UNIVERSITÀ DEGLI STUDI DI NAPOLI

"FEDERICO II"

Scuola di Dottorato in Medicina Molecolare

Dottorato di Ricerca in Genetica e Medicina Molecolare

SORTING AND MEMBRANE ORGANIZATION OF GPI-ANCHORED PROTEINS IN POLARIZED EPITHELIAL CELLS

Coordinatore:
Prof. Carmelo Bruno Bruni

Candidata:
Dott.ssa Simona Sanda Tivodar

Anno

2007

UNIVERSITÀ DEGLI STUDI DI NAPOLI

"FEDERICO II"

Dipartimento di Biologia e Patologia Cellulare e Molecolare "Luigi Califano"

Dottorato di Ricerca in Genetica e Medicina Molecolare

Coordinatore Prof. Carmelo Bruno Bruni

Sede amministrativa:
Dipartimento di Biologia e Patologia Cellulare e Molecolare "Luigi Califano"

UNIVERSITÀ DEGLI STUDI DI NAPOLI

"FEDERICO II"

Dipartimento di Biologia e Patologia Cellulare e Molecolare "Luigi Califano"

Tesi di Dottorato di Ricerca in Genetica e Medicina Molecolare
XIX

SORTING AND MEMBRANE ORGANIZATION OF GPI-ANCHORED PROTEINS IN POLARIZED EPITHELIAL CELLS

Candidata: Dott.ssa Simona Sanda Tivodar

Docente guida: Prof.ssa Chiara Zurzolo

TABLE OF CONTENTS

1. SYNOPSIS

The plasma membrane of epithelial cells is divided into distinct domains, apical and basolateral, which have different protein and lipid compositions (Rodriguez-Boulan and Powell, 1992; Mostov, 2003), achieved by the continuous specific sorting of newly synthesized molecules and recycling of membrane components (Matter, 2000; Nelson and Yeaman, 2001; Rodriguez-Boulan et al., 2005).

Glycosylphosphatidylinositol (GPI)-anchored proteins (GPI-APs) are apically sorted in a range of epithelial cell lines (Lisanti et al., 1989; Brown and Rose, 1992). It has been proposed that GPI-APs are sorted to the apical surface via their incorporation in sphingolipid- and cholesterol-rich microdomanins called rafts (Simons and Ikonen, 1997). However this hypothesis has been challenged by the finding that:

- in FRT (Fischer Rat Thyroid) cells GPI-APs are mainly delivered to the basolateral membrane (Zurzolo et al., 1993; Lipardi et al., 2000)
- both apical and basolateral GPI-APs are associated with rafts in MDCK (Madin-Darby canine kidney) cells, indicating that rafts are not sufficient to determine their apical sorting (Sarnataro et al., 2002; Paladino et al., 2004; Paladino et al., 2007).

Furthermore, we demonstrated that protein oligomerization, which could promote the stabilization of GPI-APs into rafts, is the key event for their apical sorting (Paladino et al., 2004; Paladino et al., 2007).

Another fundamental characteristic of the sorting process is that proteins are not exclusively apical or basolateral. The plasticity of epithelia is evidenced by the fact that in different epithelial cell types the same proteins can be differently sorted and/or can follow variable routes to be delivered to their final domain of residence (reviewed in (Rodriguez-Boulan et al., 2005). In addition it has been shown that apical sorting can be mediated by at least two mechanisms, raft-dependent and raft-independent (Benting et al., 1999b; Lipardi et al., 2000). Hence we have asked whether oligomerization is a requirement for apical sorting of GPI-APs in polarized cell lines other than MDCK cells and whether this mechanism is also used for apical sorting of transmembrane non raft- associated proteins. In order to answer these questions we have used FRT cells as epithelial cell model and we analyzed the behaviour of several GPI-APs differently sorted.

The factors that could promote protein oligomerization and consequently apical sorting are still under investigation and two different hypotheses could be the most possible:
1) the protein ectodomain may have a key role in determining first oligomerization and then stabilization into rafts or,

2) it is possible that apical and basolateral proteins associate with different lipid rafts that would determine the rate of their clustering and therefore be responsible for the differential sorting. The latter hypothesis is supported by the fact that caveolae, which are specialized lipid microdomains, have been found enriched on the basolateral domain of several epithelial cell lines (Lipardi *et al.*, 1998; Vogel *et al.*, 1998; Lahtinen *et al.*, 2003). In addition, Thy-1 and PrPc, two GPI-APs that traffic differently in neuronal cells (Madore *et al.*, 1999), were found within lipid microdomains with different composition (Brugger et al., 2004).

Furthermore it is unknown if different apical GPI-APs are in the same or distinct oligomeric complex and/or lipid microdomains.

Several lines of evidence indicate that in living cells GPI-APs are confined in restricted domains of the membrane. GPI-APs do not exhibit Brownian motion, but undergo random walks in a transient confinement zone (Fujiwara et al., 2002). By single particle diffusion or single particle tracking GPI-APs were found to be confined within 200-400 nm zones (Sheets *et al.*, 1997; Schutz *et al.*, 2000; Fujiwara *et al.*, 2002). Other studies using FRET, single particle tracking, or biochemical cross-linking (Friedrichson and Kurzchalia, 1998; Varma and Mayor, 1998; Pralle *et al.*, 2000) have shown that GPI-APs are restricted to submicron-sized domains on the cell surface. Findings based on FRET analysis proposed that GPI-APs are organized in three-to-four molecule hetero-clusters which depend on cholesterol (Sharma et al., 2004). On the other hand, a common biochemical criterion to define raft association has been the resistance to extraction in cold non-ionic detergent which results in the purification on sucrose density gradients of fractions enriched in glycosphingolipid, cholesterol and GPI-APs denoted DRMs (detergent-resistant membranes or detergent-resistant microdomains) (Brown and London, 1998). Using this assay it has been shown that different non-ionic detergents can extract different sets of proteins and lipids (Roper et al., 2000; Schuck et al., 2003; Slimane et al., 2003), which may indicate that different sets of proteins can associate with various types of membrane domains that could have different functional roles.

To answer all these open questions we studied how different GPI-APs are organized on the plasma membrane and we analysed the DRMs in which these protein are enriched.

In particular my thesis is organized in three major chapters:

1) Study of the GPI-AP oligomerization as specific requirement for apical sorting. This work has been published see Annex 1.

2) Analysis of lipid composition of DRMs associated to apical and basolateral GPI-APs. This work has been published see Annex 2.

3) Study of organization of GPI-APs at the apical plasma membrane in polarized epithelial cells. This work is in revision see ANNEX 3.

2. INTRODUCTION

2.1 EPITHELIAL POLARIZED CELLS

2.1.1 Plasma membrane asymmetry

Epithelial layers form the boundary between different compartments, separating the internal system of the organism from the outside world. Dependent on the organ or the state of differentiation, epithelial cells are specialized in particular functions as absorption, secretion and vectorial trans epithelial transport of fluids, electrolytes and proteins. To allow an appropriate development of these functions and to control material flow into one precise direction, epithelial cells have to maintain a polarized organization (Delacour and Jacob, 2006). The process of cell polarisation is guided by different polarisation events: the initial step is an influx of information from the extracellular milieu (Delacour and Jacob, 2006), and the following step is the establishment of cell-cell and cell-extracellular matrix contacts, which finally results in the formation of tight junctions (Figure 1) and in the reorganization of the cytoskeleton (Yeaman *et al.*, 1999; Rodriguez-Boulan *et al.*, 2005). The reorganization of the microtubule network to an apico-basolateral array also contributes to the acquisition of cell polarity (Yeaman et al., 1999). This process leads to the division of the plasma membrane in two structurally, functional and biochemical domains, known as apical and basolateral domains (Mostov *et al.*, 2003).
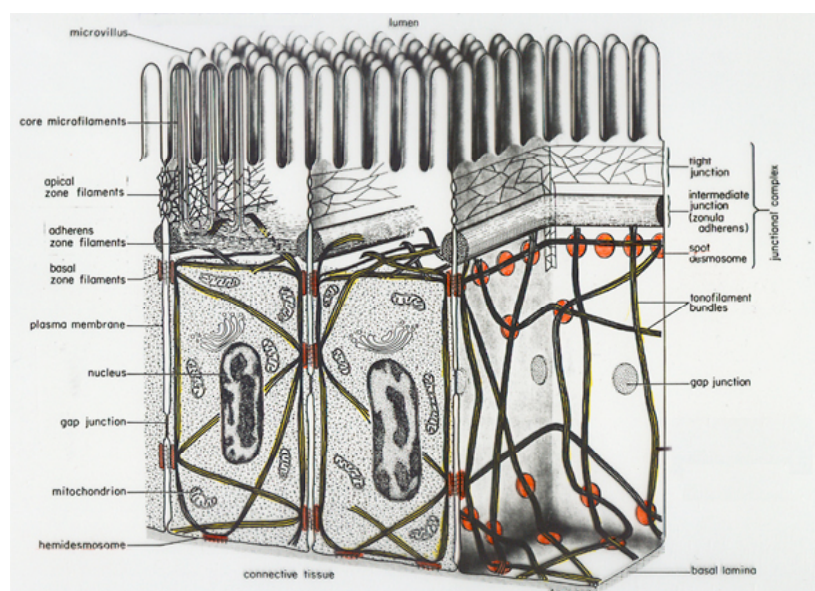
**Figure 1. Epithelial cells and organization of the junctional complex.**

The apical domain of epithelial cells is usually in contact with the external surface of an organism or with the body cavities, while the basolateral surface can be divided into two regions: the basal surface lies on a basement membrane and it is in close proximity to blood vessels and capillaries, whereas the lateral surface is adjacent to other cells in the same epithelium, and contains specialized junctional domains that allow interactions among adjacent cells (either simple mechanical adhesion as in the case of tight junctions, adherent junctions and desmosomes (Figure 1), or metabolic cooperation via gap junction) (Brown and Breton, 2000). Tight junctions prevent the mixing of proteins and lipids between the two domains of plasma membrane, beyond to regulate the paracellular transport (Mostov et al., 2003).

The cell polarity is maintained during the lifetime of an epithelium by constant plasma membrane turnover of lipids and proteins and remodelling. Hence a continuous sorting of newly synthesized molecules and recycling of membrane components are required to maintain this *molecular asymmetry at the cell surface*. The defective targeting of membrane ion channels, transporters, enzymes and receptors leads to a variety of patho-physiological conditions that cause different human diseases. To understand the so-called "diseases of protein sorting" (Brown and Breton, 2000) it is essential to understand the basic mechanisms that are used by the cell to sort, deliver, insert and maintain proteins in their correct cellular location.

2.1.2 MDCK cells, the model cells

One of the fundamental questions is how epithelial cells establish and maintain their polarized phenotype. The understanding of these processes became experimentally approachable when it was discovered that Madin-Darby canine kidney (MDCK) cells develop a tight epithelial monolayer when they are plated on a permeable substratum (Cereijido et al., 1978). Therefore MDCK cells became *the model system to study polarized protein targeting* (Figure 2). Subsequently other cell lines, like FRT (Fisher Rat Thyroid) or CaCo-2 (Colon Carcinoma) cells, were discovered to retain the ability to form polarized membrane domains in tissue culture and provided good experimental system to study mechanisms of protein sorting (Nelson and Rodriguez-Boulan, 2004). At this point a "new epoch" opened to elucidate biosynthetic and recycling pathways for apical and basolateral membrane proteins and to identify the components that guide apical and basolateral proteins along these pathways (Rodriguez-Boulan *et al.*, 2005).
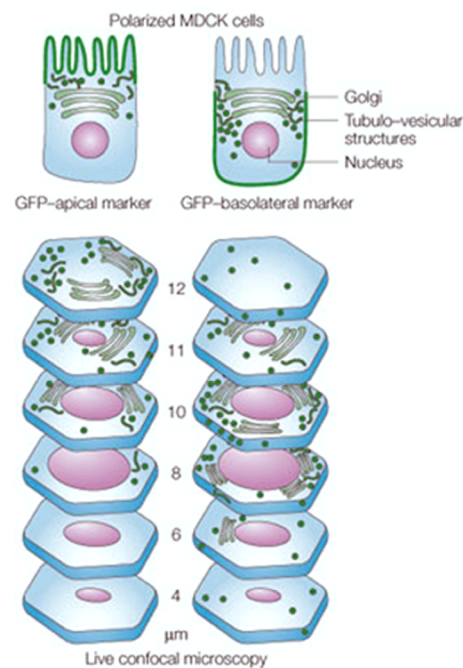
Figure 2. The Madin-Darby canine kidney (MDCK) cell model. *(From Nature Reviews, Molecular Cell Biology, March 2005, Vol. 6, No 3; Rodriguez-Boulan et al., 2005).*
The exit from the Golgi complex and delivery to the cell plasma membrane of the apical or basolateral proteins is monitored by using GFP (green fluorescent protein)-tagged proteins. This movement can be followed by different microscopic techniques.

The important impact of the MDCK cellular model is revealed by increasing the number of publications on epithelial polarity, epithelial morphogenesis and the epithelial junctional complex.

Polarized cells establish and maintain functionally distinct surface domains by an elaborate sorting process, which ensures accurate delivery of biosynthetic cargo to different parts of the plasma membrane (Matter, 2000; Mostov et al., 2003; Nelson and Rodriguez-Boulan, 2004; Schuck and Simons, 2004). Moreover, different epithelia cells show *"flexibility"* in their polarized trafficking, which was defined as the ability to localize a given protein to different regions of the

cell or to use a different targeting route to reach the same region of plasma membrane (Rodriguez-Boulan and Powell, 1992).

Epithelial cells use not only biosynthetic sorting from the TGN but also a selective recycling/transcytosis to deliver proteins to the correct surface, although the relative importance of these two pathways varies among the different cell types (Mostov et al., 2003). For example, hepatocytes use mainly an indirect pathway (transcytosis), which passes trough the basolateral membrane, to deliver proteins from the TGN to the apical surface, although some proteins are delivered directly from the TGN to the apical surface (Kipp and Arias, 2000; Bastaki *et al.*, 2002). In MDCK cells, 50% of the cell surface is endocytosed per hour, and a typical membrane protein has a half-life of approximately 20 h. In MDCK cells, which are heavily reliant on TGN sorting, the flux through the endocytic pathway is approximately ten times greater than through the biosynthetic pathway, indicating that selective recycling/transcytosis is essential for steady-state polarity (Bomsel et al., 1989).

2.1.3 Plasma membrane sorting determinants

As aforementioned the functional polarity of epithelial cells depends upon the selective insertion of proteins and lipids into distinct plasma membrane domains. This polarized distribution is an important event for different categories of proteins including membrane transporters, channels, enzymes, cell adhesion molecules and junctional components allowing cells to carry out the vectorial transport of fluid, ions and other molecules across the epithelial barrier (Brown and Breton, 2000). The polarized distribution of the proteins on the plasma membrane is considered to be the result of three processes:

1. newly synthesized proteins, destined to the apical or the basolateral cell surface, are synthesized at the level of the rough endoplasmic reticulum and transported through the Golgi to the trans-Golgi network (TGN) (Figure 3), where they are sorted into distinct vesicular carriers (Griffiths and Simons, 1986) directed to different domains of the plasma membrane. Other proteins are transported from the TGN to endosomes, and only then to the cell surface (Orzech *et al.*, 2001; Ang *et al.*, 2004).
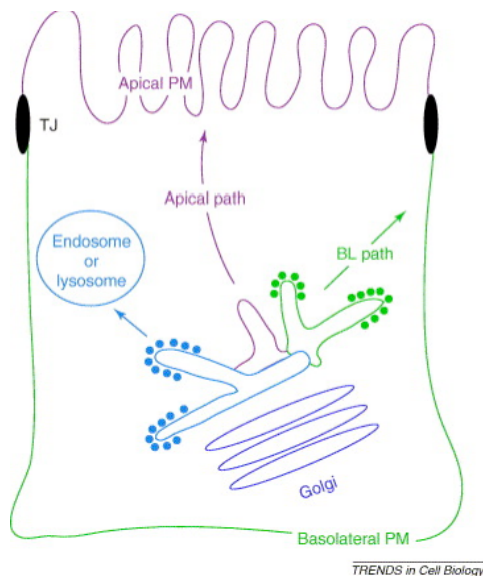
Figure 3. The scheme of the different sorting pathways that exist in polarized epithelial cells. *(From Trends in Cell Biology Volume 15, Issue 4, Heike Fölsch, 2005).*
Newly synthesized transmembrane proteins move together from the endoplasmic reticulum to the Golgi and through the Golgi apparatus. From the TGN they are sorted away from each other and delivered to endosomes or lysosomes (blue pathway), the apical plasma membrane (purple) or the basolateral plasma membrane (green).

2. some proteins are selectively retained at the cell surface, often through an interaction of their carboxyl termini with PDZ-domain-containing proteins (Harris and Lim, 2001).

3. components that are not retained at the surface are rapidly endocytosed and delivered to early endosomes, from where they can be recycled back to the cell surface, transferred to late endosomes or transported across the cell and delivered to the opposite surface, a process known as *transcytosis* (Mostov et al., 2000).

These three processes contribute to define the site of protein sorting which can be the TGN, the endosomes and the plasma membrane, all with potentially similar mechanisms for sorting different classes of membrane proteins (Nelson and Rodriguez-Boulan, 2004).

The mechanisms and carriers responsible for exocytic protein trafficking between the TGN and the plasma membrane could depend on microtubules, actin filaments and actin-associated proteins. The role of the microtubules cytoskeleton in these processes was analysed for vesicular stomatitis virus G protein tagged with GFP. These studies demonstrated that exocytic cargo moves along microtubule tracks toward the basolateral surface (Toomre *et al.*, 1999). Moreover studies using a two-colour labelling technique of live imaging in mammalian cells highlight a role for the actin cytoskeleton in the post-Golgi transport of apical sucrase-isomaltase, whereas lactase-phlorizin hydrolase-carrying apical vesicles are transferred in an actin-independent fashion to the apical membrane (Jacob et al., 2003). However recent studies showed that the actin dynamics participates in the TGN egress of both apical- and basolateral-targeted proteins but is not needed for apical raft-associated cargo (Lazaro-Dieguez *et al.*, 2007).

Pathological conditions can arise as result of the inappropriate removal or insertion of itinerant proteins, stressing the importance of proper sorting or endocytic and transcytotic transport in maintenance of polarized protein expression (Stein et al., 2002).

Protein sorting is based on different motifs, which can reside in their *cytoplasmic domains, membrane anchors or extracellular domains*. The sorting information is often referred as a *sorting signal, sorting determinant, or trafficking signal* (Muth and Caplan, 2003). These sorting motifs can interact with components of the sorting machinery and direct the proteins, through the distinct transport routes to the correct membrane domain.

Basolateral sorting determinants

Basolateral protein sorting signals are generally confined to their cytoplasmic regions. Indeed they have been identified in the cytosolic tails of a variety of transmembrane proteins by deleting or transferring them to other differently sorted proteins (Mostov *et al.*, 1986; Casanova *et al.*, 1991; Hunziker *et al.*, 1991). For example the addition of a 14 amino acids-long fragment from the cytoplasmic domain of polymeric immunoglobulin receptor (pIgA-R) to PLAP (Placental Alkaline Phosphates) reverted its sorting from the apical to the basolateral cell surface (Casanova et al., 1991).

Motifs containing Tyr, Leu-Leu or Leu-Val are localized in the cytoplasmic region near the transmembrane domain and direct these proteins to the basolateral plasma membrane domains

(Rodriguez-Boulan and Powell, 1992). In particular the aminoacid sequence YXXФ has been found mediating basolateral sorting (Nelson and Yeaman, 2001).

Furthermore tyrosine-based motif (Matter *et al.*, 1992; Matter and Mellman, 1994) are also involved in localization to coated pits and clathrin-mediated endocytosis (Chen et al., 1990; Collawn et al., 1990), and for some proteins it coincides with basolateral determinants (Hunziker *et al.*, 1991; Hunziker and Mellman, 1991). These signals were identified in several proteins as in the low density lipoprotein (LDL)-receptor (NPXY) (Matter et al., 1992), the transferrin receptor (YXRF) and the pIgA-R (YXXФ) (Matter and Mellman, 1994). For example 10 residues (including the tyrosine) in the cytoplasmic domain of the human asialoglycoprotein receptor are sufficient for its basolateral polarity and efficient endocytosis (Geffen *et al.*, 1993). Differently, the LDL-receptor contains two basolateral sorting signals, the inactivation of one signal can cause mistargeting of LDL-receptor and result in hypercholesterolemia (Matter *et al.*, 1992; Koivisto *et al.*, 2001). Furthermore, for the influenza virus hemagglutinin the conversion of cysteine 543 to tyrosine is enough to be basolaterally sorted and internalized (Lin et al., 1997).

The basolateral sorting activity of the signal is essential to establish the polarity of the protein, whereas the endocytosis signal permits proper surface regulation of the protein (Muth and Caplan, 2003). The importance of a correct regulation of these processes has been demonstrated in the case of familial hypercholesterolemia, where mutations to the LDL-receptor internalization domain prevent the uptake of low-density lipoproteins from the plasma membrane and into liver cells (Chen et al., 1990; Goldstein and Brown, 2001).

Another amino acid motif, acting as basolateral determinant, is the dileucine (LL) motif found within the cytoplasmic tail of some proteins, as the glucose transporter GLUT4 (Corvera et al., 1994; Verhey and Birnbaum, 1994; Verhey et al., 1995) and the vasopressin V2 receptor (Birnbaumer et al., 1992). A novel signal based on a single leucine motif was described in the stem cell factor (Wehrle-Haller and Imhof, 2001).

The basolateral signals are recognized by adaptor coat proteins, like AP-1B, an isoform of the AP-1 clathrin adaptor protein, but which contains an alternative epithelial-specific subunit (Mostov et al., 2003). The expression of AP-1B is sufficient to confer correct basolateral sorting in LLC-PK1 kidney epithelial cells that lack this protein (Folsch et al., 1999).

Apical sorting determinants

Delivery of proteins to the apical surfaces of epithelial cells depends on the coordination of multiple distinct mechanisms. In contrast to basolateral sorting signals apical sorting signals are localized in exoplasmic, membrane or cytoplasmic domains of the proteins (Mostov *et al.*, 2003; Muth and Caplan, 2003; Rodriguez-Boulan *et al.*, 2004; Rodriguez-Boulan *et al.*, 2005; Delacour and Jacob, 2006).

A putative apical sorting signal has been found independently in the cytoplasmic tail of two seven-transmembrane-spanning proteins, rhodopsin (Chuang and Sung, 1998) and the apical Na^+-dependent bile acid transporter (Sun *et al.*, 1998). In fact, 39 and 40 amino acids, respectively, of the cytoplasmic tail of these two proteins were able to redirect two different basolateral proteins to the apical surface in MDCK cells. Interestingly, these sequences are peculiar to these specific classes of proteins, and there are no conserved residues between the two signals of the two cytoplasmic tails.

Another specific case is that of megalin, the main endocytic receptor of the proximal tubule responsible for reabsorption of many filtered proteins. The cytoplasmic tail of megalin contains three NPXY motifs, YXXØ, SH3, and dileucine motifs beyond to PDZ-binding motif at its COOH terminus. By deletion analysis Takeda et al. found that amino acids 107-136 of the cytoplasmic tail of megalin containing the second NPXY-like motif are critical for apical sorting and targeting, whereas the regions containing the first and third NPXY motifs are required for efficient endocytosis (Takeda et al., 2003).

These studies indicated that cytoplasmic sorting machinery analogous to the one described for basolateral proteins also might exist for apically targeted proteins.

Other apical signals were found in the ectodomain of proteins by using glycosylation-deficient cell lines, showing that glycans are requested for apical protein sorting (Le Bivic et al., 1993). In the same way treatment of MDCK cells with tunicamycin, that is a GlcNAc-analogue which inhibits the first step of N-glycosylation, determined the missorting of apical gp80 to both membrane domains of MDCK cells (Urban et al., 1987).

N-glycosylation, is not a universal apical sorting signal; indeed there are some proteins that are apically sorted independently of presence or absence of N-glycosyl chains, like in the case of p75NTR in MDCK cells (Yeaman et al., 1997). Instead, deletion of O-linked glycosyl chains induced a mistargeting of p75NTR from the apical to basolateral domain of plasma membrane (Yeaman *et al.*, 1997; Jacob *et al.*, 2000).

In addition in some cases the position of O-glycans is crucial for apical sorting of the protein (Jacob *et al.*, 2000; Breuza *et al.*, 2002). At the moment several studies tend to define which part of

the glycan chain is involved in apical targeting. It was proposed that terminal oligosaccharides constitute apical determinants of endolyn (Potter et al., 2004), while the apical sorting signals are located in the core region of glycans of the H,K-ATPase beta subunit and in this case the terminal region functions to stabilize only the protein at the apical plasma membrane (Vagin et al., 2004).

Furthermore it seems that N- and O-glycans function as recessive signals respect to basolateral signals and their wide distribution in plasma membrane and secretory proteins explains the frequent finding that removal of basolateral signals from a protein results in its apical localization (Matter and Mellman, 1994; Fiedler and Simons, 1995; Yeaman *et al.*, 1997).

Although those findings highlight an involvement of N- or O-glycosylation in accurate apical delivery, the underlying mechanism by which glycosylation could determine apical trafficking is unknown. The point that remains to be determined is whether glycans motifs are directly involved in apical targeting or whether they contribute indirectly to apical protein sorting. It was postulated that glycans can act either by stabilizing proteins, allowing access to a hidden apical sorting signal or by fixation of a competent conformation for apical sorting. Alternatively, glycosylation could have an impact on the lateral mobility of the protein in the membrane, which could affect the incorporation into membrane microdomains (see after) and delivery into apical carrier vesicles (Scheiffele *et al.*, 1995; Simons and Ikonen, 1997; Rodriguez-Boulan and Gonzalez, 1999).

A particular case of apical sorting is represented by *glycosylphosphatidylinositol (GPI) anchored proteins (GPI-APs)* that are attached to the external leaflet by a glycolipid anchor (see after chapter 2.4). The GPI-APs were found to be preferential localized at the apical plasma membrane of epithelial cells, and are enriched in the sphingolipid/cholesterol membrane microdomains called *lipid rafts* (Fiedler *et al.*, 1993; Arreaza and Brown, 1995; Nosjean *et al.*, 1997). *Rafts* were proposed to form spontaneously by lateral-lateral interactions between the long and saturated chains of sphingolipids and cholesterol which is intercalated among them favouring their tight packing (Simons and Ikonen, 1997; Simons and Vaz, 2004). Because of their capacity to segregate specific classes of lipids and proteins, rafts can act as platforms of sorting. An important biochemical property of rafts is their insolubility to the cold non-ionic detergent like Triton X-100, for this motif rafts are also called detergent resistant microdomains or membranes (DRMs). Proteins associated with rafts are insoluble in this non-ionic detergent. Brown & Rose by using this method in a pulse & chase experiments have found that the GPI-APs are soluble in the ER and became progressively insoluble to Triton X-100 extraction when reach the Golgi complex indicating that in this compartment GPI-APs start to associate with rafts (Brown and Rose, 1992). Therefore, it was postulated that *GPI anchor* could be an apical sorting signal by mediating the association of GPI-APs with lipids rafts, because of natural affinity of their GPI-anchor for these membrane

microdomains (Simons and Ikonen, 1997). However this hypothesis has been recently questioned by the fact that in FRT cells the major part of endogenous GPI-APs are basolaterally sorted and GPI-APs, although DRM-associated, are apically and basolaterally sorted in MDCK cells (Zurzolo *et al.*, 1993; Lipardi *et al.*, 1998; Paladino *et al.*, 2002; Paladino *et al.*, 2004; Paladino *et al.*, 2006; Paladino *et al.*, 2007). Hence this indicates that rafts are not sufficient for apical sorting of GPI-APs (Paladino *et al.*, 2004; Paladino *et al.*, 2007). Furthermore, we found that only apical and not basolateral GPI-APs are able to oligomerize into high molecular weight complexes (Paladino *et al.*, 2004; Paladino *et al.*, 2007) and protein oligomerization begins in the medial Golgi, concomitantly with DRM association (Paladino et al., 2004). We demonstrated that impairment of oligomerization leads to protein missorting indicating that protein oligomerization is an essential step for apical sorting of GPI-APs (Paladino *et al.*, 2004; Paladino *et al.*, 2007). Oligomerization stabilizing proteins into rafts could lead the coalescence of small rafts to constitute a larger functional sorting platform (Helms and Zurzolo, 2004; Paladino *et al.*, 2004; Paladino *et al.*, 2007). It is likely that there exist some factors that promote oligomerization. Some proteins, like as VIP17/MAL (Puertollano et al., 1999), caveolins (Scheiffele et al., 1998), flotilins (Neumann-Giesen et al., 2004) and somatins (Snyers et al., 1999), which are raft-associated and form oligomers, have been hypothesized to act in promoting GPI-APs clustering. In addition it was postulated that galectin-4 could function an organizer/stabilizer within microvillar lipid *superrafts* (Braccia et al., 2003). Braccia et al. hypothesized that this lectin, tightly associated with rafts on the outside of the brush border membrane of intestinal cells, defines the core of a raft, while the GPI-anchored alkaline phosphatase and the transmembrane aminopeptidase N may could represent more peripheral raft proteins with decreasing affinity for these microdomains (Braccia et al., 2003).

Table 1. Schematic representation of basal-lateral (left) and apical (right) transport vesicles budding from the TGN. *(From Trends in Cell Biology, 483-488 Nelson & Yeaman 2001)*. Membrane proteins are sorted based on specific sorting signals (center) and sorting mechanisms (bottom) specific for either the basal-lateral (left) or apical pathways (right). Abbreviations: AP1, adaptor protein 1; Fc-R, crystalizable fragment receptor; LDL-R, low-density lipoprotein receptor.
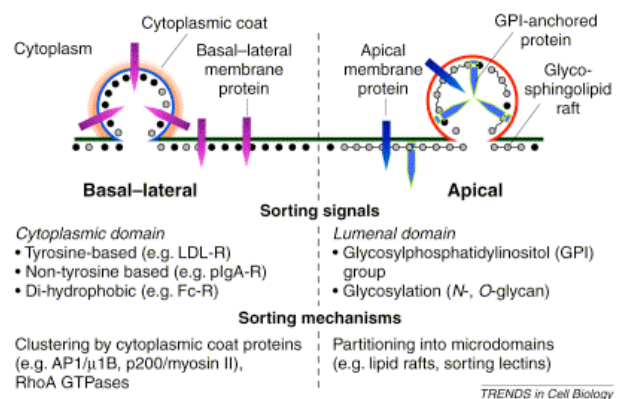
Apical sorting signals, which mediate the incorporation into membrane microdomains, have also been identified in the transmembrane (TM) domains of proteins, like in the case of the influenza virus hemagglutinin (HA) (Scheiffele *et al.*, 1997; Lin *et al.*, 1998). Furthermore it was proposed that the length of the TM domain determines the affinity of the protein for membrane microdomains thus determining its sorting (Schuck and Simons, 2004). Indeed it has been found that long TM domains could have a preference for lipid microdomains, whereas proteins that have short TM domains might be excluded because probably raft membranes are thicker than non-raft membranes (Schuck and Simons, 2004).

Basolateral and apical retention signals

Selective retention on specific domain of the plasma membrane of many proteins requires interaction with scaffold proteins, which contain the cytoplasmic PDZ-domains (Rongo *et al.*, 1998; Muth and Caplan, 2003) (Schuck and Simons, 2004). PDZ (Postsynaptic density protein 95/Drosophila Disks large/Zona occludens-1, name of three proteins where this domain was first described) domain-containing proteins have been identified as playing a critical role in membrane trafficking and sorting of ion transporters, receptors and other signalling proteins (Glynne and Evans, 2002). These scaffolding proteins coordinate the assembly of functional plasma membrane multiprotein complexes, through binding of PDZ domain to a consensus amino acid motif within the carboxyl-terminus of target proteins. Carboxy-terminal PDZ-binding motifs might direct the apical targeting of the GABA transporter GAT-3 and the cystic fibrosis transmembrane conductance regulator (CFTR) (Milewski *et al.*, 2001; Muth and Caplan, 2003).

PDZ proteins that preferentially accumulate at the apical epithelial surface include EBP50/NHERF1, E3KARP/NHERF2, PDZK1/CAP70/NaPi-Cap1 and IKEPP/NaPi-Cap2 (Wang *et al.*, 2000; Gisler *et al.*, 2001; Scott *et al.*, 2002). NHERF1/EBP50 (Na^+/H^+ exchanger regulatory factor 1, or ezrin-radixin-moesin binding phosphoprotein of 50 kDa) and NHERF2/E3KARP (Na^+/H^+ exchanger regulatory factor 2 or NHE3 kinase A regulatory protein) contain two PDZ domains and a carboxy-terminal domain that mediates association with MERM proteins (merlin, ezrin, radixin, moesin), while CAP70 and IKEPP contain four tandem PDZ domains (Bretscher *et al.*, 2000; Wang *et al.*, 2000; Gisler *et al.*, 2001; Scott *et al.*, 2002). Two studies have shown that EBP50, as well as PDZK1 can directly increase conductance via the CFTR channel through binding of the PDZ domains to the C-terminal tail of the channel (Wang *et al.*, 2000; Bezprozvanny and Maximov, 2001; Raghuram *et al.*, 2001). These authors suggest a model in which binding and/or tethering of two separate channel subunits through the tandem PDZ domains causes an activating conformational change which stabilize the localization of the channels at the surface. This model is

supported by the following observations: first, the tandem PDZ domains of EBP50 or CAP70 are required for activation; second, no other regulatory co-factor appears to be required; and third, overexpression of the PDZ proteins above a certain level eventually leads to a decrease in channel activity. In this situation, the PDZ-domain containing proteins are not acting as simple scaffold molecules (Bezprozvanny and Maximov, 2001).

Polarization of the CFTR, a cAMP-activated chloride channel, to the apical plasma membrane of epithelial cells is critical for vectorial transport of chloride in a variety of epithelia, including the airway, pancreas, intestine, and kidney (Stanton, 1997). In CFTR the sequences QDTRL at the C-terminus of the protein is responsible of the interaction with PDZ domains and in particular the leucine (position 0) and threonine (position -2) residues, are required for the efficient polarized expression of CFTR in the apical plasma membrane by interaction with EBP50. Mutations that delete the C-terminus of CFTR cause cystic fibrosis because CFTR is not polarized and not connected with EBP50 (Moyer *et al.*, 1999; Moyer *et al.*, 2000), thus indicating that PDZ-interacting domains and PDZ domain-containing proteins play a key role in the apical polarization of ion channels in epithelial cells.

The epithelial gamma-aminobutyric acid (GABA) transporter (BGT-1) contains a PDZ target motif that mediates the interaction with the PDZ protein LIN-7 in MDCK cells, and it responsible of the basolateral localization of the transporter by promoting its retention at the basolateral surface. It was found that although the transporters from which the PDZ target motif was deleted were still targeted to the basolateral surface, they were not retained but internalized in an endosomal recycling compartment (Perego *et al.*, 1999).

In conclusion both for apical and basolateral proteins, interactions with PDZ proteins could determine the polarized distribution by a retention mechanism and not by an active sorting mechanisms. PDZ proteins may, therefore, constitute an important part of membrane protein sorting machinery, by recognizing retention signals (the PDZ target sequences) and therefore preventing protein internalization.

Finally it has been suggested that a protein destined for expression at the cell surface, but lacking its sorting determinant, is not sorted at all, and its appearance at both surfaces results from a stochastic partitioning process at the level of the TGN. The absence of sorting information in other cases causes the protein or multisubunit protein complex to fail quality control check points, resulting in its retention and degradation in the ER (Ellgaard & Helenius 2001, Reddy & Corley 1998). However, the removal of the primary sorting determinant results in the exposure or

activation of a previously cryptic sorting determinant. For example, when the basolateral sorting signals of LDL-R and pIg-R are absent, these proteins are delivered to the apical surface, instead to being trapped within the ER or targeted to both membrane surfaces as would be expected if these proteins possess only a single sorting determinant (Casanova et al. 1991, Hunziker et al. 1991). Carboxypeptidase M and lactase phlorizin hydrolase provide additional examples of proteins that appear to embody both apical and basolateral sorting information (Jacob et al. 1999, McGwire et al. 1999). This hierarchy of sorting signals suggests that apical and basolateral sorting information competes in common compartment along the exocytic route. The mechanisms that determine the hierarchy of multiple signals in a single protein are still poor elucidated.

In view of the complexity of these trafficking processes, it is not surprising that a growing number of disease pathologies have been identified, involving defective targeting or trafficking of membrane proteins. These diseases can be grouped under the name "sorting disorders," and they result from abnormal delivery of functionally important proteins to the cell surface. In some cases, the mutated protein is retained and degraded intracellularly, while in others cases the mutated protein may not be delivered to the cell surface after the appropriate physiological stimulation.

2.2 MEMBRANE STRUCTURE

Cell membranes are very intensely studied because of their vital role in separating the cell from the outside world and in defining different compartments inside the cell in order to allow and protect important intracellular processes and events. Cellular membranes have diverse functions in the different regions and organelles of a cell, thus it is important to study the membrane structure and dynamics of its components. During the last 70 years different models were proposed for the membrane structure. In 1935 Davison & Danielli proposed sandwich model (Figure 4A), where a phospholipid bilayer is covered in a globular protein coat. Next, it was proposed the *fluid mosaic model* by Singer and Nicolson (Singer and Nicolson, 1972). In this model, membranes are organized in a liquid fluid bilayer in which integral proteins with their amphipathic structure (with the ionic and highly polar groups protruding from the membrane into the aqueous phase, and the non-polar groups largely buried in the hydrophobic interior of the membrane) are dispersed mediating the various functions of membranes. The fluid mosaic structure is therefore formally analogous to a two-dimensional oriented solution of integral proteins (or lipoproteins) in the viscous phospholipid bilayer solvent (Figure 4B). The bilayer provides the basic structure of the membrane and serves as a relatively impermeable barrier to the flow of water soluble molecules. Then several studies highlighted an important feature of biological membranes: they are characterized by the presence of regions with compositions and physical properties that differ from the average properties of membrane (Thompson and Tillack, 1985). In contrast to the simplified vision of Singer and Nicolson, by using enveloped viruses to sample apical or basolateral host cell membranes it was demonstrated that lipids from the apical membranes are enriched in glycoshingolipids respect to basolateral membranes (van Meer and Simons, 1982). This difference in composition appeared to be due to the sorting of lipids and proteins in the Golgi complex and trans-Golgi membranes and directed trafficking of these molecules to the cell surface (van Meer, 1989). The correlation of these biological observations with model membrane and other physical chemical studies has lead to the conclusion that there exist small clusters of glycosphingolipids (about 15 molecules maximum) in model and native bilayer membranes (Thompson and Tillack, 1985; Rock *et al.*, 1990). Subsequent studies established that GPI-APs are insoluble in Triton X-100 at 4°C and were purified in the light buoyant density on sucrose gradients similarly to cholesterol and sphingolipids (Brown and Rose, 1992). On the basis of all these data Simons and Ikonen proposed the *rafts hypothesis* (Figures 4C & 5A) (Simons and Ikonen, 1997). Cholesterol and sphingolipids, spontaneously associate together segregating from the rest of phospholipids (Simons and Ikonen, 1997). The sphingolipids have the capacity to pack tightly together because of their long and saturated acyl chains (Simons and van Meer, 1988; van Meer and Simons, 1988;

Brown and Rose, 1992) constituting a liquid-ordered phase surrounded by disordered, fluid phase composed of glycerophospolipids (Simons and Vaz, 2004). Because of their capacity to segregate proteins and lipids, lipid rafts have been implicated in several cell functions such as signalling and sorting (Simons and Ikonen, 1997; Simons and Toomre, 2000). In addition it has supposed that these lipid domains might also could affect membrane protein conformation, and thus the function of the protein (London, 2005).
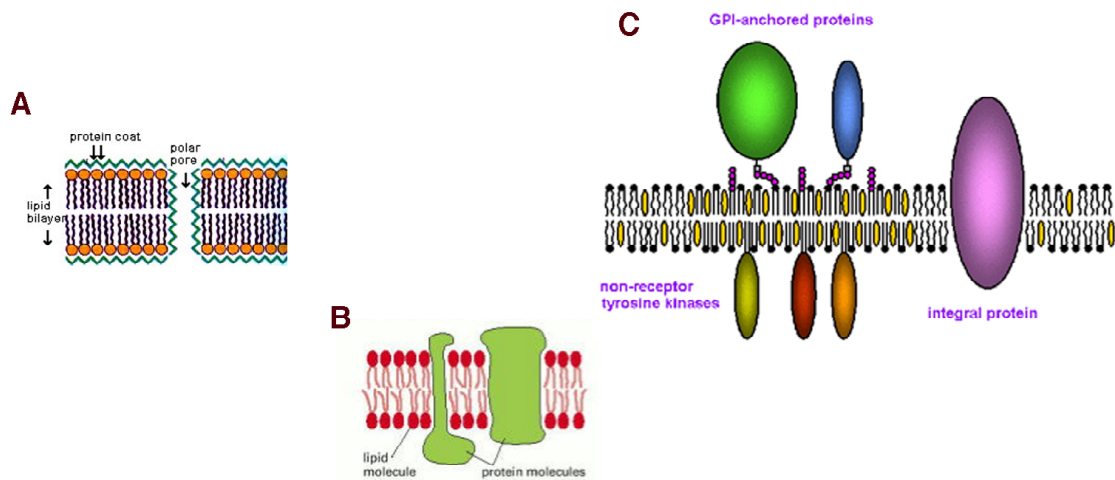
Figure 4. Different membrane structure models.
Davison & Danielli's sandwich model (A). The fluid mosaic model proposed by Singer & Nicolson (B). The Simons & Ikonen model based on the existence of distinct membrane domains called rafts (C).

In the last years many studies by using different and more sophisticated techniques have been used to proof directly the existence of lipid rafts and to determine their characteristics (size, composition, dynamics, **etc**.). Studies of domain formation in model membrane concluded that lipids could be present in three different phases: the gel phase (l_b), the liquid ordered phase (l_0), and the liquid crystalline phase or fluid phase (l_d). The mixtures of cholesterol with high melting temperature (Tm) lipids having saturated acyl chains (like dipalmitoylphosphatidylcholine (DPPC) and sphingomyelin (SM)) form a tightly packed and ordered phase similar to the gel phase, but in which lateral motion was almost as rapid as in the l_d state (Almeida et al., 1992). Fluorescence quenching studies in model membrane vesicles showed that high cholesterol concentrations could promote l_d/l_o co-existence in mixtures of high and low Tm lipids (Silvius et al., 1996), including sphingolipid-containing mixtures (Ahmed et al., 1997). Furthermore depletion of rafts components (either sphingolipids or cholesterol) perturbed sorting and signalling of different membrane proteins (Keller *et al.*, 1992; Harder and Simons, 1997). In addition, several studies made in living cells using different approaches (from diffusion methods to probe partioning, FRET and FRAP studies) suggest that lipid segregation in distinct domains also occurs in biological membranes (Maxfield, 2002;

Ritchie *et al.*, 2003; Rao and Mayor, 2005; Meder *et al.*, 2006). Indeed GPI-APs have been found confined in restricted domains of the membrane: i) GPI-APs do not exhibit Brownian motion, but undergo random walks in a transient confinement zone (Fujiwara *et al.*, 2002); ii) single particle tracking experiments revealed that GPI-APs were found to be confined within 200-400 nm zones (Sheets *et al.*, 1997; Schutz *et al.*, 2000; Fujiwara *et al.*, 2002) ; iii) other studies using FRET, single particle tracking, or biochemical cross-linking have shown that GPI-APs are restricted to submicron-sized domains on the cell surface (Friedrichson and Kurzchalia, 1998; Varma and Mayor, 1998; Pralle *et al.*, 2000).

To date, it is clear that different types of lipid/protein microdomains exist in biological membranes: rafts (Simons and Ikonen, 1997; Edidin, 2003; Simons and Vaz, 2004); caveolae which represent specific lipid microdomains coated by caveolin and involved in endocytosis of some receptors and entry of viruses and pathogens (Pelkmans and Helenius, 2002; Pelkmans, 2005; Stan, 2005); transient confinement zone (Dietrich *et al.*, 2002) and small regions enriched in fluid lipids or tetraspanin-enriched microdomain, distinct from lipid rafts and composed of a core of several tetraspanin proteins (highly hydrophobic membrane proteins) that organize other membrane proteins such as integrins, human leukocyte antigens and some growth factor receptors in cholesterol and gangliosides enriched environment. These latter complexes can have effects on cellular adhesion and motility, interactions with stroma or affecting signalling by growth factors (Lazo, 2007).

The exact mechanism by which this heterogeneity is achieved is still unknown, but is likely that complex mechanisms involving lipid synthesis, turnover and active transport (Mayor and Rao, 2004) are involved.

2.3 DIFFERENT VIEW OF LIPID MEMBRANE MICRODOMAINS

Lipid rafts have been considered as a new compartmentalization of biological membrane (Simons and Ikonen, 1997), where specific lipids can form dynamically platforms in which proteins can be enriched in order to be sorted or recruited to activate signalling cascade (Zurzolo et al., 2003).

However on the basis of recent results different views have been proposed. Some researchers envisaged rafts as *"lipid shells"* that are small, dynamic molecular-scale assemblies in which 'raft' proteins preferentially associate with certain types of lipids which transform into functional structures by dynamic and regulated processes. Indeed they believed that raft proteins have a light buoyant density not because they are in a lipid domain, but because they are encased in a shell of cholesterol and sphingolipids (Figure 5B) (Anderson and Jacobson, 2002). They speculated that a lipid shell is formed by long-term interactions between specific lipids and selected proteins in the membrane The estimated diameter of a cholesterol-sphingolipid-rich shell containing 80 lipid molecules is ~7 nm.
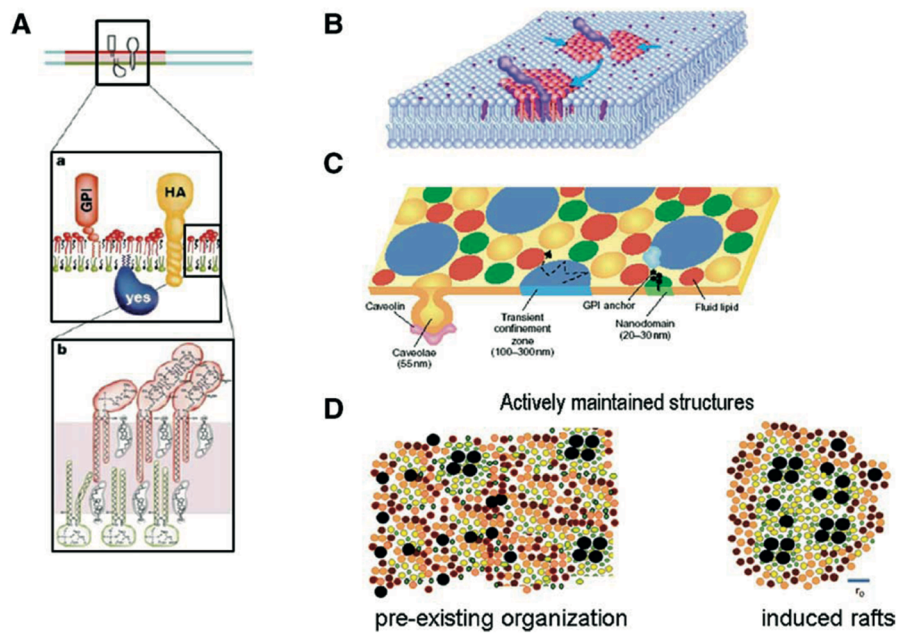
Figure 5. Models for the lateral organization of the plasma membrane. *(From Traffic 5, 231-240, Satyajit Mayor & Madan Rao, 2004).*
Rafts are represented as relatively large structures (~50 nm) (83), enriched **in** cholesterol and sphingolipids (SL), with which proteins are likely to associate (Simons and Ikonen, 1997) (A). Rafts are visualized as lipid shells that are small, dynamic molecular-scale assemblies in which raft proteins preferentially associate with certain types of lipids (Anderson and Jacobson, 2002) (B). "Mosaic of domains" model proposed that cells regulate the amount of the different types of domains via a cholesterol-based mechanism (Maxfield, 2002) (C). A different picture, which is consistent with data from GPI-anchored protein studies in living cells suggests that pre-existing lipid assemblies are small and dynamic, and coexist with monomers (D). They are actively induced to form large-scale stable rafts (Varma and Mayor, 1998; Sharma *et al.*, 2004). Black circles, GPI-anchored proteins; red and pink circles, non-raft associated lipids; yellow circles, raft-associated lipids; green, cholesterol.

Because the chemical composition of membranes is very dynamic, Maxfield considered that the view of the plasma membrane organized exclusively in rafts and non-rafts domains was an oversimplification. Therefore, in his view the plasma membrane was depicted as a mosaic of different lipid domains regulated via a cholesterol-based mechanism including caveolae, nano-domains enriched in GPI-APs, glycoshpingolipids and cholesterol and small regions enriched in fluid lipids (Figure 5C) (Maxfield, 2002). In addition, transient confinement zone (TCZ) of varying size with a diameter about 200-300 nm represents areas where different components were trapped for a few seconds, as in the case of GM_1 and Thy-1 (Dietrich *et al.*, 2002).

A different picture suggested that at steady-state there are no "functional rafts", instead small and dynamic lipid assemblies could co-exist with monomers (Figure 5D) (Mayor and Rao, 2004). These structures, then, could actively induce to form large stable " functional rafts" (Mayor and Rao, 2004). By FRET analysis they proposed that GPI-APs are organized in three-to-four molecule hetero-clusters which depend upon cholesterol (Sharma *et al.*, 2004).

Thus, the size of the membrane rafts can vary from a few nanometers to a few hundred and are very dynamic structures (Simons and Vaz, 2004; Rao and Mayor, 2005).

Recently Helms & Zurzolo have proposed in the raft model, the new concept where various proteins could have different affinities for the lipids raft, whereby the affinity can be increased by oligomerization inducing the formation of *functional rafts* (Helms and Zurzolo, 2004). Indeed both apical and basolateral GPI-APs are extracted as DRMs because of affinity of GPI anchor for these lipids microdomains, but exclusively apical GPI-APs oligomerised and are apically sorted (Paladino et al. 2004).
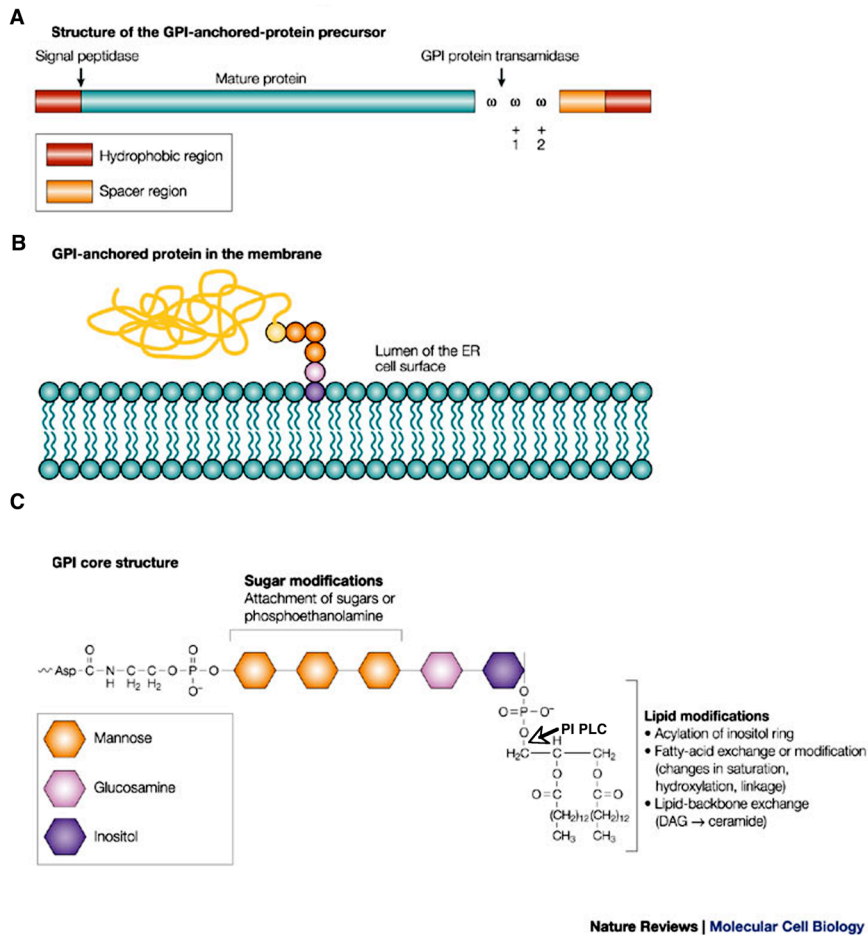
2.4 GPI-ANCHORED PROTEINS

Many membrane proteins are covalently linked to various lipids as fatty acids (Schmidt et al., 1979), isoprenoids (Glomset et al., 1990), diacylglycerols (Hantke and Braun, 1973) and glycosylphosphatidylinositols (GPI) (Ferguson et al., 1985) through post-translational modifications.

GPI-anchored proteins are synthesized as precursors with a cleavable, hydrophobic amino-terminal signal sequence that targets the protein to the lumen of the ER and a cleavable, carboxy-terminal signal sequence that directs GPI anchoring (Figure 6A). The GPI-anchoring signal consists of a hydrophobic region separated from the GPI-attachment site (ω-site) by a hydrophilic spacer region (Figure 6A). Amino-acid residues with small side chains are highly preferred for the two amino acids that follow the ω-site. At the end of the process of modification, GPI-APs are proteins bound to the membrane by the GPI-anchor (Figure 6B). The glyco-lipid anchor is attached to the ω-site by the action of a GPI transamidase in the lumen of the endoplasmic reticulum (ER). The core structure of GPI-anchor is conserved among all species that have so far been investigated (Ferguson, 1999; Ikezawa, 2002) and contained a phosphodiester linkage of phosphoethanolamine (PE) to a trimannosyl-glucosamine (Man3-GlcN) core (Figure 6C). The reducing end of GlcN is linked to phosphatidylinositol (PI). PI is then anchored through another phosphodiester linkage with diacylglycerol to the cell membrane through its hydrophobic region (Figure 6C). The core can be modified and, indeed it is subjected to various remodelling reactions, during the secretion from the cell. Variations can occur by addition of extra sugars or ethanolamine phosphates to the mannose residues, acylation of the inositol ring, changes in the fatty acids (length, saturation, hydroxylation), or their types of linkage to the glycerol backbone (acyl to alkyl), or remodelling of the entire diacylglycerol to ceramide (Mayor and Riezman, 2004).

The release from the plasma membrane of GPI anchored proteins can be obtained by treatment with phosphatidylinositol specific phospholipase C (PI-PLC) (Figure 6C). The enzyme specifically hydrolyzes the phosphodiester bond of phosphatidylinositol to form a free 1,2-diacylglycerol and glycopeptide-bound inositol cyclic-1, 2-phosphate.

The functionality of GPI-APs ranges from enzymatic to antigenic and adhesion properties. GPI-anchored proteins also play a critical role in a variety of receptor-mediated signal transduction pathways. The larger number of functions supported by GPI-APs does not help to have a precise idea on general role of GPI anchor. The stability and the modulation of their functions in cellular membrane could dependent on many different parameters such as the nature of the surrounding lipids or cytoskeleton proteins and some other factors as the accessibility to phospholipase.

Figure 6. Structure of GPI-APs on plasma membrane. *(From Satyajit Mayor & Howard Riezman Nature Reviews Molecular Cell Biology 5, 110-120, 2004).*
GPI-anchored proteins are positioned in the extracellular or luminal leaflet of membranes through their glycolipid moieties (A). A typical nascent GPI-AP contains signal peptide fragment, ω-site for addition of preformed GPI anchor, spacer and hydrophobic regions (B). The conserved GPI consists of ethanolamine phosphate in an amide linkage to the carboxyl terminus of the protein, three mannose residues (orange), glucosamine (blue) and phosphatidylinositol (purple). GPI-anchor can be modified and is subjected to various remodelling reactions of the lipid moiety. Variations can occur by addition of extra sugars or ethanolamine phosphates to the mannose residues; acylation of the inositol ring; changes in the fatty acids (length, saturation, hydroxylation), or their types of linkage to the glycerol backbone (acyl to alkyl); or remodelling of the entire diacylglycerol to ceramide (C).

The GPI-APs have been found enriched in lipid rafts as assayed in detergent insolubility experiments. Indeed GPI-APs were found resistant to solubilization by non-ionic detergents as Triton X-100. This detergent insolubility appears to be an intrinsic property of GPI anchor due to its natural affinity for the long and saturated acyl chains of glycosphingolipid/cholesterol-rich domains (Benting *et al.*, 1999a; Lipardi *et al.*, 2000; Mayor and Riezman, 2004; Paladino *et al.*, 2004; Legler *et al.*, 2005).

3. THE AIM OF THE STUDY

Rafts represent specialized membrane domains enriched in glycosphingolipids and cholesterol resistant to detergent extraction (DRMs), which may serve to segregate proteins in a specific environment in order to improve their function. Association of GPI-APs with lipid rafts has been proposed to be involved in their sorting to the apical membrane in polarized epithelial cells (Simons and Ikonen, 1997). However, the finding that in FRT cells endogenous GPI-APs are mainly delivered to the basolateral membrane (Lipardi *et al.*, 2000; Sarnataro *et al.*, 2002) and that in MDCK cells both apical and basolateral GPI-APs associate with DRMs (detergent-resistant membranes) indicate that rafts are not sufficient to determine their apical sorting (Paladino *et al.*, 2004). Furthermore, we have found that in MDCK cells protein oligomerization, which could promote the stabilization of GPI-APs into rafts, is needed for their apical sorting (Paladino *et al.*, 2004). Indeed the impairment of oligomerization impairs apical sorting of GPI-APs.

Another fundamental characteristic of the sorting process is that proteins are not exclusively apical or basolateral. The plasticity of epithelia is evidenced by the fact that in different epithelial cell types the same proteins can be differently sorted and/or can follow variable routes to be delivered to their final domain of residence (reviewed in (Rodriguez-Boulan *et al.*, 2005).

In addition it has been shown that apical sorting can be mediated by at least two mechanisms, raft-dependent and raft-independent (Benting *et al.*, 1999b; Lipardi *et al.*, 2000).

This work has three major objectives:

1) To understand whether oligomerization is a specific and universal requisite for apical sorting of GPI-APs

2) To analyse the role of the DRM specific lipid composition in apical sorting and oligomerization

3) To analyse the organization (and its requirements) of GPI-APs in the apical membrane of polarized cells

To understand whether oligomerization is a mechanism working in different epithelia and whether it specific for GPI-APs or is used also by transmembrane non-raft associated proteins I have used FRT cells as model of a different epithelium and have analysed the behaviour of four stably transfected GPI-APs: PLAP, a native GPI-AP, NTR-PLAP, in which the ectodomain of neurotrophin receptor p75 NTR is fused to the GPI-attachment signal of PLAP (Lipardi *et al.*, 2000), GFP-GPI and GH-DAF, two fusion proteins in which the green fluorescent protein (GFP) and the rat growth hormone (GH) are respectively fused to the GPI attachment signal of the folate receptor and the decay accelerating factor (DAF). We then analyzed the behaviour of these four

proteins regarding their capacity to be apically or basolateraly sorted and to be incorporated into oligomeric complexes.

In the second part of my thesis I have studied the lipid composition of the apical and basolateral DRMs and asked whether they maintained their specific composition after Triton extraction. To this aim we analyzed the lipid fraction co-immunoprecipitated with apical and basolateral GPI-AP from purified DRMs. Specifically, as model proteins I have used two DRMs associated GPI-APs, PLAP and GH-DAF, which are differently sorted in FRT cells. Cells expressing PLAP or GH-DAF were radiolabelled with $[1-^3H]$-sphingosine, then extracted in TX100, purified on sucrose density gradients, immunoprecipitated with specific antibodies against the two proteins. The labelled sphingolipids in the immunoprecipitates were analysed by TLC and digital autoradiography.

The factors that promote protein oligomerization are still unclear. Furthermore it is unknown if different apical GPI-APs are in the same or distinct oligomeric complex and/or lipid microdomains. To this aim in the last part of my thesis I studied how GPI-APs are organized at the plasma membrane and the specific requirements. In our previous work we found that GPI-AP oligomers appear to be protein specific and once formed are not sensitive to cholesterol depletion, suggesting that they are maintained by protein-protein interactions (Paladino et al., 2004). To understand what is the driving force for GPI-AP oligomerization and how this affects the reciprocal organization of different GPI-APs at the plasma membrane we have co-transfected in MDCK cells two different pairs of apical GPI-APs with the same (GFP-GPI/FR, folate receptor) or different (GFP-GPI/PLAP, placental alkaline phosphatase) GPI-attachment signal. We then analyzed the behaviour of the two different pairs of proteins regarding their capacity to be apically sorted and to be incorporated into oligomeric complexes as well as their dependence on cholesterol and their relative spatial organization.

4. MATERIALS AND METHODS

4.1 Reagents and Antibodies

Cell culture reagents were purchased from Gibco Laboratories (Grand Island, NY). Antibodies were purchased from the following companies: polyclonal anti-PLAP from Rockland (Gilgertslville, PA), monoclonal anti-PLAP from Sigma Chemical Co. (St Louis, MO), polyclonal anti-GFP from Clontech Laboratories (East Meadow Circle, CA), polyclonal anti-GFP from Santa Cruz Biotechnology (Santa Cruz, CA), monoclonal anti-GFP from Q-BIOgene (Morgan Irvine, CA), Cy3- and Cy5- conjugated secondary antibodies from Molecular Probes (PoortGebouw, Netherlands). Monoclonal anti-FR (Mov 19) was a gift of Dr. S. Miotti (Istituto Nazionale per lo Studio e la Cura dei Tumori, Milan, Italy) and polyclonal anti-GP114 and monoclonal p75NTR were a gift of Dr. A. Le Bivic (Faculté des Sciences de Luminy, Marseille, France) and the anti-GH antibody was from Biotrend GMBH (Germany). Biotin, BS_3 and HRP-conjugated streptavidin were from Pierce (Rockford, IL). Protein G- and A-coupled magnetic beads (Dynabeads) were from Dynal ASA (Oslo, Norway). All other reagents were purchased from Sigma Chemical Co. Sphingosine was prepared from cerebroside (Carter et al., 1961). $[1-^3H]$-sphingosine was prepared by specific chemical oxidation of the primary hydroxyl group of sphingosine followed by reduction with sodium boro $[^3H]$ hydride (radiochemical purity over 98%; specific radioactivity 2 Ci/mmol) (Tettamanti et al., 1973).

4.2 Cell culture and transfections

FRT cells were grown in F12 Coon's medium containing 5% FBS. FRT cells were transfected with GH-DAF cDNA (gift of Dr. Teymuras Kurzchalia) using the calcium phosphate procedure as previously described (Zurzolo et al., 1993) and stable clones were selected by resistance to neomycin. PLAP expressing cells were previously obtained in the laboratory (Lipardi et al., 2000). MDCK cells were grown in DMEM (Dulbecco's modified eagle medium) containing 5% FBS. MDCK cells were co-transfected with sequences encoding for GFP-GPI and PLAP, while cDNA for FR is transfected in MDCK cells already stably expressing GFP-GPI as previously described (Paladino et al., 2004).

4.3 Fluorescence Microscopy

Cells, grown on transwell filters for 4 days or coverslips, were washed with PBS containing 1 mM $CaCl_2$ and 1 mM $MgCl_2$, fixed with 2% or 4% paraformaldehyde and quenched with 50 mM NH_4Cl. Primary antibodies were detected with TRITC conjugated secondary antibodies. In double

imunofluorescence assay primary antibodies were detected with Cy3- and Cy5- (as anti-mouse and anti-rabbit, respectively) conjugate secondary antibodies.

Images were collected using a laser scanning microscope (LSM 510 META, Carl Zeiss Microimaging, Inc.) equipped with a planapo 63x oil-immersion (NA 1.4) objective lens. Laser lines at 543 nm and 633 were used to excite respectively the fluorophores Cy3 and Cy5 and the emission signal was collected by the META head. All image processing was done using LSM 510 software.

4.4 Biotinylation assay

Cells grown on transwell filters for 4-5 days were selectively biotinylated and processed as previously described (Zurzolo et al., 1994). Biotinylated proteins were immunoprecipitated with specific antibodies and revealed with HRP-conjugated streptavidin.

4.5 Assays for DRM-association

TX-100 Extraction

Cells grown to confluence on dishes were washed twice with PBS containing 1 mM $CaCl_2$ and 1 mM $MgCl_2$ and then lysed for 20 min on ice in 1 ml TNE/TX-100 buffer (25 mM Tris-HCl pH 7.5, 150 mM NaCl, 5 mM EDTA, 1% TX-100) and separated by centrifugation in soluble and insoluble pellets as previously described (Brown and Rose, 1992)

Sucrose density gradients multi steps

Cells were grown to confluency in 150-mm dishes, washed in PBS containing $CaCl_2$ and $MgCl_2$ and lysed for 20 min in TNE/TX-100 buffer on ice. Lysates were scraped from dishes, brought to 40% sucrose, and then placed at the bottom of a centrifuge tube. A discontinuous sucrose gradient (5-35% in TNE) was layered on the top of the lysates and the samples were centrifuged at 39,000 rpm for 17 hours in ultracentrifuge (model SW41 Beckman Inst., Fullerton, CA). One ml fractions were harvested from the top of the gradient.

Sucrose density gradients two steps

Cells that had just reached confluence in 150-mm dishes were subject to ultracentrifugation on discontinuous sucrose gradients as previously described (Prinetti et al., 2000). Briefly, cells harvested in PBS containing 0.4 mM Na_3VO_4 were suspended in 1 ml lysis buffer (1% TX-100, 10 mM Tris buffer, pH 7.5, 150 mM NaCl, 5 mM EDTA, 1 mM Na_3VO_4, 1 mM PMSF and 75 mU/ml aprotinin), allowed to stand on ice for 20 min and Dounce homogenized (10 strokes, tight). Post-nuclear supernatants were mixed with an equal volume of 85% sucrose (wt/vol) in 10 mM Tris buffer pH 7.5, 150 mM NaCl, 5 mM EDTA, 1 mM Na_3VO_4, placed at the bottom of a discontinuous sucrose gradient (30–5%) in the same buffer and centrifuged at 200,000 g for 17 hrs

at 4°C. After ultracentrifugation, eleven 1 ml fractions were collected starting from the top of the tube. Fraction 5 located at the interface between 5 and 30% sucrose was regarded as the sphingolipid-enriched membrane fraction. The bottom fraction (fraction 11) contained a pellet, which was carefully homogenized before analysis. The entire procedure was performed on ice.

4.6 Labelling with [³H]-sphingosine

Cells were incubated in the presence of 4 x 10^{-8} M [1-³H]-sphingosine (7 ml/dish) in culture medium for 2 hrs and then chased for 48 hrs in fresh culture medium. Under these conditions all sphingolipids (including ceramide, sphingomyelin, neutral glycolipids and gangliosides) and phosphatidylethanolamine were metabolically radiolabelled (Chigorno et al., 1997).

4.7 Analysis of lipids

The cell lysate, postnuclear supernatant and sucrose gradient fractions obtained after cell metabolic radiolabelling were analyzed to determine the content of radiolabelled lipids. Samples were dialyzed and lyophilized, and lipids were extracted twice with 0.4 ml chloroform/methanol 2:1 (v/v) (Riboni et al., 1992). [³H] lipids were separated by monodimensional HPTLC carried out with the solvent systems chloroform/methanol/0.2% aqueous $CaCl_2$, 55:45:10 (v/v/v). The radioactivity associated with cells and with cell fractions was determined by liquid scintillation counting. Digital autoradiography of the HPTLC plates (250 dpm applied on a 3 mm line) was performed with a Beta-Imager 2000 instrument (Biospace, Paris) using an acquisition time of about 65 hrs. The radioactivity associated with individual lipids was determined by autoradiography with the specific β-Vision software provided by Biospace. Cholesterol was separated by monodimensional HPTLC using the solvent system hexane/diethylether/acetic acid, 80:20:1 (v/v/v) and quantified after separation on HPTLC followed by visualization with 15% concentrated sulphuric acid in 1-butanol Phosphatidylcholine was separated by a two-run monodimensional HPTLC using the solvent system chloroform/methanol 9:1 (v/v), followed by the solvent system chloroform/methanol/acid acetic/water 30:20:2:1 (v/v/v/v) and quantified after separation on HPTLC followed by specific detection with a molybdate reagent. The quantity of cholesterol and phosphatidylcholine were determined by densitometry and comparison with known amounts of standard lipids using the Molecular Analyst program (Bio-Rad Laboratories).

4.8 Velocity gradients

Velocity gradients were performed using previously protocols (Doms et al., 1987; Paladino et al., 2004). Cells, grown to confluence in 100 mm dishes, were lysed either on ice or at room

temperature for 30 min in 20 mM Tris, pH 7.4, 100 mM NaCl, 1% TX-100 (with or without 0.4% SDS). Lysates were scraped from dishes, sheared through a 26-g needle and layered on top of a discontinuous sucrose gradient (30-5%) in the same buffer of the lysis containing 0.1% TX-100. After centrifugation at 45,000 rpm for 16 h in a Beckman SW 50 ultracentrifuge, fractions of 500 μl were harvested from the top of the gradient. Proteins from each fraction were TCA-precipitated or immunoprecipitated using specific antibodies depending on the experiment, run on SDS-PAGE and revealed by western blotting using specific antibodies. The lysis buffer does not contain SDS in the case of FR because SDS disrupts the antigenicity of the specific MOV-19 antibody. In the other two cases the results was unchanged (Paladino et al., 2004).

4.9 Pulse-chase

Cells grown in 100 mm dishes were starved of methionine and cysteine for 1 hour, and pulse labelled for 10 min with medium containing 100 μCi/ml of Pro-mix-[^{35}S] cell labelling (GE Healthcare) and incubated in chase medium (DMEM containing 5% FBS and met/cys 10x) for different times.

4.10 Endo H digestion

Digestion with Endo H was carried out on immunoprecipitated materials. The antigen-antibody complexes were removed from sepharose beads using 50 μl of 0.1 M Na citrate/0.1% SDS and boiling for 3 min. Samples were then incubated with 5 mU of Endo H for 16 hours at 37°C. Samples were run on SDS-PAGE and revealed by fluorography.

4.11 Cross-linking

Bis(sulfosuccinimidyl)suberate (BS$_3$) (0.5 mM) was added to the cells grown on dishes for different incubation times depending on the experiment and quenched for 15 min with 20 mM Tris pH 7.5, as described elsewhere (Friedrichson and Kurzchalia, 1998). Proteins were TCA-precipitated or immunoprecipitated with specific antibodies, separated on SDS-PAGE and revealed by western blot using specific antibodies.

4.12 Cholesterol depletion assays

To deplete the cells of cholesterol we used two different treatments: βCD (10 mM) or saponin (0.2%). In both cases, cells were grown to confluence on dishes or on coverslips for 3 d. βCD was added to the cells in medium containing 20 mM Hepes pH 7.5 and 0.2% bovine albumin for 1 h at 37°C (Keller and Simons, 1998; Lipardi et al., 2000). Alternatively, cells were incubated 30 min on

ice with saponin in medium containing 150 mM NaCl, 5 mM KCl, 1 mM $CaCl_2$, 1 mM $MgCl_2$, 20 mM Hepes pH 7.4 as previously described (Mayor and Maxfield, 1995).

To determine the rate of cholesterol depletion we measured cholesterol cellular levels by a colorimetric assay. Cells were washed twice with PBS containing $CaCl_2$ and $MgCl_2$, lysed with appropriate lysis buffer and Infinity Cholesterol Reagent (Sigma Chemical Co.) was added to the lysates in the ratio 1:10. Absorbance of samples was read at 550 nm.

5. RESULTS

Protein apical sorting in polarized epithelial cells is mediated by two different mechanisms, raft-dependent and raft independent. It has been shown that GPI-APs are organized in micro-clusters at the cell surface. In MDCK cells an essential step for apical sorting of GPI-APs is their coalescence into high molecular weight oligomers (Paladino et al. 2004). We showed that this mechanism is also functional in FRT cells, which possess a different sorting phenotype compared with MDCK cells. We demonstrated that, as in MDCK cells, both apical and basolateral GPI-APs associate with DRMs, but only the apical proteins are able to oligomerize into high molecular weight complexes during their passage through the medial Golgi.

The lipid species co-immunoprecipitating with an apical and a basolateral GPI-APs, from their associated DRMs contain the same lipid species although in different ratios and this specific ratio is maintained after mixing the cells before the lysis indicating that they maintain their identity after Triton extraction.

We also showed that oligomerization is a specific requirement for apical sorting of GPI-APs and is not used by transmembrane, non-raft associated apical proteins.

Furthermore in polarized epithelial cells GPI-APs travel to the apical surface in high molecular weight complexes in cholesterol-independent homo-clusters, which can fuse with each other into cholesterol-dependent hetero-clusters. We also showed that GPI-AP monomers cannot be cross-linked in hetero-clusters and that homo-oligomerization of GPI-APs leads to subsequent hetero-clustering.

I have divided the results of my thesis in three parts, which correspond to the three main questions that I have studied during my PhD. These are:

1) The study of oligomerization as specific requirement for apical sorting of GPI-APs in polarized epithelial cells.

2) The analysis of lipid composition of DRMs, which are associated with apical and basolateral GPI-APs.

3) The study of the organization of GPI-APs at the apical plasma membrane in polarized epithelial cells.

The papers corresponding to these result sections are added at the end of the thesis as Annex 1, Annex 2 and ANNEX 3.

5.1 OLIGOMERIZATION IS A SPECIFIC REQUIREMENT FOR APICAL SORTING OF GPI-APs BUT NOT FOR NON-RAFT ASSOCIATED APICAL PROTEINS

Both apical and basolateral GPI-APs associate with DRMs in FRT cells

In contrast to MDCK cells, FRT cells sort the majority of endogenous and transfected GPI-APs to the basolateral domain of the plasma membrane (Zurzolo *et al.*, 1993; Lipardi *et al.*, 2000). To understand if oligomerization is a general mechanism to promote apical sorting of GPI-APs in different epithelia, we studied the sorting of four different GPI-APs transfected in FRT cells: PLAP, a native GPI-AP, NTR-PLAP, in which the ectodomain of neurotrophin receptor p75 NTR is fused to the GPI-attachment signal of PLAP (Lipardi *et al.*, 2000), GFP-GPI and GH-DAF, two fusion proteins in which the green fluorescent protein (GFP) and the rat growth hormone (GH) are respectively fused to the GPI attachment signal of the folate receptor and the decay accelerating factor (DAF) (Paladino *et al.*, 2004).
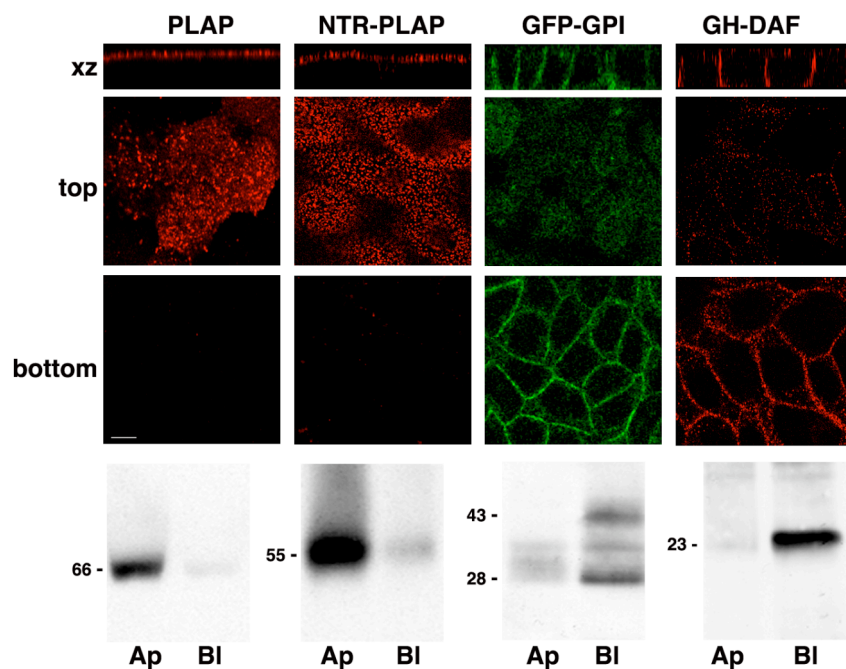

Figure 7. GPI-APs are apically and basolaterally sorted.
FRT cells stably expressing PLAP, NTR-PLAP, GFP-GPI and GH-DAF were grown on filters for 4 days. Cells were fixed and in the case of PLAP, NTR-PLAP and GH-DAF stained with specific antibodies followed by a TRITC-conjugated secondary antibody in non-permeabilized conditions. Serial confocal sections were collected from the top to the bottom of cell monolayers. Bar, 10 μm (upper panels).
Alternatively, cells were labelled with LC-biotin respectively added to the apical (Ap) or the basolateral (Bl) surface. After immunoprecipitation with specific antibodies samples were run on SDS-PAGE and biotinylated proteins revealed using HRP-streptavidin. In the case of NTR-PLAP, samples, labelled with [^{35}S]-cys overnight as described in materials and methods, after immunoprecipitation were precipitated with streptavidin beads, run on SDS-PAGE and analysed by fluorography. The band of GFP-GPI at 43 kDa represents a partially denatured GFP dimer as previously described in MDCK cells (Paladino *et al.*, 2004) (lower panels).

We confirmed by confocal microscopy (Figure 7 upper panels) that PLAP and NTR-PLAP were predominantly enriched on the apical surface, as previously shown in both FRT and MDCK cells (Lipardi *et al.*, 2000; Paladino *et al.*, 2006). On the contrary, we found that GFP-GPI and GH-DAF were predominantly localized on the basolateral membrane. Quantization by domain-selective biotinylation showed that 85% and 90%, respectively, of PLAP and NTR-PLAP was enriched on the apical membrane, while ~ 80% and 90%, respectively, of GFP-GPI and GH-DAF was basolaterally distributed (Figure 7 lower panels), thus indicating that all proteins are fully polarized respectively on the apical or basolateral cell surface.

Because in MDCK cells both apical and basolateral GPI-APs are associated with DRMs (Paladino *et al.*, 2004) we analysed DRM-association of apical and basolateral GPI-APs in FRT cells by cold Triton X-100 (TX-100) extraction and centrifugation to equilibrium on sucrose density gradients, as previously described (Brown and Rose, 1992; Zurzolo *et al.*, 1994; Paladino *et al.*, 2004). We found that both apical and basolateral proteins floated to the lighter fractions (4-7) of sucrose gradients, fractions which are also enriched in the ganglioside GM1 (Figure 8). It is interesting to note that higher amounts of apical GPI-APs were found in DRMs compared with the basolateral proteins. Indeed, averages from three independent experiments (see graph in Figure 8) showed that ~ 55-60% of apical GPI-APs are in DRMs, in contrast to only ~ 30-40% for the basolateral proteins, indicating that**,** like in MDCK cells, apical and basolateral GPI-APs have different behaviours with respect to detergent extraction (Paladino *et al.*, 2004). In addition, as in MDCK cells, (Paladino *et al.*, 2004) in the majority of the experiments there was a shift of one fraction between the floatation of apical and basolateral GPI-APs indicating that the composition of the associated DRMs could be different.
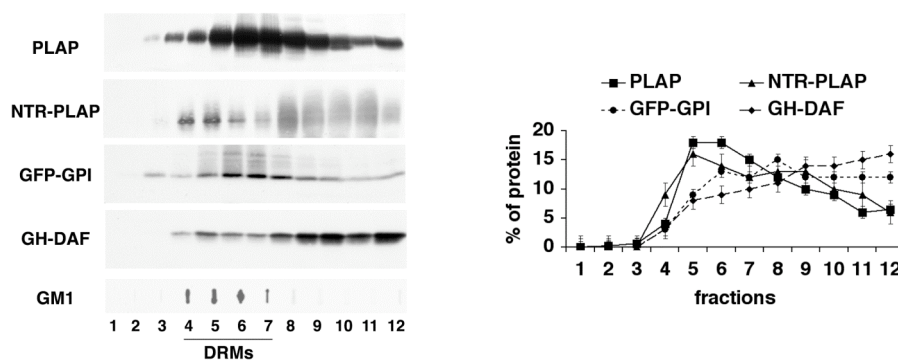

Figure 8. Both apical and basolateral GPI-APs associate with DRMs.
FRT cells stably expressing PLAP, NTR-PLAP, GFP-GPI and GH-DAF were lysed in TNE/TX-100 buffer at 4°C and run through 5-40% sucrose gradients. Fractions of 1 ml were collected from top (fraction 1) to bottom (fraction 12) after centrifugation to equilibrium. After TCA-precipitation samples were run on SDS-PAGE and detected by specific antibodies. An aliquot of each fraction was spotted on the nitrocellulose membrane and GM1 was revealed using cholera toxin conjugated to HRP. The graph shows the mean value of protein distribution on sucrose density gradients from three different experiments.

Only apical GPI-APs form HMW complexes and are found in cross-linkable complexes at the cell surface

Because in MDCK cells oligomerization appears to be a key step for apical sorting of GPI-APs (Paladino *et al.*, 2004), to test whether this could be a general mechanism for different epithelia, we purified apical and basolateral GPI-proteins from FRT cells on sucrose velocity gradients in which a protein sediments according to its molecular weight (Paladino *et al.*, 2004). As in MDCK cells (Paladino *et al.*, 2004) only apical GPI-APs oligomerize in FRT cells. Indeed while a portion of PLAP and NTR-PLAP migrated as HMW complexes containing more than a trimer, basolaterally sorted GFP-GPI and GH-DAF were purified almost exclusively from the gradient fractions corresponding to their expected monomeric molecular weights (Figure 9A).
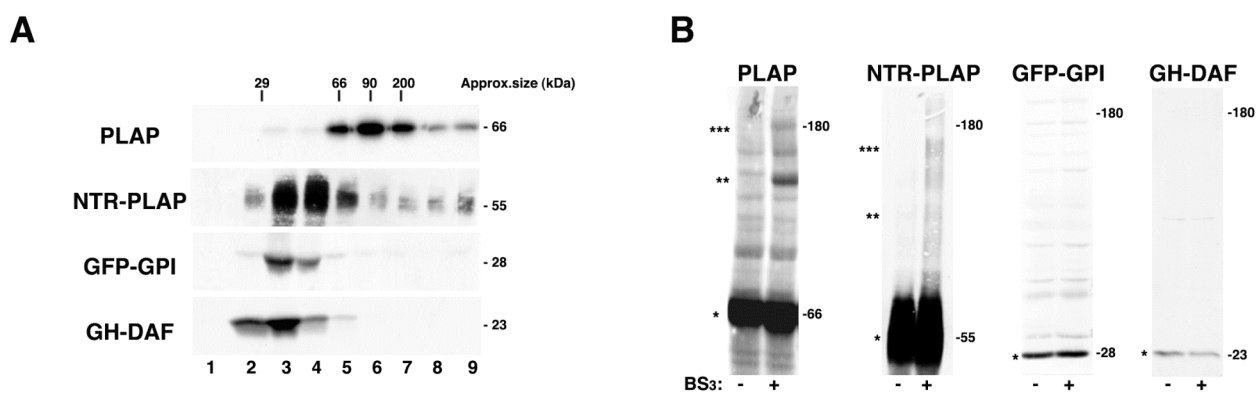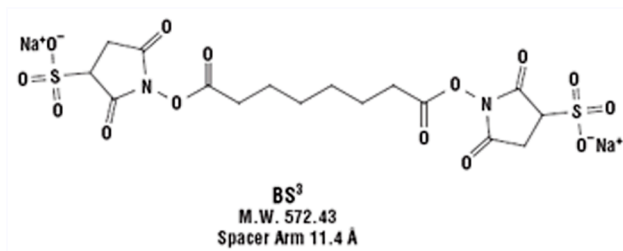

Figure 9. Only apical GPI-APs form oligomers and are in cross-linkable complexes at the cell surface.
FRT cells stably expressing PLAP, NTR-PLAP, GFP-GPI and GH-DAF were lysed in buffer containing 0.4% SDS and 0.2% TX-100 and run through a non-linear 5-30% sucrose gradient. Fractions of 500 μl were collected from the top (fraction 1) to the bottom (fraction 9) of the gradients. Proteins were TCA-precipitated and detected by western blotting using specific antibodies. In the case of PLAP, samples, labelled with Pro-mix-[^{35}S] overnight, were immunoprecipitated from each fraction, run on SDS-PAGE and revealed by fluorography. The molecular weight of the monomeric forms of each protein is indicated. The position on the gradients of molecular weight markers is indicated on top of the panel (A).
FRT cells stably expressing PLAP, NTR-PLAP, GFP-GPI and GH-DAF grown on filters were incubated with BS$_3$ (0,5 mM). After lysis, proteins were TCA-precipitated, run on SDS-PAGE (in a 6-12% gradient gel for GFP-GPI and GH-DAF or 8% gel for PLAP and NTR-PLAP). The molecular weight of the monomeric forms (*) of each protein is indicated, together with the position of a 180 kDa marker. (**) and (***) indicate respectively the expected molecular weight of the dimeric and trimeric forms of each protein (B).

To rule out the possibility that HMW complexes were formed as a consequence of detergent addition, we applied an impermeable cross-linking agent, bis(sulphosuccinimidyl)suberate (BS$_3$) (Figure 10), that is able to link molecules that are in very close proximity (arm length 11.4 Å) (Friedrichson and Kurzchalia, 1998; Paladino *et al.*, 2004), to the apical and basolateral surface of unperturbed FRT cells grown on filters.

BS₃ is a homobifunctional, water-soluble, non-cleavable and membrane impermeable crosslinker. It contains an amine-reactive N-hydroxysulfosuccinimide (NHS) ester at each end of an 8-carbon spacer arm. NHS esters react with primary amines at pH 7-9 to form stable amide bonds. BS₃ is used to determine near-neighbour relationships analyze protein structure and provide information on the distance between interacting molecules.

Figure 10. The structure of BS₃.

In the presence of BS₃, bands corresponding to dimers, trimers and higher molecular weights were detected only for PLAP and NTR-PLAP (Figure 9B). In contrast, neither GFP-GPI nor GH-DAF were found in cross-linkable complexes at the basolateral surface (Figure 9B), thus suggesting that only apical GPI-APs are in HMW complexes at the cell surface.

Oligomer formation occurs during passage of the protein through the Golgi

If oligomerization plays a role in apical sorting in FRT cells, as is the case in MDCK cells (Paladino *et al.*, 2004), we would expect this event to occur during sorting of the proteins. To address this question, we analysed the kinetics of PLAP oligomerization by pulse-chase experiments combined with endoglycosidase H (Endo H) digestion (Figure 11).
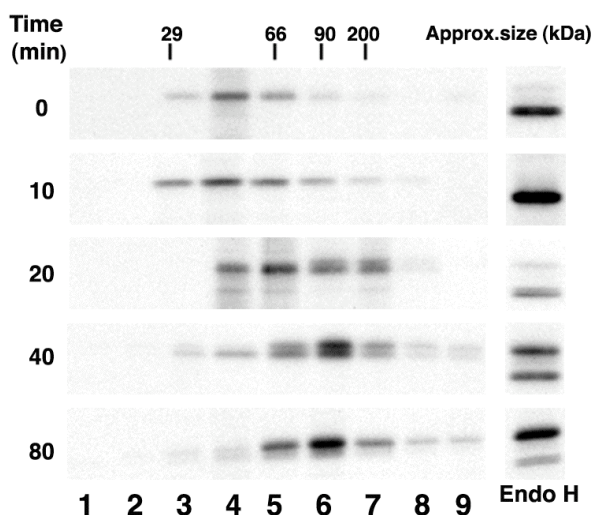
**Figure 11**. **HMW complex formation occurs during passage through the Golgi apparatus.**
FRT cells expressing PLAP were pulsed for 10 min with Pro-mix-[³⁵S] and then chased for the indicated times. At the end of each chase time the cells were lysed and purified on velocity gradients. Samples were immunoprecipitated from each fraction, run on SDS-PAGE and revealed by fluorography. An aliquot of the lysate for each chase time was immunoprecipitated (before ultracentrifugation) and treated with Endo H to monitor passage through the medial Golgi.

The acquisition of resistance to Endo H allowed us to monitor the passage of the protein through the Golgi apparatus (Dunphy and Rothman, 1985; Kornfeld and Kornfeld, 1985). After a brief pulse of 10 min with [³⁵S]-met/cys, cells were chased for the indicated times, lysed in SDS/TX-100 containing buffer and run on velocity gradients (Figure 11). PLAP began to form HMW complexes after 20 min of chase when a portion of the protein had acquired Endo H

resistance (therefore after the medial Golgi). After 40 min of chase, when almost all PLAP was Endo H resistant, ~ 30% of the protein was found in HMW complexes (Figure 11). Consistent with the cross-linking experiments (Figure 10B), PLAP was then recovered in HMW complexes also after 80 min of chase, i.e., when the majority of the protein had already reached the plasma membrane [as previously shown by targeting experiments (Lipardi et al., 2000)]. These results demonstrate that also in FRT cells apical GPI-APs oligomerize during their passage through the Golgi apparatus, where sorting is likely to occur (Wandinger-Ness et al., 1990; Rodriguez-Boulan and Powell, 1992; Mostov et al., 2000; Keller et al., 2001; Hua et al., 2006; Paladino et al., 2006).

Only the GPI-anchored but not the transmembrane or secretory forms of NTR are able to oligomerize

A question that we then addressed is whether protein oligomerization is a specific mechanism for apical sorting of raft-associated GPI-APs or is a general mechanism utilized also for non raft-associated apical proteins. To this aim we compared the behaviour of the GPI-anchored form of NTR (NTR-PLAP) with the transmembrane (TM) (p75 NTR) and secretory (NTR-sec) forms, which are both apically sorted but are not associated with DRMs (Lipardi et al., 2000). Differently to NTR-PLAP we found that neither the native TM form nor its secretory form were able to oligomerize (Figure 12). These results indicate that oligomerization is a specific requirement for apical sorting of GPI-APs associated to DRMs, and that this mechanism is not used by TM or secretory non-raft associated proteins.
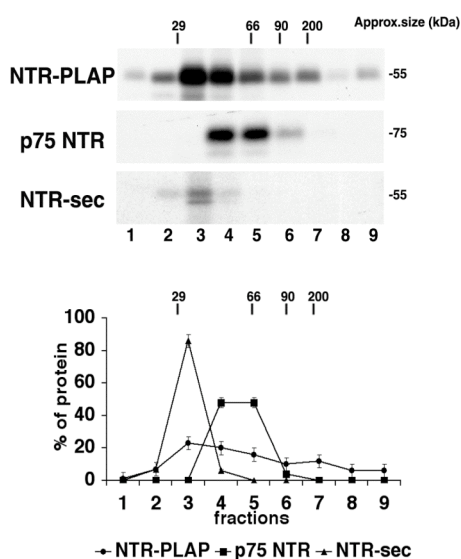
Figure 12. NTR-PLAP, but not its transmembrane or secretory forms oligomerizes in HMW complexes. FRT cells stably expressing NTR-PLAP, p75 NTR and NTR-sec were pulsed overnight with [^{35}S]-cys (250 μCi/ml). Then cells were lysed in buffer containing 0.4% SDS and 0.2% TX-100 and run through a non-linear 5-30% sucrose gradient. Fractions of 500 μl were collected from the top (fraction 1) to the bottom (fraction 9) of the gradients. Proteins were immunoprecipitated with an antibody against the ectodomain of p75 NTR, run on SDS-PAGE and revealed by fluorography. The molecular weight of the monomeric forms of each protein is indicated. The position on the gradients of molecular weight markers is indicated on top of the panel. The graph shows the mean value of protein distribution on sucrose density gradients from three different experiments.

5.2 LIPID COMPOSITION ANALYSIS OF DRMs ASSOCIATED WITH DIFFERENT GPI-APs

Analysis of DRM association of PLAP and GH-DAF in FRT cells.

In order to study the lipid composition of the apical and basolateral DRMs (Brown and Rose, 1992; Paladino *et al.*, 2004) we used as model proteins PLAP and GH-DAF which are sorted on apical and basolateral surface respectively in FRT cells (Figure 7 upper panels). As aforementioned PLAP and GH-DAF associated with detergent-resistant membranes (DRMs) and indeed at steady state both proteins (respectively ~ 80% of total PLAP and ~ 61% of total GH-DAF) were insoluble in TX-100 (Figure 13A).

In this case we decided to use a two step sucrose gradient instead of multistep gradient in order to concentrate DRMs in one fraction. Indeed after centrifugation to equilibrium on sucrose density gradients both proteins peaked in fraction 5 at the interface between 5% and 30% sucrose which is the most representative fraction of DRMs as previously described (Prinetti et al., 2000) (Figure 13B). In contrast to the majority of the proteins in the cell lysates that accumulated in the soluble fractions (8-11) (data not shown) about 63% of PLAP and 68% of GH-DAF were enriched in fractions 4 to 6 (Figure 13B), thus indicating that DRMs are likely to be present at both the apical and basolateral membranes.
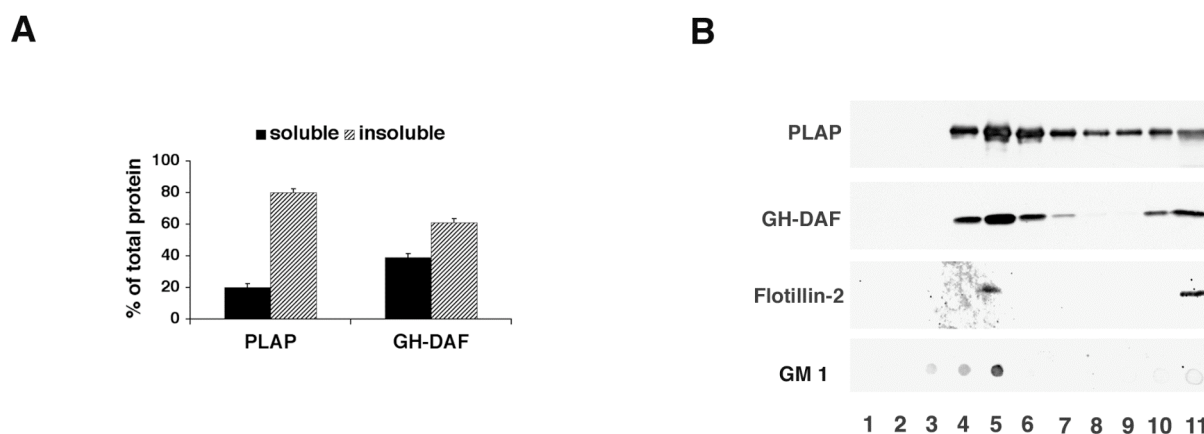
Figure 13. Both PLAP and GH-DAF associate with DRMs.
PLAP or GH-DAF clones were lysed in TNE/TX-100 buffer at 4°C and separated by centrifugation into insoluble and soluble fractions. Percentages of insoluble and soluble proteins in TX-100 from three experiments are shown. Errors bars are indicated (A).
Eleven 1 ml fractions were collected from top (1) to bottom (11) from sucrose density gradients. Proteins were analyzed by SDS-PAGE and detected by western blotting using specific anti-PLAP and anti-GH antibodies (B).

Analysis of the lipid composition of DRMs in PLAP or GH-DAF expressing FRT cells.

In order to understand whether the DRM composition was affected by the exogenous expression of apical or basolateral GPI-APs, we analyzed the lipid composition of the DRM fraction in FRT cells expressing either PLAP or GH-DAF. Cells were labelled with $[1\text{-}^3\text{H}]$ sphingosine, which is converted into more complex sphingolipids, while the catabolic tritiated ethanolamine fragment is recycled for the biosynthesis of phosphatidylethanolamine (PE), a glycerophospholipid that is a marker of non-DRM fractions (Prinetti *et al.*, 2000; Prinetti *et al.*, 2001). The radioactive lipid pattern was determined by HPTLC and radioimaging of the 11 fractions collected from sucrose density gradient centrifugation (Figure 14A). Sphingolipids (SL) were highly enriched in fraction 5 (Figure 14B), while the majority of PE was found, as expected, in the soluble fractions of the sucrose density gradients in both the cell lines (Figure 14B) as well as in wild type cells.

Phosphatidylcholine (PC) analysed by HPTLC and a colorimetric assay was also quite enriched in fraction 5 from both clones (Figure 14C), as previously described (Prinetti *et al.*, 2000; Prinetti *et al.*, 2001). Finally ~ 42 nmol/mg protein of cholesterol was found in the post-nuclear supernatants and about 50% of it was associated with fraction 5 in both FRT clones (Figure 14D). Thus these data show that the lipid distribution along sucrose density gradients is similar in both clones (Figure 14) as in wild type cells and is not affected by protein expression.
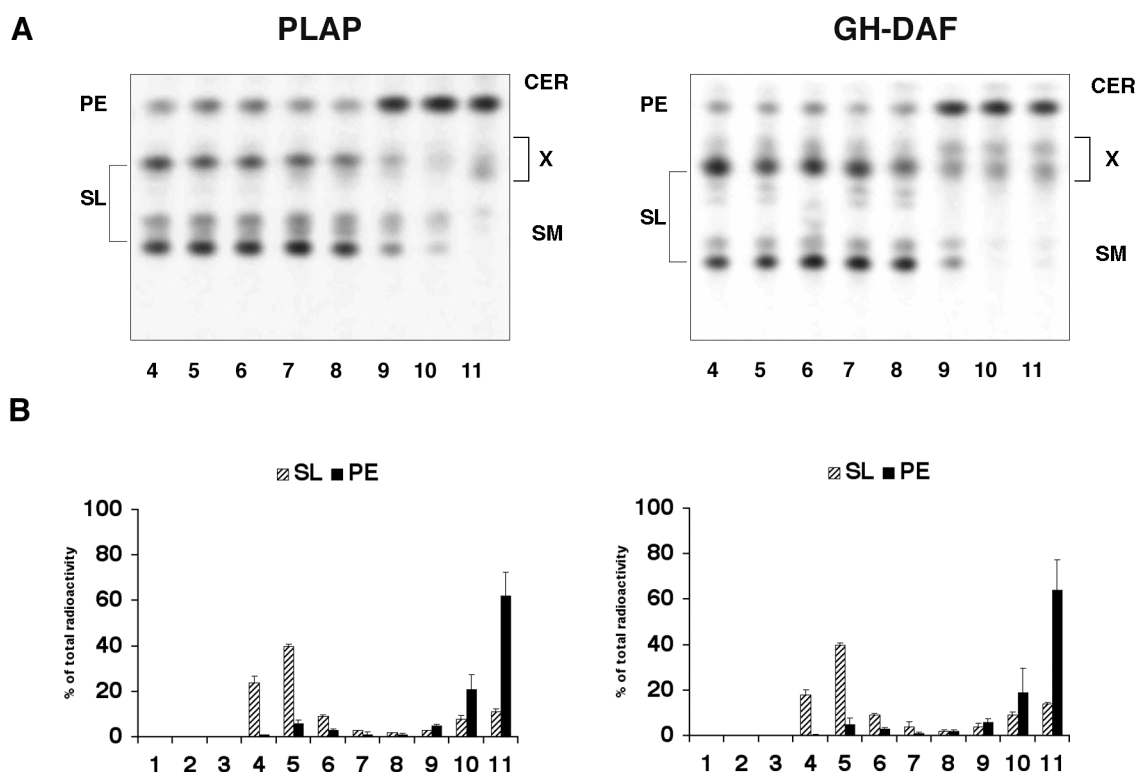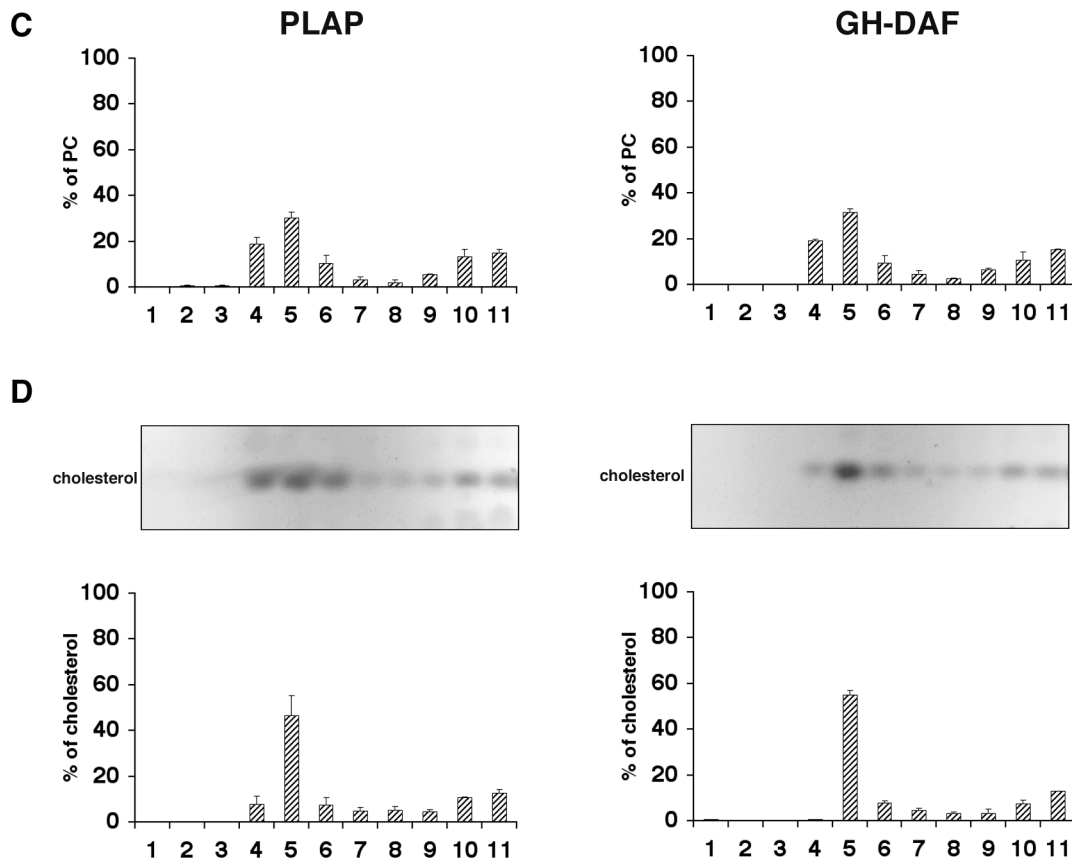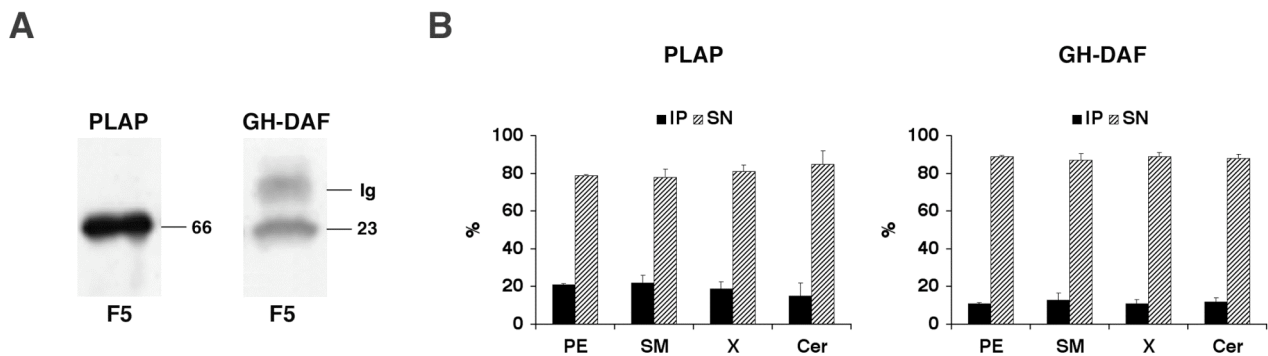
Figure 14. Lipid distribution on sucrose density gradients.
PLAP or GH-DAF clones were labelled with [³H]-sphingosine, lysed in TNE/TX-100 at 4°C and run on sucrose density gradients. Lipids from each of the 11 fractions were extracted in chloroform/methanol and separated by HPTLC. Radioactive lipids were detected by autoradiography (A). Quantitation of sphingolipid and PE radioactivity distribution within the gradient fractions. Data are expressed as % of total radioactivity associated with each lipid present in homogenate (B).
The distribution of PC and cholesterol, measured by colorimetric assays, are respectively shown in C and D. Data are expressed as % of each lipid present in homogenate. Data are the means of three different experiments ± standard deviation.

Lipid analysis of DRM fractions associated with PLAP or GH-DAF.

To analyze whether apical and basolateral GPI-APs associated to similar DRMs we specifically immunoprecipitated each protein from fraction 5 of the gradients after [³H] sphingosine-labelling (Figure 15A). About 19% and 11%, respectively, of the total radioactivity present in fraction 5 was recovered respectively in the PLAP or GH-DAF immunoprecipitates, representing co-immunoprecipitated labelled sphingolipids (Table 1). After chloroform/methanol 2:1 (v/v) extraction, HPTLC and digital autoradiography ~ 22% of SM, ~ 15% of Cer and ~ 21% of PE were associated with PLAP immunoprecipitates while ~ 13% of SM, ~ 12% of Cer and ~ 11% of PE were found in the GH-DAF immunoprecipitates (Figure 15B).

Figure 15. Lipid analysis of DRMs associated with PLAP or GH-DAF.
PLAP or GH-DAF clones were labelled with [^{3}H]-sphingosine, lysed in TNE/TX-100 at 4°C and purified by centrifugation to equilibrium on sucrose density gradients. Fraction 5 was immunoprecipitated using either PLAP or GH-DAF antibodies. Proteins (1/5 of immunoprecipitate) were run on SDS-PAGE and revealed by western blotting (A). Lipids associated with immunoprecipitates (IP) were extracted in chloroform/methanol and separated by HPTLC. The quantitation of radioactive lipids (SM, Cer, X, PE) is shown in B. We have indicated with X the unknown species of sphingolipids labelled with [^{3}H]-sphingosine. For each lipid species values are expressed as percent of radioactivity present in immunoprecipitates and in the supernatant (B). Data are the means of three different experiments ± standard deviation.

The relative percentage of each type of labelled lipid in PLAP and GH immunoprecipitates of fraction 5 was very similar (Table 2). The total lipid extracts of the immunoprecipitates were then analysed for cholesterol (~ 24.5 nmols for PLAP and ~ 16.6 nmols for GH-DAF) (Table 3) and for PC (~ 19% for PLAP and ~ 6% for GH-DAF) (Table 4). The ratio between [^{3}H]-SM:cholesterol:PC was 2663:2.24:1 (dpm:nmols:nmols) for PLAP and 4346:4.48:1 (dpm:nmols:nmols) for GH-DAF indicating that there were no significant qualitative differences in the lipid composition of DRMs associated with the apical or basolateral GPI-AP. However the calculation of the relative lipid enrichment (SL or cholesterol over PC) clearly shows that DRMs associated with basolateral GH-DAF contain double the amounts of SL and cholesterol with respect to apical PLAP (Table 5).

Effect of TX-100 on DRM formation.
To rule out the possibility that TX-100 had an effect in mixing apical and basolateral DRMs we performed TX-100 extraction and separation on sucrose density gradients after mixing the two cell lines previously labelled with [^{3}H]-sphingosine. As shown in Figure 16 the distribution of proteins (Figure 16A), radioactive lipids (Figure 16B), PC (Figure 16C) and cholesterol (Figure 16D) after separation of the mixed lysates on sucrose density gradients was similar to that from gradients derived from the single cell line extracts (compare Figure 16 with Figure 14).
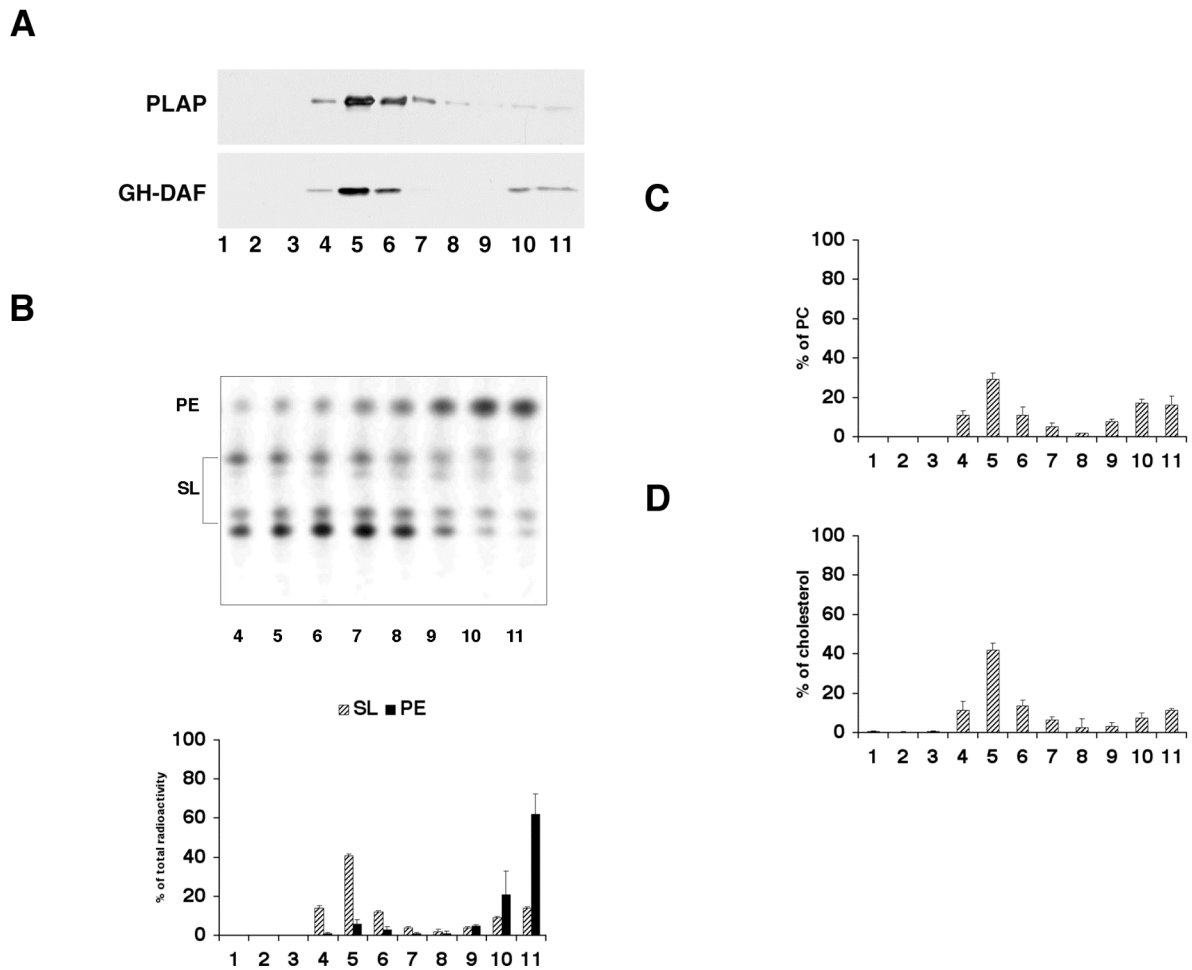
Figure 16. Protein and lipid distribution on sucrose density gradients from mixed lysates of cells expressing PLAP and GH-DAF.
PLAP and GH-DAF clones (plated in the same number) were labelled with [^{3}H]-sphingosine, harvested, mixed together and lysed in TNE/TX-100 buffer at 4°C. TX-100 extracts were purified by centrifugation to equilibrium on sucrose density gradients. Proteins were run on SDS-PAGE and PLAP and GH-DAF were detected by western blotting (A).
Lipids were extracted and detected as described in Figure 15. The distribution of sphingosine-labelled species on sucrose density gradients and their quantitation are shown in B (upper and lower panel, respectively). PC and cholesterol distributions are shown in C and D, respectively. Data are expressed as % of each lipid present in the homogenate. Data are the means of two different experiments ± standard deviation.

Fraction 5 was then immunoprecipitated using either anti-PLAP or anti-GH antibodies and proteins were analyzed by SDS-PAGE and western blotting (Figure 17A). In these mixed lysates GH-DAF was not co-immunoprecipitated with the anti-PLAP antibody and vice-versa (Figure 17A), therefore suggesting that the two proteins resided in different environments.

44

A

IP: α-PLAP   α-PLAP   α-GH   α-GH
WB: α-PLAP   α-GH   α-GH   α-PLAP

—66   —66   —66   —66
—Ig   —Ig
                       —Ig
—23   —23   —23   —23

F5   F5   F5   F5

B

IP: α-PLAP   IP: α-GH-DAF

■IP ⊠SN   ■IP ⊠SN

PE SM X Cer   PE SM X Cer
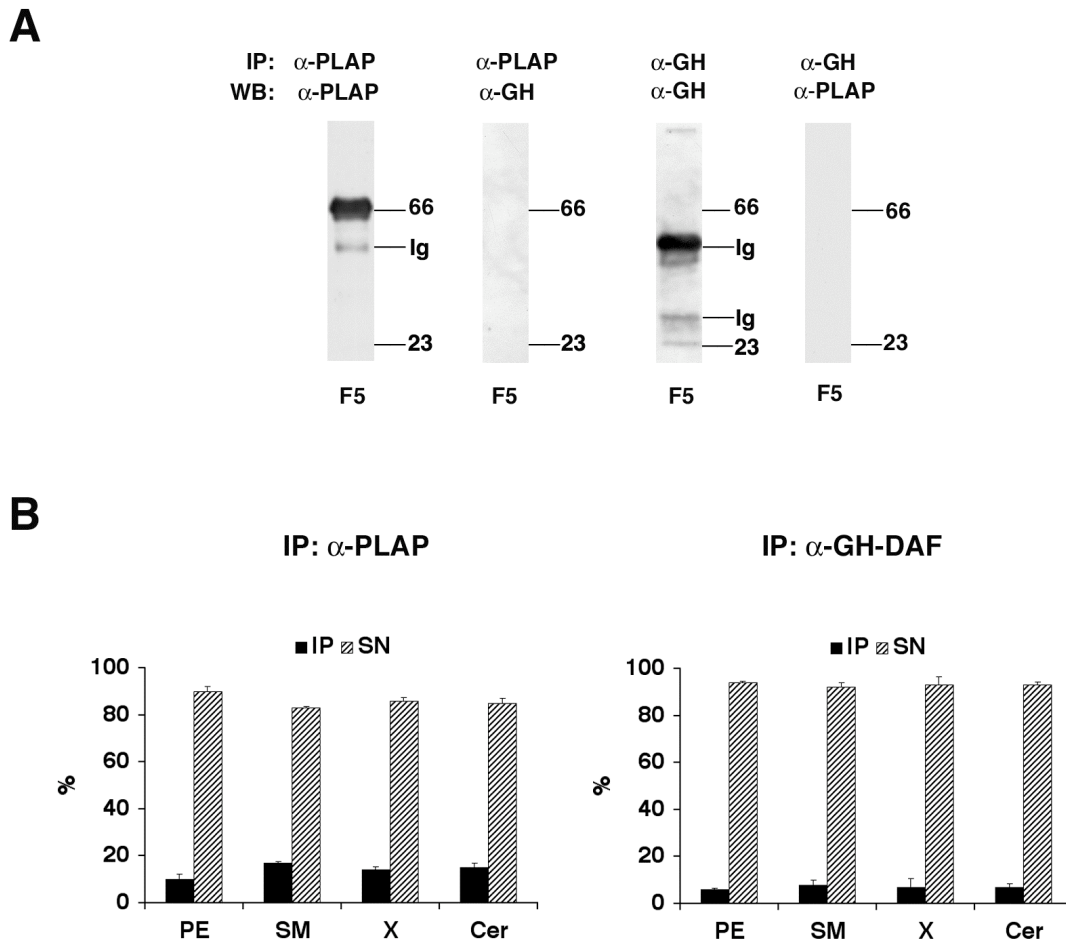
Figure 17. Lipid analysis of DRMs associated with PLAP- or GH-DAF-associated DRMs derived from mixed cell lysates.
FRT cells expressing PLAP and GH-DAF were labelled with [^{3}H]-sphingosine, harvested, mixed together and lysed in TNE/TX-100 buffer at 4°C. TX-100 extracts were purified by centrifugation to equilibrium on the sucrose gradients. Fraction 5 was immunoprecipitated using antibodies against PLAP or GH-DAF. Proteins (1/5 of immunoprecipitate) were run on SDS-PAGE and revealed by western blotting using specific anti-PLAP or anti-GH antibodies (A).
Lipids were extracted and detected as described in Figure 14. The distribution of radioactive lipids (SM, Cer, X, PE) is shown. For each lipid species values are expressed as percents of radioactivity present in immunoprecipitates and in the supernatants (B).

As expected about half of the total lipid radioactivity was recovered in the mixed compared to the single lysate immunoprecipates (~ 13% for PLAP and ~ 7% or GH-DAF) (Table 2). As shown in Figure 17B ~ 17% of SM, ~ 15% of Cer and ~ 10% of PE was associated with PLAP immunoprecipitates while ~ 8% (SM), ~ 7% (Cer) and ~ 5% (PE) were recovered in the GH immunoprecipitates. Thus the relative percentage of each type of radiolabelled lipid immunoprecipitated either with anti-PLAP or anti-GH remained constant between single and mixed lysates (Table 3). Interestingly we observed a higher cholesterol recovery, both in PLAP (~ 20 nmols) and GH (~ 11 nmols) immunoprecipitates, from the mixed lysates (Table 4). Like for SL the

amount of PC recovered in the immunoprecipitates of fraction 5 from the mixed lysates was about half of the amount in the single lysates (Table 5). The ratio [^{3}H]-SM:cholesterol:PC, in the immunoprecipitates was respectively 3700:4.05:1 (dpm:nmols:nmols) for PLAP, and 5335:6.5:1 (dpm:nmols:nmols) for GF-DAF, similar to the ratio found in the immunoprecipitates from single cell lysates (Table 6). These results confirmed that the composition of DRMs associated with an apical and a basolateral GPI-AP are qualitatively very similar and showed that the relative enrichment of the different lipid species was maintained in the mixed lysates compared to single lysate (Table 6).

Table 2. Distribution of radioactivity after immunoprecipitation with anti-PLAP or anti-GH antibodies in sphingolipid-enriched membrane fractions from FRT cells in culture.

Cell lipids were previously metabolically labelled with [^{3}H]-sphingosine. Data are expressed in dpm. Percentages represent values of three independent experiments ± standard deviations.

	Total	IP	% in IP	Preclear	Supernatant
FRT cells expressing PLAP (IP αPLAP)	243100	46100	19 ± 0.6	19500	177500
FRT cells expressing GH-DAF (IP αGH)	257500	28200	11 ± 1.5	22000	207300
Mixed cells (IP αPLAP)	257000	34900	13 ± 1	16100	205700
Mixed cells (IP αGH)	257000	17100	7 ± 0.7	22400	217500

Table 3. Percent of spingosine-labelled lipid species in the anti-PLAP or anti-GH immunoprecipitates of fraction 5. Percentages represent values of three independent experiments ± standard deviations.

	PE	SM	X	Cer
FRT cells expressing PLAP (IP αPLAP)	22 ± 1	63 ± 3.6	12 ± 3.2	3 ± 0.6
FRT cells expressing GH-DAF (IP αGH)	20 ± 2	64 ± 1.5	13 ± 3.2	3 ± 1
Mixed cells (IP αPLAP)	14 ± 2.3	62 ± 1	21 ± 3.2	3 ± 1
Mixed cells (IP αGH)	14 ± 2	63 ± 2.6	20 ± 2	3 ± 1

Table 4. Distribution of cholesterol after immunoprecipitation with anti-PLAP or anti-GH antibodies in sphingolipid-enriched membrane fractions from labelled FRT cells in culture. Data are expressed in nmoles. n.a., not analysed. Percentages represent values of three independent experiments ± standard deviations.

	Total	IP	% in IP	Preclear	Supernatant
FRT cells expressing PLAP (IP αPLAP)	164.0	24.5	15 ± 1	n.a	123.3
FRT cells expressing GH-DAF (IP αGH)	184,0	16.6	9 ± 2.5	n.a	151.1
Mixed cells (IP αPLAP)	168.0	20.7	12 ± 2	n.a	133.0
Mixed cells (IP αGH)	168.0	11.1	7 ± 1	n.a	142.5

Table 5. Distribution of phosphatidylcholine after immunoprecipitation with anti-PLAP or anti-GH antibodies in sphingolipid-enriched membrane fractions from labelled FRT cells in culture.

Data are expressed in nmoles. n.a., not analysed. Percentages represent values of two independent experiments ± standard deviations.

	Total	IP	% in IP	Preclear	Supernatant
FRT cells expressing PLAP (IP αPLAP)	57,6	10,9	19 ± 2	n.a.	41,7
FRT cells expressing GH-DAF (IP αGH)	62,0	3,7	6 ± 0.7	n.a.	53,3
Mixed cells (IP αPLAP)	57,8	5,1	9 ± 1.4	n.a.	47,8
Mixed cells (IP αGH)	57,8	1,7	3 ± 0.7	n.a.	48,9

Table 6. Relative enrichment of sphingolipids and cholesterol over phosphatidylcholine (PC) in the anti-PLAP or anti-GH immunoprecipitates.

	IP single cells	IP mixed cells
$\dfrac{(\text{Sphingolipids/PC})_{DAF}}{(\text{Sphingolipids/PC})_{PLAP}}$	1.8	1.6
$\dfrac{(\text{cholesterol/PC})_{DAF}}{(\text{cholesterol/PC})_{PLAP}}$	1.9	1.8

5.3 ORGANIZATION OF GPI-APs AT THE APICAL PLASMA MEMBRANE OF EPITHELIAL CELLS

Surface localization and DRM association of FR, PLAP and GFP-GPI

GPI-APs are localized principally on the apical domain of the plasma membrane of epithelial cells (Lisanti *et al.*, 1989) where they can be crosslinked in HMW complexes (Friedrichson and Kurzchalia, 1998; Paladino *et al.*, 2004). In order to understand whether two different apical GPI-APs are in the same clusters we co-transfected MDCK cells with two pairs of cDNAs encoding different GPI-APs. Specifically, GFP-GPI, in which GFP is fused to the GPI attachment signal from the folate receptor (FR) (Paladino *et al.*, 2004; Sharma *et al.*, 2004) was co-transfected with two different native GPI-APs (FR or PLAP), which contain distinct attachment signals. Several stable clones of MDCK cells expressing the two couples of GPI-APs, MDCK: FR/GFP-GPI and MDCK: PLAP/GFP-GPI, were selected and characterized for their protein expression and plasma membrane localization.
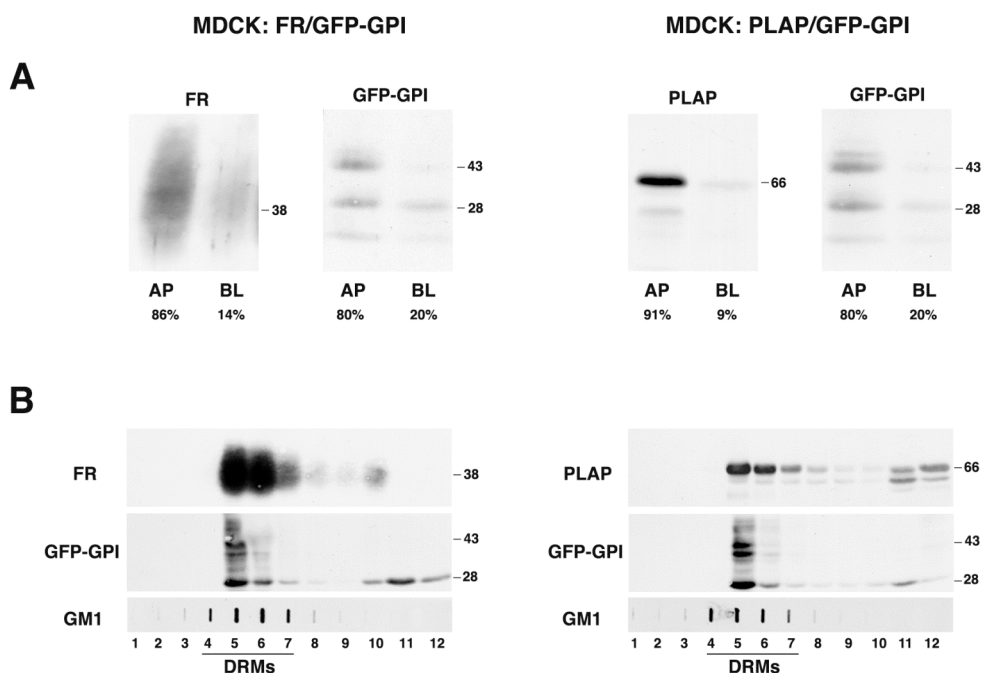
Figure 18. FR, PLAP and GFP-GPI are apically sorted and associate with DRMs in MDCK cells.
MDCK cells stably expressing FR/GFP-GPI or PLAP/GFP-GPI were grown for 4 d on filters. LC-biotin was added to the apical or the basolateral surface of the cells. After immunoprecipitation with specific antibodies, biotinylated proteins were revealed using HRP-streptavidin. Quantisation represents the mean value of three independent experiments (A). MDCK cells stably expressing FR/GFP-GPI or PLAP/GFP-GPI were lysed in buffer containing 1% TX-100 at 4°C and purified by centrifugation to equilibrium on sucrose gradients (5-40%) as described in materials and methods. Fractions of 1 ml were collected from the top (fraction 1) to the bottom (fraction 12). After TCA-precipitation, proteins were run on SDS-PAGE and detected using specific antibodies (B). An aliquot of each fraction was spotted on nitrocellulose membranes and GM1 was revealed using HRP-cholera toxin. As previously shown, the band at 43 kDa represents a partially denatured dimer of GFP (Inouye and Tsuji, 1994; Paladino *et al.*, 2004).

49

As expected from results derived from single transfected clones (Paladino *et al.*, 2004), we confirmed that GFP-GPI, PLAP and FR were all predominantly enriched on the apical surface (Figure 18A). In particular, ~ 85% and 90%, respectively, of FR and PLAP was found on the apical membrane, while ~ 80% of GFP-GPI was apically localized in both MDCK clones (Figure 18A). Interestingly each of the proteins maintained the same ratio of apical distribution in single or double transfected cells, independently of co-transfection with another GPI-AP (Figure 18A) (Paladino *et al.*, 2004).

We then analysed association to detergent-resistant membranes (DRMs) by floatation on sucrose density gradients after Triton X-100 (TX-100) extraction (Brown and Rose, 1992; Simons and Ikonen, 1997; Brown and London, 1998, 2000). Consistent with previous results (Miotti *et al.*, 2000; Paladino *et al.*, 2004), we found that all three proteins migrated to lighter density fractions (4-7) of the gradients (95%, 80% and 90%, respectively, for FR, PLAP and GFP-GPI), which were also enriched in the ganglioside GM1 (Figure 18B). These results confirmed that all three proteins associated with DRM fractions to a similar extent. Furthermore, the percentage of DRM-association on sucrose gradients was maintained constant independently of whether they were expressed alone or in pairs (Paladino *et al.*, 2004).

FR, PLAP and GFP-GPI are found in HMW homo-oligomers at the apical surface of MDCK cells

Apical GPI-APs are found in high molecular weight complexes and oligomerization appears to be a key step for their apical sorting (Paladino *et al.*, 2004). We therefore investigated whether FR, PLAP and GFP-GPI also oligomerize in the co-transfected MDCK clones. As in single transfected cells (Paladino *et al.*, 2004), in the co-transfected clones (MDCK: FR/GFP-GPI and MDCK: PLAP/GFP-GPI) FR, PLAP and GFP-GPI (about 20 - 40%) were found in oligomeric complexes after purification on velocity gradients at steady-state (Figure 19A).

To demonstrate that each protein was in HMW complexes also at the cell surface and to rule out the possibility that these complexes were formed as a consequence of detergent addition during cell lysis, we added the impermeable chemical cross linking agent, BS$_3$ to the apical surface of living cells for different times both at 4°C and 37°C.

In the presence of BS$_3$, bands corresponding to relative molecular masses of dimers (**) and trimers (***) as well as HMW oligomers were detected for each of the three proteins (Figure 19B), indicating that a relatively small portion of each protein was present in an oligomeric complex at the plasma membrane. Because the cross-linked pattern was similar at both temperatures, these data indicate that the proteins are in oligomeric complexes at physiological temperatures. In addition, the

amount of cross-linked complexes was higher at 37°C compared to 4°C, thus suggesting that at the lower temperature the formation of these complexes was drastically impaired, most likely because of the reduced mobility of the molecules involved.
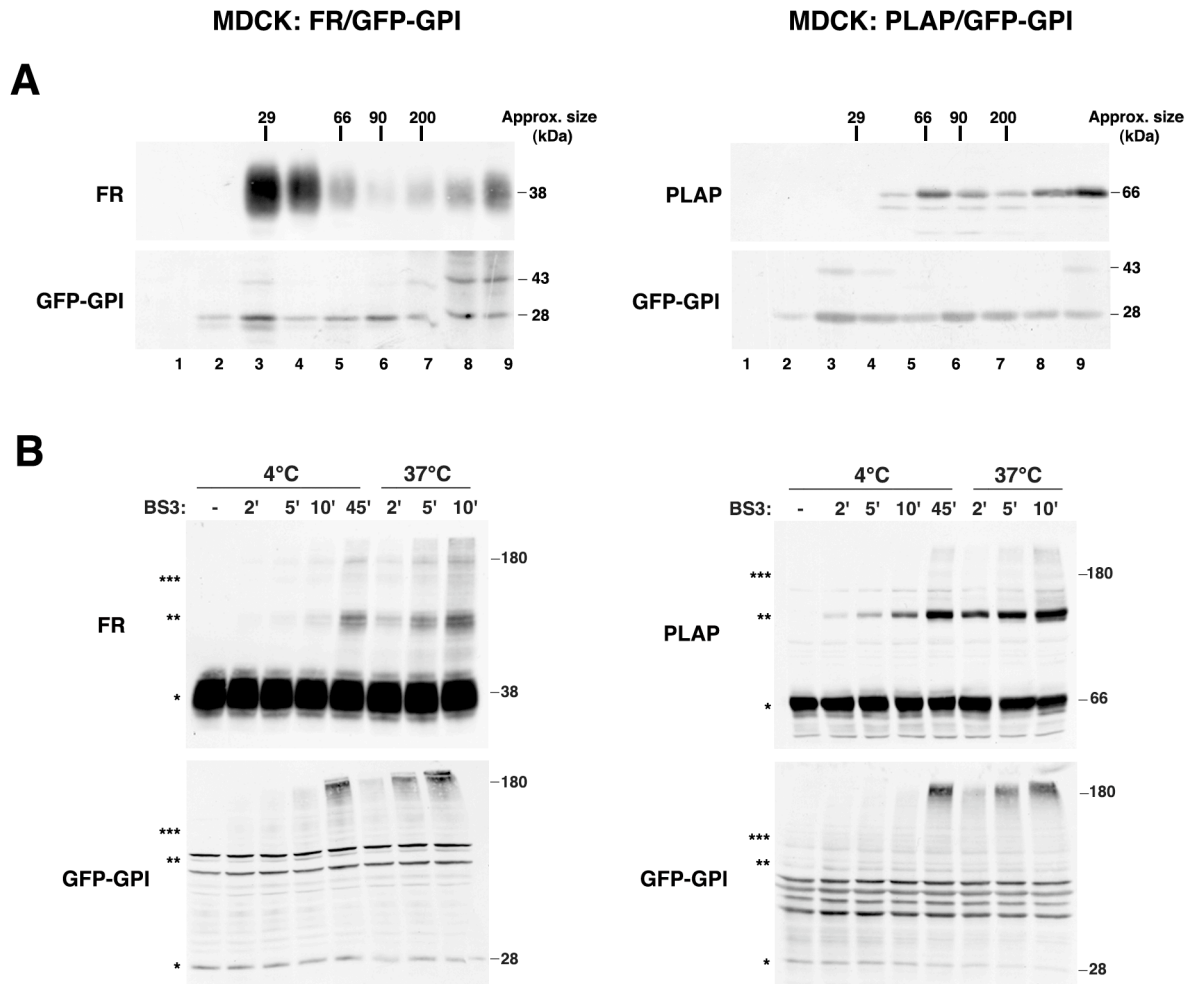

Figure 19. FR, PLAP and GFP-GPI form high molecular weight complexes in MDCK cells.
MDCK cells stably expressing FR/GFP-GPI or PLAP/GFP-GPI, grown to confluence, were purified by velocity gradient as described in materials and methods. Fractions of 0.5 ml were collected from the top (fraction 1) to the bottom (fraction 9). After TCA precipitation, samples were run on SDS-PAGE and revealed by western blotting with specific antibodies. The position on the gradients of molecular weight markers is indicated on top of the panels (A). Alternatively, cells were cross-linked by using BS_3 (0.5 mM) either at 4°C or 37°C for different indicated times. After lysis, proteins were TCA-precipitated, separated on SDS-PAGE and revealed using specific antibodies (B). The molecular weight of the monomeric forms of each protein is indicated, together with the position of a 180 kDa marker. *, **, and *** indicate, respectively, monomers, dimers and trimers of the different proteins.

GFP-GPI, FR, and PLAP oligomers can be cross-linked in hetero-clusters at the cell surface of MDCK cells

The above biochemical results indicated that each protein forms HMW homo-complexes independently of the other GPI-APs co-transfected with it. In order to understand how different GPI-APs are organized on the apical membrane within respect to each other we tested whether they could form hetero-HMW-complexes. To this aim cell lysates were immunoprecipitated using either an anti-FR or an anti-PLAP antibody and revealed with an anti-GFP antibody in the presence or absence of BS_3 addition to the apical surface (Figure 20). Although the amount of immunoprecipitated proteins detected by western blot was similar both in the presence or absence of the cross-linking agent (Figure 20), a smear between ~ 60 and ~ 300 kDa revealed with the anti-GFP antibody was detected in the immunoprecipitates from both cells only after crosslinking (Figure 20), indicating that both pairs of proteins co-immunoprecipitated after BS_3 addition.
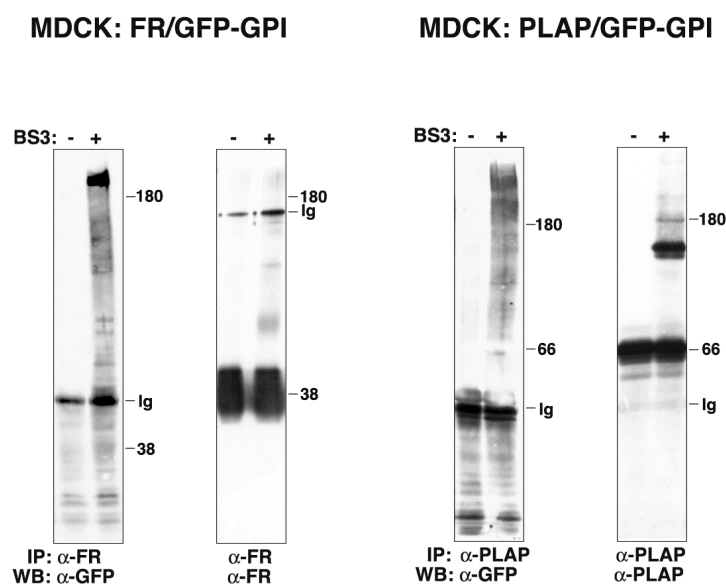
Figure 20. HMW complexes of FR, PLAP and GFP-GPI can be cross-linked in specific hetero-clusters.
MDCK cells stably expressing FR/GFP-GPI or PLAP/GFP-GPI were crosslinked at 4°C with BS_3 (0.5 mM). After lysis, proteins were immunoprecipitated either with anti-FR or anti-PLAP antibody and revealed by western blotting using specific antibodies.

This co-immunoprecipitation between GFP-GPI and FR or PLAP is specific because both anti-FR and anti-PLAP antibodies do not cross-react with GFP-GPI, as shown by control immunoprecipitations from cells expressing only GFP-GPI (Figure 21). These data clearly show that two different GPI-APs can be cross-linked in HMW complexes at the cell surface indicating that they are in close proximity.

MDCK: GFP-GPI
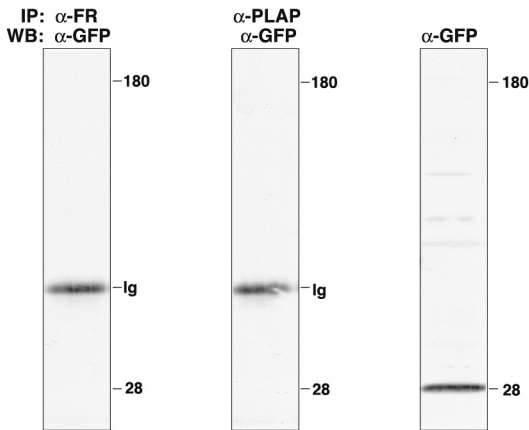
Figure 21. FR and PLAP antibodies do not show cross-reactivity for GFP-GPI.
Cell lysates from MDCK cells stably expressing GFP-GPI were immunoprecipitated either with FR or PLAP antibodies. After separation on SDS-PAGE, proteins were revealed by western blotting by using anti-GFP antibody. A control western blotting for GFP (gel on the right) shows that GFP-GPI is expressed by these cells. Note that there is no cross-reaction of the anti-GFP antibody with either FR or PLAP.

In order to understand whether these hetero-HMW complexes derived from the cross-linking of monomers or oligomers of the single proteins we purified them on velocity gradients (Figure 22). After addition of BS_3 to the cell surface, cell lysates were run on velocity gradients and each fraction was immunoprecipitated with anti-FR (Figure 22A) or anti-PLAP (Figure 22B) antibodies and revealed with the anti-GFP antibody on western blots (Figure 22 top panels). For both pairs of proteins we only observed co-immunoprecipitation with GFP-GPI in fraction 9, which contains only HMW complexes of the single proteins (Figure 22 top panels).
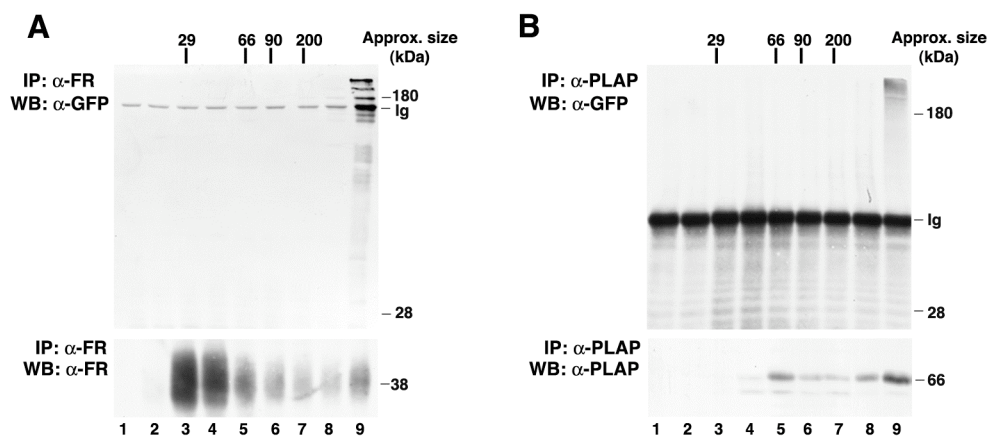

Figure 22. Purification of HMW complexes of FR, PLAP and GFP-GPI can be cross-linked in specific hetero-clusters.
MDCK cells stably expressing FR/GFP-GPI or PLAP/GFP-GPI were treated with BS_3, lysed and purified by velocity gradients. Samples were immunoprecipitated using an anti-FR (A) or anti-PLAP (B) antibody and revealed by western blotting using an anti-GFP antibody (top panels). Immunoprecipitated proteins were revealed by western blotting with the same antibody (either FR or PLAP) (bottom panels). The molecular weight of the monomeric forms of each protein is indicated, together with the position of a 180 kDa marker.

In an alternative approach we disrupted GFP-GPI oligomers, which depend on disulphide bonds (Paladino et al., 2004), by treating the cells with DTT (10 mM, 5 min) (Mezghrani et al., 2001), and then analyzed whether GFP-GPI monomers were cross-linked with PLAP or FR (whose oligomers were not affected by DTT treatment; Figure 23). As expected, in the presence of DTT GFP-GPI was present only in the monomeric, or partially denatured (band at 43 kDa) dimeric forms (Figure 23, top). In these conditions GFP-GPI did not co-immunoprecipitate with PLAP nor FR (Figure 23, bottom). These data together therefore indicated that homo-HMW-complexes of the single GPI-APs were in such close proximity as to be crosslinked and suggested that monomers/dimers cannot be cross-linked to pre-existing homo-oligomers.
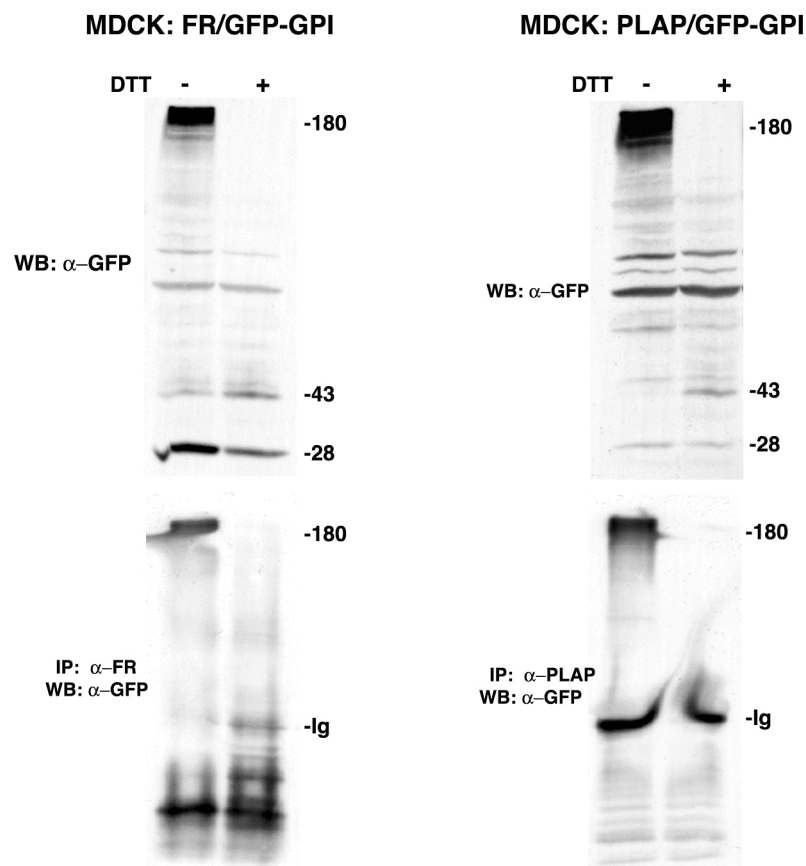
Figure 23. GFP-GPI does not co-immunoprecipitate with FR or PLAP after DTT treatment.
MDCK cells stably expressing FR/GFP-GPI or PLAP/GFP-GPI, grown to confluence, were treated with DTT for 5 min, cross-linked at 37°C for 10 min and then lysed. Lysates were immunoprecipitated either with an anti-FR or anti-PLAP antibody and revealed by western blotting by using an anti-GFP antibody (bottom). An aliquot of the lysate before immunoprecipitation was run on SDS-PAGE and revealed by western blotting using an anti-GFP antibody (top). Note that after DTT treatment GFP-GPI was present only in the monomeric or partially denatured dimeric (band at 43 kDa) form and does not co-immunoprecipitate with FR or PLAP.

Finally, in order to understand whether this clustered organization was specific for GPI-APs we analysed the behaviour of GP114, an apical endogenous non-raft transmembrane protein of MDCK cells. After BS$_3$ addition GP114 does not co-immunoprecipitate either with FR or PLAP (Figure 24) thus indicating that non-raft proteins do not cluster with GPI-APs at the apical surface.
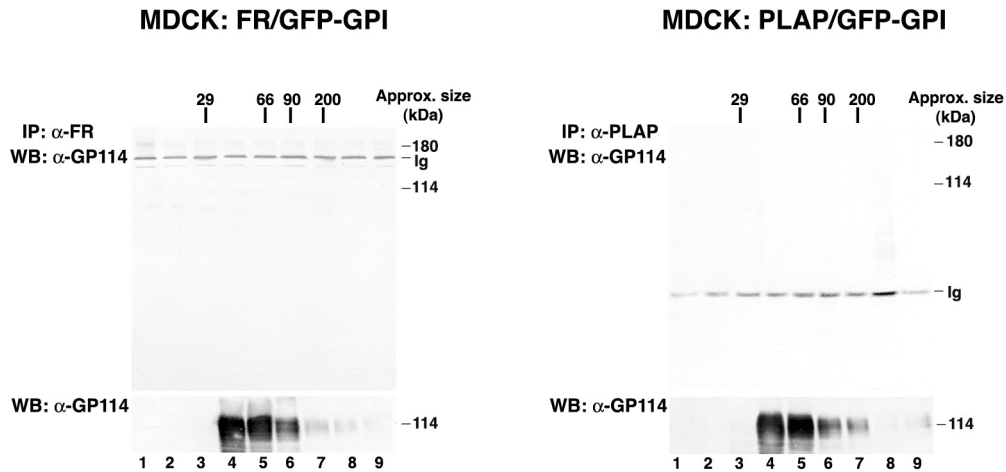
Figure 24. HMW complexes of FR and PLAP do not contain GP114.
MDCK cells stably expressing FR/GFP-GPI or PLAP/GFP-GPI were treated with BS$_3$, lysed and purified by velocity gradient. Samples were immunoprecipitated by using an anti-FR or anti-PLAP antibody and revealed by western blotting using an anti-GP114 antibody (top panels). An equal aliquot of each fraction was collected and TCA-precipitated before immunoprecipiation and revealed by western blotting with an anti-GP114 antibody (bottom panels). The molecular weight of the monomeric forms of each protein is indicated together with the position of a 180 kDa marker. Note that GP114 is not cross-linked with FR or PLAP.

Role of cholesterol in the spatial organization of GPI-AP clusters

Cholesterol has been reported to play a role in the organization of GPI-AP clusters at the surface of non-polarized cells (Sharma *et al.*, 2004). In order to understand whether the relative organization of GPI-APs at the apical membrane of MDCK cells was dependent on cholesterol, cells were treated with saponin (SAP, 0.2%, at 4°C for 30 min) and analyze the effect on homo- and hetero- GPI-AP complexes after surface cross-linking at 37°C (Figure 25).
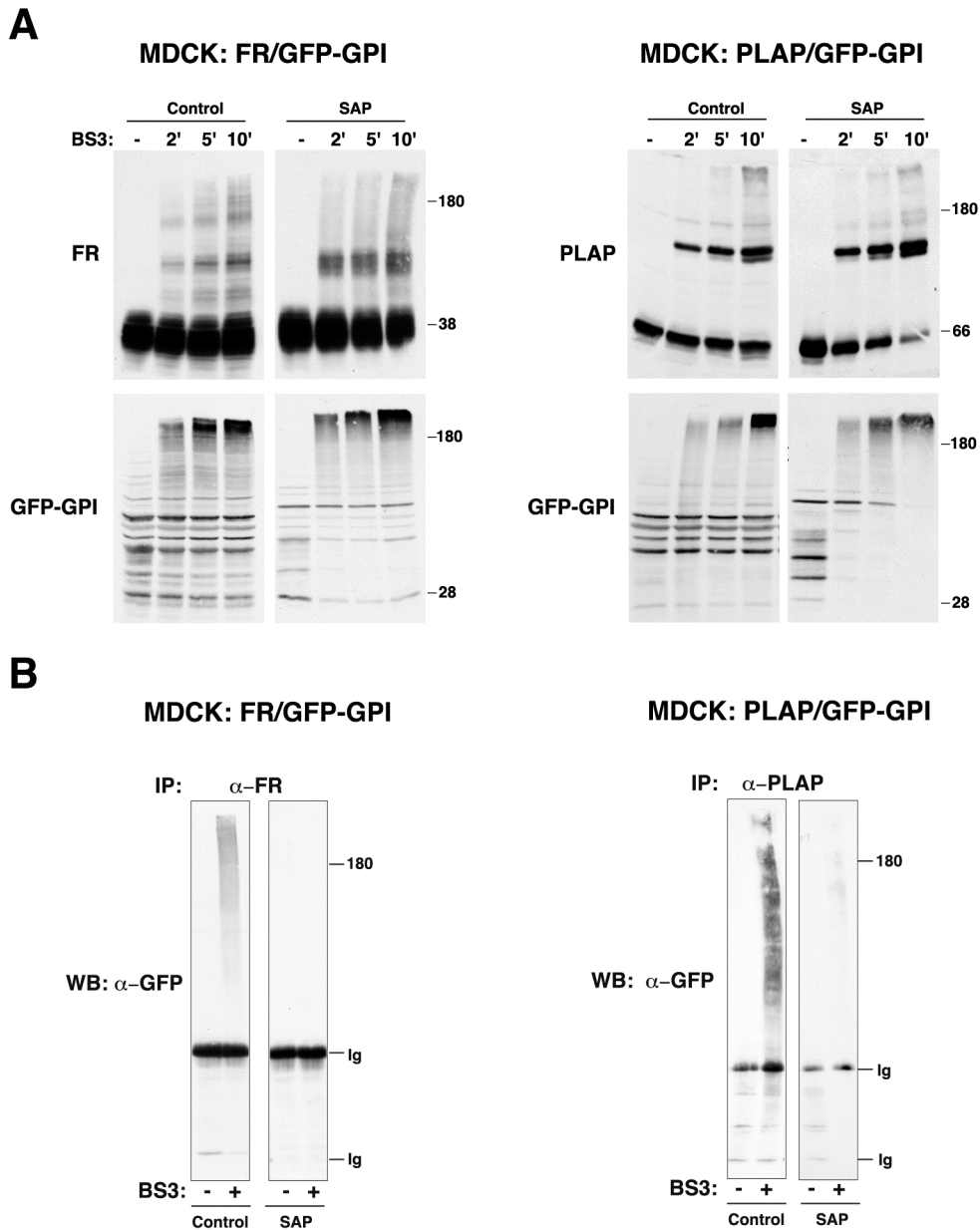
Figure 25. Saponin treatment does not affect GPI-AP homo-clusters, but affects GPI-AP hetero-clusters.
MDCK cells stably expressing FR/GFP-GPI or PLAP/GFP-GPI, either in control conditions or after saponin (SAP) addition as described in materials and methods, were cross-linked with BS$_3$ at 37°C for different times. After lysis, proteins were TCA-precipitated and revealed by western blotting with specific antibodies (A), or were immunoprecipitated by using anti-FR or anti-PLAP specific antibodies and revealed by western blotting using an anti-GFP antibody (B).

By using higher saponin concentration (Figure 26A) and/or longer incubation times (Figure 26B), it was rule out the hypothesis that homo- and hetero-clusters had different threshold sensitivity to cholesterol depletion. Also in these conditions homo-clusters were not affected clearly indicating that they did not depend on cholesterol or it is very strongly bound. On the contrary, the hetero-GPI-AP complexes were no longer cross-linkable after saponin addition (Figure 25B), indicating that co-cluster organization between two different GPI-APs requires cholesterol.
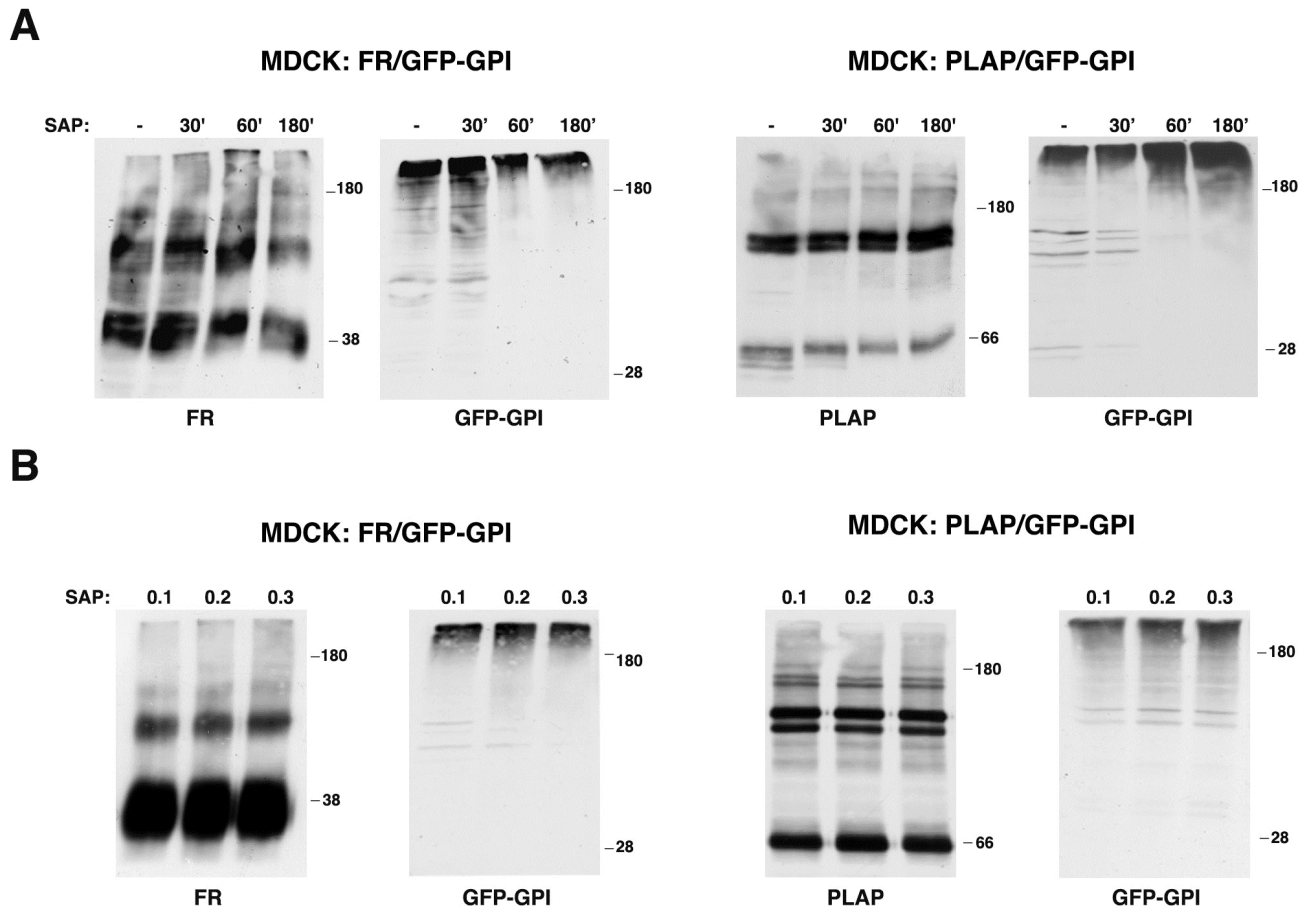
Figure 26. Longer incubation times and higher concentrations of saponin do not affect GPI-APs homo-clusters.
MDCK cells stably expressing GFP-GPI, FR or PLAP, treated with saponin (SAP) for different times (A) and different concentrations (B), were cross-linked with BS_3. After lysis, proteins were TCA-precipitated, separated on SDS-PAGE and revealed using specific antibodies.

These biochemical data on the cholesterol sensitivity of homo- and hetero- GPI-clusters were confirmed by indirect immunofluorescence and by quantitative confocal analysis. Control cells or cells treated with saponin were chemically cross-linked with BS_3, fixed and stained using specific couples of antibodies (αGFP together with αFR or αPLAP) (Figure 27). After cross-linking all three GPI-APs were organized in discrete punctate structures (Figure 27, +BS3 -SAP). The clusters

of each GPI-AP were distinct but close to each other, as indicated by the presence of some areas of co-localization either in one Z-plane (yellow areas in the overlay) (Figure 27, +BS3 -SAP).
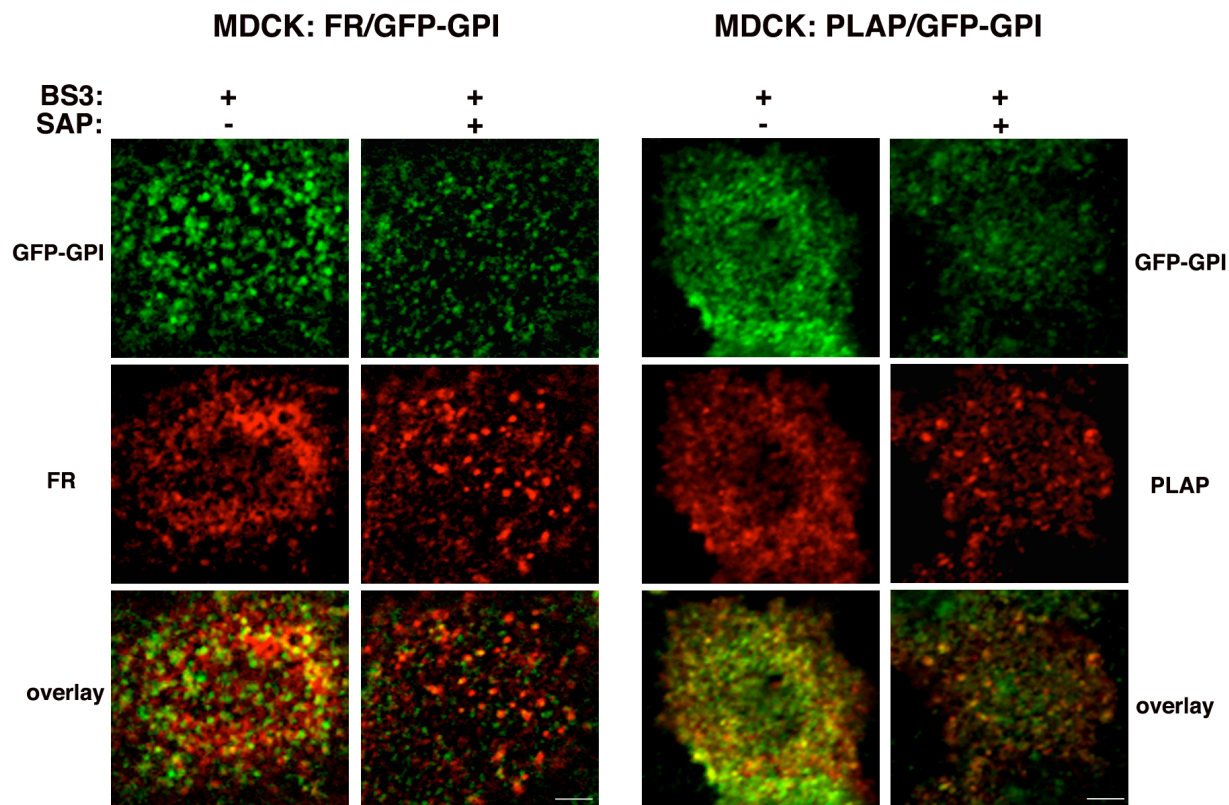
Figure 27. Cholesterol depletion affects co-clustering of both GPI-APs.
MDCK cells stably expressing FR/GFP-GPI or PLAP/GFP-GPI, either in control conditions (-) or after saponin treatment (+), were cross-linked (+) with BS_3, fixed and stained with specific antibodies and revealed by Cy3- and Cy5-conjugated secondary antibodies. Serial confocal sections were collected. Bars, 4 μm.

In order to confirm this hypothesis we have undertaken a different approach and analysed the effect of cholesterol addition on homo- and hetero- GPI-AP complexes after surface cross-linking at 37°C (Figure 28). After cholesterol addition (10mM) both FR and GFP-GPI were still cross-linked in HMW homo-complexes (Figure 28A), thus confirming that homo-clusters are cholesterol independent. In contrast, after cross-linking GFP-GPI did not co-immunoprecipitate with FR indicating that hetero-clusters between two different GPI-APs was drastically reduced with time after cholesterol addition (Figure 28B).
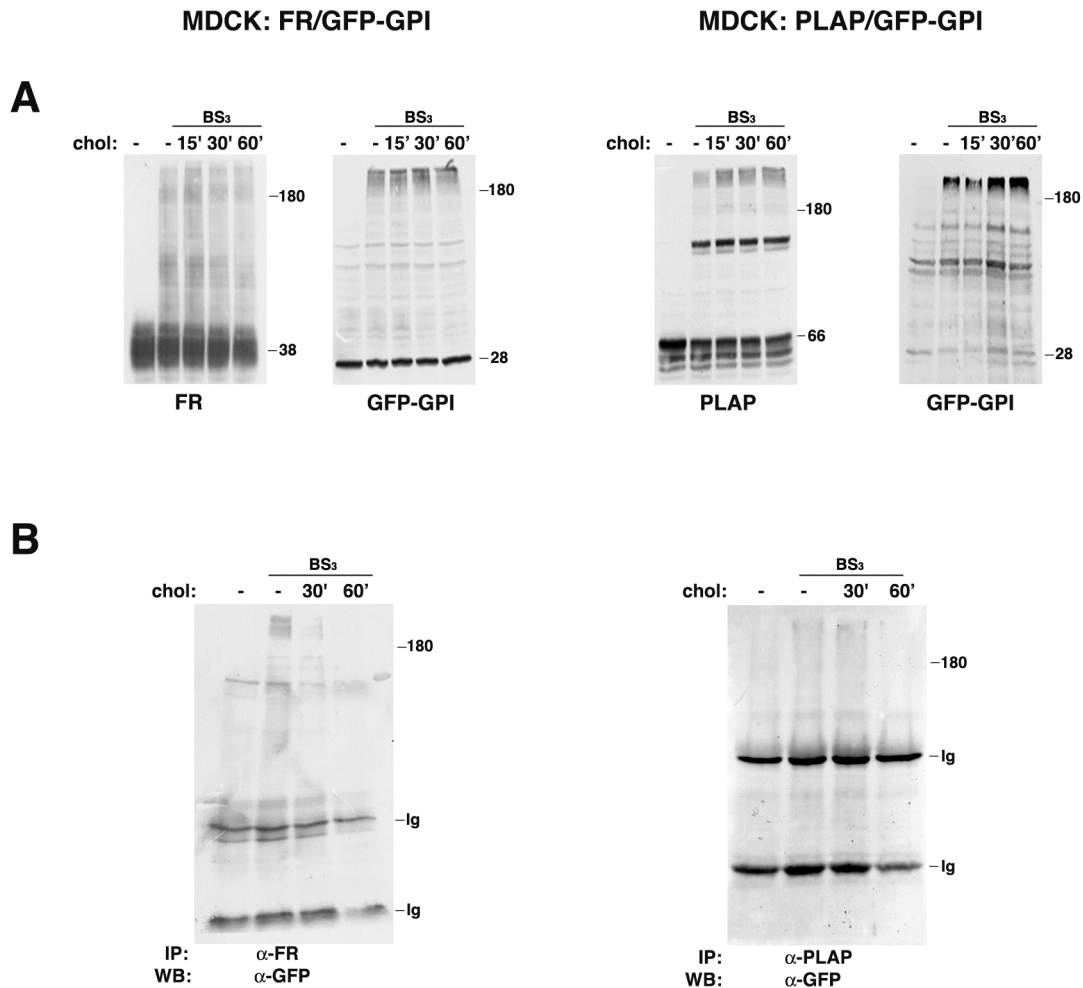
Figure 28. Effect of cholesterol addition on homo- and hetero-complexes.
MDCK cells stably expressing FR/GFP-GPI or FR/GFP-GPI or PLAP/GFP-GPI were loaded with cholesterol (chol, 10 mM) for different indicated times and then cross-linked by using BS$_3$ (0.5 mM) at 37°C for 10 min. After lysis, proteins were TCA-precipitated, separated on SDS-PAGE and revealed using specific antibodies (A) or were immunoprecipitated by using anti-FR or anti-PLAP antibodies and revealed by western blotting using an anti-GFP antibody (B). The molecular weight of the monomeric forms of each protein is indicated, together with the position of a 180 kDa marker.

In an alternative approach we investigated the effect of cholesterol depletion by metabolic inhibition, using mevinolin (MEV), or by surface extraction, using methyl-β-cyclodextrin (βCD). These treatments reduce the amount of cholesterol in the membrane in contrast to saponin which sequesters cholesterol in an hexagonal patterned lattice (Bangham *et al.*, 1962) within the bilayer. Under both these conditions we found an increase of co-immunoprecipitation between PLAP and GFP-GPI, thus suggesting that reduction of cholesterol in the plasma membrane brings the hetero-clusters closer to each other (Figure 29).

MDCK: PLAP/GFP-GPI
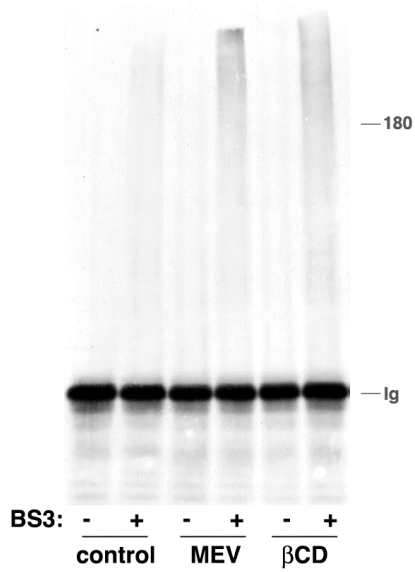
Figure 29. Cholesterol depletion (by metabolic synthesis inhibition or by βCD extraction) enhances hetero-clustering. MDCK cells stably expressing GFP-GPI and PLAP, treated or not (control) with mevinolin (MEV) or βCD were cross-linked with BS_3. After lysis, samples were immunoprecipitated using an anti-PLAP antibody and revealed by western blotting using an anti-GFP antibody. The position of immunoglobulin (Ig) and a 180 kDa marker are shown.

Thus these data clearly indicate that cholesterol influences the organization of hetero-clusters between different GPI-APs, but is not required for the organization of homo-complexes.

6. DISCUSSION

According to the raft hypothesis sphingolipids and cholesterol spontaneously associate with each other to form distinct, more ordered phases within which proteins with chemical affinity for them (such as GPI-APs) partition (Simons and Ikonen, 1997). Because of their capacity to segregate specific lipids and proteins, in cell membranes rafts can act as signalling and sorting platforms (Simons and Ikonen, 1997; Simons and Toomre, 2000). However, it has been shown that rafts are not sufficient to determine apical sorting of GPI-APs in polarized epithelial cells and that their clustering in HMW complexes is a necessary step (Paladino *et al.*, 2004). This is also supported by many reports which indicate that GPI-APs are able to cluster and segregate into specific domains (Mayor *et al.*, 1994; Anderson and Jacobson, 2002; Edidin, 2003; Meder *et al.*, 2006). Nonetheless, how apical GPI-APs are physically organized with respect to each other and to the surrounding lipids is a much-debated issue. While the original raft hypothesis postulated that lipid segregation is responsible for the organization of proteins, recent evidence indicates that functional rafts, containing GPI-APs, are generated by clustering of GPI-APs that, following oligomerization, recruit and concentrate raft lipids into a spatially segregated domain (Paladino *et al.*, 2004).

6.1 Oligomerization is a specific requirement for apical sorting of GPI-anchored proteins but not for non-raft associated apical proteins

Using MDCK cells, we have proposed that protein oligomerization constitutes a cellular sorting mechanism that recruits apical GPI-APs and excludes basolateral ones (Paladino *et al.*, 2004). Oligomerization appears to stabilize proteins into rafts, possibly because oligomers have a higher affinity for rafts than their monomers, as previously suggested (Fivaz *et al.*, 2002; Cunningham *et al.*, 2003). It could therefore lead to the coalescence of small rafts into a larger raft from which the apical vesicle could bud (Paladino *et al.*, 2004). Similarly, it has been shown that raft clustering through polymerisation of M-proteins, which interacts in rafts with neuraminidase and hemagglutinin, represents a key event in the budding of influenza viruses (Zhang *et al.*, 2000). Because protein sorting and delivery to the surface is both cell and protein specific (Rodriguez-Boulan *et al.*, 2005), we have analysed whether oligomerization represents a general requirement for apical sorting of GPI-APs in different epithelia by studying the behaviour of four different, apically and basolaterally sorted, GPI-APs in FRT cells. We have used these cell lines because they are well polarized but have a different phenotype from MDCK, in that they sort the majority of GPI-APs to the basolateral domain of the plasma membrane (Zurzolo *et al.*, 1993). We found that both apical (PLAP and NTR-PLAP) and basolateral (GFP-GPI and GH-DAF) GPI-APs are DRM-

associated (Figures 7 & 8). These data confirm previous findings showing that, independently of their sorting, GPI-APs partition into DRMs and that the GPI anchor, having specific affinity for the long and saturated acyl chains of sphingolipids, is responsible for their association with raft (Brown and London, 1998; Benting *et al.*, 1999a; Lipardi *et al.*, 2000; Mayor and Riezman, 2004; Paladino *et al.*, 2004). We also demonstrate that, as in MDCK cells, in FRT cells raft association is not sufficient to determine apical sorting of GPI-APs. Indeed, as in MDCK cells (Paladino *et al.*, 2004), only apical GPI-APs were found in HMW complexes both during sorting, specifically during the passage through the Golgi apparatus, and at the cell surface (Figure 9 and 11). These results therefore indicate that oligomerization might be the prime mechanism determining GPI-AP apical sorting in different epithelia.

Because apical proteins can be sorted both via raft-dependent and raft-independent mechanisms both in MDCK and FRT cells (Benting *et al.*, 1999b; Lipardi *et al.*, 2000), which exhibit a different sorting phenotype (Zurzolo *et al.*, 1993), another question is whether oligomerization is also required for apical sorting of non-raft proteins. To this aim we analysed the ability of oligomerization of the transmembrane and secretory forms of NTR, which are both apically sorted but are not associated with DRMs. We found that, in contrast to the GPI-anchored form (NTR-PLAP), neither the native TM (p75 NTR) nor the secretory forms (NTR-sec) are able to oligomerize (Figure 12). These results clearly indicate that oligomerization is a specific requirement for apical sorting of GPI-APs. The fact that although both the transmembrane and secretory forms of p75 NTR contained the same ectodomain of the GPI-anchored version were not able to oligomerize suggested that association with DRMs was required for oligomerization to occur. Rafts might provide a favourable environment for oligomerization to occur as shown by the fact that impairment of DRM association at the TGN also reduces oligomerization and affects apical sorting (Paladino *et al.*, 2004). Furthermore the fact that oligomer formation occurs concomitantly with DRM association in the Golgi apparatus (Paladino *et al.*, 2004) suggests that oligomerization and association to lipid rafts cooperate to promote apical sorting of GPI-APs.

In addition we found that oligomerization of GPI-APs begins in the medial Golgi (Figure 11) like in MDCK cells (Paladino *et al.*, 2006), indicating that GPI-AP in different epithelia the first sorting station for GPI-APs is the TGN.

6.2 Detergent-Resistant Membranes associated with apical and basolateral GPI-anchored proteins in polarized epithelial cells contain the same lipid species in different quantity

The analysis of the lipid composition of DRMs associated with PLAP and GH-DAF, respectively sorted to the apical and basolateral domains of FRT **cells** (Figure 7) gives information in order to understand whether apical and basolateral GPI-APs are surrounded by a different lipid environment and whether this could be linked to their different sorting. PLAP and GH-DAF were similarly distributed in a 2-step sucrose density gradient (Figure 13) and were enriched in fraction 5 to similar extents (~ 30%). This fraction contains ~ 40% of cellular sphingolipids, ~ 50% of cellular cholesterol and ~ 30% of cellular PC, but only 5% of cellular PE (Figure 14), clearly indicating a lipid segregation in the different gradient fractions. These results support the increasing evidence for the existence of specialized lipid domains in the membrane (Brown and Rose, 1992; Prinetti et al., 2000) and indicate that the lipid distribution found in FRT cells is similar to that recovered from other cell lines (Brown and Rose, 1992; Prinetti *et al.*, 2000; Pike *et al.*, 2002). Our data also show that DRM-fractions derived from different FRT clones are similar, therefore indicating that the expression of different GPI-APs does not alter lipid extraction nor their distribution on sucrose gradients.

After labelling the cells with 1-^{3}H-sphingosine we analyzed the lipids co-immunoprecipitated with PLAP and GH-DAF from the DRM fraction of sucrose gradients. The same lipid species are co-purified with apical or basolateral GPI-APs (Figure 15). However, a different ratio between the lipid species was consistently observed in different experiments and was maintained after mixing the two FRT clones before lysis (Figure 17), thus demonstrating that there is no artificial lipid mixing or domain formation caused by TX-100 extraction and suggesting that the co-immunoprecipitated lipids represent the boundary lipids around each protein (Brown and Rose, 1992; Brown and London, 2000; Simons and Vaz, 2004). Specifically we found an enrichment of SL and cholesterol over PC in the DRM fraction co-immunoprecipitated with basolateral GH-DAF compared to the ones co-immunoprecipitated with apical PLAP (Table 6). These data are in agreement with recent data demonstrating a twofold increase in the cholesterol:phospholipids ratio in the basolateral membrane of guinea pig colonic epithelia compared to the apical one (Brusche et al 2002). Cholesterol plays an important role as a linker molecule (Simons and Vaz, 2004), but it can also cause or enhance lateral separation of lipids, depending on its concentration. Higher cholesterol in the epithelial basolateral membrane leads to higher permeability compared to the apical one that needs to be better protected from the external aggression (Brusche et al 2002). Furthermore a high amount of cholesterol could lead to greater spacing between basolateral GPI-

APs, therefore impairing the possibility for them to come into closer contact with each other and ultimately impairing their oligomerization, a process that we have shown to be necessary for apical GPI-APs sorting (Paladino et al., 2004). The glycolipid anchor of GPI-APs could also have an active role in this process by promoting a different affinity for different kinds of lipid microdomains. Consequently if a GPI-AP is in a favourable lipid environment for oligomerization, then it could be apically sorted. Affinity for lipid rafts and oligomerization could work synergistically to promote apical sorting of GPI-APs.

6.3 GPI-anchored protein homo-oligomerization leads to cholesterol-dependent hetero-clustering at the surface of MDCK cells

In order to analyse the driving force behind the clustering of GPI-APs an important feature is the plasma membrane organization of GPI-APs. To this aim two pairs of apical GPI-APs were co-transfected in MDCK cells: GFP-GPI and FR, and GFP-GPI and PLAP. Consistent with previous data, all of them are apically sorted (Figure 18A) and associate with DRMs to a similar extent (Figure 18B) and could be purified as HMW homo-complexes on velocity gradients (Figure 19A) or by SDS PAGE after addition of a cell- impermeable cross-linker to the apical plasma membrane (Figure 19B). In agreement with previous observations (Mayor *et al.*, 1994; Friedrichson and Kurzchalia, 1998; Paladino *et al.*, 2004; Meder *et al.*, 2006) these data indicate that GPI-APs are organized in homo-clusters at the apical surface of polarized cells. Interestingly, GPI-APs co-immunoprecipitated only after cross-linking (Figure 20). This co-immunoprecipitation is specific for GPI-APs because it does not include other apical, non-raft proteins (Figure 24), indicating that raft and non-raft proteins are segregated into distinct environment, as recently shown (Meder *et al.*, 2006). Furthermore, co-immunoprecipitation occurs exclusively between HMW homo-complexes and not between GPI-AP monomers or dimers (Figure 22), thus suggesting that homo-GPI-AP clusters are in close proximity to each other whereas monomers, excluded by the cross-linking, are much more dispersed or actively excluded by the spatial organization of the clusters. The fact that the arm of the cross-linker is very small (1.14 nm) (Figure 10), that cross-linking occurs at 37°C in a very short time (< 2 min) and is independent of internalization and temperature, demonstrates that GPI-AP homo-clusters are in close proximity to each other at the cell surface of unperturbed cells.

The next question was then to understand how this spatial organization of GPI-APs was related to the organization of membrane lipids and to determine the principal driving forces. The raft hypothesis, based principally on lipid behaviour in simple model membranes, postulates that lipids would drive protein segregation (Simons and Vaz, 2004). On the same line, Sharma and colleagues proposed that cholesterol is an active player in the organization of GPI-AP nanoclusters, which are

sensitive to saponin. Based on sophisticated FRET analysis, it was also shown that they should be composed at most of four different GPI-APs. This is in contrast with previous observations that GPI-APs are organized in homo-clusters formed by the same protein species (Mayor *et al*., 1994; Harder *et al*., 1998; Paladino *et al*., 2004) and with our observation that cholesterol depletion does not affect organization of GPI-APs in HMW homo-complexes (Figure 25A). In contrast, we found that hetero-clusters are completely disrupted by saponin treatment (Figures 25 & 27)**,** suggesting that while hetero-cluster organization depends on cholesterol, homo-GPI-AP clusters are cholesterol-independent. We also excluded that there is a different threshold required to disrupt homo- and hetero-clusters by treating the cells for longer duration and by using different saponin concentrations (Figure 26). In addition, all alternative methods used to perturb cholesterol balance in the membranes affected exclusively the organization of hetero-clusters. Specifically, while addition of cholesterol inhibited hetero-clustering between different GPI-APs (Figure 28), cholesterol depletion (by metabolic synthesis inhibition or by βCD extraction) enhanced it (Figure 29). Strikingly, both these treatments, similar to saponin, left homo-clusters unperturbed. The different effect induced by βCD and saponin on hetero-clusters could be explained by the different action of these two compounds. Saponin inserts into the plasma membrane and sequesters cholesterol by forming multimeric globular deposits of approximately 80-100 Å (Bangham *et al*., 1962) which could result in a spatial segregation of the homo-complexes (see model in Figure 30). On the other hand, the lack of effect of saponin on homo-clusters could be explained in two ways: either saponin doesn't have access to the cholesterol tightly bound/hidden in these clusters or there is not sufficient cholesterol to bind. Differently from saponin, βCD selectively extracts cholesterol from membrane, preferentially from outside the GPI-APs complex (Ilangumaran and Hoessli, 1998), thus favouring the coalescence of hetero-clusters (see model in Figure 30). This interpretation is consistent with previous findings showing that lowering cholesterol levels by βCD induces formation of large-scale (micrometers) domains in the plasma membrane but does not alter the distribution of cross-linked or uncross-linked GPI-APs (Hao *et al*., 2001). Conversely, if cholesterol had been essential for homo-clusters organization we would have expected an effect of its depletion by either the biochemical inhibition of the synthesis or by βCD extraction.

Based on all of the above results we propose that at the plasma membrane GPI-APs are organized in homo-clusters independently of cholesterol and that they are maintained by protein-protein interactions. Because GPI-APs have a high affinity for cholesterol and saturated sphingolipids, during clustering they may generate a local enrichment of raft lipids including cholesterol within a confined zone (Figure 30), thus creating specialized membrane domains that

actively exclude GPI-AP monomers and other apical components. These GPI-AP clusters have high affinity for each other and so can fuse into cholesterol-dependent hetero-clusters (Figure 30).
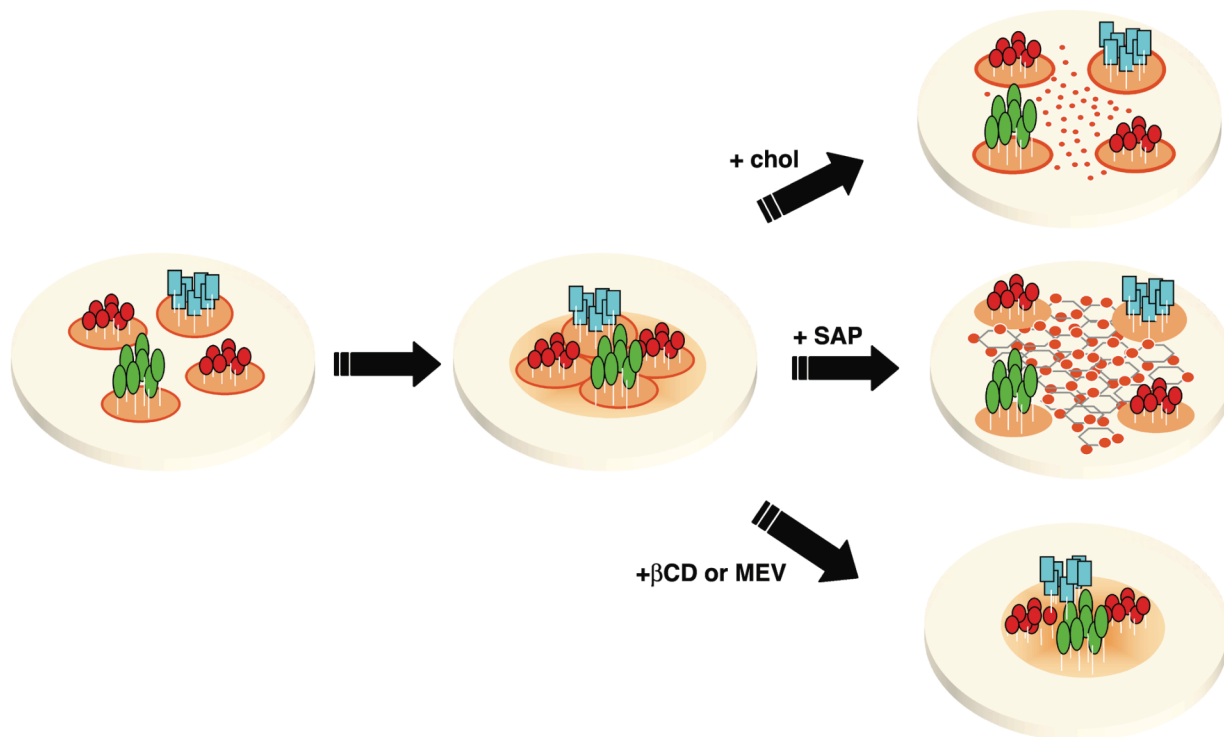
Figure 30. Model of GPI-AP membrane organization.
At the apical surface of MDCK cells GPI-APs are proposed to be organized in homo-clusters independent of cholesterol but dependent on protein-protein interactions. The proteinaceous complexes determine a local enrichment of raft lipids in a confined zone with cholesterol likely to be enriched at their boundaries (orange ring) thus creating specialized membrane domains that actively exclude GPI-AP monomers or other apical components. Because they are surrounded by a similar saturated-lipid environment these GPI-AP clusters have high affinity for each other and can fuse into cholesterol-dependent hetero-clusters. Cholesterol unbalance in the membrane by different means affects only hetero-clusters and not homo-clusters organization. The different effect of saponin (grey hexagones) metabolic inhibition, (MEV) or cyclodextrin treatments (depletion/addition) are illustrated.

Data based on velocity gradients (Figure 22) show that they are in HMW complexes containing more than four molecules, in contrast to what has been recently proposed (Sharma *et al.*, 2004). Consequently, more than four molecules are likely to be required to drive a change in the lipid microenvironment surrounding GPI-APs, which would then permit coalescence of hetero-clusters (that might represent a raft). In support of this hypothesis we do not find co-immunoprecipitation between different GPI-APs in the low molecular weight fractions of velocity gradients (Figure 22) demonstrating that hetero-oligomerization occurs only between HMW homo-complexes. Similarly we show that homo-cluster forms independently of each other because the antibody cross-linking of one specific GPI-AP does not recruit the others.

Our model is supported by studies of GPI-APs in model and cell membranes which have shown that i) monomeric GPI-APs do not show a particular affinity for liquid ordered phases

(Brown and London, 2000), ii) partitioning of GPI-APs into lipid ordered phases is dramatically increased by antibody cross-linking compared to non-raft molecules (Dietrich *et al.*, 2001; Edidin, 2003), and iii) GPI-APs do not show a particular confinement using single molecule tracking at 25 μsec resolution (Kusumi *et al.*, 2005).

Similarly, in the case of T cell signalling it has been clearly demonstrated that the clustering of CD2, the adaptor protein LAT and the tyrosine kinase Lck into discrete microdomains in the plasma membranes is maintained by protein-protein interactions and does not depend on cholesterol or preformed lipid rafts (Douglass and Vale, 2005).

Although we cannot yet exclude that rafts pre-exist in cellular membranes, our data are also supported by a significant body of literature from which it appears that all the biological functions where lipid rafts are involved require segregation and coalescence into large structures which can be explained by the action of proteins in recruiting and concentrating lipids, rather than vice versa (Brown and London, 2000; Edidin, 2003; Munro, 2003).

7. CONCLUSION & PERSPECTIVES

GPI-APs are proteins attached to the external leaflet of the plasma membrane and are involved in different cellular processes. The subcellular localization and the distribution in specific regions of the plasma membrane of GPI-APs are essential to accomplish their function and hence it is fundamental to study the mechanisms underlying their sorting.

Because GPI-APs are enriched to the apical domain of the majority of epithelial cells and partition in cholesterol/sphingolipid assemblies (lipid rafts, also called DRMs because of their resistance to detergent extraction), it has been postulated that the GPI anchor functions as an apical sorting determinant by segregating them into these membrane microdomains.

However, we have previously shown that both apical and basolateral GPI-APs associate with lipid rafts in MDCK cells (a polarized epithelial cell line), thus suggesting that rafts are not sufficient to determine their apical sorting (Paladino et al. 2004). We found that GPI-APs travel to the apical surface in HMW complexes and impairment of their oligomerization blocks their apical sorting (Paladino et al. 2004).

In my thesis I have analysed three fundamental aspects of GPI-APs protein sorting: the role of oligomerization, the composition of DRMs and the requirements for their spatial organization at the apical plasma membrane of polarized epithelial cells.

The main findings of my work are summarized below:

1) Oligomerization represents a specific and essential step for apical sorting of GPI-APs in different cell lines. Hence we have demonstrated that oligomerization is a general mechanism for apical sorting of GPI-APs working in different epithelia. In addition we showed that oligomerization is a specific requirement for GPI-APs and it is not used by transmembrane, non-raft associated apical proteins.

2) Apical and basolateral DRMs contain the same lipid species although in different ratios. Therefore we propose that apical and basolateral GPI-APs partition in a different lipid environment, which could play a role in their sorting. In addition we showed that the specific lipid ratio is maintained after lysis indicating that DRMs maintain their identity after Triton extraction and they are not an experimental artefact.

3) GPI-APs are organized in cholesterol-independent homo-clusters, which can fuse with each other into cholesterol-dependent hetero-clusters at the apical plasma membrane of MDCK cells.

We also showed that GPI-AP monomers cannot be cross-linked in hetero-clusters and the homo-oligomerization of GPI-APs leads to subsequent hetero-clustering, thus indicating that protein-protein interaction is needed to promote the organization of GPI-APs in cholesterol-dependent domains.

The fact that apical and basolateral GPI-APs segregate in a different lipid environment could be due a different affinity of GPI-anchor for different lipid microdomains. Therefore the glycolipid anchor of GPI-APs could also have an active role in their sorting. Further studies to better characterize the structural composition of the GPI anchors of differently sorted proteins and the chemical-physical properties of lipid microdomains at the level of Golgi apparatus are required.

Furthermore our data suggest that oligomerization is promoted by protein-protein interactions, therefore it will be useful to study the role of ectodomain in promoting oligomerization and consequently apical sorting of GPI-APs. Our results will allow further analysis that will aim to address the role of the proteinaceus ectodomain and the role of the GPI-anchor.

Only when all these additional possibilities have been explored will we be able to have a complete picture of the mechanism and of the different factors involved in apical sorting of GPI-APs. Specifically, important information could be obtained analyzing the trafficking and the site of sorting of apical and basolateral GPI-APs fused to different colour mutants of the GFP in living cells.

8. ABBREVIATIONS

AP, apical;

βCD, beta methyl cyclodextrin

BL, basolateral;

BS$_3$, Bis(sulphosuccinimidyl)Suberate;

CFTR, Cystic Fibrosis Transmembrane conductance Regulator;

DRMs, Detergent Resistant Membranes;

FR, Folate Receptor;

FRET, Fluorescence Resonance Energy Transfer;

FRAP, Fluorescence Recovery After Photobleaching;

FRT cells, Fischer Rat Thyroid cells;

GFP, Green Fluorescence Protein;

GH-DAF, Growth Hormone-Decay Accelerating Factor;

GPI-APs, glycosylphosphatidylinositol-anchored proteins;

HMW, High molecular weigh

HPTLC, High Performance Thin Chromatography;

LDL, Low Density Lipoprotein;

MEV, mevilonin

MDCK cells, Madin-Darby canine kidney cells;

PC, phosphatidylcholine;

PDZ, Postsynaptic density protein 95/Drosophila Disks large/Zona occludens-1

PE, phosphatidyletanolamine;

pIgA-R, polymeric Immunoglogulin A Receptor;

PLAP, placental alkaline phosphatase;

PM, plasma membrane;

SL, sphingolipids;

SM, sphingomyelin;

TCZ, Transient Confiment Zone

TGN, trans-Golgi network;

TJ, tight junction

TX-100, Triton X-100;

9. REFERENCES

Ahmed, S.N., Brown, D.A., and London, E. (1997). On the origin of sphingolipid/cholesterol-rich detergent-insoluble cell membranes: physiological concentrations of cholesterol and sphingolipid induce formation of a detergent-insoluble, liquid-ordered lipid phase in model membranes. Biochemistry *36*, 10944-10953.

Almeida, P.F., Vaz, W.L., and Thompson, T.E. (1992). Lateral diffusion in the liquid phases of dimyristoylphosphatidylcholine/cholesterol lipid bilayers: a free volume analysis. Biochemistry *31*, 6739-6747.

Anderson, R.G., and Jacobson, K. (2002). A role for lipid shells in targeting proteins to caveolae, rafts, and other lipid domains. Science (New York, N.Y *296*, 1821-1825.

Ang, A.L., Taguchi, T., Francis, S., Folsch, H., Murrells, L.J., Pypaert, M., Warren, G., and Mellman, I. (2004). Recycling endosomes can serve as intermediates during transport from the Golgi to the plasma membrane of MDCK cells. The Journal of cell biology *167*, 531-543.

Arreaza, G., and Brown, D.A. (1995). Sorting and intracellular trafficking of a glycosylphosphatidylinositol-anchored protein and two hybrid transmembrane proteins with the same ectodomain in Madin-Darby canine kidney epithelial cells. J Biol Chem *270*, 23641-23647.

Bangham, A.D., Horne, R.W., Glauert, A.M., Dingle, J.T., and Lucy, J.A. (1962). Action of saponin on biological cell membranes. Nature *196*, 952-955.

Bastaki, M., Braiterman, L.T., Johns, D.C., Chen, Y.H., and Hubbard, A.L. (2002). Absence of direct delivery for single transmembrane apical proteins or their "Secretory" forms in polarized hepatic cells. Molecular biology of the cell *13*, 225-237.

Benting, J., Rietveld, A., Ansorge, I., and Simons, K. (1999a). Acyl and alkyl chain length of GPI-anchors is critical for raft association in vitro. FEBS letters *462*, 47-50.

Benting, J.H., Rietveld, A.G., and Simons, K. (1999b). N-Glycans mediate the apical sorting of a GPI-anchored, raft-associated protein in Madin-Darby canine kidney cells. The Journal of cell biology *146*, 313-320.

Bezprozvanny, I., and Maximov, A. (2001). PDZ domains: More than just a glue. Proceedings of the National Academy of Sciences of the United States of America *98*, 787-789.

Birnbaumer, M., Seibold, A., Gilbert, S., Ishido, M., Barberis, C., Antaramian, A., Brabet, P., and Rosenthal, W. (1992). Molecular cloning of the receptor for human antidiuretic hormone. Nature *357*, 333-335.

Bomsel, M., Prydz, K., Parton, R.G., Gruenberg, J., and Simons, K. (1989). Endocytosis in filter-grown Madin-Darby canine kidney cells. The Journal of cell biology *109*, 3243-3258.

Braccia, A., Villani, M., Immerdal, L., Niels-Christiansen, L.L., Nystrom, B.T., Hansen, G.H., and Danielsen, E.M. (2003). Microvillar membrane microdomains exist at physiological temperature. Role of galectin-4 as lipid raft stabilizer revealed by "superrafts". J Biol Chem *278*, 15679-15684.

Bretscher, A., Chambers, D., Nguyen, R., and Reczek, D. (2000). ERM-Merlin and EBP50 protein families in plasma membrane organization and function. Annual review of cell and developmental biology *16*, 113-143.

Breuza, L., Garcia, M., Delgrossi, M.H., and Le Bivic, A. (2002). Role of the membrane-proximal O-glycosylation site in sorting of the human receptor for neurotrophins to the apical membrane of MDCK cells. Experimental cell research *273*, 178-186.

Brown, D., and Breton, S. (2000). Sorting proteins to their target membranes. Kidney international *57*, 816-824.

Brown, D.A., and London, E. (1998). Functions of lipid rafts in biological membranes. Annual review of cell and developmental biology *14*, 111-136.

Brown, D.A., and London, E. (2000). Structure and function of sphingolipid- and cholesterol-rich membrane rafts. J Biol Chem *275*, 17221-17224.

Brown, D.A., and Rose, J.K. (1992). Sorting of GPI-anchored proteins to glycolipid-enriched membrane subdomains during transport to the apical cell surface. Cell *68*, 533-544.

Brugger, B., Graham, C., Leibrecht, I., Mombelli, E., Jen, A., Wieland, F., and Morris, R. (2004). The membrane domains occupied by glycosylphosphatidylinositol-anchored prion protein and Thy-1 differ in lipid composition. J Biol Chem *279*, 7530-7536. Epub 2003 Dec 7534.

Carter, H.E., Hendry, R.A., Nojima, S., Stanacev, N.Z., and Ohno, K. (1961). Biochemistry of the sphingolipids. XIII. Determination of the structure of cerebrosides from wheat flour. J Biol Chem *236*, 1912-1916.

Casanova, J.E., Apodaca, G., and Mostov, K.E. (1991). An autonomous signal for basolateral sorting in the cytoplasmic domain of the polymeric immunoglobulin receptor. Cell *66*, 65-75.

Cereijido, M., Robbins, E.S., Dolan, W.J., Rotunno, C.A., and Sabatini, D.D. (1978). Polarized monolayers formed by epithelial cells on a permeable and translucent support. The Journal of cell biology *77*, 853-880.

Chen, W.J., Goldstein, J.L., and Brown, M.S. (1990). NPXY, a sequence often found in cytoplasmic tails, is required for coated pit-mediated internalization of the low density lipoprotein receptor. J Biol Chem *265*, 3116-3123.

Chigorno, V., Riva, C., Valsecchi, M., Nicolini, M., Brocca, P., and Sonnino, S. (1997). Metabolic processing of gangliosides by human fibroblasts in culture--formation and recycling of separate pools of sphingosine. European journal of biochemistry / FEBS *250*, 661-669.

Chuang, J.Z., and Sung, C.H. (1998). The cytoplasmic tail of rhodopsin acts as a novel apical sorting signal in polarized MDCK cells. The Journal of cell biology *142*, 1245-1256.

Collawn, J.F., Stangel, M., Kuhn, L.A., Esekogwu, V., Jing, S.Q., Trowbridge, I.S., and Tainer, J.A. (1990). Transferrin receptor internalization sequence YXRF implicates a tight turn as the structural recognition motif for endocytosis. Cell *63*, 1061-1072.

Corvera, S., Chawla, A., Chakrabarti, R., Joly, M., Buxton, J., and Czech, M.P. (1994). A double leucine within the GLUT4 glucose transporter COOH-terminal domain functions as an endocytosis signal. The Journal of cell biology *126*, 979-989.

Cunningham, O., Andolfo, A., Santovito, M.L., Iuzzolino, L., Blasi, F., and Sidenius, N. (2003). Dimerization controls the lipid raft partitioning of uPAR/CD87 and regulates its biological functions. The EMBO journal *22*, 5994-6003.

Delacour, D., and Jacob, R. (2006). Apical protein transport. Cell Mol Life Sci *63*, 2491-2505.

Dietrich, C., Volovyk, Z.N., Levi, M., Thompson, N.L., and Jacobson, K. (2001). Partitioning of Thy-1, GM1, and cross-linked phospholipid analogs into lipid rafts reconstituted in supported model membrane monolayers. Proceedings of the National Academy of Sciences of the United States of America *98*, 10642-10647.

Dietrich, C., Yang, B., Fujiwara, T., Kusumi, A., and Jacobson, K. (2002). Relationship of lipid rafts to transient confinement zones detected by single particle tracking. Biophysical journal *82*, 274-284.

Doms, R.W., Keller, D.S., Helenius, A., and Balch, W.E. (1987). Role for adenosine triphosphate in regulating the assembly and transport of vesicular stomatitis virus G protein trimers. The Journal of cell biology *105*, 1957-1969.

Douglass, A.D., and Vale, R.D. (2005). Single-molecule microscopy reveals plasma membrane microdomains created by protein-protein networks that exclude or trap signaling molecules in T cells. Cell *121*, 937-950.

Dunphy, W.G., and Rothman, J.E. (1985). Compartmental organization of the Golgi stack. Cell *42*, 13-21.

Edidin, M. (2003). The state of lipid rafts: from model membranes to cells. Annu Rev Biophys Biomol Struct *32*, 257-283.

Ferguson, M.A. (1999). The structure, biosynthesis and functions of glycosylphosphatidylinositol anchors, and the contributions of trypanosome research. Journal of cell science *112 (Pt 17)*, 2799-2809.

Ferguson, M.A., Low, M.G., and Cross, G.A. (1985). Glycosyl-sn-1,2-dimyristylphosphatidylinositol is covalently linked to Trypanosoma brucei variant surface glycoprotein. J Biol Chem *260*, 14547-14555.

Fiedler, K., Kobayashi, T., Kurzchalia, T.V., and Simons, K. (1993). Glycosphingolipid-enriched, detergent-insoluble complexes in protein sorting in epithelial cells. Biochemistry *32*, 6365-6373.

Fiedler, K., and Simons, K. (1995). The role of N-glycans in the secretory pathway. Cell *81*, 309-312.

Fivaz, M., Vilbois, F., Thurnheer, S., Pasquali, C., Abrami, L., Bickel, P.E., Parton, R.G., and van der Goot, F.G. (2002). Differential sorting and fate of endocytosed GPI-anchored proteins. The EMBO journal *21*, 3989-4000.

Folsch, H., Ohno, H., Bonifacino, J.S., and Mellman, I. (1999). A novel clathrin adaptor complex mediates basolateral targeting in polarized epithelial cells. Cell *99*, 189-198.

Friedrichson, T., and Kurzchalia, T.V. (1998). Microdomains of GPI-anchored proteins in living cells revealed by crosslinking. Nature *394*, 802-805.

Fujiwara, T., Ritchie, K., Murakoshi, H., Jacobson, K., and Kusumi, A. (2002). Phospholipids undergo hop diffusion in compartmentalized cell membrane. The Journal of cell biology *157*, 1071-1081.

Geffen, I., Fuhrer, C., Leitinger, B., Weiss, M., Huggel, K., Griffiths, G., and Spiess, M. (1993). Related signals for endocytosis and basolateral sorting of the asialoglycoprotein receptor. J Biol Chem *268*, 20772-20777.

Gisler, S.M., Stagljar, I., Traebert, M., Bacic, D., Biber, J., and Murer, H. (2001). Interaction of the type IIa Na/Pi cotransporter with PDZ proteins. J Biol Chem *276*, 9206-9213.

Glomset, J.A., Gelb, M.H., and Farnsworth, C.C. (1990). Prenyl proteins in eukaryotic cells: a new type of membrane anchor. Trends in biochemical sciences *15*, 139-142.

Glynne, P.A., and Evans, T.J. (2002). Role of the PDZ scaffolding protein in tubule cells in maintenance of polarised function. Experimental nephrology *10*, 307-312.

Goldstein, J.L., and Brown, M.S. (2001). Molecular medicine. The cholesterol quartet. Science (New York, N.Y *292*, 1310-1312.

Griffiths, G., and Simons, K. (1986). The trans Golgi network: sorting at the exit site of the Golgi complex. Science (New York, N.Y *234*, 438-443.

Hantke, K., and Braun, V. (1973). Covalent binding of lipid to protein. Diglyceride and amide-linked fatty acid at the N-terminal end of the murein-lipoprotein of the Escherichia coli outer membrane. European journal of biochemistry / FEBS *34*, 284-296.

Hao, M., Mukherjee, S., and Maxfield, F.R. (2001). Cholesterol depletion induces large scale domain segregation in living cell membranes. Proceedings of the National Academy of Sciences of the United States of America *98*, 13072-13077.

Harder, T., Scheiffele, P., Verkade, P., and Simons, K. (1998). Lipid domain structure of the plasma membrane revealed by patching of membrane components. The Journal of cell biology *141*, 929-942.

Harder, T., and Simons, K. (1997). Caveolae, DIGs, and the dynamics of sphingolipid-cholesterol microdomains. Current opinion in cell biology *9*, 534-542.

Harris, B.Z., and Lim, W.A. (2001). Mechanism and role of PDZ domains in signaling complex assembly. Journal of cell science *114*, 3219-3231.

Helms, J.B., and Zurzolo, C. (2004). Lipids as targeting signals: lipid rafts and intracellular trafficking. Traffic (Copenhagen, Denmark) *5*, 247-254.

Hua, W., Sheff, D., Toomre, D., and Mellman, I. (2006). Vectorial insertion of apical and basolateral membrane proteins in polarized epithelial cells revealed by quantitative 3D live cell imaging. The Journal of cell biology *172*, 1035-1044.

Hunziker, W., Harter, C., Matter, K., and Mellman, I. (1991). Basolateral sorting in MDCK cells requires a distinct cytoplasmic domain determinant. Cell *66*, 907-920.

Hunziker, W., and Mellman, I. (1991). Relationships between sorting in the exocytic and endocytic pathways of MDCK cells. Seminars in cell biology *2*, 397-410.

Ikezawa, H. (2002). Glycosylphosphatidylinositol (GPI)-anchored proteins. Biological & pharmaceutical bulletin *25*, 409-417.

Ilangumaran, S., and Hoessli, D.C. (1998). Effects of cholesterol depletion by cyclodextrin on the sphingolipid microdomains of the plasma membrane. The Biochemical journal *335 (Pt 2)*, 433-440.

Inouye, S., and Tsuji, F.I. (1994). Aequorea green fluorescent protein. Expression of the gene and fluorescence characteristics of the recombinant protein. FEBS letters *341*, 277-280.

Jacob, R., Alfalah, M., Grunberg, J., Obendorf, M., and Naim, H.Y. (2000). Structural determinants required for apical sorting of an intestinal brush-border membrane protein. J Biol Chem *275*, 6566-6572.

Jacob, R., Heine, M., Alfalah, M., and Naim, H.Y. (2003). Distinct cytoskeletal tracks direct individual vesicle populations to the apical membrane of epithelial cells. Curr Biol *13*, 607-612.

Keller, G.A., Siegel, M.W., and Caras, I.W. (1992). Endocytosis of glycophospholipid-anchored and transmembrane forms of CD4 by different endocytic pathways. The EMBO journal *11*, 863-874.

Keller, P., and Simons, K. (1998). Cholesterol is required for surface transport of influenza virus hemagglutinin. The Journal of cell biology *140*, 1357-1367.

Keller, P., Toomre, D., Diaz, E., White, J., and Simons, K. (2001). Multicolour imaging of post-Golgi sorting and trafficking in live cells. Nature cell biology *3*, 140-149.

Kipp, H., and Arias, I.M. (2000). Newly synthesized canalicular ABC transporters are directly targeted from the Golgi to the hepatocyte apical domain in rat liver. J Biol Chem *275*, 15917-15925.

Koivisto, U.M., Hubbard, A.L., and Mellman, I. (2001). A novel cellular phenotype for familial hypercholesterolemia due to a defect in polarized targeting of LDL receptor. Cell *105*, 575-585.

Kornfeld, R., and Kornfeld, S. (1985). Assembly of asparagine-linked oligosaccharides. Annu Rev Biochem *54*, 631-664.

Kusumi, A., Ike, H., Nakada, C., Murase, K., and Fujiwara, T. (2005). Single-molecule tracking of membrane molecules: plasma membrane compartmentalization and dynamic assembly of raft-philic signaling molecules. Semin Immunol *17*, 3-21.

Lahtinen, U., Honsho, M., Parton, R.G., Simons, K., and Verkade, P. (2003). Involvement of caveolin-2 in caveolar biogenesis in MDCK cells. FEBS letters *538*, 85-88.

Lazaro-Dieguez, F., Colonna, C., Cortegano, M., Calvo, M., Martinez, S.E., and Egea, G. (2007). Variable actin dynamics requirement for the exit of different cargo from the trans-Golgi network. FEBS letters *581*, 3875-3881.

Lazo, P.A. (2007). Functional implications of tetraspanin proteins in cancer biology. Cancer science *98*, 1666-1677.

Le Bivic, A., Garcia, M., and Rodriguez-Boulan, E. (1993). Ricin-resistant Madin-Darby canine kidney cells missort a major endogenous apical sialoglycoprotein. J Biol Chem *268*, 6909-6916.

Legler, D.F., Doucey, M.A., Schneider, P., Chapatte, L., Bender, F.C., and Bron, C. (2005). Differential insertion of GPI-anchored GFPs into lipid rafts of live cells. Faseb J *19*, 73-75.

Lin, S., Naim, H.Y., Rodriguez, A.C., and Roth, M.G. (1998). Mutations in the middle of the transmembrane domain reverse the polarity of transport of the influenza virus hemagglutinin in MDCK epithelial cells. The Journal of cell biology *142*, 51-57.

Lin, S., Naim, H.Y., and Roth, M.G. (1997). Tyrosine-dependent basolateral sorting signals are distinct from tyrosine-dependent internalization signals. J Biol Chem *272*, 26300-26305.

Lipardi, C., Mora, R., Colomer, V., Paladino, S., Nitsch, L., Rodriguez-Boulan, E., and Zurzolo, C. (1998). Caveolin transfection results in caveolae formation but not apical sorting of glycosylphosphatidylinositol (GPI)-anchored proteins in epithelial cells. The Journal of cell biology *140*, 617-626.

Lipardi, C., Nitsch, L., and Zurzolo, C. (2000). Detergent-insoluble GPI-anchored proteins are apically sorted in fischer rat thyroid cells, but interference with cholesterol or sphingolipids differentially affects detergent insolubility and apical sorting. Molecular biology of the cell *11*, 531-542.

Lisanti, M.P., Caras, I.W., Davitz, M.A., and Rodriguez-Boulan, E. (1989). A glycophospholipid membrane anchor acts as an apical targeting signal in polarized epithelial cells. The Journal of cell biology *109*, 2145-2156.

London, E. (2005). How principles of domain formation in model membranes may explain ambiguities concerning lipid raft formation in cells. Biochimica et biophysica acta *1746*, 203-220.

Madore, N., Smith, K.L., Graham, C.H., Jen, A., Brady, K., Hall, S., and Morris, R. (1999). Functionally different GPI proteins are organized in different domains on the neuronal surface. The EMBO journal *18*, 6917-6926.

Matter, K. (2000). Epithelial polarity: sorting out the sorters. Curr Biol *10*, R39-42.

Matter, K., Hunziker, W., and Mellman, I. (1992). Basolateral sorting of LDL receptor in MDCK cells: the cytoplasmic domain contains two tyrosine-dependent targeting determinants. Cell *71*, 741-753.

Matter, K., and Mellman, I. (1994). Mechanisms of cell polarity: sorting and transport in epithelial cells. Current opinion in cell biology *6*, 545-554.

Maxfield, F.R. (2002). Plasma membrane microdomains. Current opinion in cell biology *14*, 483-487.

Mayor, S., and Maxfield, F.R. (1995). Insolubility and redistribution of GPI-anchored proteins at the cell surface after detergent treatment. Molecular biology of the cell *6*, 929-944.

Mayor, S., and Rao, M. (2004). Rafts: scale-dependent, active lipid organization at the cell surface. Traffic (Copenhagen, Denmark) *5*, 231-240.

Mayor, S., and Riezman, H. (2004). Sorting GPI-anchored proteins. Nat Rev Mol Cell Biol *5*, 110-120.

Mayor, S., Rothberg, K.G., and Maxfield, F.R. (1994). Sequestration of GPI-anchored proteins in caveolae triggered by cross-linking. Science (New York, N.Y *264*, 1948-1951.

Meder, D., Moreno, M.J., Verkade, P., Vaz, W.L., and Simons, K. (2006). Phase coexistence and connectivity in the apical membrane of polarized epithelial cells. Proceedings of the National Academy of Sciences of the United States of America *103*, 329-334.

Milewski, M.I., Mickle, J.E., Forrest, J.K., Stafford, D.M., Moyer, B.D., Cheng, J., Guggino, W.B., Stanton, B.A., and Cutting, G.R. (2001). A PDZ-binding motif is essential but not sufficient to localize the C terminus of CFTR to the apical membrane. Journal of cell science *114*, 719-726.

Miotti, S., Bagnoli, M., Tomassetti, A., Colnaghi, M.I., and Canevari, S. (2000). Interaction of folate receptor with signaling molecules lyn and G(alpha)(i-3) in detergent-resistant complexes from the ovary carcinoma cell line IGROV1. Journal of cell science *113 Pt 2*, 349-357.

Mostov, K., Su, T., and ter Beest, M. (2003). Polarized epithelial membrane traffic: conservation and plasticity. Nature cell biology *5*, 287-293.

Mostov, K.E. (2003). Epithelial polarity and morphogenesis. Methods *30*, 189-190.

Mostov, K.E., de Bruyn Kops, A., and Deitcher, D.L. (1986). Deletion of the cytoplasmic domain of the polymeric immunoglobulin receptor prevents basolateral localization and endocytosis. Cell *47*, 359-364.

Mostov, K.E., Verges, M., and Altschuler, Y. (2000). Membrane traffic in polarized epithelial cells. Current opinion in cell biology *12*, 483-490.

Moyer, B.D., Denton, J., Karlson, K.H., Reynolds, D., Wang, S., Mickle, J.E., Milewski, M., Cutting, G.R., Guggino, W.B., Li, M., and Stanton, B.A. (1999). A PDZ-interacting domain in CFTR is an apical membrane polarization signal. The Journal of clinical investigation *104*, 1353-1361.

Moyer, B.D., Duhaime, M., Shaw, C., Denton, J., Reynolds, D., Karlson, K.H., Pfeiffer, J., Wang, S., Mickle, J.E., Milewski, M., Cutting, G.R., Guggino, W.B., Li, M., and Stanton, B.A. (2000).

The PDZ-interacting domain of cystic fibrosis transmembrane conductance regulator is required for functional expression in the apical plasma membrane. J Biol Chem *275*, 27069-27074.

Munro, S. (2003). Lipid rafts: elusive or illusive? Cell *115*, 377-388.

Muth, T.R., and Caplan, M.J. (2003). Transport protein trafficking in polarized cells. Annual review of cell and developmental biology *19*, 333-366.

Nelson, W.J., and Rodriguez-Boulan, E. (2004). Unravelling protein sorting. Nature cell biology *6*, 282-284.

Nelson, W.J., and Yeaman, C. (2001). Protein trafficking in the exocytic pathway of polarized epithelial cells. Trends in cell biology *11*, 483-486.

Neumann-Giesen, C., Falkenbach, B., Beicht, P., Claasen, S., Luers, G., Stuermer, C.A., Herzog, V., and Tikkanen, R. (2004). Membrane and raft association of reggie-1/flotillin-2: role of myristoylation, palmitoylation and oligomerization and induction of filopodia by overexpression. The Biochemical journal *378*, 509-518.

Nosjean, O., Briolay, A., and Roux, B. (1997). Mammalian GPI proteins: sorting, membrane residence and functions. Biochimica et biophysica acta *1331*, 153-186.

Orzech, E., Livshits, L., Leyt, J., Okhrimenko, H., Reich, V., Cohen, S., Weiss, A., Melamed-Book, N., Lebendiker, M., Altschuler, Y., and Aroeti, B. (2001). Interactions between adaptor protein-1 of the clathrin coat and microtubules via type 1a microtubule-associated proteins. J Biol Chem *276*, 31340-31348.

Paladino, S., Pocard, T., Catino, M.A., and Zurzolo, C. (2006). GPI-anchored proteins are directly targeted to the apical surface in fully polarized MDCK cells. J Cell Biol *172*, 1023-1034.

Paladino, S., Sarnataro, D., Pillich, R., Tivodar, S., Nitsch, L., and Zurzolo, C. (2004). Protein oligomerization modulates raft partitioning and apical sorting of GPI-anchored proteins. The Journal of cell biology *167*, 699-709.

Paladino, S., Sarnataro, D., and Zurzolo, C. (2002). Detergent-resistant membrane microdomains and apical sorting of GPI-anchored proteins in polarized epithelial cells. Ijmm International Journal of Medical Microbiology. *291*, 439-445.

Pelkmans, L. (2005). Secrets of caveolae- and lipid raft-mediated endocytosis revealed by mammalian viruses. Biochimica et biophysica acta *1746*, 295-304.

Pelkmans, L., and Helenius, A. (2002). Endocytosis via caveolae. Traffic (Copenhagen, Denmark) *3*, 311-320.

Perego, C., Vanoni, C., Villa, A., Longhi, R., Kaech, S.M., Frohli, E., Hajnal, A., Kim, S.K., and Pietrini, G. (1999). PDZ-mediated interactions retain the epithelial GABA transporter on the basolateral surface of polarized epithelial cells. The EMBO journal *18*, 2384-2393.

Pike, L.J., Han, X., Chung, K.N., and Gross, R.W. (2002). Lipid rafts are enriched in arachidonic acid and plasmenylethanolamine and their composition is independent of caveolin-1 expression: a quantitative electrospray ionization/mass spectrometric analysis. Biochemistry *41*, 2075-2088.

Potter, B.A., Ihrke, G., Bruns, J.R., Weixel, K.M., and Weisz, O.A. (2004). Specific N-glycans direct apical delivery of transmembrane, but not soluble or glycosylphosphatidylinositol-anchored forms of endolyn in Madin-Darby canine kidney cells. Molecular biology of the cell *15*, 1407-1416.

Pralle, A., Keller, P., Florin, E.L., Simons, K., and Horber, J.K. (2000). Sphingolipid-cholesterol rafts diffuse as small entities in the plasma membrane of mammalian cells. The Journal of cell biology *148*, 997-1008.

Prinetti, A., Chigorno, V., Prioni, S., Loberto, N., Marano, N., Tettamanti, G., and Sonnino, S. (2001). Changes in the lipid turnover, composition, and organization, as sphingolipid-enriched membrane domains, in rat cerebellar granule cells developing in vitro. J Biol Chem *276*, 21136-21145.

Prinetti, A., Chigorno, V., Tettamanti, G., and Sonnino, S. (2000). Sphingolipid-enriched membrane domains from rat cerebellar granule cells differentiated in culture. A compositional study. J Biol Chem *275*, 11658-11665.

Puertollano, R., Martin-Belmonte, F., Millan, J., de Marco, M.C., Albar, J.P., Kremer, L., and Alonso, M.A. (1999). The MAL proteolipid is necessary for normal apical transport and accurate sorting of the influenza virus hemagglutinin in Madin-Darby canine kidney cells. The Journal of cell biology *145*, 141-151.

Raghuram, V., Mak, D.O., and Foskett, J.K. (2001). Regulation of cystic fibrosis transmembrane conductance regulator single-channel gating by bivalent PDZ-domain-mediated interaction. Proceedings of the National Academy of Sciences of the United States of America *98*, 1300-1305.

Rao, M., and Mayor, S. (2005). Use of Forster's resonance energy transfer microscopy to study lipid rafts. Biochimica et biophysica acta *1746*, 221-233.

Riboni, L., Bassi, R., Sonnino, S., and Tettamanti, G. (1992). Formation of free sphingosine and ceramide from exogenous ganglioside GM1 by cerebellar granule cells in culture. FEBS letters *300*, 188-192.

Ritchie, K., Iino, R., Fujiwara, T., Murase, K., and Kusumi, A. (2003). The fence and picket structure of the plasma membrane of live cells as revealed by single molecule techniques (Review). Mol Membr Biol *20*, 13-18.

Rock, P., Allietta, M., Young, W.W., Jr., Thompson, T.E., and Tillack, T.W. (1990). Organization of glycosphingolipids in phosphatidylcholine bilayers: use of antibody molecules and Fab fragments as morphologic markers. Biochemistry *29*, 8484-8490.

Rodriguez-Boulan, E., and Gonzalez, A. (1999). Glycans in post-Golgi apical targeting: sorting signals or structural props? Trends in cell biology *9*, 291-294.

Rodriguez-Boulan, E., Kreitzer, G., and Musch, A. (2005). Organization of vesicular trafficking in epithelia. Nat Rev Mol Cell Biol *6*, 233-247.

Rodriguez-Boulan, E., Musch, A., and Le Bivic, A. (2004). Epithelial trafficking: new routes to familiar places. Current opinion in cell biology *16*, 436-442.

Rodriguez-Boulan, E., and Powell, S.K. (1992). Polarity of epithelial and neuronal cells. Annu Rev Cell Biol *8*, 395-427.

Rongo, C., Whitfield, C.W., Rodal, A., Kim, S.K., and Kaplan, J.M. (1998). LIN-10 is a shared component of the polarized protein localization pathways in neurons and epithelia. Cell *94*, 751-759.

Roper, K., Corbeil, D., and Huttner, W.B. (2000). Retention of prominin in microvilli reveals distinct cholesterol-based lipid micro-domains in the apical plasma membrane. Nature cell biology *2*, 582-592.

Sarnataro, D., Paladino, S., Campana, V., Grassi, J., Nitsch, L., and Zurzolo, C. (2002). PrPC is sorted to the basolateral membrane of epithelial cells independently of its association with rafts. Traffic (Copenhagen, Denmark) *3*, 810-821.

Scheiffele, P., Peranen, J., and Simons, K. (1995). N-glycans as apical sorting signals in epithelial cells. Nature *378*, 96-98.

Scheiffele, P., Roth, M.G., and Simons, K. (1997). Interaction of influenza virus haemagglutinin with sphingolipid-cholesterol membrane domains via its transmembrane domain. The EMBO journal *16*, 5501-5508.

Scheiffele, P., Verkade, P., Fra, A.M., Virta, H., Simons, K., and Ikonen, E. (1998). Caveolin-1 and -2 in the exocytic pathway of MDCK cells. The Journal of cell biology *140*, 795-806.

Schmidt, M.F., Bracha, M., and Schlesinger, M.J. (1979). Evidence for covalent attachment of fatty acids to Sindbis virus glycoproteins. Proceedings of the National Academy of Sciences of the United States of America *76*, 1687-1691.

Schuck, S., Honsho, M., Ekroos, K., Shevchenko, A., and Simons, K. (2003). Resistance of cell membranes to different detergents. Proceedings of the National Academy of Sciences of the United States of America *100*, 5795-5800.

Schuck, S., and Simons, K. (2004). Polarized sorting in epithelial cells: raft clustering and the biogenesis of the apical membrane. Journal of cell science *117*, 5955-5964.

Schutz, G.J., Kada, G., Pastushenko, V.P., and Schindler, H. (2000). Properties of lipid microdomains in a muscle cell membrane visualized by single molecule microscopy. The EMBO journal *19*, 892-901.

Scott, R.O., Thelin, W.R., and Milgram, S.L. (2002). A novel PDZ protein regulates the activity of guanylyl cyclase C, the heat-stable enterotoxin receptor. J Biol Chem *277*, 22934-22941.

Sharma, P., Varma, R., Sarasij, R.C., Ira, Gousset, K., Krishnamoorthy, G., Rao, M., and Mayor, S. (2004). Nanoscale organization of multiple GPI-anchored proteins in living cell membranes. Cell *116*, 577-589.

Sheets, E.D., Lee, G.M., Simson, R., and Jacobson, K. (1997). Transient confinement of a glycosylphosphatidylinositol-anchored protein in the plasma membrane. Biochemistry *36*, 12449-12458.

Silvius, J.R., del Giudice, D., and Lafleur, M. (1996). Cholesterol at different bilayer concentrations can promote or antagonize lateral segregation of phospholipids of differing acyl chain length. Biochemistry *35*, 15198-15208.

Simons, K., and Ikonen, E. (1997). Functional rafts in cell membranes. Nature *387*, 569-572.

Simons, K., and Toomre, D. (2000). Lipid rafts and signal transduction. Nat Rev Mol Cell Biol *1*, 31-39.

Simons, K., and van Meer, G. (1988). Lipid sorting in epithelial cells. Biochemistry *27*, 6197-6202.

Simons, K., and Vaz, W.L. (2004). Model systems, lipid rafts, and cell membranes. Annu Rev Biophys Biomol Struct *33*, 269-295.

Singer, S.J., and Nicolson, G.L. (1972). The fluid mosaic model of the structure of cell membranes. Science (New York, N.Y *175*, 720-731.

Slimane, T.A., Trugnan, G., Van, I.S.C., and Hoekstra, D. (2003). Raft-mediated trafficking of apical resident proteins occurs in both direct and transcytotic pathways in polarized hepatic cells: role of distinct lipid microdomains. Molecular biology of the cell *14*, 611-624.

Snyers, L., Umlauf, E., and Prohaska, R. (1999). Association of stomatin with lipid-protein complexes in the plasma membrane and the endocytic compartment. European journal of cell biology *78*, 802-812.

Stan, R.V. (2005). Structure of caveolae. Biochimica et biophysica acta *1746*, 334-348.

Stanton, B.A. (1997). Cystic fibrosis transmembrane conductance regulator (CFTR) and renal function. Wiener klinische Wochenschrift *109*, 457-464.

Stein, M., Wandinger-Ness, A., and Roitbak, T. (2002). Altered trafficking and epithelial cell polarity in disease. Trends in cell biology *12*, 374-381.

Sun, A.Q., Ananthanarayanan, M., Soroka, C.J., Thevananther, S., Shneider, B.L., and Suchy, F.J. (1998). Sorting of rat liver and ileal sodium-dependent bile acid transporters in polarized epithelial cells. The American journal of physiology *275*, G1045-1055.

Takeda, T., Yamazaki, H., and Farquhar, M.G. (2003). Identification of an apical sorting determinant in the cytoplasmic tail of megalin. American journal of physiology *284*, C1105-1113.

Tettamanti, G., Bonali, F., Marchesini, S., and Zambotti, V. (1973). A new procedure for the extraction, purification and fractionation of brain gangliosides. Biochimica et biophysica acta *296*, 160-170.

Thompson, T.E., and Tillack, T.W. (1985). Organization of glycosphingolipids in bilayers and plasma membranes of mammalian cells. Annual review of biophysics and biophysical chemistry *14*, 361-386.

Toomre, D., Keller, P., White, J., Olivo, J.C., and Simons, K. (1999). Dual-color visualization of trans-Golgi network to plasma membrane traffic along microtubules in living cells. Journal of cell science *112*, 21-33.

Urban, J., Parczyk, K., Leutz, A., Kayne, M., and Kondor-Koch, C. (1987). Constitutive apical secretion of an 80-kD sulfated glycoprotein complex in the polarized epithelial Madin-Darby canine kidney cell line. The Journal of cell biology *105*, 2735-2743.

Vagin, O., Turdikulova, S., and Sachs, G. (2004). The H,K-ATPase beta subunit as a model to study the role of N-glycosylation in membrane trafficking and apical sorting. J Biol Chem *279*, 39026-39034.

van Meer, G. (1989). Lipid traffic in animal cells. Annu Rev Cell Biol *5*, 247-275.

van Meer, G., and Simons, K. (1982). Viruses budding from either the apical or the basolateral plasma membrane domain of MDCK cells have unique phospholipid compositions. The EMBO journal *1*, 847-852.

van Meer, G., and Simons, K. (1988). Lipid polarity and sorting in epithelial cells. J Cell Biochem *36*, 51-58.

Varma, R., and Mayor, S. (1998). GPI-anchored proteins are organized in submicron domains at the cell surface. Nature *394*, 798-801.

Verhey, K.J., and Birnbaum, M.J. (1994). A Leu-Leu sequence is essential for COOH-terminal targeting signal of GLUT4 glucose transporter in fibroblasts. J Biol Chem *269*, 2353-2356.

Verhey, K.J., Yeh, J.I., and Birnbaum, M.J. (1995). Distinct signals in the GLUT4 glucose transporter for internalization and for targeting to an insulin-responsive compartment. The Journal of cell biology *130*, 1071-1079.

Vogel, U., Sandvig, K., and van Deurs, B. (1998). Expression of caveolin-1 and polarized formation of invaginated caveolae in Caco-2 and MDCK II cells. Journal of cell science *111 (Pt 6)*, 825-832.

Wandinger-Ness, A., Bennett, M.K., Antony, C., and Simons, K. (1990). Distinct transport vesicles mediate the delivery of plasma membrane proteins to the apical and basolateral domains of MDCK cells. The Journal of cell biology *111*, 987-1000.

Wang, S., Yue, H., Derin, R.B., Guggino, W.B., and Li, M. (2000). Accessory protein facilitated CFTR-CFTR interaction, a molecular mechanism to potentiate the chloride channel activity. Cell *103*, 169-179.

Wehrle-Haller, B., and Imhof, B.A. (2001). Stem cell factor presentation to c-Kit. Identification of a basolateral targeting domain. J Biol Chem *276*, 12667-12674.

Yeaman, C., Grindstaff, K.K., and Nelson, W.J. (1999). New perspectives on mechanisms involved in generating epithelial cell polarity. Physiological reviews *79*, 73-98.

Yeaman, C., Le Gall, A.H., Baldwin, A.N., Monlauzeur, L., Le Bivic, A., and Rodriguez-Boulan, E. (1997). The O-glycosylated stalk domain is required for apical sorting of neurotrophin receptors in polarized MDCK cells. The Journal of cell biology *139*, 929-940.

Zhang, J., Pekosz, A., and Lamb, R.A. (2000). Influenza virus assembly and lipid raft microdomains: a role for the cytoplasmic tails of the spike glycoproteins. Journal of virology *74*, 4634-4644.

Zurzolo, C., Lisanti, M.P., Caras, I.W., Nitsch, L., and Rodriguez-Boulan, E. (1993). Glycosylphosphatidylinositol-anchored proteins are preferentially targeted to the basolateral surface in Fischer rat thyroid epithelial cells. The Journal of cell biology *121*, 1031-1039.

Zurzolo, C., van Meer, G., and Mayor, S. (2003). The order of rafts. Conference on microdomains, lipid rafts and caveolae. EMBO Rep *4*, 1117-1121.

Zurzolo, C., van't Hof, W., van Meer, G., and Rodriguez-Boulan, E. (1994). VIP21/caveolin, glycosphingolipid clusters and the sorting of glycosylphosphatidylinositol-anchored proteins in epithelial cells. The EMBO journal *13*, 42-53.

ANNEX 1

Oligomerization Is a Specific Requirement for Apical Sorting of Glycosyl-Phosphatidylinositol-Anchored Proteins but Not for Non-Raft-Associated Apical Proteins

Simona Paladino[1,2], Daniela Sarnataro[1], Simona Tivodar[1] and Chiara Zurzolo[1,3,*]

[1]*Dipartimento di Biologia e Patologia Cellulare e Molecolare, Università degli Studi di Napoli Federico II, Napoli 80131 Italy*
[2]*CEINGE Biotecnologie Avanzate s.c.a.r.l., Napoli 80131 Italy*
[3]*Unité de Trafic Membranaire et Pathogénèse, Institut Pasteur, 25 rue du Docteur Roux, 75015 Paris, France*
Corresponding author: Chiara Zurzolo, zurzolo@pasteur.fr; zurzolo@unina.it

Protein apical sorting in polarized epithelial cells is mediated by two different mechanisms, raft dependent and raft independent. In Madin–Darby canine kidney (MDCK) cells, an essential step for apical sorting of glycosyl-phosphatidylinositol (GPI)-anchored proteins (GPI-APs) is their coalescence into high-molecular-weight (HMW) oligomers. Here we show that this mechanism is also functional in Fischer rat thyroid cells, which possess a different sorting phenotype compared with MDCK cells. We demonstrate that, as in MDCK cells, both apical and basolateral GPI-APs associate with detergent-resistant microdomains, but that only the apical proteins are able to oligomerize into HMW complexes during their passage through the medial Golgi. We also show that oligomerization is a specific requirement for apical sorting of GPI-APs and is not used by transmembrane, non-raft-associated apical proteins.

The plasma membrane of epithelial cells is divided by tight junctions into two domains, apical and basolateral, which have different protein and lipid compositions that are necessary for their proper specialized functions (1,2). The generation and maintenance of distinct apical and basolateral identities is achieved largely by the continuous sorting of newly synthesized and recycling components to one or other domain of the cell surface (3–5). Hence, sorting determinants in the cargo molecules and molecular machinery responsible for interpreting targeting signals are required.

Basolateral sorting signals have been identified as short amino acid sequences, often containing tyrosine or dileucine-based motifs and confined to the cytosolic tails of membrane proteins, which are recognized by the clathrin adaptor complex (6,7). In contrast, apical signals are more variable. Lumen-localized domains, transmembrane (TM) domains and membrane-binding features have all been shown to be important for apical sorting (8–12). Furthermore, different from basolateral sorting, apical recognition is not only based on protein–protein interactions but on lipid–lipid and lipid–protein interactions also. In particular, it has been postulated that sphingolipid- and cholesterol-rich microdomains (rafts) can act as sorting platforms for inclusion of proteins into apical post-*trans* Golgi network (TGN) sorting vesicles (13) because of their capacity to segregate specific classes of lipids and proteins (14,15). The best example of raft-mediated apical sorting is represented by glycosyl-phosphatidylinositol (GPI)-anchored proteins (GPI-APs), which associate into detergent-resistant microdomains (DRMs) during their passage through the Golgi apparatus (13,16), where sorting is believed to occur (17,18). It was, therefore, proposed that the GPI anchor itself acts as an apical sorting determinant by mediating raft association (13,14). However, the roles of the GPI anchor and of lipid rafts as apical determinants have been recently questioned by the finding that both apically and basolaterally sorted GPI-APs associate with DRMs in Madin–Darby canine kidney (MDCK) cells (19,20). Furthermore, it has been demonstrated that association with DRMs is not sufficient to determine apical sorting of GPI-APs and that oligomerization in high-molecular-weight (HMW) complexes is required (19).

Another fundamental characteristic of the sorting process is that proteins are not exclusively apical or basolateral. The plasticity of epithelia is evidenced by the fact that in different epithelial cell types the same proteins can be differently sorted and/or can follow variable routes to be delivered to their final domain of residence [reviewed by Rodriguez-Boulan et al. (21)]. In addition, it has been shown that apical sorting can be mediated by at least two mechanisms, raft dependent and raft independent (12,20). Here, we ask two specific questions: 1) Is oligomerization a requirement for apical sorting of GPI-APs in polarized cell lines other than MDCK cells? 2) Is this a mechanism also used for apical sorting of TM non-raft-associated proteins?

In order to answer these questions, we have used Fischer rat thyroid (FRT) cells. Although they possess DRMs enriched in sphingomyelin, glycosphingolipids and

cholesterol (22), these cells deliver most of their endogenous GPI-APs to the basolateral surface (23), therefore representing a good model to understand whether protein oligomerization could be a general requirement for apical sorting of GPI-APs. Furthermore, because it has been shown that, as in MDCK cells, FRT cells can use at least two mechanisms, raft dependent and raft independent, to deliver apical proteins (12,20), they also represent a good model to understand whether oligomerization is required for apical sorting of non-raft-associated proteins.

Thus, we analysed here the DRM association of four GPI-APs with opposite polarities in FRT cells: placental alkaline phosphatase (PLAP) and NTR-PLAP (in which the ectodomain of p75 NTR (neurotrophin receptor) is fused to the GPI attachment signal of PLAP), which are apically sorted, and GFP-GPI [in which green fluorescent protein (GFP) is fused to the GPI anchor attachment signal from the folate receptor] and growth hormone–decay accelerating factor (GH-DAF) (in which the rat GH is fused to the GPI attachment signal of DAF), which are basolateral. We show that both apical and basolateral GPI-APs are associated with DRMs, indicating that also in FRT cells lipid rafts do not provide an exclusive mechanism for driving apical sorting. We also found that only the apically sorted GPI-APs are able to form HMW complexes and that oligomerization of apical GPI-APs occurs during transport to the plasma membrane. In addition, we demonstrate that only GPI-APs and not TM proteins oligomerize in HMW complexes prior to apical sorting. These data indicate that oligomerization is a specific requirement for apical sorting of GPI-APs in different epithelia and that this mechanism is not used by nonraft TM apical proteins.

Results

Both apical and basolateral GPI-APs associate with DRMs in FRT cells

In contrast to MDCK cells, FRT cells sort the majority of endogenous and transfected GPI-APs to the basolateral domain of the plasma membrane (12,23). To understand if oligomerization is a general mechanism to promote apical sorting of GPI-APs in different epithelia, we studied the sorting of four different GPI-APs transfected in FRT cells: PLAP, a native GPI-AP, NTR-PLAP, in which the ectodomain of neurotrophin receptor p75 NTR is fused to the GPI attachment signal of PLAP (12), GFP-GPI and GH-DAF, two fusion proteins in which the GFP and the rat GH are, respectively, fused to the GPI attachment signal of the folate receptor and the DAF (19).

We confirmed by confocal microscopy (Figure 1A) that PLAP and NTR-PLAP were predominantly enriched on the apical surface, as previously shown in both FRT and MDCK cells (12,18). On the contrary, we found that GFP-GPI and GH-DAF were predominantly localized on the basolateral membrane. Quantitation by domain-selective biotinylation (Figure 1B) showed that 85 and 90%, respectively, of PLAP and NTR-PLAP was enriched on the apical membrane, while ~80 and 90%, respectively, of GFP-GPI and GH-DAF was basolaterally distributed (Figure 1B), thus indicating that all proteins are fully polarized, respectively, on the apical or basolateral cell surface.

Because in MDCK cells both apical and basolateral GPI-APs are associated with DRMs (19), we analysed DRM association of apical and basolateral GPI-APs in FRT cells
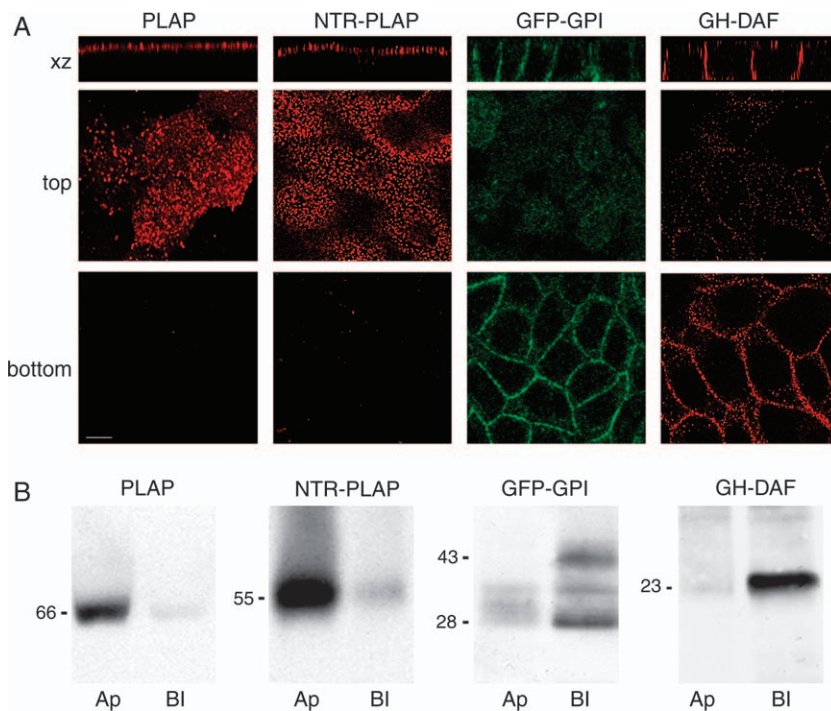
Figure 1: GPI-APs are apically and basolaterally sorted. A) FRT cells stably expressing PLAP, NTR-PLAP, GFP-GPI and GH-DAF were grown on filters for 4 days. Cells were fixed, and in the case of PLAP, NTR-PLAP and GH-DAF stained with specific antibodies followed by a TRITC-conjugated secondary antibody in nonpermeabilized conditions. Serial confocal sections were collected from the top to the bottom of cell monolayers. Bar, 10 μm. B) Alternatively, cells were labelled with long chain (LC)-biotin added to the apical (Ap) or the basolateral (Bl) surface. After immunoprecipitation with specific antibodies, samples were run on SDS-PAGE and biotinylated proteins revealed using HRP-streptavidin. In the case of NTR-PLAP, samples, labelled with [35S]cys overnight as described in *Materials and Methods*, after immunoprecipitation were precipitated with streptavidin beads, run on SDS-PAGE and analysed by fluorography. The band of GFP-GPI at 43 kDa represents a partially denatured GFP dimer as previously described in MDCK cells (19).

by cold Triton-X-100 (TX-100) extraction and centrifugation to equilibrium on sucrose density gradients, as previously described (16,19,22). We found that both apical and basolateral proteins floated to the lighter fractions (4–7) of sucrose gradients, fractions which are also enriched in the ganglioside GM1 (Figure 2). It is interesting to note that higher amounts of apical GPI-APs were found in DRMs compared with the basolateral proteins. Indeed, averages from three independent experiments (see graph in Figure 2) showed that ∼55–60% of apical GPI-APs are in DRMs, in contrast to only ∼30–40% of the basolateral proteins, indicating that like in MDCK cells, apical and basolateral GPI-APs have different behaviours with respect to detergent extraction (19). In addition, as in MDCK cells (19), in the majority of the experiments, there
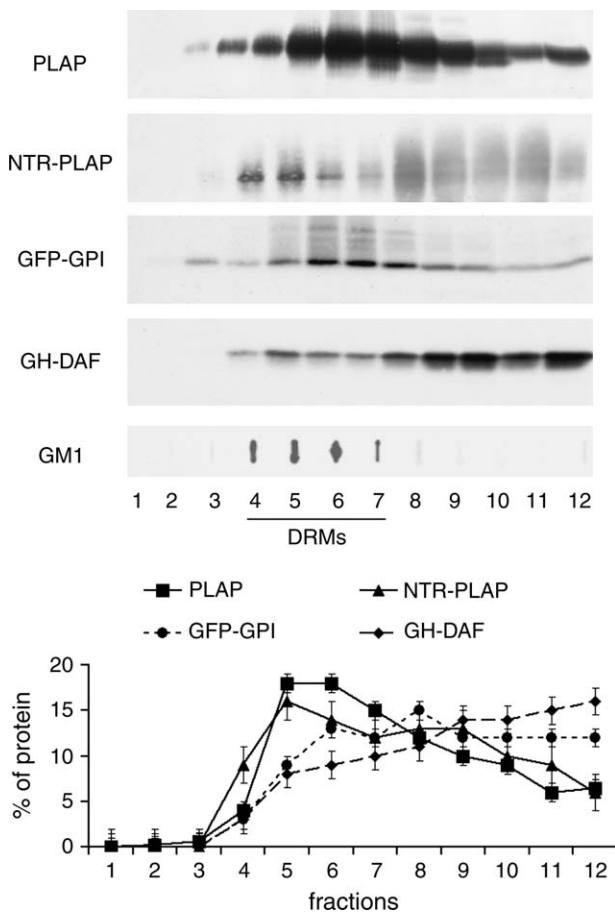
Figure 2: Both apical and basolateral GPI-APs associate with DRMs. FRT cells stably expressing PLAP, NTR-PLAP, GFP-GPI and GH-DAF were lysed in TNE/TX-100 buffer at 4°C and run through 5–40% sucrose gradients. Fractions of 1 ml were collected from top (fraction 1) to bottom (fraction 12) after centrifugation to equilibrium. After TCA precipitation, samples were run on SDS-PAGE and detected by specific antibodies. An aliquot of each fraction was spotted on the nitrocellulose membrane, and GM1 was revealed using cholera toxin conjugated to HRP. The graph shows the mean value of protein distribution on sucrose density gradients from three different experiments.

was a shift of one fraction between the floatation of apical and basolateral GPI-APs, indicating that the composition of the associated DRMs could be different, as recently suggested (24).
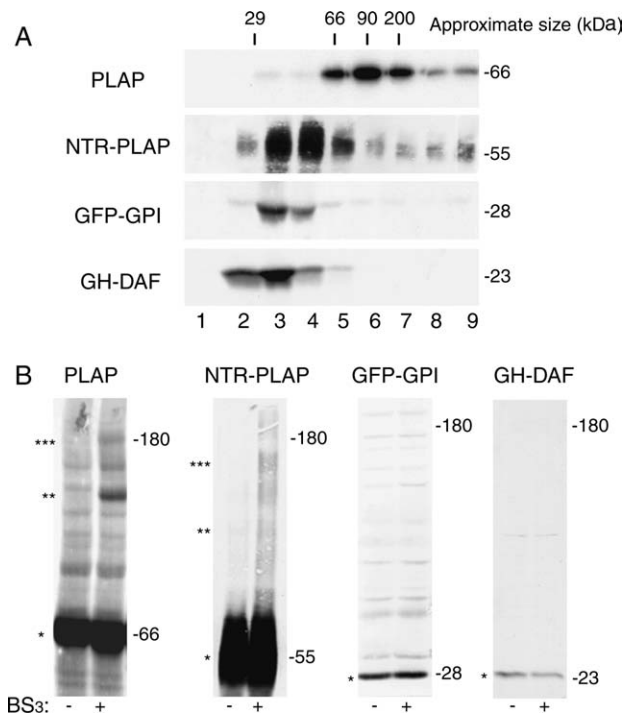
Only apical GPI-APs form HMW complexes and are found in cross-linkable complexes at the cell surface

Because in MDCK cells oligomerization appears to be a key step for apical sorting of GPI-APs (19), to test whether this could be a general mechanism for different epithelia, we purified apical and basolateral GPI proteins from FRT cells on sucrose velocity gradients in which a protein sediments according to its molecular weight (19). As in MDCK cells (19), only apical GPI-APs oligomerize in FRT cells. Indeed, while a portion of PLAP and NTR-PLAP migrated as HMW complexes containing more than a trimer, basolaterally sorted GFP-GPI and GH-DAF were purified almost exclusively from the gradient fractions corresponding to their expected monomeric molecular weights (Figure 3A).

To rule out the possibility that HMW complexes were formed as a consequence of detergent addition, we applied an impermeable cross-linking agent, bis(sulpho-succinimidyl)suberate (BS_3), that is able to link molecules that are in very close proximity (arm length 11.4 Å) (19,25) to the apical and basolateral surface of unperturbed FRT cells grown on filters. In the presence of BS_3, bands corresponding to dimers, trimers and HMWs were detected only for PLAP and NTR-PLAP (Figure 3B). In contrast, neither GFP-GPI nor GH-DAF was found in cross-linkable complexes at the basolateral surface (Figure 3B), thus suggesting that only apical GPI-APs are in HMW complexes at the cell surface. To rule out the possibility that these differences were because the apical proteins were more highly expressed/more concentrated per unit area of membrane due to exogenous expression and/or that they are better chemical substrates for the cross-linker, we used as control two apical and basolateral TM proteins endogenously expressed in FRT cells. Specifically, DPPIV, a TM nonraft apical protein, was used as a negative control for apical cross-linking, while Na,K-adenosine triphosphatase (ATPase), a nonraft basolateral marker for which multiple isoforms of three subunits, α, β and γ, form the Na,K-ATPase oligomer (26), was used as a positive control for basolateral cross-linking. We found that DPPIV is not in cross-linkable complexes although it is expressed at high levels, indicating that not all proteins on the apical surface form oligomers (Figure S1). In contrast, Na,K-ATPase migrates as HMW complexes after BS_3 addition (Figure S1). These results clearly indicate that the efficiency of the cross-linker is independent of the surface of residency, or of a different accessibility of the cross-linker to the two surfaces.
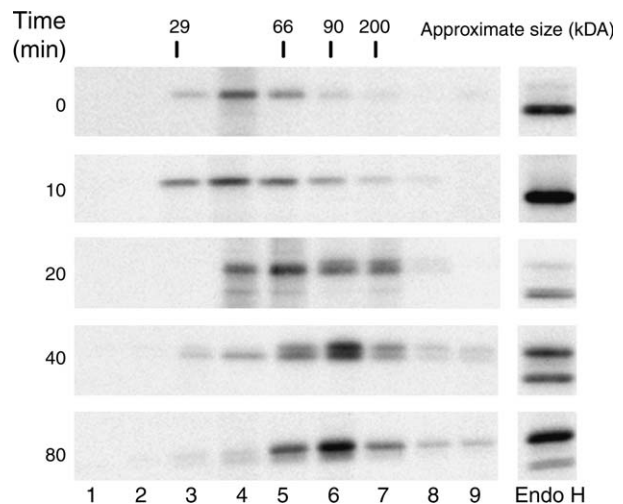
Oligomer formation occurs during passage of the protein through the Golgi

If oligomerization plays a role in apical sorting in FRT cells, as is the case in MDCK cells (19), we would expect this

A

B

Figure 3: Only apical GPI-APs form oligomers and are in cross-linkable complexes at the cell surface. A) FRT cells stably expressing PLAP, NTR-PLAP, GFP-GPI and GH-DAF were lysed in buffer containing 0.4% SDS and 0.2% TX-100 and run through a nonlinear 5–30% sucrose gradient. Fractions of 500 µl were collected from the top (fraction 1) to the bottom (fraction 9) of the gradients. Proteins were TCA precipitated and detected by Western blotting using specific antibodies. In the case of PLAP, samples, labelled with Pro-mix-[^{35}S] overnight, were immunoprecipitated from each fraction, run on SDS-PAGE and revealed by fluorography. The molecular weight of the monomeric forms of each protein is indicated. The position on the gradients of molecular weight markers is indicated on top of the panel. B) FRT cells stably expressing PLAP, NTR-PLAP, GFP-GPI and GH-DAF grown on filters were incubated with BS$_3$ (0.5 mM). After lysis, proteins were TCA precipitated, run on SDS-PAGE (in a 6–12% gradient gel for GFP-GPI and GH-DAF or 8% gel for PLAP and NTR-PLAP). The molecular weight of the monomeric forms (*) of each protein is indicated, together with the position of a 180-kDa marker. ** and *** indicate the expected molecular weight of the dimeric and trimeric forms of each protein, respectively.

event to occur during sorting of the proteins. To address this question, we analysed the kinetics of PLAP oligomerization by pulse-chase experiments combined with endoglycosidase H (Endo H) digestion (Figure 4). The acquisition of resistance to Endo H allowed us to monitor the passage of the protein through the Golgi apparatus (26,27). After a brief pulse of 10 min with [^{35}S]met/cys, cells were chased for the indicated times, lysed in SDS/TX-100 containing buffer and run on velocity gradients (Figure 4). PLAP began to form HMW complexes after 20 min of chase when a portion of the protein had acquired Endo H resistance (therefore after the medial Golgi). After 40 min of chase, when almost all PLAP was Endo H resistant,

Figure 4: HMW complex formation occurs during passage through the Golgi apparatus. FRT cells expressing PLAP were pulsed for 10 min with Pro-mix-[^{35}S] and then chased for the indicated times. At the end of each chase time, the cells were lysed and purified on velocity gradients. Samples were immunoprecipitated from each fraction, run on SDS-PAGE and revealed by fluorography. An aliquot of the lysate for each chase time was immunoprecipitated (before ultracentrifugation) and treated with Endo H to monitor passage through the medial Golgi.

~30% of the protein was found in HMW complexes (Figure 4). Consistent with the cross-linking experiments (Figure 3B), PLAP was then recovered in HMW complexes also after 80 min of chase, i.e. when the majority of the protein had already reached the plasma membrane [as previously shown by targeting experiments (12)]. These results demonstrate that also in FRT cells, apical GPI-APs oligomerize during their passage through the Golgi apparatus, where sorting is likely to occur (1,17,18,28–30).

Only the GPI-anchored but not the TM or secretory forms of NTR are able to oligomerize

A question that we then addressed is whether protein oligomerization is a specific mechanism for apical sorting of raft-associated GPI-APs or is a general mechanism utilized also for non-raft-associated apical proteins. To this aim, we compared the behaviour of the GPI-anchored form of NTR (NTR-PLAP) with those of TM (p75 NTR) and secretory (NTR-sec) forms, which are both apically sorted but are not associated with DRMs (12). Different from NTR-PLAP, we found that neither the native TM form nor its secretory form was able to oligomerize (Figure 5). These results indicate that oligomerization is a specific requirement for apical sorting of GPI-APs associated to DRMs, and that this mechanism is not used by TM or secretory non-raft-associated proteins.

Discussion

Cell membranes are organized into compositionally and functionally distinct membrane domains, a subset of which
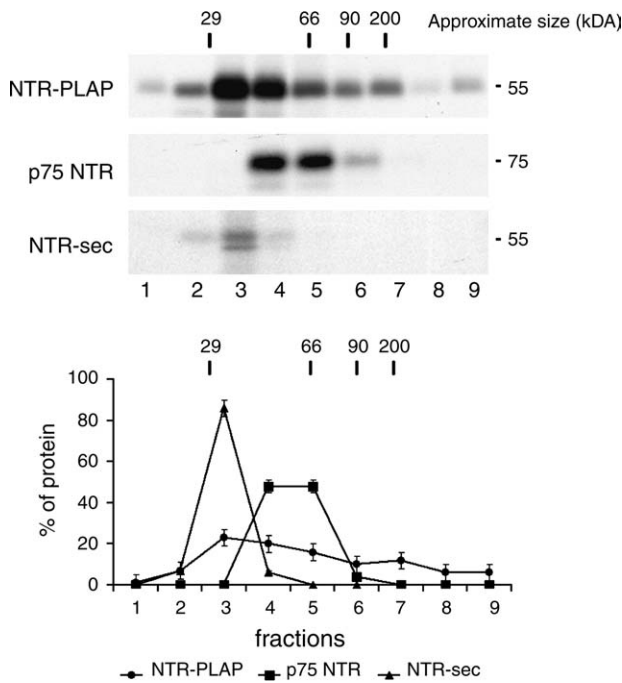
Figure 5: NTR-PLAP, but not its transmembrane or secretory forms, oligomerizes in HMW complexes. FRT cells stably expressing NTR-PLAP, p75 NTR and NTR-sec were pulsed overnight with [^{35}S]cys (250 μCi/mL). Then, cells were lysed in buffer containing 0.4% SDS and 0.2% TX-100 and run through a nonlinear 5–30% sucrose gradient. Fractions of 500 μl were collected from the top (fraction 1) to the bottom (fraction 9) of the gradients. Proteins were immunoprecipitated with an antibody against the ectodomain of p75 NTR, run on SDS-PAGE and revealed by fluorography. The molecular weight of the monomeric forms of each protein is indicated. The position on the gradients of molecular weight markers is indicated on top of the panel. The graph shows the mean value of protein distribution on sucrose density gradients from three different experiments.

are lipid rafts that represent areas enriched in sphingolipids and cholesterol. Because of their capacity to segregate specific lipids and proteins, rafts assembled within the fluid bilayer of the TGN may act as sorting platforms for inclusion of cargo proteins destined for delivery to the apical membrane (13). However, it has been recently demonstrated that raft association is not sufficient to determine apical sorting of GPI-APs (12,19,20).

Several evidences indicate that lipid rafts have to cluster together in order to engage in different membrane functions. Clustering of individual small rafts should reinforce the segregation of different lipid phases and consequently of membrane components associated with them [reviewed by Schuck and Simons (31)]. Antibodies, antigens and raft-binding proteins, such as cholera toxin, can all cluster rafts, thus promoting protein internalization, pathogen entry and/or virus budding (32–34). Similarly, by using MDCK cells, we have proposed that protein oligomeriza-

tion constitutes a cellular sorting mechanism that recruits apical GPI-APs and excludes basolateral ones (19). Oligomerization appears to stabilize proteins into rafts, possibly because oligomers have a higher affinity for rafts than their monomers, as previously suggested (35,36). It could, therefore, lead to the coalescence of small rafts into a larger raft from which the apical vesicle could bud (19). Similarly, it has been shown that raft clustering through polymerization of M-proteins, which interacts in rafts with neuraminidase and haemagglutinin, represents a key event in the budding of influenza viruses (37).

Because protein sorting and delivery to the surface is both cell and protein specific (21), in this article, we have analysed whether oligomerization represents a general requirement for apical sorting of GPI-APs in different epithelia by studying the behaviour of four different, apically and basolaterally sorted, GPI-APs in FRT cells. We have used these cells because they are well polarized but have a phenotype different from that of MDCK, in that they sort the majority of GPI-APs to the basolateral domain of the plasma membrane (23). We found that both apical (PLAP and NTR-PLAP) and basolateral (GFP-GPI and GH-DAF) GPI-APs are DRM associated (Figure 2). These data confirm previous findings showing that, independently of their sorting, GPI-APs partition into DRMs and that the GPI anchor, having specific affinity for the long and saturated acyl chains of sphingolipids, is responsible for their association with rafts (12,15,19,38,39). We also demonstrate that, as in MDCK cells, in FRT cells, raft association is not sufficient to determine apical sorting of GPI-APs. Indeed, as in MDCK cells (19), only apical GPI-APs were found in HMW complexes both during sorting, specifically during the passage through the Golgi apparatus, and at the cell surface (Figures 3 and 4). These results, therefore, indicate that oligomerization might be the prime mechanism determining GPI-AP apical sorting in different epithelia.

We cannot yet understand the mechanism that determines selective oligomerization of apical GPI-APs. One possibility is that differences in ectodomain glycosylation might be important in promoting or impairing this process because previous work indicated that glycosylation may play a major role in apical sorting (20). Another possibility, which we are also currently studying, is that differences in the GPI anchor may promote association with different lipid domains. Interestingly, like in MDCK cells, we found a shift in the migration of apical and basolateral GPI-APs on sucrose gradients. Although the DRM experiments are of limited value because they are based on the use of detergents and may not therefore represent the real *in vivo* situation (40), this result may indicate that clustered rafts associated with apical proteins have a composition different from that of rafts associated with basolateral proteins. In line with this hypothesis, we have recently shown that although there are no qualitative differences in the lipid composition of DRMs associated with apical and basolateral GPI-APs in

FRT cells, the ratio between sphingolipids and cholesterol is different (24).

Because apical proteins can be sorted both via raft-dependent and raft-independent mechanisms both in MDCK and FRT cells (12,20), which exhibit a different sorting phenotype (23), another question is whether oligomerization is also required for apical sorting of nonraft proteins. To this aim, we analysed the ability of oligomerization of the TM and secretory forms of NTR, which are both apically sorted but are not associated with DRMs. We found that, in contrast to the GPI-anchored form (NTR-PLAP), neither the native TM (p75 NTR) nor the secretory forms (NTR-sec) are able to oligomerize (Figure 5). These results clearly indicate that oligomerization is a specific requirement for apical sorting of GPI-APs. The fact that although both the TM and secretory forms of p75 NTR contained the same ectodomain of the GPI-anchored version, they were not able to oligomerize suggested that association with DRMs was required for oligomerization to occur. Rafts might provide a favourable environment for oligomerization to occur as shown by the fact that impairment of DRM association at the TGN also reduces oligomerization and affects apical sorting (19). Furthermore, the fact that oligomer formation occurs concomitantly with DRM association in the Golgi apparatus (data not shown and (19) suggests that oligomerization and association to lipid rafts co-operate to promote apical sorting of GPI-APs.

Finally, we found that oligomerization of GPI-APs begins in the medial Golgi (Figure 4) like in MDCK cells (18), indicating that in different epithelia the first sorting station for GPI-APs is the TGN. However, we cannot exclude the possibility that GPI-APs travel through post-TGN compartments before reaching the apical membrane, which might constitute a second sorting station, as previously shown for some basolateral proteins (41,42). Further studies using live imaging approach (17,18) will shed light on this issue.

Materials and Methods

Reagents and antibodies

Cell culture reagents were purchased from Gibco Laboratories (Grand Island, NY, USA). Antibodies were purchased from the following companies: polyclonal αGFP from Clontech Laboratories (East Meadow Circle, CA, USA), monoclonal αGFP from Molecular Probes (PoortGebouw, the Netherlands), αPLAP from Rockland (Gilbertsville, PA, USA), αGH from Biotrend GMBH (Cologne, Germany). The antibody against p75 was a gift from Dr A. Le Bivic (Faculté des Sciences de Luminy, Marseille, France). Biotin, horseradish peroxidase (HRP)-linked streptavidin and BS$_3$ were from Pierce (Rockford, IL, USA). All other reagents were purchased from Sigma Chemical Co. (St Louis, MO, USA).

Cell culture and transfections

The FRT cells were grown in F12 Coon's modified medium containing 5% FBS. The FRT cells were transfected with complementary DNA coding for the different proteins, using the calcium phosphate procedure, as previously described (23). Stable clones were selected by resistance to neomycin.

Fluorescence microscopy

The FRT cells were grown on transwell filters for 4 days, washed with PBS containing CaCl$_2$ and MgCl$_2$, fixed with 4% paraformaldehyde and quenched with 50 mM NH$_4$Cl. Primary antibodies were detected with TRITC-conjugated secondary antibodies. Images were collected using a Zeiss Laser Scanning Confocal Microscope (LSM 510) equipped with a planapo 63× oil-immersion (NA 1.4) objective lens.

Biotinylation assay

Cells were grown on polycarbonate filters for 4 days. Cells were selectively biotinylated from the apical and basolateral sides, and lysates were immunoprecipitated with specific antibodies and revealed on blots with HRP-streptavidin. In the case of NTR-PLAP, cells were metabolically labelled with ^{35}S-cys (100 μCi/mL) overnight, and after biotinylation, lysates were immunoprecipitated with a specific antibody and then precipitated with streptavidin beads. Sample were run on SDS-PAGE and analysed by fluorography.

Sucrose density gradients

Sucrose gradient analysis of TX-100-insoluble material was performed using previously published protocols (16,22). Cells were grown to confluency in 150-mm dishes, washed in PBS containing CaCl$_2$ and MgCl$_2$ and lysed for 20 min in TNE/1% TX-100 buffer on ice. Lysates were scraped from dishes, brought to 40% sucrose and then placed at the bottom of a centrifuge tube. A discontinuous sucrose gradient (5–35% in TNE) was layered on the top of the lysates, and the samples were centrifuged at 188000 × g for 17 h in ultracentrifuge (model SW41 Beckman Inst., Fullerton, CA, USA). One-millilitre fractions were harvested from the top of the gradient and trichloroacetic acid (TCA) precipitated. Proteins were run on SDS-PAGE and revealed by Western blotting using specific antibodies.

Velocity gradients

Velocity gradients were performed using previously published protocols (19,43). Cells were grown to confluency in 100-mm dishes, washed in PBS containing CaCl$_2$ and MgCl$_2$ and lysed for 30 min in 20 mM Tris, pH 7.4, 100 mM NaCl, 0.4% SDS and 0.2% TX-100 on ice. Lysates were scraped from dishes and sheared through a 26-g needle, and nuclei were pelleted. A sucrose gradient (5–30%) was layered, and the lysate, added on the 5% fraction, was centrifuged at 190000 × g for 16 h in ultracentrifuge (model SW 50 Beckman). Fractions of 500 μL were harvested from the top of the gradient, and then they were TCA precipitated or immunoprecipitated depending on the experiment.

Pulse chase

Cells grown in 100-mm dishes were starved of methionine and cysteine for 1 h and pulse labelled for 10 min with medium containing 100 μCi/mL of Pro-mix-[^{35}S] cell labelling (GE Healthcare, Little Chalfont, England) and incubated in chase medium (DMEM containing 5% FBS and met/cys 10×) for different times.

Endo H digestion

Digestion with Endo H was carried out on immunoprecipitated materials. The antigen–antibody complexes were removed from sepharose beads using 50 μL of 0.1 M Na citrate/0.1% SDS and boiling for 3 min. Samples were then incubated with 5 mU of Endo H for 16 h at 37°C. Samples were run on SDS-PAGE and revealed by fluorography.

Cross-linking

Cells were grown on polycarbonate filters for 4 days. BS$_3$ (0.5 mM) was added to the apical or basolateral surface for 45 min and quenched for 15 min with 20 mM Tris, pH 7.5, as described elsewhere (24). Proteins were TCA precipitated, separated on SDS-PAGE and revealed by specific antibodies.

Acknowledgments

Supplementary Material

Figure S1: DPPIV is not present in cross-linkable complexes on the apical membrane, while Na,K-ATPase is in an oligomeric complex at the basolateral surface. BS_3 (0.5 mM) was added on the apical or basolateral surface of FRT cells grown on filters. After lysis, proteins were TCA precipitated, run on SDS-PAGE (10% polyacrylamide) and revealed by Western blots using specific antibody against DPPIV [generous gift from Dr A. Quaroni (Cornell University, Ithaca, New York)] and against the subunit α1 of Na,K-ATPase (from Santa Cruz Biotechnology, Santa Cruz, CA). The molecular weight of the monomeric forms (*) of each protein is indicated, together with the position of standard markers.

Supplemental materials are available as part of the online article at http://www.blackwell-synergy.com

References

1. Rodriguez-Boulan E, Powell SK. Polarity of epithelial and neuronal cells. Annu Rev Cell Biol 1992;8:395–427.
2. Drubin DG, Nelson WJ. Origins of cell polarity. Cell 1996;84:335–344.
3. Mellman I. Endocytosis and molecular sorting. Annu Rev Cell Dev Biol 1996;12:575–625.
4. Matter K. Epithelial polarity: sorting out the sorters. Curr Biol 2000;10:R39–R42.
5. Nelson WJ, Yeaman C. Protein trafficking in the exocytic pathway of polarized epithelial cells. Trends Cell Biol 2001;11:483–486.
6. Folsch H, Ohno H, Bonifacino JS, Mellman I. A novel clathrin adaptor complex mediates basolateral targeting in polarized epithelial cells. Cell 1999;99:189–198.
7. Sugimoto H, Sugahara M, Folsch H, Koide Y, Nakatsu F, Tanaka N, Nishimura T, Furukawa M, Mullins C, Nakatura N, Mellman I, Ohno H. Differential recognition of tyrosine-based basolateral signals by AP-1B subunit mu1B in polarized epithelial cells. Mol Biol Cell 2002;13:2374–2382.
8. Scheiffele P, Peranen J, Simons K. N-Glycans as apical sorting signals in epithelial cells. Nature 1995;378:96–98.
9. Scheiffele P, Roth MG, Simons K. Interaction of influenza virus haemagglutinin with sphingolipid-cholesterol membrane domains via its transmembrane domain. EMBO J 1997;16:5501–5508.
10. Chuang JZ, Sung CH. The cytoplasmic tail of rhodopsin acts as a novel apical sorting signal in polarized MDCK cells. J Cell Biol 1998;142:1245–1256.
11. Sun AQ, Ananthanarayanan M, Soroka CJ, Thevananther S, Shneider BL, Suchy FJ. Sorting of rat liver and ileal sodium-dependent bile acid transporters in polarized epithelial cells. Am J Physiol 1998;275:G1045–G1055.
12. Lipardi C, Nitsch L, Zurzolo C. Detergent-insoluble GPI-anchored proteins are apically sorted in Fischer rat thyroid cells, but interference with cholesterol or sphingolipids differentially affects detergent insolubility and apical sorting. Mol Biol Cell 2000;11:531–542.
13. Simons K, Ikonen E. Functional rafts in cell membranes. Nature 1997;387:569–572.
14. Simons K, van Meer G. Lipid sorting in epithelial cells. Biochemistry 1988;27:6197–6202.
15. Brown DA, London E. Functions of lipid rafts in biological membranes. Annu Rev Cell Dev Biol 1998;14:111–136.
16. Brown DA, Rose JK. Sorting of GPI-anchored proteins to glycolipid-enriched membrane subdomains during transport to the apical cell surface. Cell 1992;68:533–544.
17. Hua W, Sheff D, Toomre D, Mellman I. Vectorial insertion of apical and basolateral membrane proteins in polarized epithelial cells revealed by quantitative 3D live cell imaging. J Cell Biol 2006;172:1035–1044.
18. Paladino S, Pocard T, Catino MA, Zurzolo C. GPI-anchored proteins are directly targeted to the apical surface in fully polarized MDCK cells. J Cell Biol 2006;172:1023–1034.
19. Paladino S, Sarnataro D, Pillich R, Tivodar S, Nitsch L, Zurzolo C. Protein oligomerization modulates raft partitioning and apical sorting of GPI-anchored proteins. J Cell Biol 2004;167:699–709.
20. Benting JH, Rietveld AG, Simons K. N-Glycans mediate the apical sorting of a GPI-anchored, raft-associated protein in Madin-Darby canine kidney cells. J Cell Biol 1999;146:313–320.
21. Rodriguez-Boulan E, Kreitzer G, Musch A. Organization of vesicular trafficking in epithelia. Nat Rev Mol Cell Biol 2005;6:233–247.
22. Zurzolo C, van't Hof W, van Meer G, Rodriguez-Boulan E. VIP21/caveolin, glycosphingolipid clusters and the sorting of glycosylphosphatidylinositol-anchored proteins in epithelial cells. EMBO J 1994;13:42–53.
23. Zurzolo C, Lisanti MP, Caras IW, Nitsch L, Rodriguez-Boulan E. Glycosylphosphatidylinositol-anchored proteins are preferentially targeted to the basolateral surface in Fischer rat thyroid epithelial cells. J Cell Biol 1993;121:1031–1039.
24. Tivodar S, Paladino S, Pillich R, Prinetti A, Chigorno V, van Meer G, Sonnino S, Zurzolo C. Analysis of detergent-resistant membranes associated with apical and basolateral GPI-anchored proteins in polarized epithelial cells. FEBS Lett 2006;580:5705–5712.
25. Friedrichson T, Kurzchalia TV. Microdomains of GPI-anchored proteins in living cells revealed by crosslinking. Nature 1998;394:802–805.
26. Kornfeld R, Kornfeld S. Assembly of asparagine-linked oligosaccharides. Annu Rev Biochem 1985;54:631–664.
27. Dunphy WG, Rothman JE. Compartmental organization of the Golgi stack. Cell 1985;42:13–21.
28. Keller P, Toomre D, Diaz E, White J, Simons K. Multicolour imaging of post-Golgi sorting and trafficking in live cells. Nat Cell Biol 2001;3:140–149.
29. Wandinger-Ness A, Bennett MK, Antony C, Simons K. Distinct transport vesicles mediate the delivery of plasma membrane proteins to the apical and basolateral domains of MDCK cells. J Cell Biol 1990;111:987–1000.
30. Mostov KE, Verges M, Altschuler Y. Membrane traffic in polarized epithelial cells. Curr Opin Cell Biol 2000;12:483–490.
31. Schuck S, Simons K. Polarized sorting in epithelial cells: raft clustering and the biogenesis of the apical membrane. J Cell Sci 2004;117:5955–5964.
32. Abrami L., van Der Goot FG. Plasma membrane microdomains act as concentration platforms to facilitate intoxication by aerolysin. J Cell Biol 1999;147:175–184.
33. Pelkmans L, Helenius A. Endocytosis via caveolae. Traffic 2002;3:311–320.
34. Parton RG, Richards AA. Lipid rafts and caveolae as portals for endocytosis: new insights and common mechanisms. Traffic 2003;4:724–738.

35. Cunningham O, Andolfo A, Santovito ML, Iuzzolino L, Blasi F, Sidenius N. Dimerization controls the lipid raft partitioning of uPAR/CD87 and regulates its biological functions. EMBO J 2003;22:5994–6003.

36. Fivaz M, Vilbois F, Thurnheer S, Pasquali C, Abrami L, Bickel PE, Parton RG, van der Goot FG. Differential sorting and fate of endocytosed GPI-anchored proteins. EMBO J 2002;21:3989–4000.

37. Zhang J, Pekosz A, Lamb RA. Influenza virus assembly and lipid raft microdomains: a role for the cytoplasmic tails of the spike glycoproteins. J Virol 2000;74:4634–4644.

38. Benting J, Rietveld A, Ansorge I, Simons K. Acyl and alkyl chain length of GPI-anchors is critical for raft association in vitro. FEBS Lett 1999;462:47–50.

39. Mayor S, Riezman H. Sorting GPI-anchored proteins. Nat Rev Mol Cell Biol 2004;5:110–120.

40. Schuck S, Honsho M, Ekroos K, Shevchenko A, Simons K. Resistance of cell membranes to different detergents. Proc Natl Acad Sci USA 2003;100:5795–5800.

41. Salas-Cortes L, Ye F, Tenza D, Wilhelm C, Theos A, Louvard D, Raposo G, Coudrier E, Warrent G, Mellman I. Myosin Ib modulates the morphology and the protein transport within multi-vesicular sorting endosomes. J Cell Sci 2005;118:4823–4832.

42. Ang AL, Taguchi T, Francis S, Folsch H, Murrells LJ, Pypaert M et al. Recycling endosomes can serve as intermediates during transport from the Golgi to the plasma membrane of MDCK cells. J Cell Biol 2004;167:531–543.

43. Scheiffele P, Verkade P, Fra AM, Virta H, Simons K, Ikonen E. Caveolin-1 and -2 in the exocytic pathway of MDCK cells. J Cell Biol 1998;140:795–806.

ANNEX 2

Analysis of detergent-resistant membranes associated with apical and basolateral GPI-anchored proteins in polarized epithelial cells

Simona Tivodar[a], Simona Paladino[a,b], Rudolf Pillich[a], Alessandro Prinetti[c], Vanna Chigorno[c], Gerrit van Meer[d], Sandro Sonnino[c], Chiara Zurzolo[a,e,*]

[a] *Dipartimento di Biologia e Patologia Cellulare e Molecolare, Università degli Studi di Napoli Federico II, via S. Pansini 5, 80131 Napoli, Italy*
[b] *CEINGE Biotecnologie Avanzate S.C.A.R.L., 80145 Napoli, Italy*
[c] *Center of Excellence on Neurodegenerative Diseases, Department of Medical Chemistry, Biochemistry and Biotechnology, University of Milan, 20090 Segrate, Italy*
[d] *Department of Membrane Enzymology, Padualaan 8, 3584 CH, Utrecht University, The Netherlands*
[e] *Unité de Trafic Membranaire et Pathogénèse, Institut Pasteur, 25 rue du Docteur Roux, 75724 Paris Cedex 15, France*

Abstract Detergent-resistant membranes (DRMs) represent specialized membrane domains resistant to detergent extraction, which may serve to segregate proteins in a specific environment in order to improve their function. Segregation of glycosylphosphatidylinositol-anchored proteins (GPI-APs) in DRMs has been shown to be involved in their sorting to the apical membrane in polarized epithelial cells. Nonetheless, we have shown that both apical and basolateral GPI-APs associate with DRMs. In this report we investigated the lipid composition of DRMs associated with an apical and a basolateral GPI-AP.

We found that apical and basolateral DRMs contain the same lipid species although in different ratios. This specific lipid ratio is maintained after mixing the cells before lysis indicating that DRMs maintain their identity after Triton extraction.
© 2006 Federation of European Biochemical Societies. Published by Elsevier B.V. All rights reserved.

1. Introduction

Lipid rafts constitute distinct liquid ordered phases enriched in sphingolipids and cholesterol that are resistant to extraction in cold detergents [1–3]. Because they segregate proteins and lipids in specific regions of the membranes, they have been implicated in several cell functions such as signalling and sorting [4]. One case in point is the one of glycosylphosphatidylinositol (GPI)-anchored proteins (GPI-APs) that are apically sorted in a range of polarized epithelial cell lines [2,5,6]. It has been proposed that GPI-APs are sorted to the apical surface via their incorporation in rafts [7]. However, the finding that in FRT cells GPI-APs are mainly delivered to the basolateral membrane [8,9] and that in MDCK cells both apical and basolateral GPI-APs associate with DRMs (detergent-resistant membranes) indicate that rafts are not sufficient to determine their apical sorting [10]. Furthermore, we have found that protein oligomerization, which could promote the stabilization of GPI-APs into rafts, is needed for their apical sorting [10]. The factors that promote protein oligomerization and apical sorting are still unclear. We consider two different hypotheses to be most likely: (1) the protein ectodomain may have a key role in determining first oligomerization and then stabilization into rafts, or (2) apical and basolateral proteins associate with different microdomains that would determine the rate of their clustering and therefore be responsible for the differential sorting. The latter hypothesis is supported by the fact that caveolae, which are specialized lipid microdomains, have been found enriched on the basolateral domain of several epithelial cell lines [11,12]. In addition, Thy-1 and PrPc, two GPI-APs respectively enriched in the axon and in the cell body of neurons, resembling the apical and basolateral domain of epithelial cells, associate with lipid microdomains of different composition [13].

In order to study the lipid composition of the apical and basolateral DRMs and to understand whether they maintain their specific composition after Triton extraction we analyzed the lipid fraction that co-immunoprecipitated with an apical (PLAP) and basolateral (GH-DAF) GPI-AP in DRMs from single or mixed FRT/PLAP and FRT/GH-DAF clones.

2. Material and methods

2.1. Reagents and antibodies

Cell culture reagents were purchased from Gibco Laboratories (Grand Island, NY). The anti-PLAP antibody was from Rockland (Gilgertsville, PA), the anti-GH antibody was from Biotrend GMBH (Germany) and the anti-flotillin antibody was from BD Biosciences Pharmingen (San Jose, CA). Biotin and HRP-conjugated streptavidin were from Pierce (Rockford, IL). Protein G- and A-coupled magnetic beads (dynabeads) were from Dynal ASA (Oslo, Norway). All other reagents were purchased from Sigma Chemical Co. (St Louis, MO).

*Corresponding author. Fax: +33 (0) 1 40613238.
E-mail addresses:* zurzolo@pasteur.fr,
zurzolo@unina.it (C. Zurzolo).

[1-^{3}H]-sphingosine (radiochemical purity over 98%; specific radioactivity 2 Ci/mmol) was prepared as previously described [14].

2.2. Cell culture and transfections

FRT cells were grown in F12 Coon's medium containing 5% FBS and stably transfected with GH-DAF cDNA as previously described [15]. FRT clones expressing PLAP were previously obtained [9]. Surface expression of transfected GPI-APs was analyzed by confocal microscopy (Zeiss 510 LSM) and by biotinylation of cells grown on filters for 4 days as previously described [10].

2.3. Assays for DRM association

2.3.1. Triton X-100 (TX-100) extraction.
Cells grown to confluency from one 60-mm dish ($\sim 2 \times 10^6$) were washed twice with PBS containing 1 mM CaCl$_2$ and 1 mM MgCl$_2$ and then lysed for 20 min on ice in 1 ml TNE/TX-100 buffer (25 mM Tris–HCl, pH 7.5, 150 mM NaCl, 5 mM EDTA, 1% TX-100) and separated by centrifugation into soluble and insoluble fraction as previously described [2].

2.3.2. Sucrose density gradients.
Cells that had just reached confluency in 150-mm dishes (20-25 $\times 10^6$) were subject to ultracentrifugation on discontinuous sucrose gradients as previously described [16]. Briefly, cells harvested in PBS containing 0.4 mM Na$_3$VO$_4$ were suspended in 1 ml lysis buffer on ice (1% TX-100, 10 mM Tris buffer, pH 7.5, 150 mM NaCl, 5 mM EDTA, 1 mM Na$_3$VO$_4$, 1 mM PMSF and 75 mU/ml aprotinin), Dounce homogenized. Post-nuclear supernatants (~ 8 mg proteins) were mixed with an equal volume of 85% sucrose (wt/vol) in 10 mM Tris buffer, pH 7.5, 150 mM NaCl, 5 mM EDTA, 1 mM Na$_3$VO$_4$, and run on discontinuous sucrose gradients (30–5%) at $200000 \times g$ for 17 h at 4 °C. Eleven 1 ml fractions were collected starting from the top of the tube. Fraction 5, located at the interface between 5% and 30% sucrose, was regarded as the sphingolipid-enriched membrane fraction.

2.4. [^{3}H]-sphingosine labelling and lipid analysis

Cells from two 150-mm dishes ($40-50 \times 10^6$) were incubated in the presence of 4×10^{-8} M [1-^{3}H]-sphingosine (7 ml/dish) in culture medium for 2 h and then chased for 48 h in fresh culture medium [16]. The radioactivity associated with cells and with cell fractions was determined by liquid scintillation counting. Labelled samples were dialyzed and lyophilized. [^{3}H] lipids were extracted twice with 0.4 ml chloroform/methanol 2:1 (v/v), separated by mono-dimensional HPTLC using the solvent system chloroform/methanol/0.2% acqueous CaCl$_2$ 55:45:10 (v/v/v), revealed by digital autoradiography (250 dpm applied on a 3 mm line) with a Beta-Imager 2000 instrument, and analyzed by β-Vision software (Biospace, Paris) [16]. Cholesterol was quantified after separation on HPTLC by visualization with 15% concentrated sulphuric acid in 1-butanol [16]. Phosphatidylcholine was separated by a two-run mono-dimensional HPTLC using the solvent system chloroform/methanol 9:1 (v/v), followed by the solvent system chloroform/methanol/acid acetic/water 30:20:2:1 (v/v/v/v) and quantified after separation on HPTLC followed by specific detection with a molybdate reagent. Cholesterol and phosphatidylcholine were quantified by densitometry and comparison with known amounts of standard lipids (Molecular Analyst program, Bio-Rad Laboratories).

2.5. Immunoprecipitation

Cells grown to confluency from two 150-mm dishes ($40-50 \times 10^6$) were labelled with [1-^{3}H]-sphingosine and subject to ultracentrifugation on discontinuous sucrose gradients as aforementioned. Aliquots of fraction 5 (800 μl) diluted with 200 μl lysis buffer (5% TX-100, 10 mM Tris buffer, pH 7.5, 150 mM NaCl, 5 mM EDTA, 1 mM Na$_3$VO$_4$, 1 mM PMSF and 75 mU/ml aprotinin) were precleared twice with dynabeads for 2 h and incubated overnight at 4 °C with anti-PLAP or anti-GH antibodies. Immunoprecipitates were recovered using protein A- or protein G-coupled magnetic beads [16]. Lipids
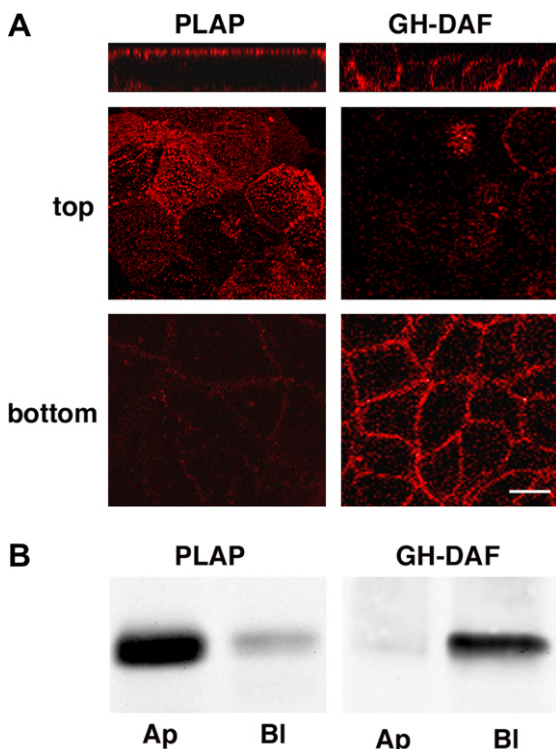

Fig. 1. PLAP and GH-DAF are differently sorted in FRT cells. PLAP or GH-DAF FRT clones were grown to confluency on filters, fixed and stained with specific antibodies against PLAP and GH followed by TRITC-conjugated secondary antibody in non-permeabilized conditions. Serial confocal sections were collected from the top to the bottom of cell monolayers (A). LC-biotin was added to the apical or the basolateral surface of FRT clones. Biotinylated proteins were immunoprecipitated using specific antibodies to PLAP or GH and revealed with HRP-conjugated streptavidin (B). Bar = 10 μm.

Fig. 2. Both PLAP and GH-DAF associate with DRMs. PLAP or GH-DAF clones were lysed in TNE/TX-100 buffer at 4 °C and separated by centrifugation into insoluble and soluble fractions. Percentages of insoluble and soluble proteins in TX-100 from three experiments are shown. Errors bars are indicated (A). Eleven 1 ml fractions were collected from top (1) to bottom (11) from sucrose density gradients. Proteins were analyzed by SDS–PAGE and detected by Western blotting using specific anti-PLAP, anti-GH and anti-flotillin-2 antibodies. An aliquot of each fraction was spotted on the nitrocellulose membrane and GM$_1$ was revealed using cholera-toxin conjugated to HRP (B).

were extracted from the immunoprecipitates and analyzed as described above. 1/5 of the samples were analyzed by SDS–PAGE.

3. Results

3.1. Analysis of surface distribution and DRM association of PLAP and GH-DAF in FRT cells

The surface distribution of PLAP (placental alkaline phosphatase, a native GPI-AP) and GH-DAF (in which growth hormone is fused with the GPI-attachment signal from DAF) was analyzed by immunofluorescence and confocal microscopy in stably transfected FRT cells grown in polarized conditions on transwell filters (Fig. 1A). These experiments confirmed that PLAP was preferentially localized on the apical domain [9], while GH-DAF was preferentially localized on the basolateral domain, in agreement with what has been shown in MDCK cells [10]. By surface biotinylation we quantified the surface distribution of the two proteins that was respectively
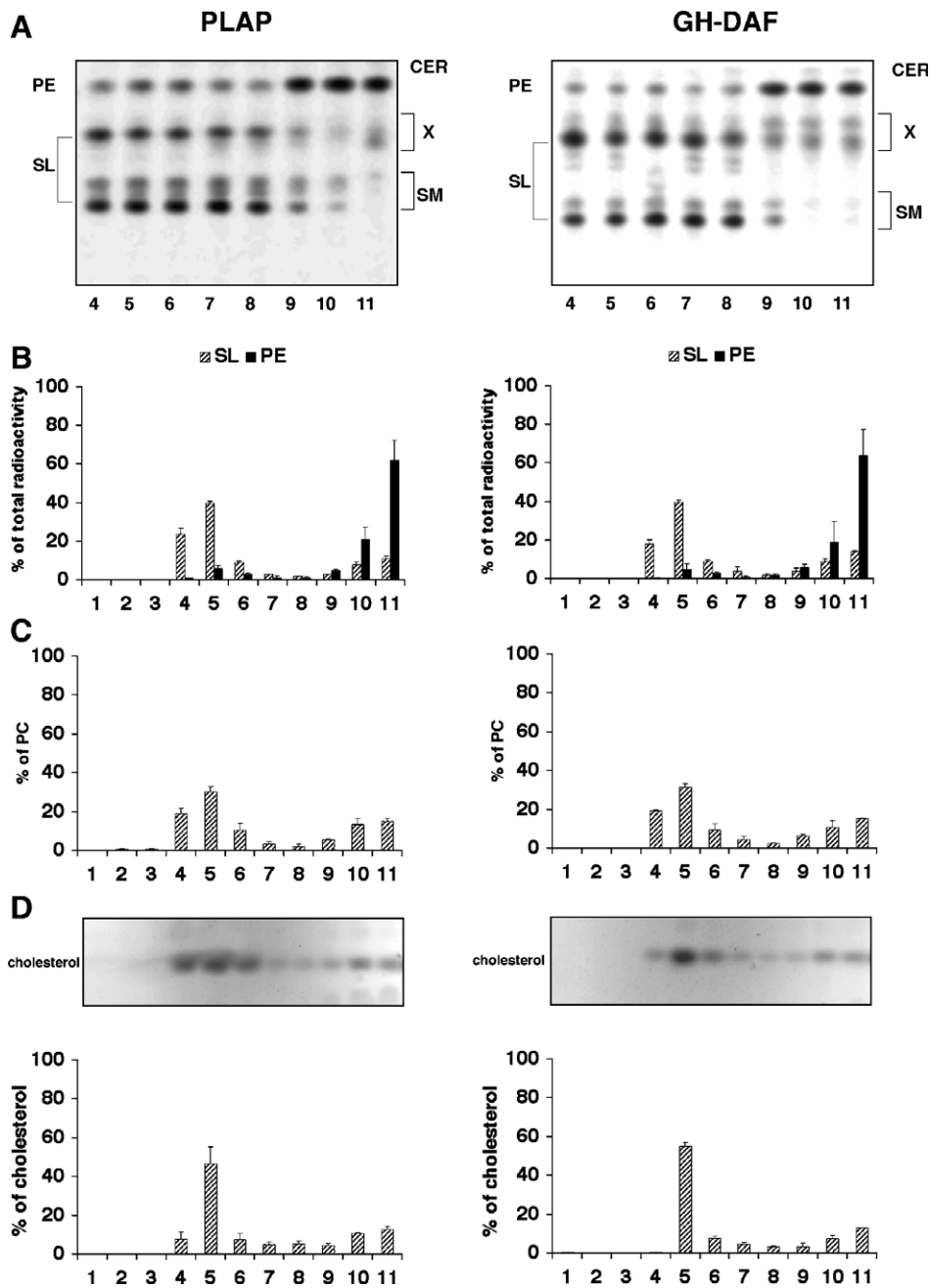
Fig. 3. Lipid distribution on sucrose density gradients. PLAP or GH-DAF clones were labelled with [³H]-sphingosine, lysed in TNE/TX-100 at 4 °C and run on sucrose density gradients. Lipids from each of the 11 fractions were extracted in chloroform/methanol. 250 dpm/fraction was separated by HPTLC and detected by autoradiography (A). We have indicated with X the unknown species of sphingolipids labelled with [³H]-sphingosine. Quantitation of sphingolipid and PE radioactivity distribution within the gradient fractions. Data are expressed as % of total radioactivity associated with each lipid present in homogenate (B). The distribution of PC and cholesterol, measured by colorimetric assays, are respectively shown in (C) and (D). Data are expressed as % of each lipid present in homogenate. Data are the means of three independent experiments ± S.D.
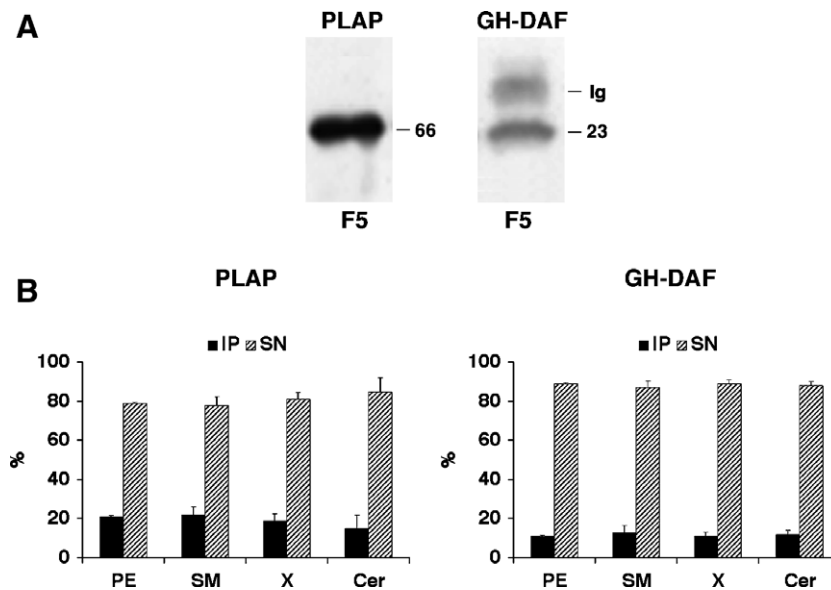
Fig. 4. Lipid analysis of DRMs associated with PLAP or GH-DAF. PLAP or GH-DAF clones were labelled with [^{3}H]-sphingosine, lysed in TNE/ TX-100 at 4 °C and purified by centrifugation to equilibrium on sucrose density gradients. Fraction 5 was immunoprecipitated using either PLAP or GH-DAF antibodies. Proteins (1/5 of immunoprecipitate) were run on SDS–PAGE and revealed by Western blotting (A). Lipids associated with immunoprecipitates (IP) were extracted in chloroform/methanol and separated by HPTLC. The quantitation of radioactive lipids (SM, Cer, X, PE) is shown in (B). For each lipid species values are expressed as percent of radioactivity present in immunoprecipitates and in the supernatant (SN) (B). Data are the means of three independent experiments ± S.D.

Table 1
Distribution of radioactivity after immunoprecipitation with anti-PLAP or anti-GH antibodies in sphingolipid-enriched membrane fractions from FRT cells in culture

	Total	IP	% in IP	Preclear	Supernatant
FRT cells expressing PLAP (IP αPLAP)	243 100	46 100	19 ± 0.6	19 500	177 500
FRT cells expressing GH-DAF (IP αGH)	257 500	28 200	11 ± 1.5	22 000	207 300
Mixed cells (IP αPLAP)	257 000	34 900	13 ± 1	16 100	205 700
Mixed cells (IP αGH)	257 000	17 100	7 ± 0.7	22 400	217 500

Cell lipids were previously metabolically labelled with [^{3}H]-sphingosine. Data are expressed in dpm. Percentages represent values of three independent experiments ± S.D.

Table 2
Percent of spingosine-labelled lipid species in the anti-PLAP or anti-GH immunoprecipitates of fraction 5

	PE	SM	X	Cer
FRT cells expressing PLAP (IP αPLAP)	22 ± 1	63 ± 3.6	12 ± 3.2	3 ± 0.6
FRT cells expressing GH-DAF (IP αGH)	20 ± 2	64 ± 1.5	13 ± 3.2	3 ± 1
Mixed cells (IP αPLAP)	14 ± 2.3	62 ± 1	21 ± 3.2	3 ± 1
Mixed cells (IP αGH)	14 ± 2	63 ± 2.6	20 ± 2	3 ± 1

Percentages represent values of three independent experiments ± S.D.

~90% apical for PLAP and ~99% basolateral for GH-DAF (Fig. 1B).

In order to analyze the amount of PLAP and GH-DAF associated with DRMs we performed TX-100 extraction and flotation on sucrose density gradients, as previously described [2,10,16]. At steady state both proteins (respectively ~80% of total PLAP and ~61% of total GH-DAF) were insoluble in TX-100 (Fig. 2A). After centrifugation to equilibrium on sucrose density gradients both proteins peaked in fraction 5 at the interface between 5% and 30% sucrose which is the most representative fraction of DRMs [16], as shown by the flota-

Table 3
Distribution of cholesterol after immunoprecipitation with anti-PLAP or anti-GH antibodies in sphingolipid-enriched membrane fractions from labelled FRT cells in culture

	Total	IP	% in IP	Preclear	Supernatant
FRT cells expressing PLAP (IP αPLAP)	164.0	24.5	15 ± 1	n.a	123.3
FRT cells expressing GH-DAF (IP αGH)	184.0	16.6	9 ± 2.5	n.a	151.1
Mixed cells (IP αPLAP)	168.0	20.7	12 ± 2	n.a	133.0
Mixed cells (IP αGH)	168.0	11.1	7 ± 1	n.a	142.5

Data are expressed in nmol. n.a., not analyzed. Percentages represent values of three independent experiments ± S.D.

tion profiles of flotillin-2 and GM_1 used as control bona-fide DRM markers (Fig. 2B). In contrast to the majority of the proteins in the cell lysates that accumulated in the soluble fractions (8–11) (data not shown) about 63% of PLAP and 68% of GH-DAF were enriched in fractions 4–6 (Fig. 2B), thus indicating that both apical and basolateral GPI-APs are associated with DRMs.

3.2. Analysis of the lipid composition of DRMs in PLAP or GH-DAF expressing FRT cells

In order to understand whether the DRM composition was affected by the exogenous expression of apical or basolateral GPI-APs, we analyzed the lipid composition of the DRM fraction in FRT cells expressing either PLAP or GH-DAF. Cells were labelled with $[1-^3H]$-sphingosine, which is converted into more complex sphingolipids, while the catabolic tritiated ethanolamine fragment is recycled for the biosynthesis of phosphatidylethanolamine (PE), a glycerophospholipid that is a marker of non-DRM fractions [16,17]. The radioactive lipid pattern was determined by HPTLC and radioimaging of the 11 fractions collected from sucrose density gradient centrifugation (Fig. 3A). Sphingolipids (SL) (sphingomyelin (SM) and the unknown X species of sphingolipids labelled with $[1-^3H]$-sphingosine) were highly enriched in fraction 5 (Fig. 3B), while the majority of PE was found, as expected, in the soluble fractions of the sucrose density gradients in both the cell lines (Fig. 3B).

Phosphatidylcholine (PC) analyzed by HPTLC and a colorimetric assay was also quite enriched in fraction 5 from both clones (Fig. 3C), as previously described [16,17]. Finally, ~42 nmol/mg protein of cholesterol was found in the post-nuclear supernatants and about 50% of it was associated with fraction 5 in both FRT clones (Fig. 3D). Thus these data show that the lipid distribution along sucrose density gradients is similar in both clones (Fig. 3) and is not affected by protein expression.

3.3. Lipid analysis of DRM fractions associated with PLAP or GH-DAF

To analyze whether apical and basolateral GPI-APs associated to similar DRMs we specifically immunoprecipitated each protein from fraction 5 of the gradients after $[^3H]$-sphingosine-labelling (Fig. 4A). About 19% and 11%, respectively, of the total radioactivity present in fraction 5 was recovered respectively in the PLAP or GH-DAF immunoprecipitates, representing co-immunoprecipitated labelled sphingolipids (Table 1). After chloroform/methanol 2:1 (v/v) extraction, HPTLC and digital autoradiography ~22% of SM, ~15% of Cer and ~21% of PE were associated with PLAP immunoprecipitates while ~13% of SM, ~12% of Cer and ~11% of PE were found in the GH-DAF immunoprecipitates (Fig. 4B). The relative

percentage of each type of labelled lipid in PLAP and GH immunoprecipitates of fraction 5 was very similar (Table 2). The total lipid extracts of the immunoprecipitates were then analyzed for cholesterol (~24.5 nmol for PLAP and ~16.6 nmol for GH-DAF) (Table 3) and for PC (~19% for PLAP and ~6% for GH-DAF) (Table 4). The ratio between $[^3H]$-SM:cholesterol:PC was 2663:2.24:1 (dpm:nmol:nmol) for PLAP and 4346:4.48:1 (dpm:nmol:nmol) for GH-DAF indicating that there were no significant qualitative differences in the lipid composition of DRMs associated with the apical or basolateral GPI-AP. However, the calculation of the relative lipid enrichment (SL or cholesterol over PC) clearly shows that DRMs associated with basolateral GH-DAF contain higher amounts of SL and cholesterol with respect to apical PLAP (Table 5).

3.4. Effect of TX-100 on DRM formation

To rule out the possibility that TX-100 had an effect in mixing apical and basolateral DRMs we performed TX-100 extraction and separation on sucrose density gradients after mixing the two cell lines previously labelled with $[^3H]$-sphingosine. As shown in Fig. 5 the distribution of proteins (Fig. 5A), radioactive lipids (Fig. 5B), PC (Fig. 5C) and cholesterol (Fig. 5D) after separation of the mixed lysates on sucrose density gradients was similar to that from gradients derived from the single cell line extracts (compare Fig. 5 with Fig. 3).

Fraction 5 was then immunoprecipitated using either anti-PLAP or anti-GH antibodies and proteins were analyzed by SDS–PAGE and Western blotting (Fig. 6A). In these mixed lysates GH-DAF was not co-immunoprecipitated with the anti-PLAP antibody and vice-versa (Fig. 6A), therefore indicating that the addition of the detergent does not lead to a mixing of the two proteins or their surrounding environments. As expected about half of the total lipid radioactivity was recovered in the mixed compared to the single lysate immunoprecipates (~13% for PLAP and ~7% for GH-DAF) (Table 1). As shown in Fig. 6B ~17% of SM, ~15% of Cer and ~10% of PE was associated with PLAP immunoprecipitates while ~8% (SM), ~7% (Cer) and ~5% (PE) were recovered in the GH immunoprecipitates. Thus the relative percentage of each type of radiolabelled lipid immunoprecipitated either with anti-PLAP or

Table 5
Relative enrichment of sphingolipids and cholesterol over phosphatidylcholine (PC) in the anti-PLAP or anti-GH immunoprecipitates

	IP single cells	IP mixed cells
$\frac{(\text{Sphingolipids/PC})_{DAF}}{(\text{Sphingolipids/PC})_{PLAP}}$	1.8	1.6
$\frac{(\text{cholesterol/PC})_{DAF}}{(\text{cholesterol/PC})_{PLAP}}$	1.9	1.8

Table 4
Distribution of phosphatidylcholine after immunoprecipitation with anti-PLAP or anti-GH antibodies in sphingolipid-enriched membrane fractions from labelled FRT cells in culture

	Total	IP	% in IP	Preclear	Supernatant
FRT cells expressing PLAP (IP αPLAP)	57.6	10.9	19 ± 2	n.a.	41.7
FRT cells expressing GH-DAF (IP αGH)	62.0	3.7	6 ± 0.7	n.a.	53.3
Mixed cells (IP αPLAP)	57.8	5.1	9 ± 1.4	n.a.	47.8
Mixed cells (IP αGH)	57.8	1.7	3 ± 0.7	n.a.	48.9

Data are expressed in nmoles. n.a., not analyzed. Percentages represent values of two independent experiments ± S.D.
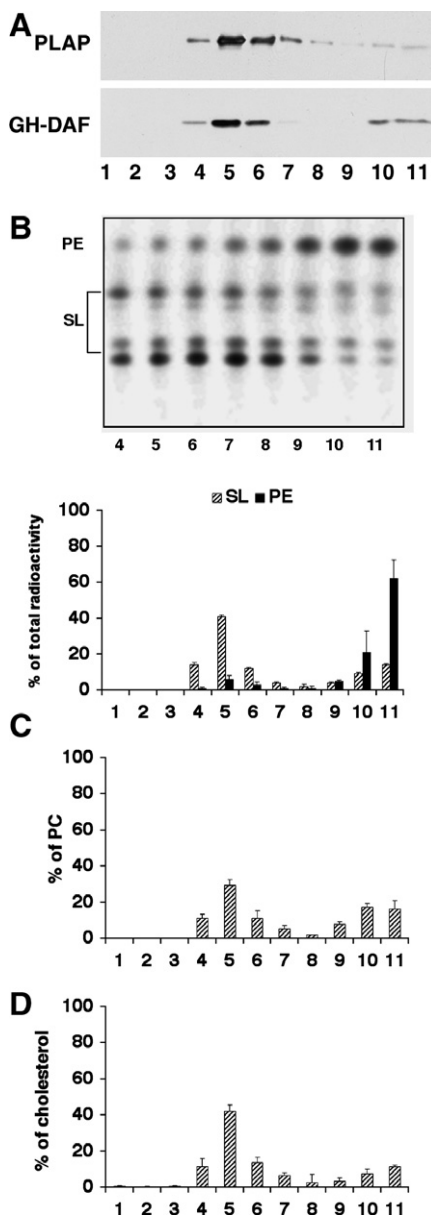
Fig. 5. Protein and lipid distribution on sucrose density gradients from mixed lysates of cells expressing PLAP and GH-DAF. PLAP and GH-DAF clones (plated in the same number) were labelled with [³H]-sphingosine, harvested, mixed together and lysed in TNE/TX-100 buffer at 4 °C. TX-100 extracts were purified by centrifugation to equilibrium on sucrose density gradients. Proteins were run on SDS–PAGE and PLAP and GH-DAF were detected by Western blotting (A). Lipids were extracted and detected as described in Fig. 3. The distribution of sphingosine-labelled species on sucrose density gradients and their quantitation are shown in (B) (upper and lower panel, respectively). PC and cholesterol distributions are shown in (C) and (D), respectively. Data are expressed as % of each lipid present in the homogenate. Data are the means of two independent experiments ± S.D.

anti-GH remained constant between single and mixed lysates (Table 2). Interestingly, we observed a higher cholesterol recovery, both in PLAP (∼20 nmol) and GH (∼11 nmol) immunoprecipitates, from the mixed lysates (Table 3). Like for SL the amount of PC recovered in the immunoprecipitates of fraction 5 from the mixed lysates was about half of the

amount in the single lysates (Table 4). The ratio [³H]-SM: cholesterol:PC, in the immunoprecipitates was respectively 3700:4.05:1 (dpm:nmol:nmol) for PLAP, and 5335:6.5:1 (dpm:nmol:nmol) for GF-DAF, similar to the ratio found in the immunoprecipitates from single cell lysates (Table 5). These results confirmed that the composition of DRMs associated with an apical and a basolateral GPI-AP are qualitatively very similar and showed that the relative enrichment of the different lipid species was maintained in the mixed lysates compared to single lysate (Table 5).

4. Discussion

We have investigated here the lipid composition of DRMs associated with PLAP and GH-DAF, respectively sorted to the apical and basolateral domains of FRT cells, in order to understand whether apical and basolateral GPI-APs are surrounded by a different lipid environment and whether this could be linked to their different sorting. We found that PLAP and GH-DAF were similarly distributed in a 2-step sucrose density gradient (Fig. 2) and were enriched in fraction 5 to similar extents (∼30%). This fraction contains ∼40% of cellular sphingolipids, ∼50% of cellular cholesterol and ∼30% of cellular PC (Fig. 3), but only 5% of cellular PE (Fig. 3), clearly indicating a lipid segregation in the different gradient fractions. These results support the increasing evidence for the existence of specialized lipid domains in the membrane [2,16] and indicate that the lipid distribution found in FRT cells is similar to that recovered from other cell lines [2,16,18]. Our data also show that DRM-fractions derived from different FRT clones are similar, therefore indicating that the expression of different GPI-APs does not alter lipid extraction nor their distribution on sucrose gradients.

After labelling the cells with [1-³H]-sphingosine we analyzed the lipids co-immunoprecipitated with PLAP and GH-DAF from the DRM fraction of sucrose gradients. We found no qualitative differences in the lipid species co-purified with apical or basolateral GPI-APs (Fig. 4). However, a different ratio between the lipid species was consistently observed in different experiments and was maintained after mixing the two FRT clones before lysis (Fig. 6), thus demonstrating that there is no artificial lipid mixing or domain formation caused by TX-100 extraction and suggesting that the co-immunoprecipitated lipids represent the boundary lipids around each protein [3]. Specifically we found an enrichment of SL and cholesterol over PC in the DRM fraction co-immunoprecipitated with basolateral GH-DAF compared to the ones co-immunoprecipitated with apical PLAP (Table 5). These data are in agreement with recent data demonstrating a twofold increase in the cholesterol:phospholipids ratio in the basolateral membrane of guinea pig colonic epithelia compared to the apical one [19]. Cholesterol plays an important role as a linker molecule [3], but it can also cause or enhance lateral separation of lipids, depending on its concentration. Higher cholesterol in the epithelial basolateral membrane leads to higher permeability compared to the apical one that needs to be better protected from the external aggression [19]. Furthermore, a high amount of cholesterol could lead to greater spacing between basolateral GPI-APs, therefore impairing the possibility for them to come into closer contact with each other and ultimately
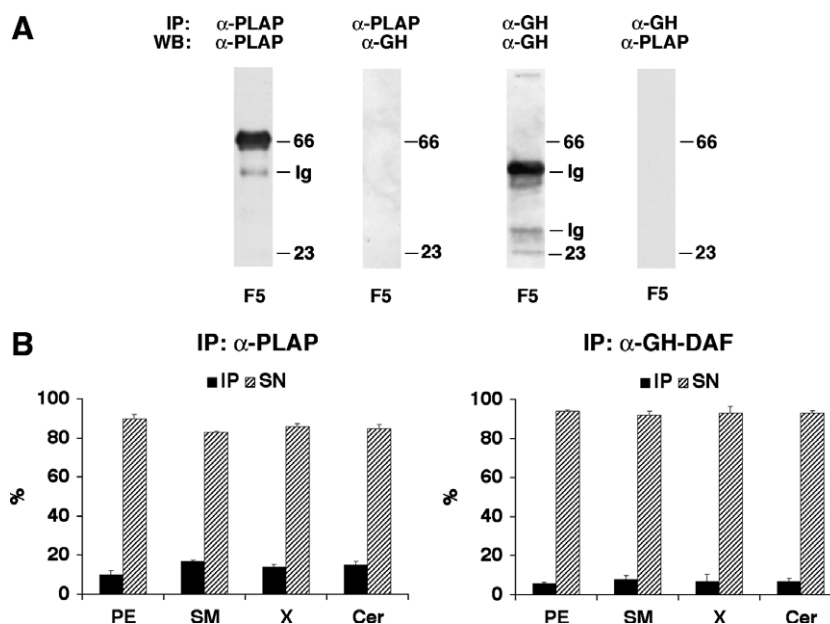
Fig. 6. Lipid analysis of DRMs associated with PLAP- or GH-DAF-associated DRMs derived from mixed cell lysates. FRT cells expressing PLAP and GH-DAF were labelled with [³H]-sphingosine, harvested, mixed together and lysed in TNE/TX-100 buffer at 4 °C. TX-100 extracts were purified by centrifugation to equilibrium on the sucrose gradients. Fraction 5 was immunoprecipitated using antibodies against PLAP or GH-DAF. Proteins (1/5 of immunoprecipitate) were run on SDS–PAGE and revealed by Western blotting using specific anti-PLAP or anti-GH antibodies (A). The molecular weights of PLAP (66 kDa) and GH-DAF (23 kDa) and immunoglobulins (Ig) are indicated. Lipids were extracted and detected as described in Fig. 3. The distribution of radioactive lipids (SM, Cer, X, PE) is shown. For each lipid species values are expressed as percents of radioactivity present in immunoprecipitates (IP) and in the supernatants (SN) (B).

impairing their oligomerization, a process that we have shown to be necessary for apical GPI-APs sorting [10]. The glycolipid anchor of GPI-APs could also have an active role in this process by promoting a different affinity for different kinds of lipid microdomains. Consequently, if a GPI-AP is in a favorable lipid environment for oligomerization, then it could be apically sorted. Affinity for lipid rafts and oligomerization could work synergistically to promote apical sorting of GPI-APs. At this stage we cannot conclude whether the quantitative differences that we have found in the lipid composition of DRMs associated with apical and basolateral GPI-APs have a direct role in apical sorting, but our results will allow further analysis that will aim to address the role of the proteinaceus ectodomain and the role of the GPI-anchor. Only when all these additional possibilities have been explored will we be able to have a complete picture of the mechanism and of the different factors involved in apical sorting of GPI-APs.

References

[1] Brown, D.A. and London, E. (2000) Structure and function of sphingolipid- and cholesterol-rich membrane rafts. J. Biol. Chem. 275, 17221–17224.

[2] Brown, D.A. and Rose, J.K. (1992) Sorting of GPI-anchored proteins to glycolipid-enriched membrane subdomains during transport to the apical cell surface. Cell 68, 533–544.

[3] Simons, K. and Vaz, W.L. (2004) Model systems, lipid rafts, and cell membranes. Annu. Rev. Biophys. Biomol. Struct. 33, 269–295.

[4] Simons, K. and Toomre, D. (2000) Lipid rafts and signal transduction. Nat. Rev. Mol. Cell Biol. 1, 31–39.

[5] Lisanti, M.P., LeBivic, A., Saltiel, A.R. and Rodriguez-Boulan, E. (1990) Preferred apical distribution of glycosyl-phosphatidyl-inositol (GPI) anchored proteins: a highly conserved feature of the polarized epithelial cell phenotype. J. Membr. Biol., 113155–113167.

[6] Rodriguez-Boulan, E., Kreitzer, G. and Musch, A. (2005) Organization of vesicular trafficking in epithelia. Nat. Rev. Mol. Cell Biol. 6, 233–247.

[7] Simons, K. and Ikonen, E. (1997) Functional rafts in cell membranes. Nature 387, 569–572.

[8] Sarnataro, D., Paladino, S., Campana, V., Grassi, J., Nitsch, L. and Zurzolo, C. (2002) PrPC is sorted to the basolateral membrane of epithelial cells independently of its association with rafts. Traffic 3, 810–821.

[9] Lipardi, C., Nitsch, L. and Zurzolo, C. (2000) Detergent-insoluble GPI-anchored proteins are apically sorted in Fischer rat thyroid cells, but interference with cholesterol or sphingolipids differentially affects detergent insolubility and apical sorting. Mol. Biol. Cell 11, 531–542.

[10] Paladino, S., Sarnataro, D., Pillich, R., Tivodar, S., Nitsch, L. and Zurzolo, C. (2004) Protein oligomerization modulates raft partitioning and apical sorting of GPI-anchored proteins. J. Cell Biol. 167, 699–709.

[11] Vogel, U., Sandvig, K. and van Deurs, B. (1998) Expression of caveolin-1 and polarized formation of invaginated caveolae in Caco-2 and MDCK II cells. J. Cell Sci. 111 (Pt 6), 825–832.

[12] Lahtinen, U., Honsho, M., Parton, R.G., Simons, K. and Verkade, P. (2003) Involvement of caveolin-2 in caveolar biogenesis in MDCK cells. FEBS Lett. 538, 85–88.

[13] Brugger, B., Graham, C., Leibrecht, I., Mombelli, E., Jen, A., Wieland, F. and Morris, R. (2004) The membrane domains occupied by glycosylphosphatidylinositol-anchored prion protein and Thy-1 differ in lipid composition. J. Biol. Chem. 279, 7530–7536.

[14] Tettamanti, G., Bonali, F., Marchesini, S. and Zambotti, V. (1973) A new procedure for the extraction, purification and fractionation of brain gangliosides. Biochim. Biophys. Acta 296, 160–170.

[15] Zurzolo, C., Lisanti, M.P., Caras, I.W., Nitsch, L. and Rodriguez-Boulan, E. (1993) Glycosylphosphatidylinositol-anchored proteins are preferentially targeted to the basolateral surface in Fischer rat thyroid epithelial cells. J. Cell Biol. 121, 1031–1039.

[16] Prinetti, A., Chigorno, V., Tettamanti, G. and Sonnino, S. (2000) Sphingolipid-enriched membrane domains from rat cerebellar granule cells differentiated in culture. A compositional study. J. Biol. Chem. 275, 11658–11665.

[17] Prinetti, A., Chigorno, V., Prioni, S., Loberto, N., Marano, N., Tettamanti, G. and Sonnino, S. (2001) Changes in the lipid turnover, composition, and organization, as sphingolipid-enriched membrane domains, in rat cerebellar granule cells developing in vitro. J. Biol. Chem. 276, 21136–21145.

[18] Pike, L.J., Han, X., Chung, K.N. and Gross, R.W. (2002) Lipid rafts are enriched in arachidonic acid and plasmenylethanolamine and their composition is independent of caveolin-1 expression: a quantitative electrospray ionization/mass spectrometric analysis. Biochemistry 41, 2075–2088.

[19] Busche, R., Dittmann, J., Meyer zu Duttingdorf, H.D., Glockenthor, U., von Engelhardt, W. and Sallmann, H.P. (2002) Permeability properties of apical and basolateral membranes of the guinea pig caecal and colonic epithelia for short-chain fatty acids. Biochim. Biophys. Acta 20, 55–63.

ANNEX 3

GPI-anchored protein homo-oligomerization leads to cholesterol-dependent hetero-clustering at the surface of MDCK cells

Simona Tivodar[a#], Simona Paladino[ab#] and Chiara Zurzolo[ac]∗

[a]Dipartimento di Biologia e Patologia Cellulare e Molecolare, Università degli Studi di Napoli Federico II, 80131 Napoli, Italy; [b]CEINGE Biotecnologie Avanzate S.C.A.R.L., 80145 Napoli, Italy; [c]Unité de Trafic Membranaire et Pathogénèse, Institut Pasteur, 25 rue du Docteur Roux, 75015 Paris, France.

Running Title: Membrane organization of GPI-anchored proteins

[#] These authors contributed equally to this work.

∗ Address correspondence to Chiara Zurzolo, Unité de Trafic Membranaire et Pathogénèse, Institut Pasteur, 25 rue du Docteur Roux, 75015 Paris, France. Tel: +33 (0)1 45688277. Fax: +33 (0)1 40613238. E-mail: zurzolo@pasteur.fr; zurzolo@unina.it

Number of characters: 56,719

Abstract

It has been shown that glycosylphosphatidylinositol (GPI)-anchored proteins (GPI-APs) are organized in micro-clusters at the cell surface. Furthermore in polarized epithelial cells GPI-APs travel to the apical surface in high molecular weight complexes and impairment of their oligomerization blocks their apical sorting. However what is the driving force for this clustered organization and whether different GPI-APs are associated in the same oligomeric complex is unknown. Here we have investigated membrane organization of three different apical GPI-APs co-expressed in pairs at the apical surface of MDCK cells. We show that GPI-APs are organized in cholesterol-independent homo-clusters, which can fuse with each other into cholesterol-dependent hetero-clusters. We also show that GPI-AP monomers cannot be cross-linked in hetero-clusters and that homo-oligomerization of GPI-APs leads to subsequent hetero-clustering. These results indicate that protein-protein interaction is needed first to promote the organization of GPI-APs in cholesterol-dependent domains.

Introduction

Increasing evidence indicates that biological membranes are organized into compositionally and functionally distinct membrane domains among which rafts represent a class of such domain enriched in sphingolipids and cholesterol (Edidin, 2003; Simons and Vaz, 2004). Lipid domains form spontaneously in binary and ternary lipid mixtures (London, 2002). In particular it has been shown that sphingolipid and cholesterol segregate from glycerophospholipids to form tightly packed liquid-ordered domains in model membranes (Brown and London, 1998, 2000; London, 2002). Several studies made in living cells using different approaches suggest that lipid segregation in distinct domains also occurs in biological membranes (Maxfield, 2002; Ritchie *et al*., 2003; Rao and Mayor, 2005; Meder *et al*., 2006).

GPI-APs, together with other lipid-anchored proteins, are enriched in rafts because of the natural affinity of the GPI anchor for the long and saturated acyl chains of sphingolipids (Benting *et al*., 1999a; Lipardi *et al*., 2000; Mayor and Riezman, 2004; Paladino *et al*., 2004; Legler *et al*., 2005). Several lines of evidence indicate that in living cells GPI-APs are confined in restricted domains of the membrane: i) GPI-APs do not exhibit Brownian motion, but undergo random walks in a transient confinement zone (Fujiwara *et al*., 2002); ii) single particle tracking experiments revealed that GPI-APs were found to be confined within 200-400 nm zones (Sheets *et al*., 1997; Schutz *et al*., 2000; Fujiwara *et al*., 2002) ; iii) other studies using FRET, single particle tracking, or biochemical cross-linking have shown that GPI-APs are restricted to submicron-sized domains on the cell surface (Friedrichson and Kurzchalia, 1998; Varma and Mayor, 1998; Pralle *et al*., 2000). Recent findings based on FRET analysis proposed that GPI-APs are organized in three-to-four molecule hetero-clusters which depend upon cholesterol (Sharma *et al*., 2004). Thus, the size of the membrane rafts can vary from a few nanometers to a few hundred and are very dynamic structures (Simons and Vaz, 2004; Rao and Mayor, 2005).

 In the original proposal, lipid rafts originate by the spontaneous segregation of specific lipids due to lipid-lipid interactions that would exclude or include other lipids and proteins, thus leading to specialized functional domains (Simons and van Meer, 1988; Simons and Ikonen, 1997). In contrast it has been proposed that rafts might originate due to the behaviour of core proteins that have particular affinities for specific classes of lipids (Anderson and Jacobson, 2002; Helms and Zurzolo, 2004; Paladino *et al*., 2004; Jacobson *et al*., 2007). Consequently, protein-protein and protein-lipid interactions rather than lipid-lipid interactions would play the major role in organizing membrane domains.

One of the proposed functions of rafts has been in determining the sorting of associated proteins in both the exocytic and endocytic pathways (Ikonen and Simons, 1998; Ikonen, 2001; Salaun *et al*.,

2004; Rajendran and Simons, 2005). However, for GPI-APs their association to rafts is not sufficient by itself to determine apical sorting in polarized epithelial cells (Paladino *et al.*, 2004; Schuck and Simons, 2004), but oligomerization into high molecular weight (HMW) complexes is also required, as shown from the fact that impairment of oligomerization by point mutations in the protein ectodomain affects apical sorting (Paladino *et al.*, 2004; Paladino *et al.*, 2007). GPI-AP oligomers appear to be protein specific and once formed are not sensitive to cholesterol depletion, suggesting that they are maintained by protein-protein interactions (Paladino *et al.*, 2004). Nonetheless, rafts may constitute a favourable environment for HMW complex formation because cholesterol depletion impairs their oligomerization in the Golgi apparatus (Paladino *et al.*, 2004). It is therefore possible that besides the protein ectodomain the lipid anchor also has a role in favouring clustering of apical GPI-APs. GPI anchors differ in their fatty acid composition (Ferguson and Williams, 1988) and probably can interact differently with raft lipids, which might affect their ability to oligomerize.

Similarly at the plasma membrane GPI-APs have been reported to be organized in microdomains (Varma and Mayor, 1998; Hao *et al.*, 2001; Kenworthy *et al.*, 2004; Sharma *et al.*, 2004; Meder *et al.*, 2006); however their abundance, size and composition is not known. Due to the lack of consensus to the driving force behind GPI-AP organization we sought to determine whether lipids or proteins are the principal force driving GPI-APs interaction/clustering. To this aim we have co-transfected in MDCK cells two different pairs of apical GPI-APs with the same (GFP-GPI/FR, folate receptor) or different (GFP-GPI/PLAP, placental alkaline phosphatase) GPI-attachment signals. We then analyzed the behaviour of the two different pairs of proteins regarding their capacity to be apically sorted and to be incorporated into oligomeric complexes as well as their dependence on cholesterol and their relative spatial organization at the apical plasma membrane. Overall our results demonstrate that GPI-APs at the plasma membrane are organized in clusters of single GPI-APs species, which we refer to as homo-complexes independently of cholesterol. These complexes can fuse into clusters of multiple GPI-APs species named hetero-clusters that are sensitive to cholesterol depletion and therefore could represent cholesterol dependent raft domains. Importantly, we demonstrate that in order to form cholesterol sensitive hetero-complexes, GPI-APs have to be organized first as homo-complexes. These data indicate that the primary driving force for GPI-APs membrane organization is based on protein-protein interactions as cholesterol-independent homo-clusters prefigure hetero-clusters. However spatially both protein-protein interactions as well as cholesterol are significant players in GPI-AP organization.

Results

Surface localization and DRM association of FR, PLAP and GFP-GPI

GPI-APs are localized principally on the apical domain of the plasma membrane of epithelial cells (Lisanti *et al*., 1989) where they can be crosslinked in HMW complexes (Friedrichson and Kurzchalia, 1998; Paladino *et al*., 2004). In order to understand whether two different species of apical GPI-APs are in the same clusters we co-transfected MDCK cells with two pairs of cDNAs encoding different GPI-APs. Specifically, GFP-GPI, in which GFP is fused to the GPI attachment signal from the folate receptor (FR) (Paladino *et al*., 2004; Sharma *et al*., 2004) was co-transfected with two different native GPI-APs (FR or PLAP), which contain distinct attachment signals. Several stable clones of MDCK cells expressing the two pairs of GPI-APs, MDCK: FR/GFP-GPI and MDCK: PLAP/GFP-GPI, were selected and characterized for their protein expression and plasma membrane localization.

As expected from results derived from single transfected clones (Paladino *et al*., 2004), we confirmed that GFP-GPI, PLAP and FR were all enriched on the apical surface (Figure 1A). In particular, ~ 85% and 90% of FR and PLAP was found on the apical membrane respectively, while ~ 80% of GFP-GPI was apically localized in both MDCK clones (Figure 1A). Each of the proteins maintained the same ratio of apical distribution in both single and double transfected cells (Figure 1A) (Paladino *et al*., 2004).

We then analysed association of these GPI-APs with detergent-resistant membranes (DRMs) by floatation on sucrose density gradients after Triton X-100 (TX-100) extraction (Brown and Rose, 1992; Simons and Ikonen, 1997; Brown and London, 1998, 2000). Consistent with previous results (Miotti *et al*., 2000; Paladino *et al*., 2004), we found that all three proteins migrated to the lighter density fractions (4-7) of the gradients (95%, 80% and 90%, respectively, for FR, PLAP and GFP-GPI), which were also enriched in the ganglioside GM1 (Figure 1B). These results confirmed that all three proteins associated with DRM fractions to a similar extent. Furthermore, the proportion of each of the GPI-APs found in DRMs was maintained constant independently of whether they were expressed alone or in pairs (Paladino *et al*., 2004).

FR, PLAP and GFP-GPI are found in HMW homo-oligomers at the apical surface of MDCK cells

Apical GPI-APs are found in HMW complexes and oligomerization appears to be a key step for their apical sorting (Paladino *et al*., 2004). We therefore investigated whether FR, PLAP and GFP-GPI also oligomerize in the co-transfected MDCK clones. As in single transfected cells (Paladino *et al*., 2004), in the co-transfected clones (MDCK: FR/GFP-GPI and MDCK: PLAP/GFP-GPI) FR,

PLAP and GFP-GPI (about 20 - 40%) were found in oligomeric complexes after fractionation of velocity gradients at steady-state (Figure 2A) in agreement with previously published data by FRET analysis (Sharma *et al.*, 2004).

To ensure that each protein was in HMW complexes also at the cell surface and to rule out the possibility that these complexes were formed as a consequence of detergent addition during cell lysis, we added the impermeable chemical crosslinking agent, BS_3 [Bis(sulfosuccinimidyl)suberate] (arm lenght 1,14 nm) to the apical surface of living cells for different times both at 37°C and at 4°C to inhibit internalization. In the presence of BS_3, bands corresponding to relative molecular masses of dimers (**) and trimers (***) as well as HMW complexes were detected for each of the three proteins (Figure 2B). This indicates that a relatively small fraction of each protein is present in an oligomeric complex at the plasma membrane similar to what has previously shown in single transfected cells (Friedrichson and Kurzchalia, 1998; Paladino *et al.*, 2004). The cross-linked pattern was similar at both temperatures, indicating that the proteins are in oligomeric complexes at physiological temperatures. In addition, the amount of cross-linked complexes was higher at 37°C compared to 4°C, thus suggesting that at the lower temperature the formation of these complexes was drastically impaired, most likely because of the reduced mobility of the molecules in the plane of the membrane. Furthermore, we could rule out the possibility that the enhanced cross-linking at 37°C was dependent on internalization in specific domains and could confirm that these complexes existed at the cell surface because none of the proteins were endocytosed during the short incubation times at 37°C (Supplementary Figure 1A and B, and data not shown).

GFP-GPI, FR, and PLAP oligomers can be cross-linked in hetero-clusters at the cell surface of MDCK cells

The above biochemical results indicated that each protein forms HMW homo-complexes independently of the other GPI-APs with which they were co-transfected. In order to understand how different GPI-APs are organized on the apical membrane with respect to each other we tested whether they could be cross-linked in hetero-HMW-complexes. To this aim lysates from cells exposed or not to the addition of BS_3 were immunoprecipitated using either an anti-FR or an anti-PLAP antibody and revealed with an anti-GFP antibody (Figure 3). Although the amount of immunoprecipitated proteins detected by western blot was similar both in the presence or absence of the cross-linking agent (Figure 3, right panels), a smear between ~ 60 and ~ 300 kDa revealed with the anti-GFP antibody was detected in the immunoprecipitates from both cells only after crosslinking (Figure 3, left panels), indicating that both pairs of proteins co-immunoprecipitated after BS_3 addition. This co-immunoprecipitation between GFP-GPI and FR or PLAP is specific

because neither the anti-FR nor the anti-PLAP antibodies cross-react with GFP-GPI, as shown by control immunoprecipitations from cells expressing only GFP-GPI (Supplementary Figure 2). These data show that two different GPI-APs can be cross-linked in HMW hetero-complexes at the cell surface indicating that they are in close proximity.

In order to understand whether this clustered organization was specific for GPI-APs we analysed the behaviour of GP114, an apical endogenous non-raft transmembrane protein of MDCK cells. After addition of BS_3 GP114 does not co-immunoprecipitate either with FR or PLAP (Supplementary Figure 3) thus supporting the concept that non-raft proteins are in a distinct environment from GPI-APs at the apical surface.

Role of cholesterol in the spatial organization of GPI-AP clusters

By using pharmacological depletion of cholesterol and a FRET approach Sharma and colleagues (Sharma *et al.*, 2004) reported that cholesterol plays a role in the organization of GPI-AP nano-clusters at the surface of non-polarized cells. In order to understand whether the relative organization of GPI-APs at the apical membrane of MDCK cells was dependent on cholesterol, we depleted cells of cholesterol using similar pharmacological conditions (eg; saponin, SAP, 0.2%, at 4°C for 30 min) and analyzed the effect on homo- and hetero- GPI-AP complexes after surface cross-linking at 37°C (Figures 4 and 5).

After cholesterol depletion all three proteins were still cross-linked in HMW homo-complexes (Figure 4). On the contrary, the hetero-GPI-AP complexes were no longer cross-linkable after saponin addition (Figure 5), indicating that co-cluster organization between two different GPI-APs requires cholesterol. To rule out the hypothesis that homo- and hetero-clusters had different threshold sensitivity to cholesterol depletion we used higher saponin concentration and/or longer incubation times (Supplementary Figure 4). Under these conditions homo-clusters remained unaffected indicating that they did not depend on cholesterol.

These biochemical data on the cholesterol sensitivity of homo- and hetero- GPI-clusters were supported by indirect immunofluorescence and by quantitative confocal analysis. Control cells or cells treated with saponin were chemically cross-linked with BS_3, fixed and stained using specific couples of antibodies (αGFP together with αFR or αPLAP) (Figure 6). Similarly to single expressing cells (Supplementary Figure 5) after cross-linking all three GPI-APs were organized in discrete punctate structures (Figure 6, +BS3 -SAP). The clusters of each GPI-AP were distinct but close to each other, as indicated by the presence of some areas of co-localization either in one Z-plane (yellow areas in the overlay) or in the 3D-reconstruction (white areas) (Figure 6, +BS3 -SAP). Although confocal microscopy does not allow the spatial resolution to discriminate GPI-APs

micro-clusters we could quantify the effect of saponin on this macro-cluster organization. Therefore we measured the degree of co-localization of 10 randomly chosen fluorescence images from two different experiments (Table I). Between 5 and 6% of co-localization was found between the two proteins in both clones. Interestingly, in agreement with the biochemical experiments, saponin treatment completely abolished the co-localization of GFP-GPI with either FR or PLAP and all three proteins were found in homo-clusters completely separated from each other (Figure 6, +BS3 +SAP), as evidenced further by the degree of co-localization that was strongly reduced to ~ 0.2-0.6% (Table I). Taken together, these data indicate that while saponin treatment does not affect GPI-AP homo-complex formation, it does disrupt their organization into hetero-complexes, indicating that these structures are likely to be dependent on cholesterol.

In order to confirm this hypothesis we have undertaken two different approaches. In the first approach we analysed the effect of cholesterol addition on homo- and hetero- GPI-AP complexes after surface cross-linking at 37°C (Figure 7). As previously shown (Patel *et al*., 2002) pretreating MDCK cells with cholesterol (10 mM) complexed to βCD resulted in an increase in cellular cholesterol levels without detectable cytotoxicity or morphological changes in the cell monolayer. Under these conditions all three proteins were still cross-linked in HMW homo-complexes (Figure 7A), thus supporting the hypothesis that homo-clusters are cholesterol independent. In contrast, after cross-linking GFP-GPI did not co-immunoprecipitate with FR or PLAP indicating that hetero-clusters between two different GPI-APs was drastically reduced with time after cholesterol addition (Figure 7B). In an alternative approach we investigated the effect of cholesterol depletion by metabolic inhibition, using mevinolin (MEV), or by surface extraction, using methyl-β-cyclodextrin (βCD). These treatments reduce the amount of cholesterol in the membrane in contrast to saponin which sequesters cholesterol in an hexagonal patterned lattice (Bangham *et al*., 1962) within the bilayer. Under both these conditions we found an increase of co-immunoprecipitation between PLAP and GFP-GPI, thus suggesting that reduction of cholesterol in the plasma membrane brings the hetero-clusters closer to each other (Supplementary Figure 6). On the contrary both these treatments do not affect the formation of homo-complexes (data not shown), similar to the saponin conditions (Figure 4). These different approaches all point to a role for cholesterol in the organization of hetero-clusters between different GPI-APs, and confirm that cholesterol is not required for the formation of homo-complexes.

To rule out the hypothesis that removal of cholesterol could have a general effect on membrane organization and therefore not be specific for raft-associated proteins we analyzed the effect of cholesterol depletion on the membrane organization of apical transmembrane non-raft associated proteins, namely the neurotrophin receptor (p75 NTR) exogenously expressed in MDCK cells (Le

Bivic et al., 1991) and the endogenous GP114 (Le Bivic et al., 1990). Interestingly saponin had the opposite effect on these proteins compared to GPI-APs. Indeed, after cross-linking we could observe a smear at high molecular weight concomitant with a decrease of the monomeric form for both proteins in saponin treated compared to non treated cells suggesting that cholesterol depletion facilitated interactions between non-raft proteins (Supplementary Figure 7). On the other hand, as expected, we did not find any co-immunoprecipitation between the two proteins (data not shown). The opposite effect of saponin in the case of non raft- and raft-associated proteins indicates that these proteins are in different phases as previously shown (Ritchie et al., 2003; Kusumi et al., 2005; Meder et al., 2006) and support the hypothesis that the effect of cholesterol depletion on GPI-APs hetero-clusters is specific.

GPI-AP homo-clusters are required to form hetero-clusters

The question arises as to whether cholesterol-independent homo-oligomerization of GPI-APs is required for the formation of cholesterol dependent hetero-clusters. Thus we analysed whether the hetero-HMW GPI-AP complexes derived from the cross-linking of monomers or oligomers of the single proteins by purifying them on velocity gradients (Figure 8). After addition of BS_3 to the cell surface, cell lysates were run on velocity gradients and each fraction was immunoprecipitated with anti-FR or anti-PLAP antibodies and revealed with the anti-GFP antibody on western blots (Figure 8). For both pairs of proteins we only observed co-immunoprecipitation with GFP-GPI in fraction 9, which contains only HMW complexes of the single proteins (Figure 8). In an alternative approach we disrupted GFP-GPI oligomers, which depend on disulphide bonds (Paladino et al., 2004), by treating the cells with DTT (10 mM, 5 min), and then analyzed whether GFP-GPI monomers were cross-linked with PLAP or FR (whose oligomers were not affected by DTT treatment; data not shown). As expected, in the presence of DTT GFP-GPI was present only in the monomeric, or partially denaturated dimeric forms (band at 43 kDa, Supplementary Figure 8, top). In these conditions GFP-GPI did not co-immunoprecipitate with PLAP nor FR (Supplementary Figure 8, bottom). Taken together these data show that only homo-HMW-complexes of the single GPI-APs were in close enough proximity to be cross-linked and suggested that monomers/dimers cannot be cross-linked to pre-existing homo-oligomers likely because they are more dispersed.

Having established that only homo-oligomers can be crosslinked in hetero-clusters the next question was to understand whether homo-oligomerization of GPI-APs leads to subsequent hetero-clustering. To this aim we artificially increased GPI-AP homo-clustering by adding simultaneously anti-GFP and anti-PLAP antibodies at 12°C to MDCK cells expressing both proteins (Figure 9A). In agreement with previous observations (Mayor et al., 1994; Harder et al., 1998; Meder et al.,

2006) following primary and secondary antibody addition, we observed the redistribution of the two proteins into punctate patterns (Figure 9A). Quantification of 10 randomly chosen images from two different experiments showed that approximately 4% of PLAP/GFP-GPI clusters were co-localizing whereas only 0.5% co-clustering was observed in untreated cells (Table II). These data show that cross-linking of GPI-APs induces hetero-clustering. However we also show that the clustering of the two proteins in specific areas of the plasma membrane is largely independent of each other. To directly test this hypothesis we stimulated clustering of one of the two proteins by antibody cross-linking and analysed the behaviour of the other one after fixation. We found that cross-linking of GFP-GPI with a specific antibody was not able to co-cluster either PLAP (Figure 9B, left panels) or FR (Figure 9B, right panels and Table III). Similar results were obtained by clustering FR or PLAP (data not shown), thus confirming that GPI-AP homo-clusters are independent of each other. These data also correlate with biochemical experiments (Figures 8 and Supplementary 8) in which only GPI-AP homo-oligomers can be cross-linked while monomers and dimers cannot.

In order to avoid possible problems caused by fixation (Mayor *et al.*, 1994; Kusumi and Suzuki, 2005), we performed the same type of experiment in living cells by following the fluorescence of GFP-GPI molecules after cross-linking of PLAP or FR with specific antibodies (Figure 9C). Cross-linking of either PLAP or FR did not induce increased co-localization with GFP-GPI (Figure 9C, panels B-D, F-H), the distribution of which was unaltered compared to the non cross-linked conditions (Figure 9C, panels A and E). The regions occupied by GFP-GPI appear to be completely segregated from those of FR or PLAP, as indicated by quantification of different experiments (about 0.2-0.4%) shown in Table III. These data indicate that no significant association between multiple GPI-APs exists and that each GPI-AP is independently recruited into homo-clusters.

Discussion

According to the raft hypothesis sphingolipids and cholesterol spontaneously associate with each other to form distinct, more ordered phases within which proteins with chemical affinity for them (such as GPI-APs) partition (Simons and Ikonen, 1997). Because of their capacity to segregate specific lipids and proteins, in cell membranes rafts can act as signalling and sorting platforms (Simons and Ikonen, 1997; Simons and Toomre, 2000). However, it has been shown that rafts are not sufficient to determine apical sorting of GPI-APs in polarized epithelial cells and that their clustering in HMW complexes is a necessary step (Paladino *et al.*, 2004). This is also supported by many reports which indicate that GPI-APs are able to cluster and segregate into specific domains (Mayor *et al.*, 1994; Anderson and Jacobson, 2002; Edidin, 2003; Meder *et al.*, 2006). Nonetheless, how apical GPI-APs are physically organized with respect to each other and to the surrounding lipids is a much-debated issue. While the original raft hypothesis postulated that lipid segregation is responsible for the organization of proteins, recent evidence indicates that functional rafts, containing GPI-APs, are generated by clustering of GPI-APs that, following oligomerization, recruit and concentrate raft lipids into a spatially segregated domain (Paladino *et al.*, 2004).

In order to analyse the driving force behind the clustering of GPI-APs we have studied the plasma membrane organization of two pairs of apical GPI-APs co-transfected in MDCK cells: GFP-GPI and FR, and GFP-GPI and PLAP. Consistent with previous data, all of them associate with DRMs to a similar extent (Figure 1B) and could be purified as HMW homo-complexes on velocity gradients (Figure 2A) or by SDS PAGE after addition of a cell- impermeable cross-linker to the apical plasma membrane (Figure 2B). In agreement with previous observations (Mayor *et al.*, 1994; Friedrichson and Kurzchalia, 1998; Paladino *et al.*, 2004; Meder *et al.*, 2006) these data indicate that GPI-APs are organized in homo-clusters at the apical surface of polarized cells. Interestingly, we found that both pairs of GPI-APs co-immunoprecipitate after cross-linking (Figure 3). This co-immunoprecipitation is specific for GPI-APs because it does not include other apical, non-raft proteins (Supplementary Figure 3), indicating that raft and non-raft proteins are segregated into distinct environment, as recently shown (Meder *et al.*, 2006). Furthermore, co-immunoprecipitation occurs exclusively between HMW homo-complexes and not between GPI-AP monomers or dimers (Figures 8 and Supplementary 8), thus suggesting that homo-GPI-AP clusters are in close proximity to each other whereas monomers, excluded by the cross-linking, are much more dispersed or actively excluded by the spatial organization of the clusters. The fact that the arm of the cross-linker is very small (1.14 nm), that cross-linking occurs at 37°C in a very short time (< 2 min) and is independent of internalization and temperature, demonstrates that GPI-AP homo-clusters are in close proximity to each other at the cell surface of unperturbed cells.

These data are also supported by quantitative analysis of confocal immunofluorescence images, showing that after chemical cross-linking the co-localization of two GPI-APs increases (Figure 6 and Table I). It therefore appears that homo-oligomerization is necessary to create the subsequent spatial organization of GPI-APs into hetero-clusters. Indeed, by artificially clustering each GPI-AP by antibody cross-linking we were able to induce GPI-AP co-clustering (Figure 9A and Table II), thus showing that homo-clustering induces a partial co-localization between two different GPI-APs. However, because clustering of GFP-GPI is not sufficient to recruit either FR or PLAP (Figure 9B and Table III), or vice-versa (Figure 9C and Table III), our data also indicate that each GPI-AP is independently recruited to form its own cluster. These data are in agreement with previously published results in both polarized (Meder *et al*., 2006) and non-polarized cells (Mayor *et al*., 1994; Harder *et al*., 1998) so far as they show that different GPI-APs are organized in distinct independent clusters that can be close enough to be co-patched by antibody addition.

The next question was then to understand how this spatial organization of GPI-APs was related to the organization of membrane lipids and to determine the principal driving forces. The raft hypothesis, based principally on lipid behaviour in simple model membranes, postulates that lipids would drive protein segregation (Simons and Vaz, 2004). On the same line, Sharma and colleagues proposed that cholesterol is an active player in the organization of GPI-AP nanoclusters, which are sensitive to saponin. Based on sophisticated FRET analysis, it was also shown that they should be composed at most of four different GPI-APs. This is in contrast with previous observations that GPI-APs are organized in homo-clusters formed by the same protein species (Mayor *et al*., 1994; Harder *et al*., 1998; Paladino *et al*., 2004) and with our observation that cholesterol depletion does not affect organization of GPI-APs in HMW complexes (Figures 4 and Supplementary 4A and B). This feature does not appear to be specific for polarized cells because GFP-GPI clusters are also insensitive to cholesterol depletion in CHO cells (Supplementary Figure 4C). In contrast, we found that hetero-clusters are completely disrupted by saponin treatment (Figures 5 and 6 and table I)**,** suggesting that while hetero-cluster organization depends on cholesterol, homo-GPI-AP clusters are cholesterol-independent. We also excluded that there is a different threshold required to disrupt homo- and hetero-clusters by treating the cells for longer duration and by using different saponin concentrations (Supplementary Figure 4A and B). Furthermore, the opposite effect of saponin in the case of non-raft-associated proteins (Supplementary Figure 7) support the hypothesis that the effect of cholesterol depletion on GPI-AP hetero-clusters is specific. In addition, all alternative methods used to perturb cholesterol balance in the membranes affected exclusively the organization of hetero-clusters. Specifically, while addition of cholesterol inhibited hetero-clustering between different GPI-APs, cholesterol depletion (by metabolic synthesis inhibition or by βCD extraction)

enhanced it (Figures 7 and Supplementary 6). Strikingly, both these treatments, similar to saponin, left homo-clusters unperturbed. The different effect induced by βCD and saponin on hetero-clusters could be explained by the different action of these two compounds. Saponin inserts into the plasma membrane and sequesters cholesterol by forming multimeric globular deposits of approximately 80-100 Å (Bangham *et al.*, 1962) which could result in a spatial segregation of the homo-complexes (see model in Figure 10). On the other hand, the lack of effect of saponin on homo-clusters could be explained in two ways: either saponin doesn't have access to the cholesterol tightly bound/hidden in these clusters or there is not sufficient cholesterol to bind. Differently from saponin, βCD selectively extracts cholesterol from membrane, preferentially from outside the GPI-APs complex (Ilangumaran and Hoessli, 1998), thus favouring the coalescence of hetero-clusters (see model in Figure 10). This interpretation is consistent with previous findings showing that lowering cholesterol levels by βCD induces formation of large-scale (micrometers) domains in the plasma membrane but does not alter the distribution of cross-linked or uncross-linked GPI-APs (Hao *et al.*, 2001). Conversely, if cholesterol had been essential for homo-clusters organization we would have expected an effect of its depletion by either the biochemical inhibition of the synthesis or by βCD extraction.

Based on all of the above results we propose that at the plasma membrane GPI-APs are organized in homo-clusters independently of cholesterol and that they are maintained by protein-protein interactions. Because GPI-APs have a high affinity for cholesterol and saturated sphingolipids, during clustering they may generate a local enrichment of raft lipids including cholesterol within a confined zone (Figure 10), thus creating specialized membrane domains that actively exclude GPI-AP monomers and other apical components. These GPI-AP clusters have high affinity for each other and so can fuse into cholesterol-dependent hetero-clusters (Figure 10). Although our approach does not permit measurement of the precise size of the cholesterol-independent GPI-AP homo-clusters our data based on velocity gradients (Figure 8) show that they are in HMW complexes containing more than four molecules, in contrast to what has been recently proposed (Sharma *et al.*, 2004). Consequently, more than four molecules are likely to be required to drive a change in the lipid microenvironment surrounding GPI-APs, which would then permit coalescence of hetero-clusters (that might represent a raft). In support of this hypothesis we do not find co-immunoprecipitation between different GPI-APs in the low molecular weight fractions of velocity gradients (Figure 8) demonstrating that hetero-oligomerization occurs only between HMW homo-complexes. Similarly we show that homo-cluster forms independently of each other because the antibody cross-linking of one specific GPI-AP does not recruit the others. However our data also

support the hypothesis that homo-oligomerization is necessary to create the subsequent spatial organization of GPI-APs into hetero-clusters (Figure 9A and Table II).

Our model is supported by studies of GPI-APs in model and cell membranes which have shown that i) monomeric GPI-APs do not show a particular affinity for liquid ordered phases (Brown and London, 2000), ii) partitioning of GPI-APs into lipid ordered phases is dramatically increased by antibody cross-linking compared to non-raft molecules (Dietrich *et al.*, 2001; Edidin, 2003), and iii) GPI-APs do not show a particular confinement using single molecule tracking at 25 μsec resolution (Kusumi *et al.*, 2005).

Similarly, in the case of T cell signalling it has been clearly demonstrated that the clustering of CD2, the adaptor protein LAT and the tyrosine kinase Lck into discrete microdomains in the plasma membranes is maintained by protein-protein interactions and does not depend on cholesterol or preformed lipid rafts (Douglass and Vale, 2005).

Although we cannot yet exclude that rafts pre-exist in cellular membranes, our data are also supported by a significant body of literature from which it appears that all the biological functions where lipid rafts are involved require segregation and coalescence into large structures which can be explained by the action of proteins in recruiting and concentrating lipids, rather than vice versa (Brown and London, 2000; Edidin, 2003; Munro, 2003).

Materials and Methods

Reagents and Antibodies

Antibodies were purchased from the following companies: polyclonal anti-PLAP from Rockland (Gilgertslville, PA), monoclonal anti-PLAP from Sigma Chemical Co. (St Louis, MO), polyclonal anti-GFP from Clontech Laboratories (East Meadow Circle, CA), polyclonal anti-GFP from Santa Cruz Biotechnology (Santa Cruz, CA), monoclonal anti-GFP from Q-BIOgene (Morgan Irvine, CA), Cy3- and Cy5- conjugated secondary antibodies from Molecular Probes (PoortGebouw, Netherlands). Monoclonal anti-FR (Mov 19) was a gift of Dr. S. Miotti (Istituto Nazionale per lo Studio e la Cura dei Tumori, Milan, Italy) and polyclonal anti-GP114 was a gift of Dr. A. Le Bivic (Faculté des Sciences de Luminy, Marseille, France). Biotin, BS_3 and HRP-conjugated streptavidin were from Pierce (Rockford, IL). Cell culture reagents and all other reagents were purchased from Sigma Chemical Co.

Cell culture and transfections

MDCK cells were grown in DMEM containing 5% FBS. MDCK cells were co-transfected with sequences encoding for GFP-GPI and PLAP, while cDNA for FR is transfected in MDCK cells already stably expressing GFP-GPI as previously described (Paladino *et al.*, 2004).

Biotinylation assay

Cells grown on the transwell filters for 4 d were selectively biotinylated and processed as previously described (Zurzolo *et al.*, 1994). Single proteins were immunoprecipitated from cell lysates using specific antibodies and run on SDS-PAGE. Biotinylated proteins were revealed by HRP-conjugated streptavidin.

Sucrose Density Gradients

Sucrose gradient analysis was performed using cells grown on 150 mm ($20\text{-}25 \times 10^6$) dishes to confluence. Cells were scraped from dishes in PBS containing $CaCl_2$ and $MgCl_2$, resuspended in 1 ml of lysis buffer containing 1% TX-100, 10 mM Tris buffer, pH 7.5, 150 mM NaCl, 5 mM EDTA and sheared through a 23-g needle. The lysate was mixed with an equal volume of 85% sucrose and run on discontinuous sucrose gradients (40–5%) at 200,000 g for 17 hrs at 4°C (Tivodar *et al.*, 2006). Fractions were collected starting from the top of the tube and TCA-precipitated. Samples were revealed by western blotting using specific antibodies.

Velocity gradients

Velocity gradients were performed using previously protocols (Doms *et al.*, 1987; Paladino *et al.*, 2004). Cells, grown to confluence in 100 mm dishes, were lysed either on ice or at room temperature for 30 min in 20 mM Tris, pH 7.4, 100 mM NaCl, 1% TX-100 (with or without 0.4% SDS). Lysates were scraped from dishes, sheared through a 26-g needle and layered on top of a discontinuous sucrose gradient (30-5%) in the same buffer of the lysis containing 0.1% TX-100. After centrifugation at 45,000 rpm for 16 h in a Beckman SW 50 ultracentrifuge, fractions of 500 μl were harvested from the top of the gradient. Proteins from each fraction were TCA-precipitated or immunoprecipitated using specific antibodies depending on the experiment, run on SDS-PAGE and revealed by western blotting using specific antibodies. The lysis buffer does not contain SDS in the case of FR because SDS disrupts the antigenicity of the specific MOV-19 antibody. In the other two cases the results was unchanged (Paladino *et al.*, 2004).

Cross-linking

Bis(sulfosuccinimidyl)suberate (BS_3) (0.5 mM) was added to the cells grown on dishes for different incubation times depending on the experiment and quenched for 15 min with 20 mM Tris pH 7.5, as described elsewhere (Friedrichson and Kurzchalia, 1998). Proteins were TCA-precipitated or immunoprecipitated with specific antibodies, separated on SDS-PAGE and revealed by western blot using specific antibodies.

Fluorescence Microscopy

After cross-linking, MDCK cells were washed with PBS containing $CaCl_2$ and $MgCl_2$, fixed with 4% PFA and quenched with 50 mM NH_4Cl. Primary antibodies were detected with Cy3- and Cy5- (as anti-mouse and anti-rabbit, respectively) conjugate secondary antibodies. Images were collected using a laser scanning microscope (LSM 510 META, Carl Zeiss Microimaging, Inc.) equipped with a planapo 63x oil-immersion (NA 1.4) objective lens. Laser lines at 543 nm and 633 were used to excite respectively the fluorophores Cy3 and Cy5 and the emission signal was collected by the META head. All image processing was done using LSM 510 software.

Antibody co-patching

Cells were incubated with specific primary antibodies in areal medium (F12 Coon's modified medium with 20 mM Hepes pH 7.5 and 0.2% bovine albumin) for 45 min at 12°C. After washings, Cy3- and Cy5- (as anti-mouse and anti-rabbit, respectively) conjugate secondary antibodies were added to the cells for 45 min at 12°C. Then cells were washed, fixed and quenched as above.

Alternatively after antibody clustering cells were imaged in vivo without fixation by confocal microscopy in CO_2 independent medium (150 mM NaCl, 5 mM KCl, 1 mM, CaCl$_2$, 1 mM MgCl$_2$, and 20 mM Hepes, pH 7.4).

Co-localization measurements

The degree of co-localization of the two fluorescence signals in the different experiments was quantified by using the LSM 510 software (Carl Zeiss Microimaging, Inc). In all images we have established for all fluorophores as threshold, above which pixels are retained co-localized, the value 150 (one example is shown in Supplementary Methods). The number of co-localized pixels was normalized for the total of pixels of a specific fluorophore in the image. The degree of co-localization of 10 cells randomly chosen of two different experiments was measured and the average values with standard deviation are shown in the tables.

Saponin treatment

Cells, grown to confluence on dishes or on coverslips for 3 d were incubated 30 min on ice with saponin (0.2%) in CO_2 independent medium as previously described (Sharma *et al.*, 2004).

Cholesterol addition assays

Addition of cholesterol (10mM) to cells was carried out using cholesterol-saturated βCD, which was prepared as previously described (Christian *et al.*, 1997; Ying *et al.*, 2003). Briefly, 1 g of βCD was dissolved in 20 ml H$_2$O, and then 30 mg of cholesterol was added. The mixed solution was incubated at 37°C overnight, filtrated and freeze-dried.

The cholesterol-saturated βCD was added to the cells in medium containing 20 mM Hepes pH 7.5 and 0.2% bovine albumin at 37°C for different indicated times. By colorimetric assay we measured that the levels of total cholesterol increased about 7-14% in cholesterol-loaded cells in comparison to the control cells.

References

Ahmed, S.N., Brown, D.A., and London, E. (1997). On the origin of sphingolipid/cholesterol-rich detergent-insoluble cell membranes: physiological concentrations of cholesterol and sphingolipid induce formation of a detergent-insoluble, liquid-ordered lipid phase in model membranes. Biochemistry *36*, 10944-10953.

Almeida, P.F., Vaz, W.L., and Thompson, T.E. (1992). Lateral diffusion in the liquid phases of dimyristoylphosphatidylcholine/cholesterol lipid bilayers: a free volume analysis. Biochemistry *31*, 6739-6747.

Anderson, R.G., and Jacobson, K. (2002). A role for lipid shells in targeting proteins to caveolae, rafts, and other lipid domains. Science (New York, N.Y *296*, 1821-1825.

Ang, A.L., Taguchi, T., Francis, S., Folsch, H., Murrells, L.J., Pypaert, M., Warren, G., and Mellman, I. (2004). Recycling endosomes can serve as intermediates during transport from the Golgi to the plasma membrane of MDCK cells. The Journal of cell biology *167*, 531-543.

Arreaza, G., and Brown, D.A. (1995). Sorting and intracellular trafficking of a glycosylphosphatidylinositol-anchored protein and two hybrid transmembrane proteins with the same ectodomain in Madin-Darby canine kidney epithelial cells. J Biol Chem *270*, 23641-23647.

Bangham, A.D., Horne, R.W., Glauert, A.M., Dingle, J.T., and Lucy, J.A. (1962). Action of saponin on biological cell membranes. Nature *196*, 952-955.

Bastaki, M., Braiterman, L.T., Johns, D.C., Chen, Y.H., and Hubbard, A.L. (2002). Absence of direct delivery for single transmembrane apical proteins or their "Secretory" forms in polarized hepatic cells. Molecular biology of the cell *13*, 225-237.

Benting, J., Rietveld, A., Ansorge, I., and Simons, K. (1999a). Acyl and alkyl chain length of GPI-anchors is critical for raft association in vitro. FEBS letters *462*, 47-50.

Benting, J.H., Rietveld, A.G., and Simons, K. (1999b). N-Glycans mediate the apical sorting of a GPI-anchored, raft-associated protein in Madin-Darby canine kidney cells. The Journal of cell biology *146*, 313-320.

Bezprozvanny, I., and Maximov, A. (2001). PDZ domains: More than just a glue. Proceedings of the National Academy of Sciences of the United States of America *98*, 787-789.

Birnbaumer, M., Seibold, A., Gilbert, S., Ishido, M., Barberis, C., Antaramian, A., Brabet, P., and Rosenthal, W. (1992). Molecular cloning of the receptor for human antidiuretic hormone. Nature *357*, 333-335.

Bomsel, M., Prydz, K., Parton, R.G., Gruenberg, J., and Simons, K. (1989). Endocytosis in filter-grown Madin-Darby canine kidney cells. The Journal of cell biology *109*, 3243-3258.

Braccia, A., Villani, M., Immerdal, L., Niels-Christiansen, L.L., Nystrom, B.T., Hansen, G.H., and Danielsen, E.M. (2003). Microvillar membrane microdomains exist at physiological temperature. Role of galectin-4 as lipid raft stabilizer revealed by "superrafts". J Biol Chem *278*, 15679-15684.

Bretscher, A., Chambers, D., Nguyen, R., and Reczek, D. (2000). ERM-Merlin and EBP50 protein families in plasma membrane organization and function. Annual review of cell and developmental biology *16*, 113-143.

Breuza, L., Garcia, M., Delgrossi, M.H., and Le Bivic, A. (2002). Role of the membrane-proximal O-glycosylation site in sorting of the human receptor for neurotrophins to the apical membrane of MDCK cells. Experimental cell research *273*, 178-186.

Brown, D., and Breton, S. (2000). Sorting proteins to their target membranes. Kidney international *57*, 816-824.

Brown, D.A., and London, E. (1998). Functions of lipid rafts in biological membranes. Annual review of cell and developmental biology *14*, 111-136.

Brown, D.A., and London, E. (2000). Structure and function of sphingolipid- and cholesterol-rich membrane rafts. J Biol Chem *275*, 17221-17224.

Brown, D.A., and Rose, J.K. (1992). Sorting of GPI-anchored proteins to glycolipid-enriched membrane subdomains during transport to the apical cell surface. Cell *68*, 533-544.

Brugger, B., Graham, C., Leibrecht, I., Mombelli, E., Jen, A., Wieland, F., and Morris, R. (2004). The membrane domains occupied by glycosylphosphatidylinositol-anchored prion protein and Thy-1 differ in lipid composition. J Biol Chem *279*, 7530-7536. Epub 2003 Dec 7534.

Carter, H.E., Hendry, R.A., Nojima, S., Stanacev, N.Z., and Ohno, K. (1961). Biochemistry of the sphingolipids. XIII. Determination of the structure of cerebrosides from wheat flour. J Biol Chem *236*, 1912-1916.

Casanova, J.E., Apodaca, G., and Mostov, K.E. (1991). An autonomous signal for basolateral sorting in the cytoplasmic domain of the polymeric immunoglobulin receptor. Cell *66*, 65-75.

Cereijido, M., Robbins, E.S., Dolan, W.J., Rotunno, C.A., and Sabatini, D.D. (1978). Polarized monolayers formed by epithelial cells on a permeable and translucent support. The Journal of cell biology *77*, 853-880.

Chen, W.J., Goldstein, J.L., and Brown, M.S. (1990). NPXY, a sequence often found in cytoplasmic tails, is required for coated pit-mediated internalization of the low density lipoprotein receptor. J Biol Chem *265*, 3116-3123.

Chigorno, V., Riva, C., Valsecchi, M., Nicolini, M., Brocca, P., and Sonnino, S. (1997). Metabolic processing of gangliosides by human fibroblasts in culture--formation and recycling of separate pools of sphingosine. European journal of biochemistry / FEBS *250*, 661-669.

Christian, A.E., Haynes, M.P., Phillips, M.C., and Rothblat, G.H. (1997). Use of cyclodextrins for manipulating cellular cholesterol content. Journal of lipid research *38*, 2264-2272.

Chuang, J.Z., and Sung, C.H. (1998). The cytoplasmic tail of rhodopsin acts as a novel apical sorting signal in polarized MDCK cells. The Journal of cell biology *142*, 1245-1256.

Collawn, J.F., Stangel, M., Kuhn, L.A., Esekogwu, V., Jing, S.Q., Trowbridge, I.S., and Tainer, J.A. (1990). Transferrin receptor internalization sequence YXRF implicates a tight turn as the structural recognition motif for endocytosis. Cell *63*, 1061-1072.

Corvera, S., Chawla, A., Chakrabarti, R., Joly, M., Buxton, J., and Czech, M.P. (1994). A double leucine within the GLUT4 glucose transporter COOH-terminal domain functions as an endocytosis signal. The Journal of cell biology *126*, 979-989.

Cunningham, O., Andolfo, A., Santovito, M.L., Iuzzolino, L., Blasi, F., and Sidenius, N. (2003). Dimerization controls the lipid raft partitioning of uPAR/CD87 and regulates its biological functions. The EMBO journal *22*, 5994-6003.

Delacour, D., and Jacob, R. (2006). Apical protein transport. Cell Mol Life Sci *63*, 2491-2505.

Dietrich, C., Volovyk, Z.N., Levi, M., Thompson, N.L., and Jacobson, K. (2001). Partitioning of Thy-1, GM1, and cross-linked phospholipid analogs into lipid rafts reconstituted in supported model membrane monolayers. Proceedings of the National Academy of Sciences of the United States of America *98*, 10642-10647.

Dietrich, C., Yang, B., Fujiwara, T., Kusumi, A., and Jacobson, K. (2002). Relationship of lipid rafts to transient confinement zones detected by single particle tracking. Biophysical journal *82*, 274-284.

Doms, R.W., Keller, D.S., Helenius, A., and Balch, W.E. (1987). Role for adenosine triphosphate in regulating the assembly and transport of vesicular stomatitis virus G protein trimers. The Journal of cell biology *105*, 1957-1969.

Douglass, A.D., and Vale, R.D. (2005). Single-molecule microscopy reveals plasma membrane microdomains created by protein-protein networks that exclude or trap signaling molecules in T cells. Cell *121*, 937-950.

Dunphy, W.G., and Rothman, J.E. (1985). Compartmental organization of the Golgi stack. Cell *42*, 13-21.

Edidin, M. (2003). The state of lipid rafts: from model membranes to cells. Annu Rev Biophys Biomol Struct *32*, 257-283.

Ferguson, M.A. (1999). The structure, biosynthesis and functions of glycosylphosphatidylinositol anchors, and the contributions of trypanosome research. Journal of cell science *112 (Pt 17)*, 2799-2809.

Ferguson, M.A., Low, M.G., and Cross, G.A. (1985). Glycosyl-sn-1,2-dimyristylphosphatidylinositol is covalently linked to Trypanosoma brucei variant surface glycoprotein. J Biol Chem *260*, 14547-14555.

Ferguson, M.A., and Williams, A.F. (1988). Cell-surface anchoring of proteins via glycosyl-phosphatidylinositol structures. Annu Rev Biochem *57*, 285-320.

Fiedler, K., Kobayashi, T., Kurzchalia, T.V., and Simons, K. (1993). Glycosphingolipid-enriched, detergent-insoluble complexes in protein sorting in epithelial cells. Biochemistry *32*, 6365-6373.

Fiedler, K., and Simons, K. (1995). The role of N-glycans in the secretory pathway. Cell *81*, 309-312.

Fivaz, M., Vilbois, F., Thurnheer, S., Pasquali, C., Abrami, L., Bickel, P.E., Parton, R.G., and van der Goot, F.G. (2002). Differential sorting and fate of endocytosed GPI-anchored proteins. The EMBO journal *21*, 3989-4000.

Folsch, H., Ohno, H., Bonifacino, J.S., and Mellman, I. (1999). A novel clathrin adaptor complex mediates basolateral targeting in polarized epithelial cells. Cell *99*, 189-198.

Friedrichson, T., and Kurzchalia, T.V. (1998). Microdomains of GPI-anchored proteins in living cells revealed by crosslinking. Nature *394*, 802-805.

Fujiwara, T., Ritchie, K., Murakoshi, H., Jacobson, K., and Kusumi, A. (2002). Phospholipids undergo hop diffusion in compartmentalized cell membrane. The Journal of cell biology *157*, 1071-1081.

Geffen, I., Fuhrer, C., Leitinger, B., Weiss, M., Huggel, K., Griffiths, G., and Spiess, M. (1993). Related signals for endocytosis and basolateral sorting of the asialoglycoprotein receptor. J Biol Chem *268*, 20772-20777.

Gisler, S.M., Stagljar, I., Traebert, M., Bacic, D., Biber, J., and Murer, H. (2001). Interaction of the type IIa Na/Pi cotransporter with PDZ proteins. J Biol Chem *276*, 9206-9213.

Glomset, J.A., Gelb, M.H., and Farnsworth, C.C. (1990). Prenyl proteins in eukaryotic cells: a new type of membrane anchor. Trends in biochemical sciences *15*, 139-142.

Glynne, P.A., and Evans, T.J. (2002). Role of the PDZ scaffolding protein in tubule cells in maintenance of polarised function. Experimental nephrology *10*, 307-312.

Goldstein, J.L., and Brown, M.S. (2001). Molecular medicine. The cholesterol quartet. Science (New York, N.Y *292*, 1310-1312.

Griffiths, G., and Simons, K. (1986). The trans Golgi network: sorting at the exit site of the Golgi complex. Science (New York, N.Y *234*, 438-443.

Hantke, K., and Braun, V. (1973). Covalent binding of lipid to protein. Diglyceride and amide-linked fatty acid at the N-terminal end of the murein-lipoprotein of the Escherichia coli outer membrane. European journal of biochemistry / FEBS *34*, 284-296.

Hao, M., Mukherjee, S., and Maxfield, F.R. (2001). Cholesterol depletion induces large scale domain segregation in living cell membranes. Proceedings of the National Academy of Sciences of the United States of America *98*, 13072-13077.

Harder, T., Scheiffele, P., Verkade, P., and Simons, K. (1998). Lipid domain structure of the plasma membrane revealed by patching of membrane components. The Journal of cell biology *141*, 929-942.

Harder, T., and Simons, K. (1997). Caveolae, DIGs, and the dynamics of sphingolipid-cholesterol microdomains. Current opinion in cell biology *9*, 534-542.

Harris, B.Z., and Lim, W.A. (2001). Mechanism and role of PDZ domains in signaling complex assembly. Journal of cell science *114*, 3219-3231.

Helms, J.B., and Zurzolo, C. (2004). Lipids as targeting signals: lipid rafts and intracellular trafficking. Traffic (Copenhagen, Denmark) *5*, 247-254.

Hua, W., Sheff, D., Toomre, D., and Mellman, I. (2006). Vectorial insertion of apical and basolateral membrane proteins in polarized epithelial cells revealed by quantitative 3D live cell imaging. The Journal of cell biology *172*, 1035-1044.

Hunziker, W., Harter, C., Matter, K., and Mellman, I. (1991). Basolateral sorting in MDCK cells requires a distinct cytoplasmic domain determinant. Cell *66*, 907-920.

Hunziker, W., and Mellman, I. (1991). Relationships between sorting in the exocytic and endocytic pathways of MDCK cells. Seminars in cell biology *2*, 397-410.

Ikezawa, H. (2002). Glycosylphosphatidylinositol (GPI)-anchored proteins. Biological & pharmaceutical bulletin *25*, 409-417.

Ikonen, E. (2001). Roles of lipid rafts in membrane transport. Current opinion in cell biology *13*, 470-477.

Ikonen, E., and Simons, K. (1998). Protein and lipid sorting from the trans-Golgi network to the plasma membrane in polarized cells. Semin Cell Dev Biol *9*, 503-509.

Ilangumaran, S., and Hoessli, D.C. (1998). Effects of cholesterol depletion by cyclodextrin on the sphingolipid microdomains of the plasma membrane. The Biochemical journal *335 (Pt 2)*, 433-440.

Inouye, S., and Tsuji, F.I. (1994). Aequorea green fluorescent protein. Expression of the gene and fluorescence characteristics of the recombinant protein. FEBS letters *341*, 277-280.

Jacob, R., Alfalah, M., Grunberg, J., Obendorf, M., and Naim, H.Y. (2000). Structural determinants required for apical sorting of an intestinal brush-border membrane protein. J Biol Chem *275*, 6566-6572.

Jacob, R., Heine, M., Alfalah, M., and Naim, H.Y. (2003). Distinct cytoskeletal tracks direct individual vesicle populations to the apical membrane of epithelial cells. Curr Biol *13*, 607-612.

Jacobson, K., Mouritsen, O.G., and Anderson, R.G. (2007). Lipid rafts: at a crossroad between cell biology and physics. Nature cell biology *9*, 7-14.

Keller, G.A., Siegel, M.W., and Caras, I.W. (1992). Endocytosis of glycophospholipid-anchored and transmembrane forms of CD4 by different endocytic pathways. The EMBO journal *11*, 863-874.

Keller, P., and Simons, K. (1998). Cholesterol is required for surface transport of influenza virus hemagglutinin. The Journal of cell biology *140*, 1357-1367.

Keller, P., Toomre, D., Diaz, E., White, J., and Simons, K. (2001). Multicolour imaging of post-Golgi sorting and trafficking in live cells. Nature cell biology *3*, 140-149.

Kenworthy, A.K., Nichols, B.J., Remmert, C.L., Hendrix, G.M., Kumar, M., Zimmerberg, J., and Lippincott-Schwartz, J. (2004). Dynamics of putative raft-associated proteins at the cell surface. The Journal of cell biology *165*, 735-746.

Kipp, H., and Arias, I.M. (2000). Newly synthesized canalicular ABC transporters are directly targeted from the Golgi to the hepatocyte apical domain in rat liver. J Biol Chem *275*, 15917-15925.

Koivisto, U.M., Hubbard, A.L., and Mellman, I. (2001). A novel cellular phenotype for familial hypercholesterolemia due to a defect in polarized targeting of LDL receptor. Cell *105*, 575-585.

Kornfeld, R., and Kornfeld, S. (1985). Assembly of asparagine-linked oligosaccharides. Annu Rev Biochem *54*, 631-664.

Kusumi, A., Ike, H., Nakada, C., Murase, K., and Fujiwara, T. (2005). Single-molecule tracking of membrane molecules: plasma membrane compartmentalization and dynamic assembly of raft-philic signaling molecules. Semin Immunol *17*, 3-21.

Kusumi, A., and Suzuki, K. (2005). Toward understanding the dynamics of membrane-raft-based molecular interactions. Biochimica et biophysica acta *1746*, 234-251.

Lahtinen, U., Honsho, M., Parton, R.G., Simons, K., and Verkade, P. (2003). Involvement of caveolin-2 in caveolar biogenesis in MDCK cells. FEBS letters *538*, 85-88.

Lazaro-Dieguez, F., Colonna, C., Cortegano, M., Calvo, M., Martinez, S.E., and Egea, G. (2007). Variable actin dynamics requirement for the exit of different cargo from the trans-Golgi network. FEBS letters *581*, 3875-3881.

Lazo, P.A. (2007). Functional implications of tetraspanin proteins in cancer biology. Cancer science *98*, 1666-1677.

Le Bivic, A., Garcia, M., and Rodriguez-Boulan, E. (1993). Ricin-resistant Madin-Darby canine kidney cells missort a major endogenous apical sialoglycoprotein. J Biol Chem *268*, 6909-6916.

Le Bivic, A., Sambuy, Y., Mostov, K., and Rodriguez-Boulan, E. (1990). Vectorial targeting of an endogenous apical membrane sialoglycoprotein and uvomorulin in MDCK cells. The Journal of cell biology *110*, 1533-1539.

Le Bivic, A., Sambuy, Y., Patzak, A., Patil, N., Chao, M., and Rodriguez-Boulan, E. (1991). An internal deletion in the cytoplasmic tail reverses the apical localization of human NGF receptor in transfected MDCK cells. The Journal of cell biology *115*, 607-618.

Legler, D.F., Doucey, M.A., Schneider, P., Chapatte, L., Bender, F.C., and Bron, C. (2005). Differential insertion of GPI-anchored GFPs into lipid rafts of live cells. Faseb J *19*, 73-75.

Lin, S., Naim, H.Y., Rodriguez, A.C., and Roth, M.G. (1998). Mutations in the middle of the transmembrane domain reverse the polarity of transport of the influenza virus hemagglutinin in MDCK epithelial cells. The Journal of cell biology *142*, 51-57.

Lin, S., Naim, H.Y., and Roth, M.G. (1997). Tyrosine-dependent basolateral sorting signals are distinct from tyrosine-dependent internalization signals. J Biol Chem *272*, 26300-26305.

Lipardi, C., Mora, R., Colomer, V., Paladino, S., Nitsch, L., Rodriguez-Boulan, E., and Zurzolo, C. (1998). Caveolin transfection results in caveolae formation but not apical sorting of glycosylphosphatidylinositol (GPI)-anchored proteins in epithelial cells. The Journal of cell biology *140*, 617-626.

Lipardi, C., Nitsch, L., and Zurzolo, C. (2000). Detergent-insoluble GPI-anchored proteins are apically sorted in fischer rat thyroid cells, but interference with cholesterol or sphingolipids differentially affects detergent insolubility and apical sorting. Molecular biology of the cell *11*, 531-542.

Lisanti, M.P., Caras, I.W., Davitz, M.A., and Rodriguez-Boulan, E. (1989). A glycophospholipid membrane anchor acts as an apical targeting signal in polarized epithelial cells. The Journal of cell biology *109*, 2145-2156.

London, E. (2002). Insights into lipid raft structure and formation from experiments in model membranes. Curr Opin Struct Biol *12*, 480-486.

London, E. (2005). How principles of domain formation in model membranes may explain ambiguities concerning lipid raft formation in cells. Biochimica et biophysica acta *1746*, 203-220.

Madore, N., Smith, K.L., Graham, C.H., Jen, A., Brady, K., Hall, S., and Morris, R. (1999). Functionally different GPI proteins are organized in different domains on the neuronal surface. The EMBO journal *18*, 6917-6926.

Matter, K. (2000). Epithelial polarity: sorting out the sorters. Curr Biol *10*, R39-42.

Matter, K., Hunziker, W., and Mellman, I. (1992). Basolateral sorting of LDL receptor in MDCK cells: the cytoplasmic domain contains two tyrosine-dependent targeting determinants. Cell *71*, 741-753.

Matter, K., and Mellman, I. (1994). Mechanisms of cell polarity: sorting and transport in epithelial cells. Current opinion in cell biology *6*, 545-554.

Maxfield, F.R. (2002). Plasma membrane microdomains. Current opinion in cell biology *14*, 483-487.

Mayor, S., and Maxfield, F.R. (1995). Insolubility and redistribution of GPI-anchored proteins at the cell surface after detergent treatment. Molecular biology of the cell *6*, 929-944.

Mayor, S., and Rao, M. (2004). Rafts: scale-dependent, active lipid organization at the cell surface. Traffic (Copenhagen, Denmark) *5*, 231-240.

Mayor, S., and Riezman, H. (2004). Sorting GPI-anchored proteins. Nat Rev Mol Cell Biol *5*, 110-120.

Mayor, S., Rothberg, K.G., and Maxfield, F.R. (1994). Sequestration of GPI-anchored proteins in caveolae triggered by cross-linking. Science (New York, N.Y *264*, 1948-1951.

Meder, D., Moreno, M.J., Verkade, P., Vaz, W.L., and Simons, K. (2006). Phase coexistence and connectivity in the apical membrane of polarized epithelial cells. Proceedings of the National Academy of Sciences of the United States of America *103*, 329-334.

Milewski, M.I., Mickle, J.E., Forrest, J.K., Stafford, D.M., Moyer, B.D., Cheng, J., Guggino, W.B., Stanton, B.A., and Cutting, G.R. (2001). A PDZ-binding motif is essential but not sufficient to localize the C terminus of CFTR to the apical membrane. Journal of cell science *114*, 719-726.

Miotti, S., Bagnoli, M., Tomassetti, A., Colnaghi, M.I., and Canevari, S. (2000). Interaction of folate receptor with signaling molecules lyn and G(alpha)(i-3) in detergent-resistant complexes from the ovary carcinoma cell line IGROV1. Journal of cell science *113 Pt 2*, 349-357.

Mostov, K., Su, T., and ter Beest, M. (2003). Polarized epithelial membrane traffic: conservation and plasticity. Nature cell biology *5*, 287-293.

Mostov, K.E. (2003). Epithelial polarity and morphogenesis. Methods *30*, 189-190.

Mostov, K.E., de Bruyn Kops, A., and Deitcher, D.L. (1986). Deletion of the cytoplasmic domain of the polymeric immunoglobulin receptor prevents basolateral localization and endocytosis. Cell *47*, 359-364.

Mostov, K.E., Verges, M., and Altschuler, Y. (2000). Membrane traffic in polarized epithelial cells. Current opinion in cell biology *12*, 483-490.

Moyer, B.D., Denton, J., Karlson, K.H., Reynolds, D., Wang, S., Mickle, J.E., Milewski, M., Cutting, G.R., Guggino, W.B., Li, M., and Stanton, B.A. (1999). A PDZ-interacting domain in CFTR is an apical membrane polarization signal. The Journal of clinical investigation *104*, 1353-1361.

Moyer, B.D., Duhaime, M., Shaw, C., Denton, J., Reynolds, D., Karlson, K.H., Pfeiffer, J., Wang, S., Mickle, J.E., Milewski, M., Cutting, G.R., Guggino, W.B., Li, M., and Stanton, B.A. (2000). The PDZ-interacting domain of cystic fibrosis transmembrane conductance regulator is required for functional expression in the apical plasma membrane. J Biol Chem *275*, 27069-27074.

Munro, S. (2003). Lipid rafts: elusive or illusive? Cell *115*, 377-388.

Muth, T.R., and Caplan, M.J. (2003). Transport protein trafficking in polarized cells. Annual review of cell and developmental biology *19*, 333-366.

Nelson, W.J., and Rodriguez-Boulan, E. (2004). Unravelling protein sorting. Nature cell biology *6*, 282-284.

Nelson, W.J., and Yeaman, C. (2001). Protein trafficking in the exocytic pathway of polarized epithelial cells. Trends in cell biology *11*, 483-486.

Neumann-Giesen, C., Falkenbach, B., Beicht, P., Claasen, S., Luers, G., Stuermer, C.A., Herzog, V., and Tikkanen, R. (2004). Membrane and raft association of reggie-1/flotillin-2: role of myristoylation, palmitoylation and oligomerization and induction of filopodia by overexpression. The Biochemical journal *378*, 509-518.

Nosjean, O., Briolay, A., and Roux, B. (1997). Mammalian GPI proteins: sorting, membrane residence and functions. Biochimica et biophysica acta *1331*, 153-186.

Orzech, E., Livshits, L., Leyt, J., Okhrimenko, H., Reich, V., Cohen, S., Weiss, A., Melamed-Book, N., Lebendiker, M., Altschuler, Y., and Aroeti, B. (2001). Interactions between adaptor protein-1 of the clathrin coat and microtubules via type 1a microtubule-associated proteins. J Biol Chem *276*, 31340-31348.

Paladino, S., Pocard, T., Catino, M.A., and Zurzolo, C. (2006). GPI-anchored proteins are directly targeted to the apical surface in fully polarized MDCK cells. J Cell Biol *172*, 1023-1034.

Paladino, S., Sarnataro, D., Pillich, R., Tivodar, S., Nitsch, L., and Zurzolo, C. (2004). Protein oligomerization modulates raft partitioning and apical sorting of GPI-anchored proteins. The Journal of cell biology *167*, 699-709.

Paladino, S., Sarnataro, D., Tivodar, S., and Zurzolo, C. (2007). Oligomerization is a specific requirement for apical sorting of glycosyl-phosphatidylinositol-anchored proteins but not for non-raft-associated apical proteins. Traffic (Copenhagen, Denmark) *8*, 251-258.

Paladino, S., Sarnataro, D., and Zurzolo, C. (2002). Detergent-resistant membrane microdomains and apical sorting of GPI-anchored proteins in polarized epithelial cells. Ijmm International Journal of Medical Microbiology. *291*, 439-445.

Patel, H.K., Willhite, D.C., Patel, R.M., Ye, D., Williams, C.L., Torres, E.M., Marty, K.B., MacDonald, R.A., and Blanke, S.R. (2002). Plasma membrane cholesterol modulates cellular vacuolation induced by the Helicobacter pylori vacuolating cytotoxin. Infection and immunity *70*, 4112-4123.

Pelkmans, L. (2005). Secrets of caveolae- and lipid raft-mediated endocytosis revealed by mammalian viruses. Biochimica et biophysica acta *1746*, 295-304.

Pelkmans, L., and Helenius, A. (2002). Endocytosis via caveolae. Traffic (Copenhagen, Denmark) *3*, 311-320.

Perego, C., Vanoni, C., Villa, A., Longhi, R., Kaech, S.M., Frohli, E., Hajnal, A., Kim, S.K., and Pietrini, G. (1999). PDZ-mediated interactions retain the epithelial GABA transporter on the basolateral surface of polarized epithelial cells. The EMBO journal *18*, 2384-2393.

Pike, L.J., Han, X., Chung, K.N., and Gross, R.W. (2002). Lipid rafts are enriched in arachidonic acid and plasmenylethanolamine and their composition is independent of caveolin-1 expression: a quantitative electrospray ionization/mass spectrometric analysis. Biochemistry *41*, 2075-2088.

Potter, B.A., Ihrke, G., Bruns, J.R., Weixel, K.M., and Weisz, O.A. (2004). Specific N-glycans direct apical delivery of transmembrane, but not soluble or glycosylphosphatidylinositol-anchored forms of endolyn in Madin-Darby canine kidney cells. Molecular biology of the cell *15*, 1407-1416.

Pralle, A., Keller, P., Florin, E.L., Simons, K., and Horber, J.K. (2000). Sphingolipid-cholesterol rafts diffuse as small entities in the plasma membrane of mammalian cells. The Journal of cell biology *148*, 997-1008.

Prinetti, A., Chigorno, V., Prioni, S., Loberto, N., Marano, N., Tettamanti, G., and Sonnino, S. (2001). Changes in the lipid turnover, composition, and organization, as sphingolipid-enriched membrane domains, in rat cerebellar granule cells developing in vitro. J Biol Chem *276*, 21136-21145.

Prinetti, A., Chigorno, V., Tettamanti, G., and Sonnino, S. (2000). Sphingolipid-enriched membrane domains from rat cerebellar granule cells differentiated in culture. A compositional study. J Biol Chem *275*, 11658-11665.

Puertollano, R., Martin-Belmonte, F., Millan, J., de Marco, M.C., Albar, J.P., Kremer, L., and Alonso, M.A. (1999). The MAL proteolipid is necessary for normal apical transport and accurate sorting of the influenza virus hemagglutinin in Madin-Darby canine kidney cells. The Journal of cell biology *145*, 141-151.

Raghuram, V., Mak, D.O., and Foskett, J.K. (2001). Regulation of cystic fibrosis transmembrane conductance regulator single-channel gating by bivalent PDZ-domain-mediated interaction. Proceedings of the National Academy of Sciences of the United States of America *98*, 1300-1305.

Rajendran, L., and Simons, K. (2005). Lipid rafts and membrane dynamics. Journal of cell science *118*, 1099-1102.

Rao, M., and Mayor, S. (2005). Use of Forster's resonance energy transfer microscopy to study lipid rafts. Biochimica et biophysica acta *1746*, 221-233.

Riboni, L., Bassi, R., Sonnino, S., and Tettamanti, G. (1992). Formation of free sphingosine and ceramide from exogenous ganglioside GM1 by cerebellar granule cells in culture. FEBS letters *300*, 188-192.

Ritchie, K., Iino, R., Fujiwara, T., Murase, K., and Kusumi, A. (2003). The fence and picket structure of the plasma membrane of live cells as revealed by single molecule techniques (Review). Mol Membr Biol *20*, 13-18.

Rock, P., Allietta, M., Young, W.W., Jr., Thompson, T.E., and Tillack, T.W. (1990). Organization of glycosphingolipids in phosphatidylcholine bilayers: use of antibody molecules and Fab fragments as morphologic markers. Biochemistry *29*, 8484-8490.

Rodriguez-Boulan, E., and Gonzalez, A. (1999). Glycans in post-Golgi apical targeting: sorting signals or structural props? Trends in cell biology *9*, 291-294.

Rodriguez-Boulan, E., Kreitzer, G., and Musch, A. (2005). Organization of vesicular trafficking in epithelia. Nat Rev Mol Cell Biol *6*, 233-247.

Rodriguez-Boulan, E., Musch, A., and Le Bivic, A. (2004). Epithelial trafficking: new routes to familiar places. Current opinion in cell biology *16*, 436-442.

Rodriguez-Boulan, E., and Powell, S.K. (1992). Polarity of epithelial and neuronal cells. Annu Rev Cell Biol *8*, 395-427.

Rongo, C., Whitfield, C.W., Rodal, A., Kim, S.K., and Kaplan, J.M. (1998). LIN-10 is a shared component of the polarized protein localization pathways in neurons and epithelia. Cell *94*, 751-759.

Roper, K., Corbeil, D., and Huttner, W.B. (2000). Retention of prominin in microvilli reveals distinct cholesterol-based lipid micro-domains in the apical plasma membrane. Nature cell biology *2*, 582-592.

Salaun, C., James, D.J., and Chamberlain, L.H. (2004). Lipid rafts and the regulation of exocytosis. Traffic (Copenhagen, Denmark) *5*, 255-264.

Sarnataro, D., Paladino, S., Campana, V., Grassi, J., Nitsch, L., and Zurzolo, C. (2002). PrPC is sorted to the basolateral membrane of epithelial cells independently of its association with rafts. Traffic (Copenhagen, Denmark) *3*, 810-821.

Scheiffele, P., Peranen, J., and Simons, K. (1995). N-glycans as apical sorting signals in epithelial cells. Nature *378*, 96-98.

Scheiffele, P., Roth, M.G., and Simons, K. (1997). Interaction of influenza virus haemagglutinin with sphingolipid-cholesterol membrane domains via its transmembrane domain. The EMBO journal *16*, 5501-5508.

Scheiffele, P., Verkade, P., Fra, A.M., Virta, H., Simons, K., and Ikonen, E. (1998). Caveolin-1 and -2 in the exocytic pathway of MDCK cells. The Journal of cell biology *140*, 795-806.

Schmidt, M.F., Bracha, M., and Schlesinger, M.J. (1979). Evidence for covalent attachment of fatty acids to Sindbis virus glycoproteins. Proceedings of the National Academy of Sciences of the United States of America *76*, 1687-1691.

Schuck, S., Honsho, M., Ekroos, K., Shevchenko, A., and Simons, K. (2003). Resistance of cell membranes to different detergents. Proceedings of the National Academy of Sciences of the United States of America *100*, 5795-5800.

Schuck, S., and Simons, K. (2004). Polarized sorting in epithelial cells: raft clustering and the biogenesis of the apical membrane. Journal of cell science *117*, 5955-5964.

Schutz, G.J., Kada, G., Pastushenko, V.P., and Schindler, H. (2000). Properties of lipid microdomains in a muscle cell membrane visualized by single molecule microscopy. The EMBO journal *19*, 892-901.

Scott, R.O., Thelin, W.R., and Milgram, S.L. (2002). A novel PDZ protein regulates the activity of guanylyl cyclase C, the heat-stable enterotoxin receptor. J Biol Chem *277*, 22934-22941.

Sharma, P., Varma, R., Sarasij, R.C., Ira, Gousset, K., Krishnamoorthy, G., Rao, M., and Mayor, S. (2004). Nanoscale organization of multiple GPI-anchored proteins in living cell membranes. Cell *116*, 577-589.

Sheets, E.D., Lee, G.M., Simson, R., and Jacobson, K. (1997). Transient confinement of a glycosylphosphatidylinositol-anchored protein in the plasma membrane. Biochemistry *36*, 12449-12458.

Silvius, J.R., del Giudice, D., and Lafleur, M. (1996). Cholesterol at different bilayer concentrations can promote or antagonize lateral segregation of phospholipids of differing acyl chain length. Biochemistry *35*, 15198-15208.

Simons, K., and Ikonen, E. (1997). Functional rafts in cell membranes. Nature *387*, 569-572.

Simons, K., and Toomre, D. (2000). Lipid rafts and signal transduction. Nat Rev Mol Cell Biol *1*, 31-39.

Simons, K., and van Meer, G. (1988). Lipid sorting in epithelial cells. Biochemistry *27*, 6197-6202.

Simons, K., and Vaz, W.L. (2004). Model systems, lipid rafts, and cell membranes. Annu Rev Biophys Biomol Struct *33*, 269-295.

Singer, S.J., and Nicolson, G.L. (1972). The fluid mosaic model of the structure of cell membranes. Science (New York, N.Y *175*, 720-731.

Slimane, T.A., Trugnan, G., Van, I.S.C., and Hoekstra, D. (2003). Raft-mediated trafficking of apical resident proteins occurs in both direct and transcytotic pathways in polarized hepatic cells: role of distinct lipid microdomains. Molecular biology of the cell *14*, 611-624.

Snyers, L., Umlauf, E., and Prohaska, R. (1999). Association of stomatin with lipid-protein complexes in the plasma membrane and the endocytic compartment. European journal of cell biology *78*, 802-812.

Stan, R.V. (2005). Structure of caveolae. Biochimica et biophysica acta *1746*, 334-348.

Stanton, B.A. (1997). Cystic fibrosis transmembrane conductance regulator (CFTR) and renal function. Wiener klinische Wochenschrift *109*, 457-464.

Stein, M., Wandinger-Ness, A., and Roitbak, T. (2002). Altered trafficking and epithelial cell polarity in disease. Trends in cell biology *12*, 374-381.

Sun, A.Q., Ananthanarayanan, M., Soroka, C.J., Thevananther, S., Shneider, B.L., and Suchy, F.J. (1998). Sorting of rat liver and ileal sodium-dependent bile acid transporters in polarized epithelial cells. The American journal of physiology *275*, G1045-1055.

Takeda, T., Yamazaki, H., and Farquhar, M.G. (2003). Identification of an apical sorting determinant in the cytoplasmic tail of megalin. American journal of physiology *284*, C1105-1113.

Tettamanti, G., Bonali, F., Marchesini, S., and Zambotti, V. (1973). A new procedure for the extraction, purification and fractionation of brain gangliosides. Biochimica et biophysica acta *296*, 160-170.

Thompson, T.E., and Tillack, T.W. (1985). Organization of glycosphingolipids in bilayers and plasma membranes of mammalian cells. Annual review of biophysics and biophysical chemistry *14*, 361-386.

Tivodar, S., Paladino, S., Pillich, R., Prinetti, A., Chigorno, V., van Meer, G., Sonnino, S., and Zurzolo, C. (2006). Analysis of detergent-resistant membranes associated with apical and basolateral GPI-anchored proteins in polarized epithelial cells. FEBS letters *580*, 5705-5712.

Toomre, D., Keller, P., White, J., Olivo, J.C., and Simons, K. (1999). Dual-color visualization of trans-Golgi network to plasma membrane traffic along microtubules in living cells. Journal of cell science *112*, 21-33.

Urban, J., Parczyk, K., Leutz, A., Kayne, M., and Kondor-Koch, C. (1987). Constitutive apical secretion of an 80-kD sulfated glycoprotein complex in the polarized epithelial Madin-Darby canine kidney cell line. The Journal of cell biology *105*, 2735-2743.

Vagin, O., Turdikulova, S., and Sachs, G. (2004). The H,K-ATPase beta subunit as a model to study the role of N-glycosylation in membrane trafficking and apical sorting. J Biol Chem *279*, 39026-39034.

van Meer, G. (1989). Lipid traffic in animal cells. Annu Rev Cell Biol *5*, 247-275.

van Meer, G., and Simons, K. (1982). Viruses budding from either the apical or the basolateral plasma membrane domain of MDCK cells have unique phospholipid compositions. The EMBO journal *1*, 847-852.

van Meer, G., and Simons, K. (1988). Lipid polarity and sorting in epithelial cells. J Cell Biochem *36*, 51-58.

Varma, R., and Mayor, S. (1998). GPI-anchored proteins are organized in submicron domains at the cell surface. Nature *394*, 798-801.

Verhey, K.J., and Birnbaum, M.J. (1994). A Leu-Leu sequence is essential for COOH-terminal targeting signal of GLUT4 glucose transporter in fibroblasts. J Biol Chem *269*, 2353-2356.

Verhey, K.J., Yeh, J.I., and Birnbaum, M.J. (1995). Distinct signals in the GLUT4 glucose transporter for internalization and for targeting to an insulin-responsive compartment. The Journal of cell biology *130*, 1071-1079.

Vogel, U., Sandvig, K., and van Deurs, B. (1998). Expression of caveolin-1 and polarized formation of invaginated caveolae in Caco-2 and MDCK II cells. Journal of cell science *111 (Pt 6)*, 825-832.

Wandinger-Ness, A., Bennett, M.K., Antony, C., and Simons, K. (1990). Distinct transport vesicles mediate the delivery of plasma membrane proteins to the apical and basolateral domains of MDCK cells. The Journal of cell biology *111*, 987-1000.

Wang, S., Yue, H., Derin, R.B., Guggino, W.B., and Li, M. (2000). Accessory protein facilitated CFTR-CFTR interaction, a molecular mechanism to potentiate the chloride channel activity. Cell *103*, 169-179.

Wehrle-Haller, B., and Imhof, B.A. (2001). Stem cell factor presentation to c-Kit. Identification of a basolateral targeting domain. J Biol Chem *276*, 12667-12674.

Yeaman, C., Grindstaff, K.K., and Nelson, W.J. (1999). New perspectives on mechanisms involved in generating epithelial cell polarity. Physiological reviews *79*, 73-98.

Yeaman, C., Le Gall, A.H., Baldwin, A.N., Monlauzeur, L., Le Bivic, A., and Rodriguez-Boulan, E. (1997). The O-glycosylated stalk domain is required for apical sorting of neurotrophin receptors in polarized MDCK cells. The Journal of cell biology *139*, 929-940.

Ying, M., Grimmer, S., Iversen, T.G., Van Deurs, B., and Sandvig, K. (2003). Cholesterol loading induces a block in the exit of VSVG from the TGN. Traffic (Copenhagen, Denmark) *4*, 772-784.

Zhang, J., Pekosz, A., and Lamb, R.A. (2000). Influenza virus assembly and lipid raft microdomains: a role for the cytoplasmic tails of the spike glycoproteins. Journal of virology *74*, 4634-4644.

Zurzolo, C., Lisanti, M.P., Caras, I.W., Nitsch, L., and Rodriguez-Boulan, E. (1993). Glycosylphosphatidylinositol-anchored proteins are preferentially targeted to the basolateral surface in Fischer rat thyroid epithelial cells. The Journal of cell biology *121*, 1031-1039.

Zurzolo, C., van Meer, G., and Mayor, S. (2003). The order of rafts. Conference on microdomains, lipid rafts and caveolae. EMBO Rep *4*, 1117-1121.

Zurzolo, C., van't Hof, W., van Meer, G., and Rodriguez-Boulan, E. (1994). VIP21/caveolin, glycosphingolipid clusters and the sorting of glycosylphosphatidylinositol-anchored proteins in epithelial cells. The EMBO journal *13*, 42-53.

Figure legends

Figure 1 FR, PLAP and GFP-GPI are apically sorted and associate with DRMs in MDCK cells.

MDCK cells stably expressing FR/GFP-GPI or PLAP/GFP-GPI were grown for 4 d on filters. LC-biotin was added to the apical or the basolateral surface of the cells. After immunoprecipitation with specific antibodies, biotinylated proteins were revealed using HRP-streptavidin. Quantitations represent the mean value of three independent experiments (**A**). MDCK cells stably expressing FR/GFP-GPI or PLAP/GFP-GPI were lysed in buffer containing 1% TX-100 at 4°C and purified by centrifugation to equilibrium on sucrose gradients (5-40%) as described in materials and methods. Fractions of 1 ml were collected from the top (fraction 1) to the bottom (fraction 12). After TCA-precipitation, proteins were run on SDS-PAGE and detected using specific antibodies (**B**). An aliquot of each fraction was spotted on nitrocellulose membranes and GM1 was revealed using HRP-cholera toxin. As previously shown, the band at 43 kDa represents a partially denatured dimer of GFP (Inouye and Tsuji, 1994; Paladino *et al.*, 2004).

Figure 2 FR, PLAP and GFP-GPI form high molecular weight complexes in MDCK cells.

MDCK cells stably expressing FR/GFP-GPI or PLAP/GFP-GPI, grown to confluence, were purified by velocity gradient as described in materials and methods. Fractions of 0.5 ml were collected from the top (fraction 1) to the bottom (fraction 9). After TCA precipitation, samples were run on SDS-PAGE and revealed by western blotting with specific antibodies. The position on the gradients of molecular weight markers is indicated on top of the panels (**A**). Alternatively, cells were cross-linked by using BS_3 (0.5 mM) either at 4°C or 37°C for different indicated times. After lysis, proteins were TCA-precipiated, separated on SDS-PAGE and revealed using specific antibodies (**B**). The molecular weight of the monomeric forms of each protein is indicated, together with the position of a 180 kDa marker. *, **, and *** indicate, respectively, monomers, dimers and trimers of the different proteins.

Figure 3 HMW complexes of FR, PLAP and GFP-GPI can be cross-linked in specific hetero-clusters.

MDCK cells stably expressing FR/GFP-GPI or PLAP/GFP-GPI were crosslinked at 4°C with BS_3 (0.5 mM). After lysis, proteins were immunoprecipitated either with anti-FR or anti-PLAP antibody and revealed by western blotting using specific antibodies.

Figure 4 Cholesterol depletion does not affect GPI-AP homo-clusters.

MDCK cells stably expressing FR/GFP-GPI or PLAP/GFP-GPI, either in control conditions or after saponin (SAP) addition as described in materials and methods, were cross-linked with BS$_3$ at 37°C for different times. After lysis, proteins were TCA-precipitated and revealed by western blotting with specific antibodies.

Figure 5 Cholesterol depletion affects GPI-AP hetero-clusters.

MDCK cells stably expressing FR/GFP-GPI or PLAP/GFP-GPI, in control conditions or after saponin treatment, were cross-linked with BS$_3$. After lysis, samples were immunoprecipitated by using anti-FR or anti-PLAP specific antibodies and revealed by western blotting using an anti-GFP antibody.

Figure 6 Cholesterol depletion affects co-clustering of both GPI-APs.

MDCK cells stably expressing FR/GFP-GPI or PLAP/GFP-GPI, either in control conditions (-) or after saponin treatment (+), were cross-linked (+) with BS$_3$, fixed and stained with specific antibodies and revealed by Cy3- and Cy5-conjugated secondary antibodies. Serial confocal sections were collected. The 3D reconstruction is shown and areas of co-localization are labelled in white. Bars, 4 µm.

Figure 7 Effect of cholesterol addition on homo- and hetero-complexes.

MDCK cells stably expressing FR/GFP-GPI or PLAP/GFP-GPI were loaded with cholesterol (chol, 10 mM) for different indicated times and then cross-linked by using BS$_3$ (0.5 mM) at 37°C for 10 min. After lysis, proteins were TCA-precipitated, separated on SDS-PAGE and revealed using specific antibodies (**A**) or were immunoprecipitated by using anti-FR or anti-PLAP antibodies and revealed by western blotting using an anti-GFP antibody (**B**). The molecular weight of the monomeric forms of each protein is indicated, together with the position of a 180 kDa marker.

Figure 8 Hetero-clusters are exclusively formed by HMW complexes of each GPI-AP.

MDCK cells stably expressing FR/GFP-GPI or PLAP/GFP-GPI were treated with BS$_3$, lysed and purified by velocity gradients. Samples were immunoprecipitated using an anti-FR or anti-PLAP antibody and revealed by western blotting using an anti-GFP antibody (top panels). Immunoprecipitated proteins were revealed by western blotting with the same antibody (either FR or PLAP; bottom panels). The molecular weight of the monomeric forms of each protein is indicated, together with the position of a 180 kDa marker.
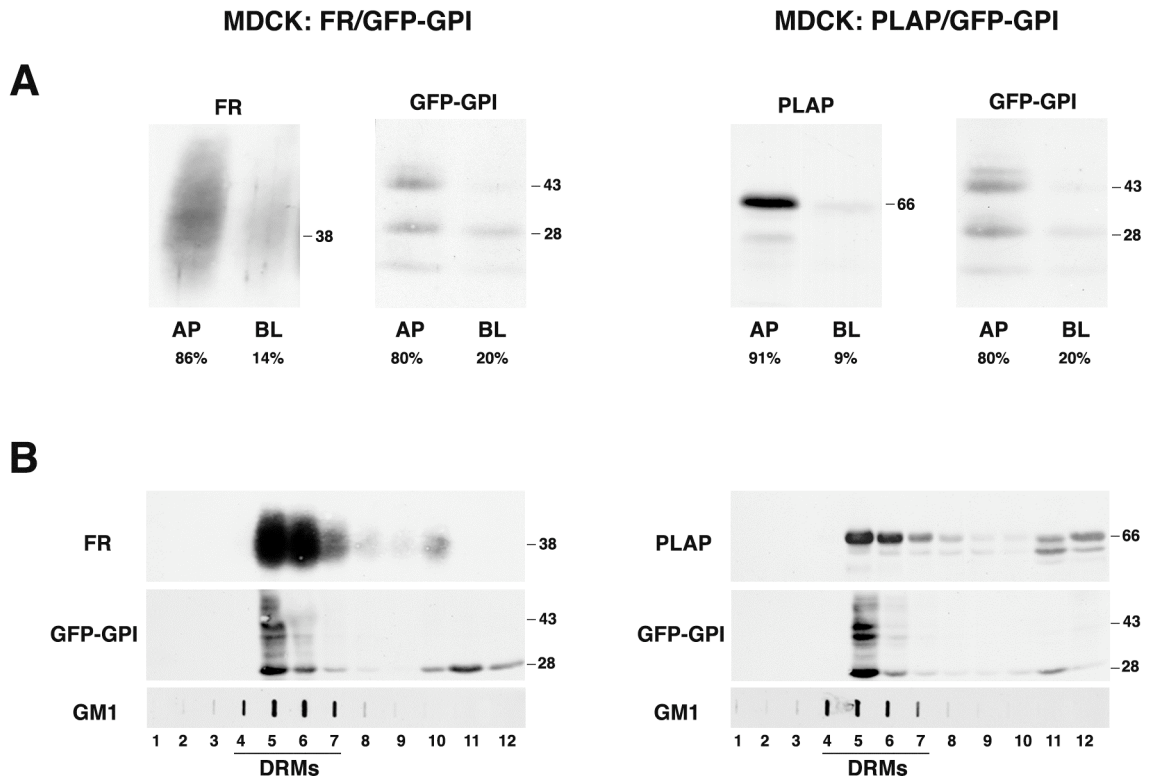
Figure 9 Analysis of co-clustering of GFP-GPI with FR or PLAP by antibody cross-linking at the cell surface.

MDCK cells stably expressing PLAP/GFP-GPI were simultaneously incubated at 12°C for 45 min with specific antibodies against GFP and PLAP (α–GFP/α–PLAP cross-linking) or left untreated (control). After washing, cells were incubated with secondary antibodies and fixed, or fixed for 1 h and incubated with primary and secondary antibodies (**A**). MDCK cells stably expressing PLAP/GFP-GPI (left panels) or FR/GFP-GPI (right panels) were incubated only with αGFP primary and secondary antibodies for 45 min at 12°C. After fixation, the other GPI-AP in the pair was stained in non-permeabilized conditions using a specific antibody and revealed with a secondary antibody (**B**). MDCK cells stably expressing FR/GFP-GPI or PLAP/GFP-GPI were incubated at 12°C with a specific antibody against either FR (pictures B-D) or PLAP (pictures F-H) and then with a secondary antibody for 45 min. Cells were imaged in vivo by confocal microscopy. In picture A and E the fluorescence of GFP-GPI in the absence of antibody clustering is shown (**C**). Serial confocal sections were collected. Bars, 4 μm.
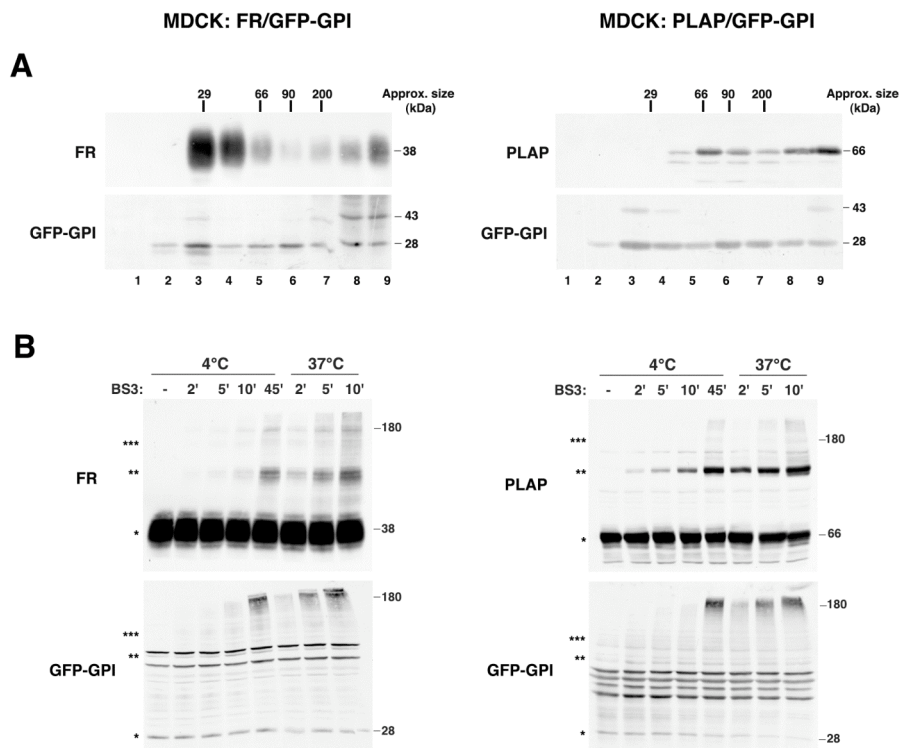
Figure 10 Model of GPI-AP membrane organization.

At the apical surface of MDCK cells GPI-APs are proposed to be organized in homo-clusters independent of cholesterol but dependent on protein-protein interactions. The proteinaceous complexes determine a local enrichment of raft lipids in a confined zone with cholesterol likely to be enriched at their boundaries (orange ring) thus creating specialized membrane domains that actively exclude GPI-AP monomers or other apical components. Because they are surrounded by a similar saturated-lipid environment these GPI-AP clusters have high affinity for each other and can fuse into cholesterol-dependent hetero-clusters. Cholesterol unbalance in the membrane by different means affects only hetero-clusters and not homo-clusters organization. The different effect of saponin (grey hexagones) metabolic inhibition, (MEV) or cyclodextrin treatments (depletion/addition) are illustrated.
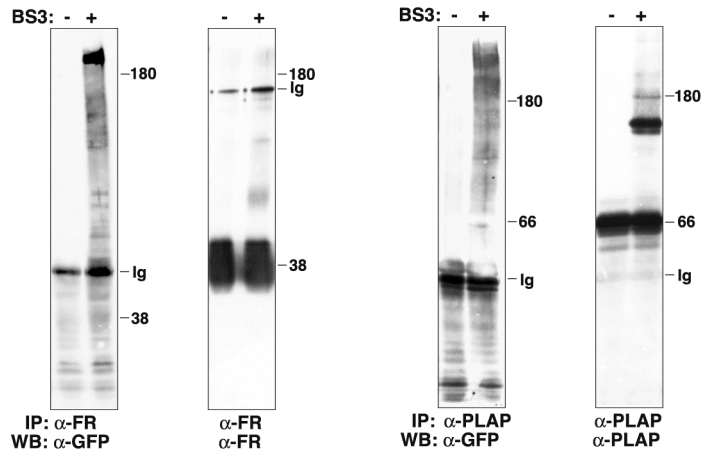
Figure 1

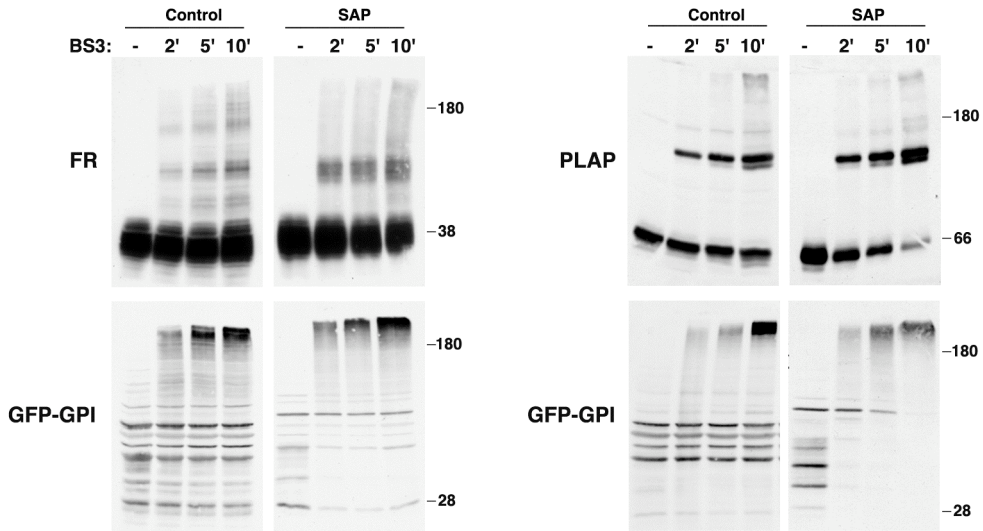**Figure 2**

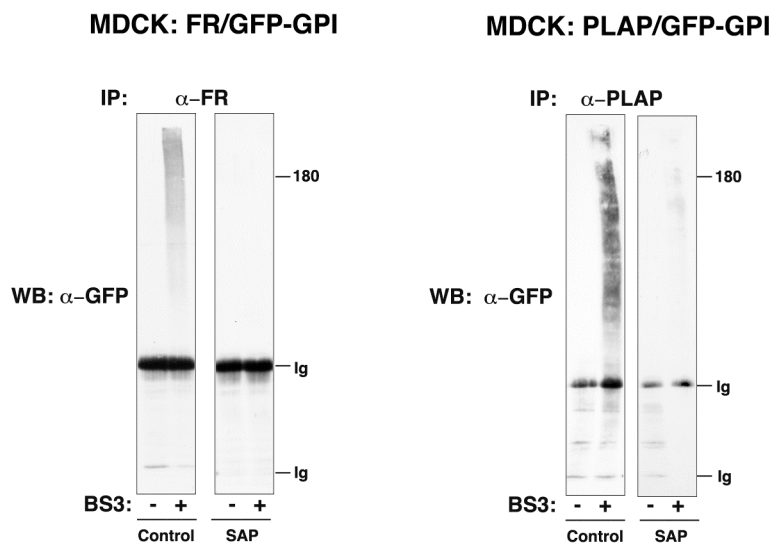**MDCK: FR/GFP-GPI**   **MDCK: PLAP/GFP-GPI**

BS3: - +   - +   BS3: - +   - +

—180   —180   —180   —180

—Ig

Ig—   —66   —66

—38

Ig—   —38   Ig—   Ig—

IP: α-FR   α-FR   IP: α-PLAP   α-PLAP
WB: α-GFP   α-FR   WB: α-GFP   α-PLAP

Figure 3

MDCK: FR/GFP-GPI   **MDCK: PLAP/GFP-GPI**

	Control	SAP			Control	SAP	

BS3: - 2' 5' 10'   - 2' 5' 10'   BS3: - 2' 5' 10'   - 2' 5' 10'

FR   —180   PLAP   —180

—38   —66

GFP-GPI   —180   GFP-GPI   —180

—28   —28

Figure 4

114

MDCK: FR/GFP-GPI
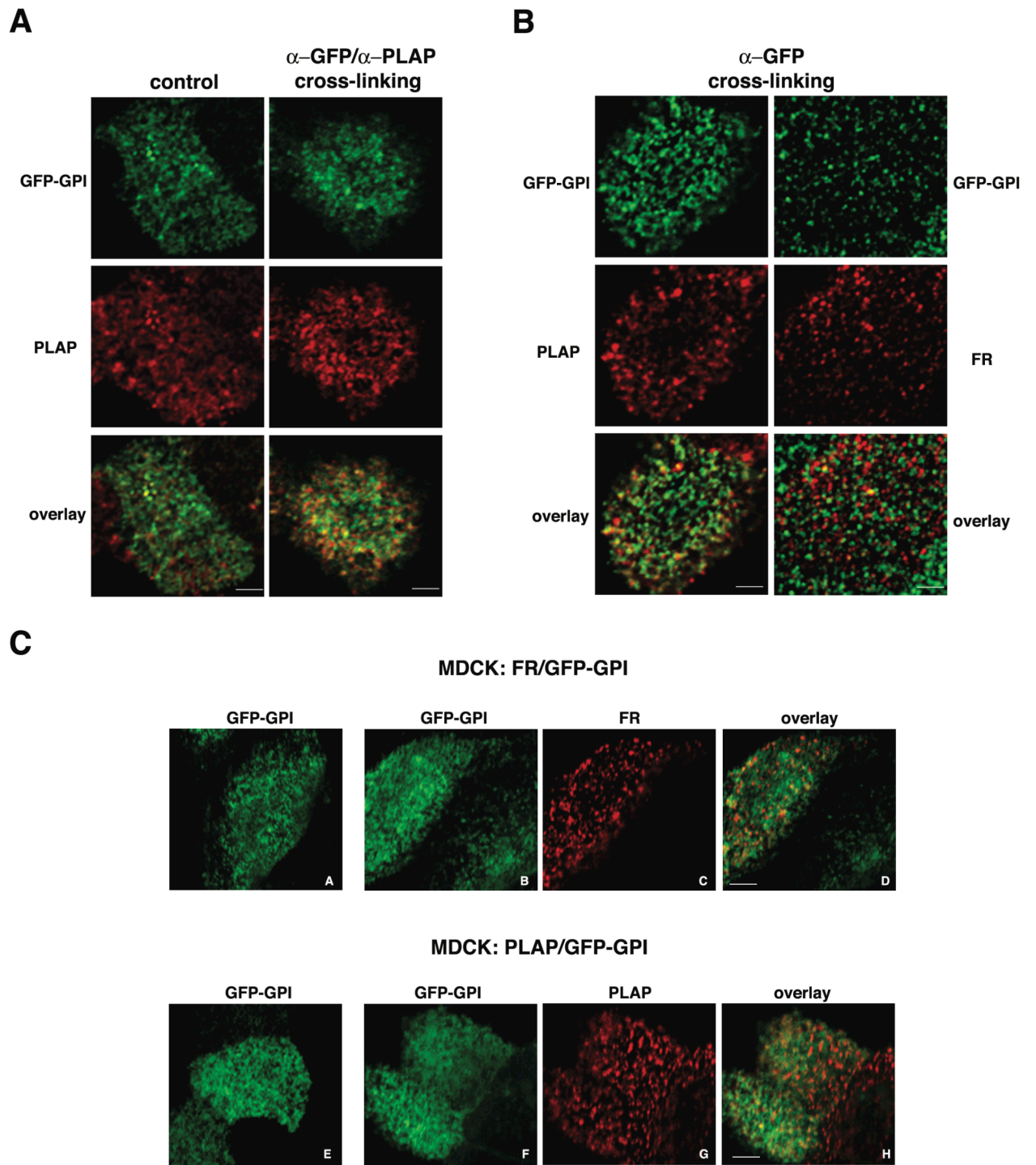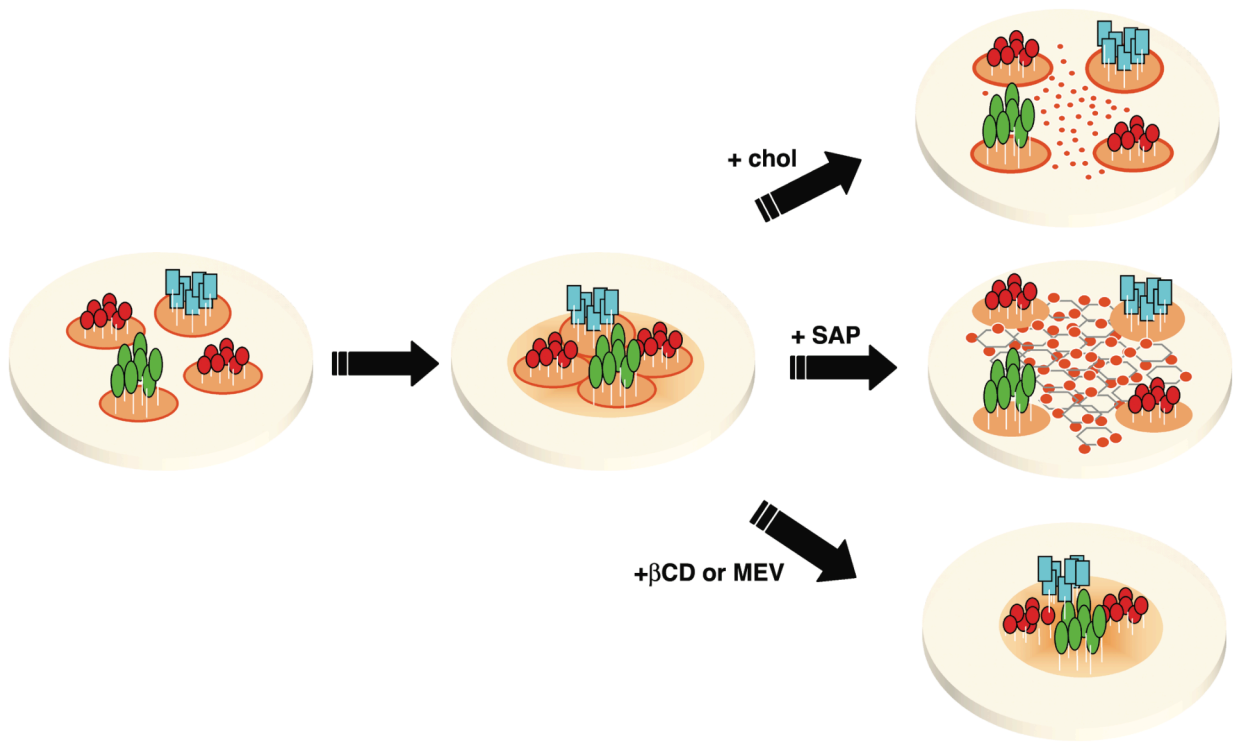
MDCK: PLAP/GFP-GPI

Figure 5

Figure 6

MDCK: FR/GFP-GPI   MDCK: PLAP/GFP-GPI

A

FR   GFP-GPI   PLAP   GFP-GPI

B

IP: α-FR   IP: α-PLAP
WB: α-GFP   WB: α-GFP

Figure 7

MDCK: FR/GFP-GPI   MDCK: PLAP/GFP-GPI

Figure 8

A

control   α–GFP/α–PLAP cross-linking

GFP-GPI

PLAP

overlay

B

α–GFP cross-linking

GFP-GPI   GFP-GPI

PLAP   FR

overlay   overlay

C

MDCK: FR/GFP-GPI

GFP-GPI   GFP-GPI   FR   overlay

A   B   C   D

MDCK: PLAP/GFP-GPI

GFP-GPI   GFP-GPI   PLAP   overlay

E   F   G   H

Figure 9

Figure 10

A

B

Figure S1

MDCK: GFP-GPI

Figure S2

MDCK: FR/GFP-GPI   MDCK: PLAP/GFP-GPI

Figure S3

A

MDCK: FR/GFP-GPI

MDCK: PLAP/GFP-GPI

FR

GFP-GPI

PLAP

GFP-GPI

B

MDCK: FR/GFP-GPI

MDCK: PLAP/GFP-GPI

FR

GFP-GPI

PLAP

GFP-GPI

C

CHO: GFP-GPI

Figure S4

GFP-GPI | FR | PLAP

Control

SAP

Figure S5

MDCK: PLAP/GFP-GPI

—180

—Ig

BS3: - +   - +   - +

control   MEV   βCD

Figure S6

p75 NTR | GP114

—180

—75

—180

—114

SAP: -   +

BS3: +   +   +   +
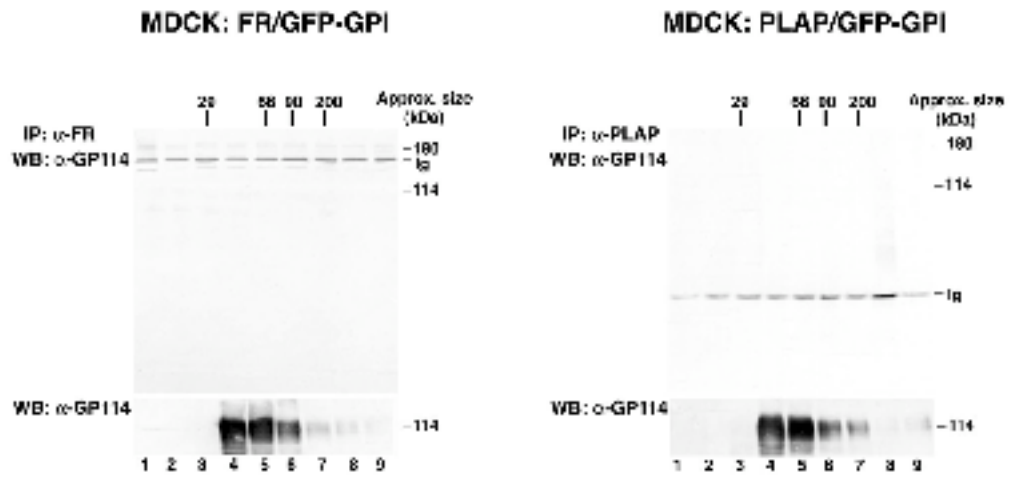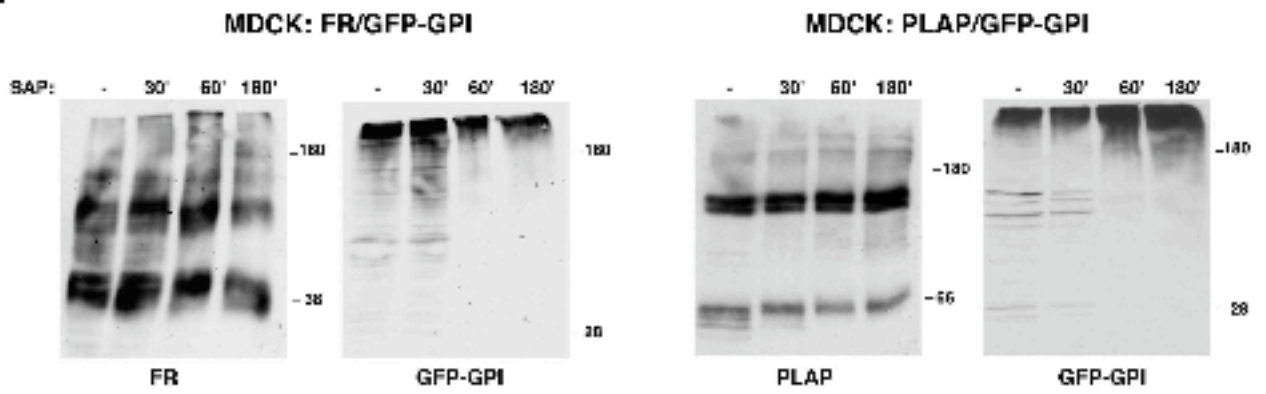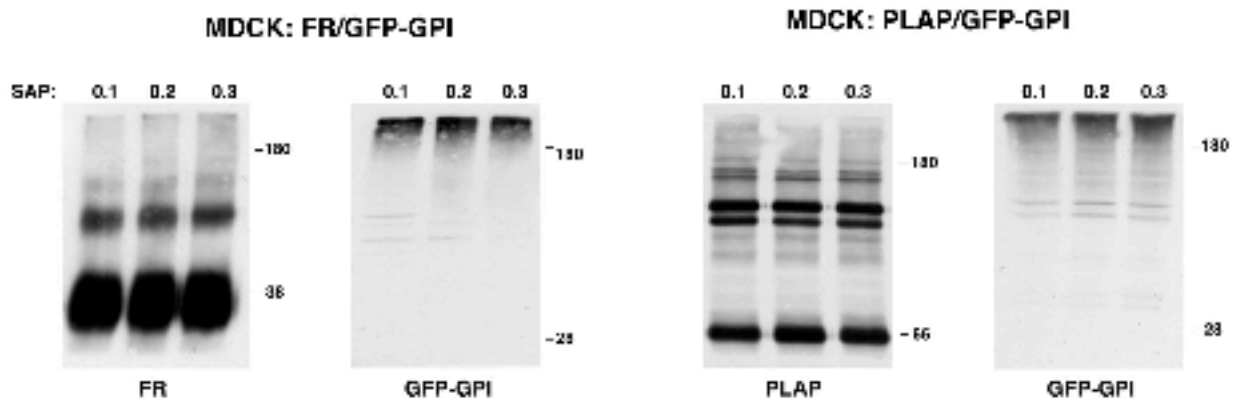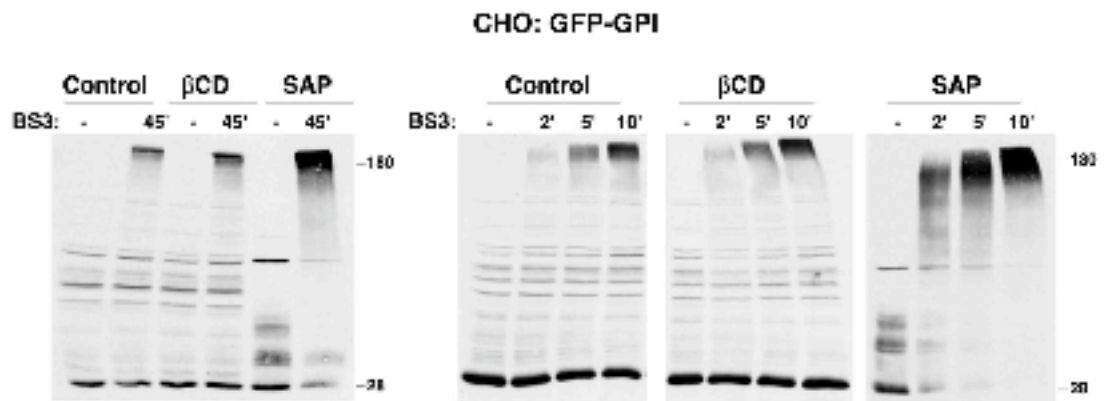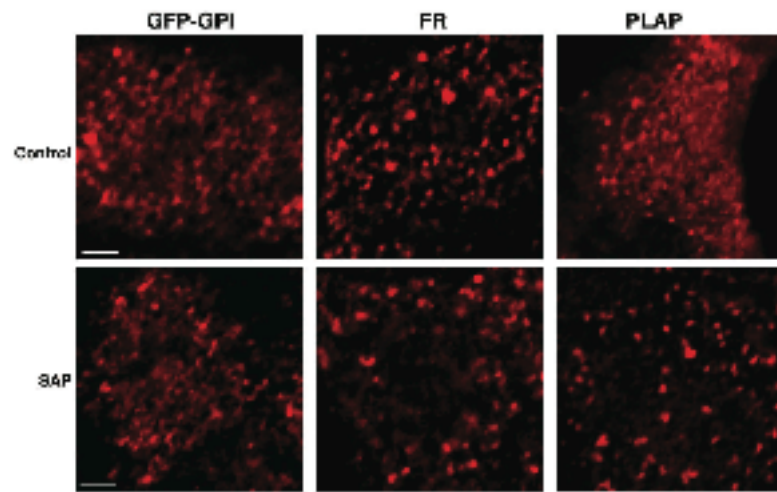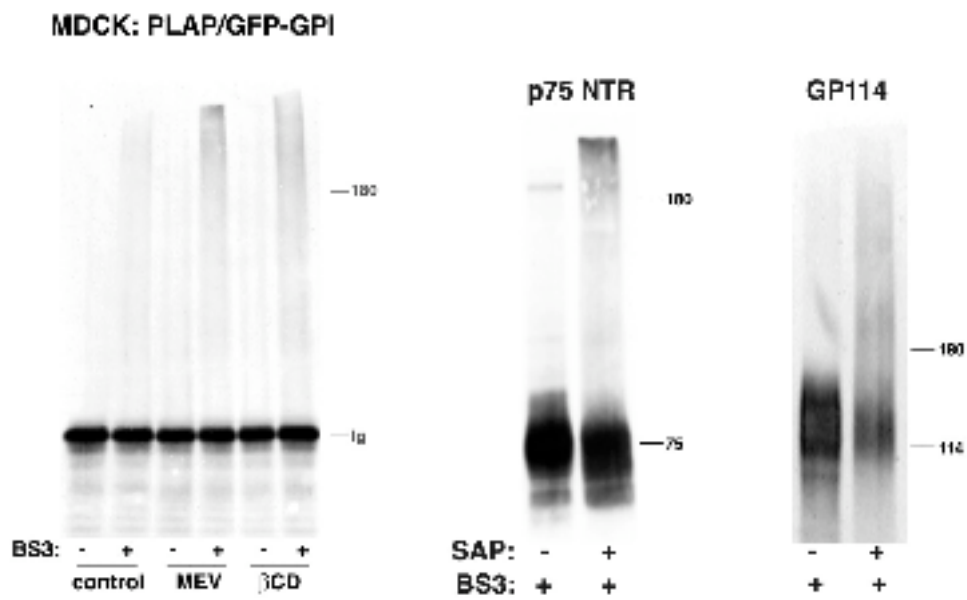
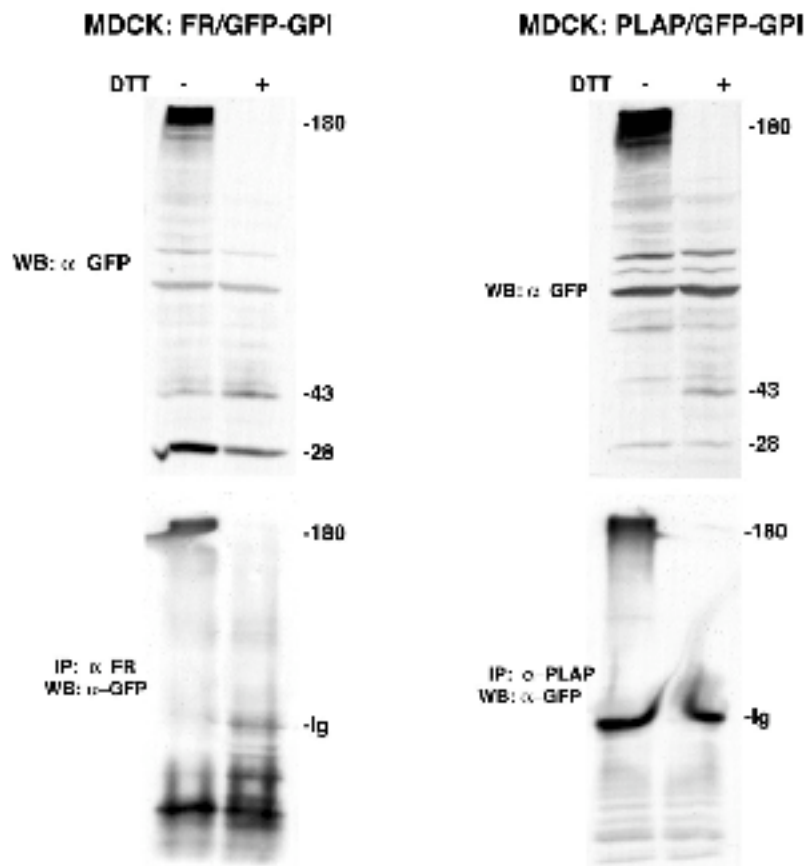## Figure S7

Figure S8

Table I. Quantitation of degree of co-localization between GFP-GPI and FR or PLAP in co-expressing MDCK cells in absence or presence of saponin.

	MDCK: FR/GFP-GPI		MDCK: PLAP/GFP-GPI	
	FR	GFP-GPI	PLAP	GFP-GPI
+BS3, -SAP	5.5 ± 0.7	5.9 ± 0.49	5.5 ± 2	5 ± 1.6
+BS3, +SAP	0.6 ± 0.2	0.6 ± 0.3	0.32 ± 0.1	0,21 ± 0.1

Table II. Quantitation of degree of co-localization between GFP-GPI and PLAP in co-expressing MDCK cells in control conditions or after antibodies (abs) clustering.

	MDCK: PLAP/GFP-GPI	
	PLAP	GFP-GPI
control	0,7 ± 0,2	0,5 ± 0.1
αGFP/PLAP abs clustering	3,6 ± 0.8	3,9 ± 0.6

Table III. Quantitation of degree of co-localization of GFP-GPI with FR or with PLAP in co-expressing MDCK cells after clustering with an anti-GFP, anti-FR or anti-PLAP antibody (ab).

	MDCK: FR/GFP-GPI	
	FR	GFP-GPI
αFR ab clustering	0.45 ± 0.15	0.3 ± 0.14
αGFP ab clustering	0.3 ±0.09	0.5 ± 0.07
	MDCK: PLAP/GFP-GPI	
	PLAP	GFP-GPI
αPLAP ab clustering	0.2 ± 0.004	0.25 ± 0.003
αGFP ab clustering	0.7 ± 0.5	0.8 ± 0.5